ECONOMIC GEOLOGY OF THE WENATCHEE MINING DISTRICT, CHELAN COUNTY, WASHINGTON

A Dissertation
Submitted in Partial Fulfillment
of the Requirements for the
DEGREE OF DOCTOR OF PHILOSOPHY
with a
Major in Geology
in the
GRADUATE SCHOOL
UNIVERSITY OF IDAHO

by
Lawrence E. Ott

March, 1988

ABSTRACT

Epithermal gold-silver mineralization in the Wenatchee district occurs as widely spaced quartz-adularia veins within pervasively silicified Eocene continental sedimentary rocks in the southeastern part of the Chiwaukum graben, a northwest-trending dextral strike-slip basin in central Washington that formed between 49 and 42 m.y.b.p. Economic mineralization occurs in the abandoned L-D and newly discovered Cannon mines.

Sedimentary rocks are divided into: (1) mineralized and complexly deformed beds of arkose, siltstone, and claystone of uncertain age which are bounded to the east by (2) the middle Eocene Chumstick Formation, and to the west by (3) the Oligocene Wenatchee Formation.

The sediments are cut by, and interlayered with felsic to intermediate volcanic and hypabyssal rocks which yield K-Ar ages of 33.5±2.0 to 50.9±3.5 m.y.b.p. (for weakly mineralized hornblende andesite west of mineralization) and 43.2±0.4 m.y.b.p. (for unaltered biotite rhyodacite porphyry east of mineralization).

Cannon mine ore minerals are electrum, pyrargyrite, tetrahedrite, and acanthite; and naummanite, aguilarite, pyrargyrite, and electrum predominate at the L-D mine. Gangue minerals are pyrite, chalcopyrite, quartz, chalcedony, calcite, and adularia (K-Ar: 44.2±1.9 m.y.b.p.). Alteration at the Cannon mine consists of a single mixed zone of selectively pervasive and vein-controlled silicification, and vein-

controlled potassium silicate and carbonate alteration that is overlain by a zone of pervasive intermediate argillic alteration. Anomalous concentrations of selenium, antimony, gold, silver, arsenic, and mercury at the Cannon mine, arsenic and mercury are also present in a halo over the ore bodies.

Cannon mine veins occupy radial and a-c extension fractures in southwest-trending, north-verging asymmetric folds that formed as a result of dextral shear on the Eagle Creek fault, a northwest-trending intra-graben fault along which magmatic and hydrothermal activity was localized during graben formation. L-D mine veins occupy northeast-trending veins that occupy release joints that developed at the end of graben formation. Ductile and brittle deformation features are present and indicate that intra-mineralization strain-rate variations were important in ore localization. Post-Oligocene, north-trending dextral strike-slip tear faults, and northwest-trending, southwest-dipping reverse faults offset ore bodies.

ACKNOWLEDGMENTS

This study was made possible by the financial backing and cooperation of Asamera Minerals (US) Incorporated and Breakwater Resources Limited, joint venture partners at the Cannon mine.

Excellent technical support was received from the geologic staff of Asamera: D. Groody, T.E. Alexander, R. Gill, E.S. McCulloch, C. Hale, W.B. Bond, R. Karlson, and E.L. Follis. The writer is grateful for their open sharing of ideas and maps.

Omni Petroleum Services of Houston, Texas conducted porosity and permeability test free of charge, and microprobe analysis of ore minerals was made possible by a grant from the Idaho Geologic Survey and the assistance of C.R. Knowles.

Dr. Peter Siems, chairman of the writer's graduate committee, is credited with seeing the project through from start to finish, and most of the ideas addressed in the following pages would not be as fully developed without his encouragement. Early versions of the manuscript were greatly improved by the editorial comments of members of the writer's graduate committee: Dr. John Bursnall, Dr. John Bush, Dr. James Reece, and Bob Hautala.

Margaret Holmes-Ott drafted all of the figures and produced the black and white prints.

DEDICATION

This dissertation is dedicated to my wife Peggy, whose patience, love, support, and encouragement made the project possible, and whose excellent drafting abilities expedited the final product.

TABLE OF CONTENTS

	Page
Authorization to submit dissertation	ii
Abstract	iii
Acknowledgments	v
Dedication	vi
Table of contents	vii
List of figures	viii
List of tables	xiii
List of plates	xiv
Introduction	1
Previous Geologic Investigations	5
Exploration and Production History	7
Regional Geology	13
Tertiary Sedimentary Rocks	13
Tertiary Igneous Rocks	16
Structural Geology	16
District Geology	20
Sedimentary Rocks	20
Sedimentary rocks of uncertain age	21
Chumstick Formation	26
Wenatchee Formation	28
Igneous Rocks	29
Amygdaloidal basalt	30
Saddle Rock andesite	33
Biotite rhyodacite porphyry	38
Andesite of the Horse Lake Mountain Complex	43

Age of emplacement..... 44
Structural Geology..... 46
Eagle Creek structure..... 48
North-trending faults..... 50
Pitcher syncline..... 51
Structures associated with mineralization..... 53
Interpretation of district structural history and its relation to mineralization..... 54
Timing and type of deformation..... 57
Introduction to the economic geology of the Wenatchee district..... 64
Geology of the "B" reef complex..... 71
Distribution and morphology of mineralized zones..... 71
Structural framework..... 75
Stratigraphy..... 95
Wall-rock alteration and mineralization..... 106
Alteration zoning..... 107
Intermediate argillic alteration..... 109
Silicification..... 113
Sericitic alteration..... 117
Wall-rock mineralization..... 119
Vein-controlled alteration and mineralization..... 122
Quartz-adularia veins..... 123
Stockwork veins..... 132
Calcite veins..... 137
Ore mineralogy..... 137

Timing of mineralization and alteration..... 143
Geology of the "D" reef..... 149
Distribution of mineralized rocks..... 149
Structural framework..... 151
Stratigraphy of the mineralized section..... 157
Mineralization and hydrothermal alteration..... 160
Other mineralized areas..... 163
Discussion..... 168
Trace Element Geochemistry..... 178
Instrumental neutron activation analytical data..... 179
Wall rock samples..... 179
Vein samples..... 183
Directly coupled emission spectrographic analytical data..... 186
Trace Element Zonation..... 189
Trace Element Patterns at Ore Boundaries..... 199
Summary..... 206
Conclusions..... 211
Recommendations for Further Research..... 214
References..... 217
APPENDIX A..... 226
APPENDIX B..... 231
APPENDIX C..... 236
APPENDIX D..... 239
APPENDIX E..... 245
APPENDIX F..... 255

LIST OF FIGURES

Page

Figure 1. Location map showing northwest-trending corridor that comprises the Wenatchee district, and geographic features referred to in text..... 2

Figure 2. Distribution of hydrothermally altered rocks, or "reefs", in the Wenatchee district..... 4

Figure 3. Generalized composite plan of the "B" reef complex, showing the location of ore zones, projected to the surface, and numbered in the order of their discovery..... 12

Figure 4. Regional geology of central Washington (modified from Gresens, 1983, Figure 2)..... 14

Figure 5. Schematic diagram of graben formation by dextral strike-slip movement on the Entiat and Leavenworth faults (modified from Gresens, 1983, Figure 7)..... 19

Figure 6. Complexly deformed Eocene-aged sedimentary rocks in the central portion of the district as exposed in the highwall excavated during preparation of the mill site at the Cannon mine..... 23

Figure 7. Heterolithic epiclastic breccia west of Rooster Comb. Drill Hole ASH-70A, 602 ft. down hole..... 25

Figure 8. Ternary diagrams showing Na_2O - K_2O - CaO content, and normative quartz - orthoclase - plagioclase in hypabyssal intrusive rocks in the Wenatchee district..... 32

Figure 9. View of the Saddle Rock andesite, looking northwest form Wenatchee Dome 34

Figure 10. Composite section of the Saddle Rock andesite, based on DDH B87-6B..... 37

Figure 11. View of Wenatchee Dome and Rooster Comb, looking southeast..... 39

Figure 12. Contact between perlite (on the left)and rhyodacite (on the right) on the west side of Wenatchee Dome..... 41

Figure 13. Principal structural features in the Wenatchee district..... 47

Figure 14. View of the Pitcher syncline, in beds of the Wenatchee Formation, looking northwest across Squilchuck Canyon..... 52

Figure 15. Interpretations of structural relations at the Pitcher syncline and "D" reef made by previous workers..... 55

Figure 16. Silicified, veined sedimentary rocks at the "D" reef..... 67

Figure 17. Surface outcrop of "B" reef prior to development of the Cannon mine..... 69

Figure 18. Generalized plan view, long section, and cross sections through the "B" reef complex..... 74

Figure 19. Geology of the "B" North ore body, 785 level, Cannon Mine..... 77

Figure 20. Geology of the "B" North ore body, 755 level, Cannon Mine..... 78

Figure 21. Geology of the "B" North ore body, 700 level, Cannon Mine..... 79

Figure 22. Geology of the "B" North ore body, 650 level, Cannon Mine..... 80

Figure 23. Geology of the "B" North ore body, 600 level, Cannon Mine..... 81

Figure 24. Geology of the "B" North ore body, 550 level, Cannon Mine..... 82

Figure 25. Geology of the "B" North ore body, 500 level, Cannon Mine..... 83

Figure 26. East-west cross section 8000N through the D stope area of the "B" North ore body, looking north..... 84

Figure 27. North-south long section 6100E through the Cannon mine, looking west..... 85

Figure 28. North-south long section 6300E throuth the Cannon mine, looking west..... 86

Figure 29. Equal area plot of bedding poles from the D stope area of the "B" North ore body..... 88

Figure 30. Southeast-trending asymmetric syncline in the D 36 stope on the 650 level of the "B" North ore body..... 89

Figure 31. Dismembered quartz-adularia veinlet in medium-grained feldspathic sandstone from the 700 level.... 91

Figure 32. Composite map of vein orientations in the "B" North ore body, including the D stope and X stope areas..... 93

Figure 33. Equal area plot of vein poles from the D stope area of the "B" North ore body..... 94

Figure 34. Local stratigraphic control of ore boundaries in the "B" North ore body..... 97

Figure 35. Generalized stratigraphic column showing mineralized sedimentary rocks in the D stope area of the "B" North ore body..... 99

Figure 36. Typical exposure of unit 1 on the 700 level of the "B" North ore body..... 101

Figure 37. Thinly laminated siltstone and sandy siltbeds of unit 2 as exposed on the 500 level..... 102

Figure 38. Carbonaceous siltstone beds of unit 4 that have been squeezed into the hinge of an anticline adjacent to the DX thrust on the 650 level, D stope area, "B" North zone..... 105

Figure 39. Vertical distribution of alteration zones at the "B" reef complex..... 108

Figure 40. Strong intermediate argillic alteration in feldspathic sandstone..... 112

Figure 41. Photomicrographs of feldspathic sandstone from unit 3 in the "B" North ore body..... 115

Figure 42. Weakly sericitized plagioclase grain in feldspathic sandstone from the 755 level..... 118

Figure 43. Core samples of hydrothermal breccia from about the 650 level of the "B" North ore body..... 120

Figure 44. Well rounded, spherical detrital grains in of polycrystalline quartz, monocrystalline quartz, and microcline in a breccia from the "B" Neath zone..... 121

Figure 45. Photograph (a) and sketch (b) of vein sample from the "B" Neath zone..... 127

Figure 46. Photograph (a) and sketch (b) of vein sample from the "B" Neath zone showing crustification of massive pyrite..... 128

Figure 47. Photograph (a) and sketch (b) of vein sample form the "B" Neath zone showing brecciated wall rock..... 129

Figure 48. Schematic drawing showing characteristic features of veins in the "B" Neath zone..... 130

Figure 49. Typical crustified quartz-adularia vein on the 700 level of the "B" North ore body..... 133

Figure 50. Vein sample from the 700 level of the "B" North ore body, showing adularia layers (stained yellow), and breccia-filled vein interior..... 134

Figure 51. Hand sample (A) and photomicrograph (B) showing lamellar boxwork texture developed from the replacement of calcite by quartz and chalcedony..... 135

Figure 52. Stockwork veining on the 650 level of the "B" North ore body..... 136

Figure 53. Vein calcite in sample from the 755 level.... 138

Figure 54. Electrum grains encapsulated in fine-grained quartz..... 141

Figure 55. Photomicrograph of electrum, pyrargyrite, and pyrite from the X stope area of the "B" North ore body on the 650 level..... 142

Figure 56. Pyrargyrite grain (medium gray) engulfed and and partially replaced by electrum (yellow)..... 147

Figure 57. Generalized paragenetic diagram showing the interpreted sequence of ore and gangue mineral deposition at the "B" reef complex..... 148

Figure 58. Plan map of the 1250 level of the L-D mine... 150

Figure 59. Geology of the 1250 level, Block 1, of the 1250 level of the "D" reef..... 152

Figure 60. Detailed geologic map of carbonaceous gouge zone in unnamed fault on the western boundary of Block 3 on the 1250 level..... 154

Figure 61. Bedding-plane vein crosscut by northeast-striking, north-dipping vein in Block 1..... 156

Figure 62. Measured stratigraphic sections in Block 1 of the 1250 level of the L-D mine..... 158

Figure 63. Style of veining in the northeast part of Block 1..... 161

Figure 64. Geologic map of the 1250 level at "A" reef... 165

Figure 65. Plan view and long section of sample base for trace element zonation investigation..... 190

Figure 66. Distribution of sample points and contoured gold values at the "B" reef complex..... 194

Figure 67. Copper and silver distribution..... 196

Figure 68. Selenium and antimony distribution..... 197

Figure 69. Arsenic and mercury distribution..... 198

Figure 70. Plan map and rib sketch of the rhyodacite-ore contact on the 755 level of the Cannon mine..... 200

Figure 71. Plan map and rib sketch of the rhyodacite-ore contact on the 700 level of the Cannon mine..... 201

Figure 72. Plan map and rib sketch of the rhyodacite-ore contact on the 550 level of the Cannon mine..... 202

Figure 73. Graphic log of drill hole TAD-10E showing concentrations of Au, Ag, As, Sb, and Hg in the lower 105 feet of the hole..... 205

LIST OF TABLES

Page

Table 1. L-D mine production, 1949 - 1967..... 10

Table 2. Major oxide and normative mineral content of hypabyssal intrusive rocks in the Wenatchee district..... 31

Table 3. Summary of age determinations on igneous rocks in and near the Wenatchee district, and adularia from the "B" North ore body..... 45

Table 4. Proven and probable ore reserves at the Cannon mine, by ore body, in ounces per short ton..... 172

Table 5. Statistical summary of instrumental neutron activation analyses for Au, Sb, As, Ag, Na, Cr, Fe, Ba, Hf, La, Mo, Cd, Co, Th, W, and U in wall rock samples from the "B" North ore body..... 181

Table 6. Comparison of average concentrations of trace elements in mineralized wall rock samples from the "B" North ore body with worldwide averages for sandstone, shale, and granite..... 182

Table 7. Statistical summary of instrumental neutron activation analyses for Au, Sb, As, Ag, Na, Cr, Fe, Ba, Hf, La, Mo, Cd, Co, Th, W, and U in vein samples from the "B" North ore body..... 185

Table 8. Statistical summary of directly coupled plasma emission spectrographic analyses for Ag, As, Sb, Cu, Zn, Se, Fe, Mn, Cr, and Ni, and cold vapor atomic absorption analyses for Hg in vein samples from the "B" North and "B" Neath ore bodies..... 187

Table 9. Average content of Cu, Pb, Zn, Ni, Cr, Mn, Ag, As, Sb, Fe, and Hg in vein samples from the "B" North and "B" Neath ore bodies, by level..... 188

Table 10. Statistical summary of atomic absorption analyses for Ag, Sb, As, Se, Te, Hg, Cu, and Pb, and fire assay analysis for Au in composite geochemical samples from the "B" reef complex..... 192

LIST OF PLATES

Plate 1.	Surface geology of the Wenatchee mining district, Chelan County, Washington.....	In Pocket
Plate 2.	Geologic cross sections through the Wenatchee mining district.....	In Pocket
Plate 3.	Reduced copy of plate 1 for reprographic use.....	In Pocket
Plate 4.	Reduced copy of plate 2 for reprographic use.....	In Pocket

INTRODUCTION

Epithermal gold-silver mineralization, genetically related to regional Eocene strike-slip faulting, has localized nearly 1.5 million ounces (47 mt) of economically recoverable gold in central Washington. Previous structural interpretations have been based on post-mineralization structures, and have been useful as exploration guides on a mine-site scale. This thesis presents new radiometric age determinations, describes geologic features of newly opened and abandoned mines, and presents a new interpretation of the pre- and intra-mineralization structural development of the district.

The Wenatchee mining district is located in the eastern foothills of the Cascade mountains, approximately 1.5 km west of the Columbia River in Chelan County, Washington (Figure 1). The district is easily accessible by paved highways and rail transportation. Other utilities are close at hand. Most of the district lies between 300 and 600 meters of elevation in moderately rugged terrain. Precipitation averages between 30 and 38 centimeters per year, and vegetation is dominated by typical Upper Sonoran species.

The district consists of Eocene-aged continental sedimentary rocks which have been hydrothermally altered in discrete zones that are spatially related to Eocene-aged intrusive and volcanic rocks of felsic to intermediate composition. Individual zones of alteration and mineralization are locally referred to as reefs. The most northerly and most southerly silicified outcrops are named "G" reef and "D" reef

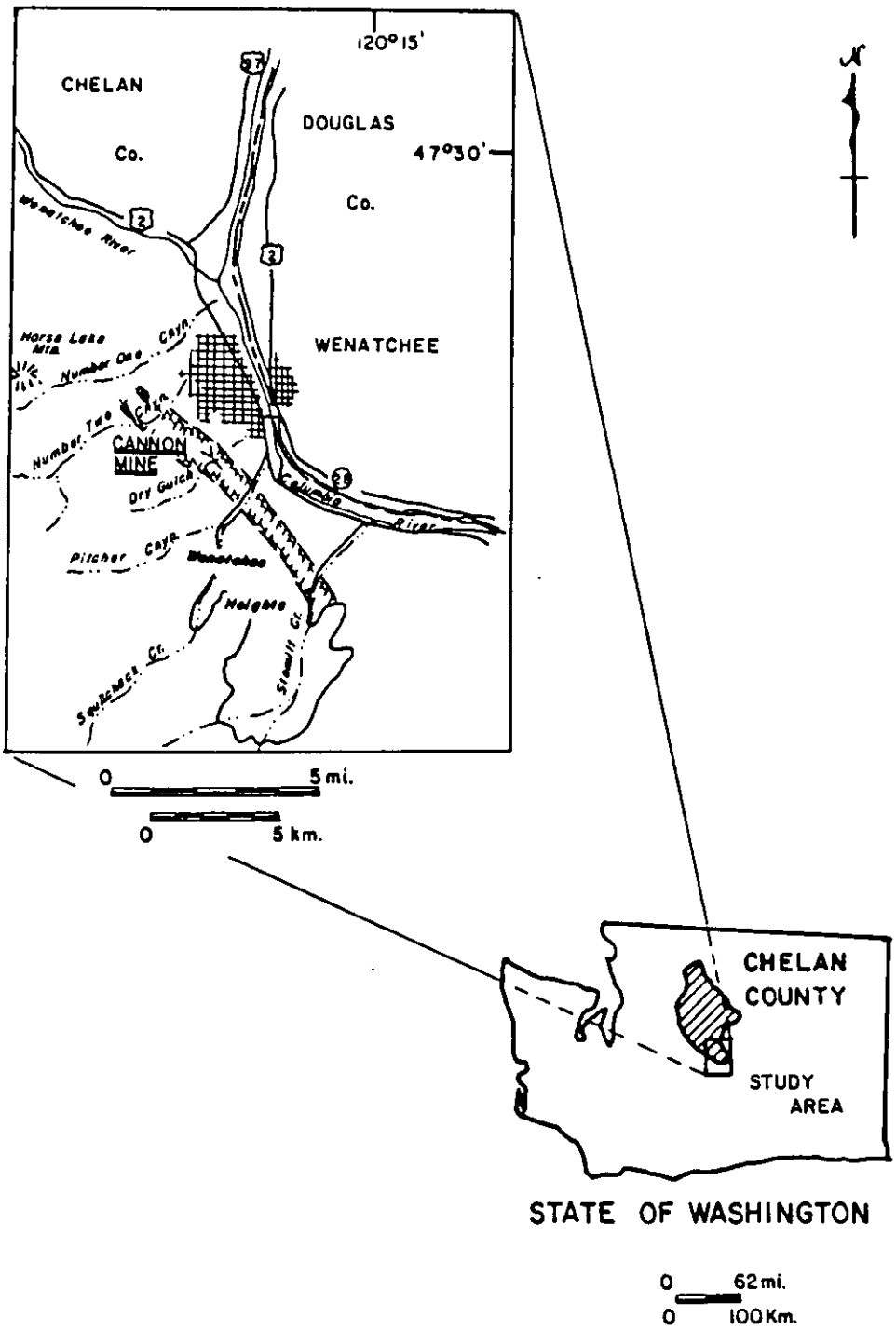

Figure 1. Location map showing northwest-trending corridor that comprises the Wenatchee district, and geographic features referred to in text.

respectively (Figure 2). The intrusions and zones of altered rock are aligned along a northwest trend that is parallel to the Columbia River for approximately eight km (Figure 1).

Gold is the principal commodity produced in the Wenatchee district; silver is the only byproduct. The Cannon mine (Figure 1) is currently the only producing mine in the district and has been in operation since mid-1985. Prior to the opening of the mine, the district had lain dormant for nearly 20 years.

The objective of this study is to describe as fully as possible the geology of the Wenatchee district, with an emphasis on features responsible for localizing individual altered and mineralized zones. Much of this document will focus on a description of the "B" reef complex, since the ore bodies there are the most recently discovered and previously have not been discussed in detail.

The initial field work for this investigation was carried out during the summer of 1985, during which time the new underground developments at the Cannon mine were mapped and sampled in detail. Cursory examinations of other mineralized zones within the district were also made during this period. Seven months of underground and surface mapping and sample collection were conducted during the period of May through December, 1986. Much of this time was spent mapping the advancing production and development headings at the Cannon mine and inspecting of several thousand feet of drill core derived from a grade control drilling program. Approximately

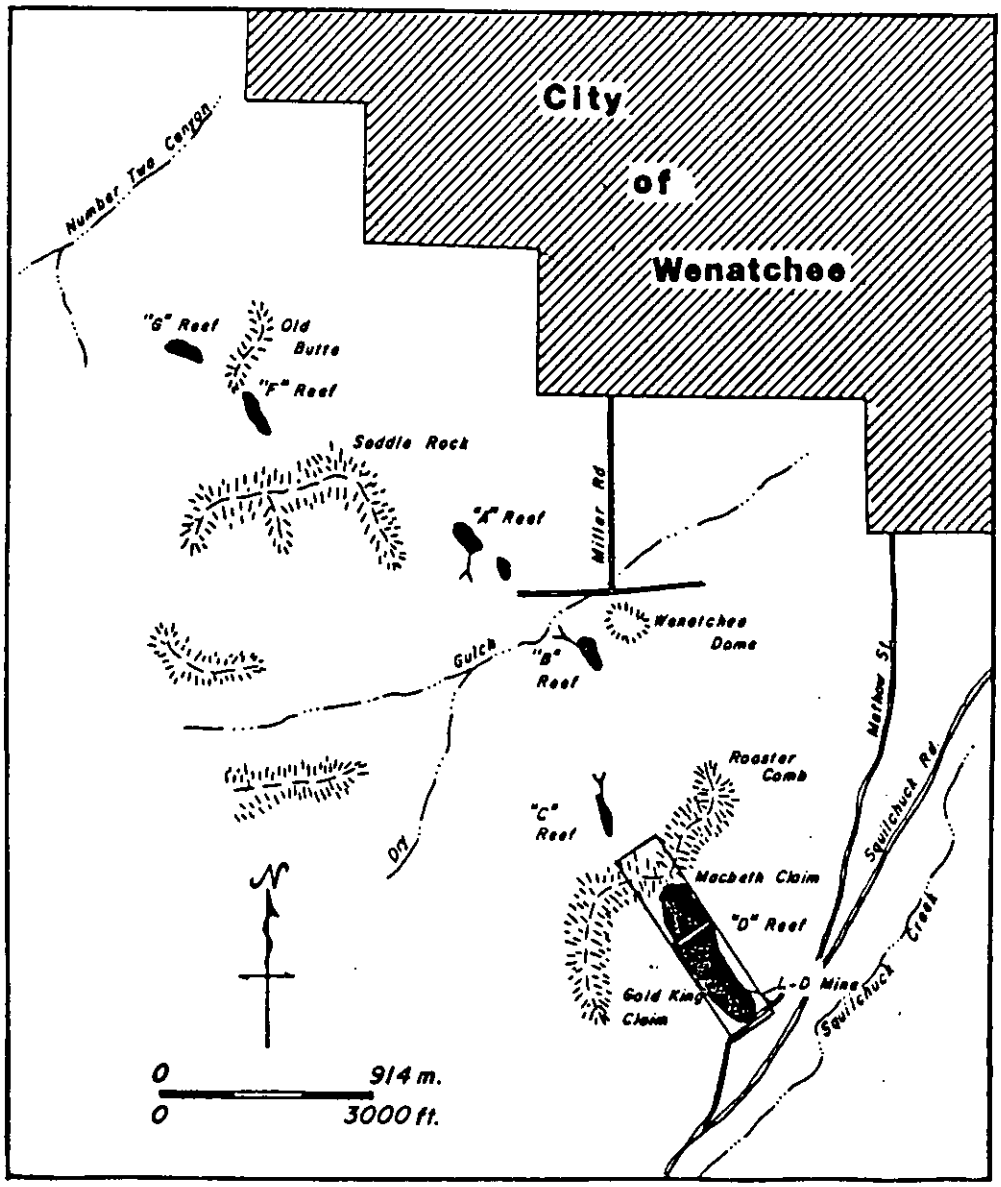

Figure 2. Distribution of hydrothermally altered rocks, or "reefs", in the Wenatchee district.

two months of this time were devoted to mapping and sampling outlying surface exposures of hypabyssal intrusive rocks and altered sedimentary rocks. Four months during the summer of 1987 were spent mapping rehabilitated portions of the L-D mine (Figure 2) and surface exposures throughout the district. Field work was augmented by petrographic study of collected samples and computer-assisted analysis of structural and geochemical data during the winter months of 1985, 1986, and 1987. Structural data were processed through KALKANI-UON FRESE software on the IBM main frame system at the University of Idaho. Petrologic calculations and plots were compiled from geochemical data using PETCAL3 (Bingler and others, 1976) and GPP GEOCHEMICAL (Geist and others, 1985) software on an IBM PC. The software packages HISTO and ISOPOLY by Geostat Systems International of Golden, Colorado were used on an IBM AT to process trace element geochemical data.

Major oxide analyses, trace element geochemical analyses, radiometric age determinations, and permeability and porosity analyses were all contracted to commercial laboratories.

Previous Geologic Investigations

The earliest recorded observations of Wenatchee area geology were made by a Pacific railway exploration party led by Gibbs. The party passed through the vicinity of the present city of Wenatchee and observed the interstratification of lava and conglomerate near the mouth of the Pisquouse (Wenatchee) river (Gibbs, 1855, as reported by Chappell,

1936). Russell (1900) collected information on, and named the Swauk Formation near Wenatchee during a reconnaissance of the North Cascade Mountains for the U. S. Geological Survey. Willis (1903) analyzed deformation features of rocks along the Columbia River between the Wenatchee and Methow valleys. Smith and Calkins (1904), enroute to the 49th parallel for a reconnaissance of the Cascade Mountains along the international border, made the first observations in the present study area. They reported rhyolite and andesite at the mouth of Dry Gulch and included petrographic descriptions of both rock types in their final report.

Research by Waters (1930), Chappell (1936), and Page (1939) produced the first detailed description of the geology of central Washington; their works have provided the basis for many later studies. Recent publications on the general geology of central Washington include Gresens (1983), Gresens and others (1977), Tabor and others (1982), and Laravie (1976).

Coombs (1950, 1952) described in detail the rhyodacite of the Wenatchee dome, and Bayley (1965) investigated the andesitic rocks in the vicinity of Horse Lake Mountain (Figure 1).

The structural geology of central Washington in general and the Chiwaukum graben in particular has been discussed by Willis (1958), Gresens (1976b, 1980, 1982a, 1982b), Johnson (1983), and Evans (1987). Silling (1979) conducted a gravity survey of the northern portion of the graben to determine graben depth.

Sedimentary rocks infilling the Chiwaukum graben are discussed by Gresens (1976a), Gresens and others (1981), Whetten (1976), Buza (1977), and McClincey (1986).

The general geology of the L-D mine is discussed by Lovitt and McDowall (1954), Lovitt and Skerl (1958), Patton (1967), and Patton and Cheney (1971). Moody (1958) and Guilbert (1963) describe the ore mineralogy of the L-D mine. Ott and others (1986) discuss the geology of the "B" North ore body, and Margolis (1987) investigated the mineralization trend southeast of the L-D mine.

Exploration and Production History

In 1885 a prospector named V. Carkeek staked the Gold King and McBeth claims on the prominent ridge of iron-stained and silicified sandstone now known as the "D" reef (Figure 2). Very little work was done on the property until 1894, one year after the Great Northern Railway began serving the newly chartered City of Wenatchee. In 1894, the Golden King Mining Company erected a five stamp mill and began driving drifts into the base of the "D" reef outcrop. Mining and milling were conducted intermittently by the Golden King Mining Company and later by the Wenatchee Mining Company until the project was abandoned in 1911. Two factors are cited as reasons for failure of the project: (1) mining efforts were directed at bulk production rather than selective removal of higher grade vein material, and (2) the milling operation failed to sufficiently liberate gold for amalgamation (Anon.,

1938a, Lovitt and McDowall, 1954). Chappell (1936) reports that 170 tons of ore were milled in 1910 from which $722.68 worth of gold and silver were recovered. Unfortunately, there are no recorded production figures for these early mining efforts in the Wenatchee district.

From 1911 to 1928 the Gold King and McBeth claims were essentially dormant. In 1928, J. J. Keegan of Wenatchee purchased the claims. In addition to his own attempts to work the claims, Keegan made several attempts to interest large mining companies in the property from 1928 to 1949. In 1938, Keegan arranged a contract to sell 100 to 300 tons per day of ore to the American Smelting and Refining Company smelter in Tacoma, Washington (Anon., 1938b). In 1940, the Keegan Mining and Development Company announced plans to construct a 1000 ton-per-day ore treatment facility in Quincy, Washington. There is no record of total tonnage or grade of ore shipped by Keegan, but the operation was apparently not profitable and the Quincy mill was never constructed.

Various mining companies evaluated the claims between 1934 and 1949, the most thorough evaluation during this period was made by the Knob Hill Mining Company from 1943 to 1945. Knob Hill considered the prospect nonprofitable as a large-tonnage, low-grade deposit.

In June, 1949, the property was examined by E. H. Lovitt of the Lovitt Mining Company (LMC). LMC examined the prospect as one which could be selectively mined on a smaller tonnage basis and was able to profitably mine the deposit almost

immediately (Anon., 1953a). Lovitt produced about 410,000 oz of gold between 1949 and 1967 (Table 1). The drop in production during 1952 (Table 1) occurred when the Anaconda Copper Mining Company took a $1,000,000 option on the property (Anon., 1953b). The focus of Anaconda was on development and exploration rather than production. Anaconda relinquished its option in 1953 (Anon., 1953b).

From 1949 to 1962 LMC shipped ore directly to the Tacoma smelter, and received a substantial credit for the high silica content, in addition to the gold and silver payments. In late 1961, LMC and Day Mines, Inc. of Wallace, Idaho entered into a joint venture agreement, forming L-D Mines, Inc. (Anon., 1962a). L-D mines began construction of a 300 ton-per-day flotation mill in late 1961 and began milling ore by July of 1962 (Anon., 1962b). From 1962 to 1967, the bulk of the shipments to Tacoma were concentrate rather than ore.

By 1965, L-D Mines had stepped up exploration efforts in the area in anticipation of the eventual depletion of "D" reef reserves. A $133,260 exploration project was undertaken at the "B" reef of which $66,630 (50%) was obtained as an Office of Minerals Exploration loan (Anon., 1965). This late exploration effort proved unsuccessful, and in March of 1967 Henry L. Day, president of Day Mines, Inc., announced the closure of the L-D Mine (Anon., 1967).

In the mid-1970's, Cyprus Mines Corporation assembled a large land package in the area and explored the "D" reef and the "B" reef,and discovered the "B" West ore body.

Table 1. L-D mine production, 1949 - 1967, in ounces per short ton. Compiled from Lovitt Mining Company records.

Year	Tons to Smelter	Grade Au	Grade Ag	Tons Milled	Grade Au	Grade Ag	Total Tons For Year	Grade Au	Grade Ag
1949	9,351	0.557	0.53	---	---	--	9,351	0.557	0.53
1950	43,417	0.744	0.66	---	---	--	43,417	0.744	0.66
1951	52,704	0.490	0.63	---	---	--	52,704	0.490	0.63
1952	38,850	0.385	0.49	---	---	--	38,850	0.385	0.49
1953	57,689	0.422	0.59	---	---	--	57,689	0.422	0.59
1954	52,747	0.419	0.52	---	---	--	52,747	0.419	0.52
1955	60,756	0.407	0.41	---	---	--	60,756	0.407	0.41
1956	61,602	0.398	0.45	---	---	--	61,602	0.398	0.45
1957	68,909	0.368	0.42	---	---	--	68,909	0.368	0.42
1958	62,972	0.351	0.44	---	---	--	62,972	0.351	0.44
1959	31,810	0.961	1.73	---	---	--	31,810	0.961	1.73
1960	40,339	0.859	1.76	---	---	--	40,339	0.859	1.76
1961	40,752	0.584	1.14	---	---	--	40,752	0.584	1.14
1962	3,622	0.348	0.71	40,554	0.393	0.34	44,176	0.389	0.37
1963	5,867	0.155	0.27	82,861	0.290	0.30	88,728	0.281	0.30
1964	6,229	0.266	0.74	88,034	0.193	0.61	94,263	0.198	0.62
1965	2,344	0.101	0.25	85,716	0.226	0.59	88,060	0.223	0.58
1966	1,512	0.230	0.38	90,984	0.190	0.46	92,496	0.191	0.46
1967	---	---	--	6,951	0.227	0.25	6,951	0.227	0.25

Total short tons, 1949 - 1967: 1,036,572 (932,915 mt)

Total ounces: Au- 410,482 (12,767 kg) Ag- 625,849 (19,454 kg)

Average Grade: Au- 0.396 oz/ton (13.85 g/mt) Ag- 0.60 oz/ton (20.73 g/mt)

Silver to Gold Ratio: 1.525:1

Became the L-D mine on December 1, 1961

In 1981, Goldbelt Mines, Inc. entered a joint venture agreement with Asamera Minerals, Inc. to explore the "B" and "B" West ore bodies under a lease agreement with Cyprus. Goldbelt required financing to maintain its position in the joint venture through mid-1982. Financing was provided by Breakwater Resources, Ltd. which gained control of Goldbelt. By the fall of 1982, Breakwater was a full partner (49%) with Asamera in the project. In early 1983, the "B" North ore was identified (Figure 3), and, by late 1984, Asamera and Breakwater had delineated of 5.2 million short tons (4.7 mt) of geologic reserves averaging 0.214 oz/ton (7.4 g/mt) gold and 0.40 oz/ton (13.8 g/mt) silver in the "B" North, "B" West, and "B" ore bodies through surface and underground drilling. During this time, a 2000 ton-per-day (1800 mt/day) flotation mill was constructed, and by mid-1985 the Cannon mine was in full production. Initial production at the Cannon mine concentrated on the larger tonnage "B" North ore body. During late 1986 and early 1987, mine-site exploration efforts identified substantial zones of ore-grade rock north of the "B" North ore body and below the "B" reef. In keeping with traditional designations for mineralized rock in the district, these ore bodies have been designated as the "B-4" and "B-Neath" ore bodies, respectively (Figure 3).

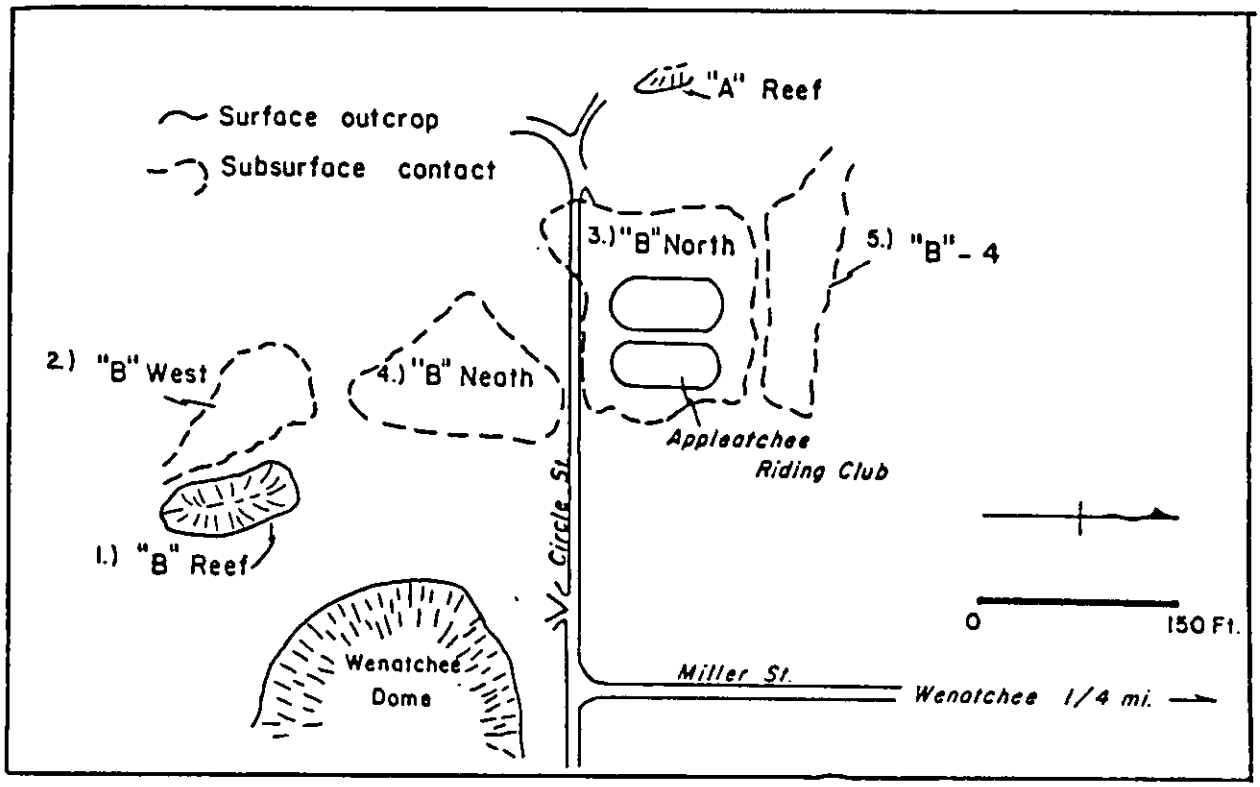

Figure 3. Generalized composite plan view of the "B" reef complex showing the location of ore zones, projected to the surface, and numbered in order of their discovery.

REGIONAL GEOLOGY

The Wenatchee district is situated within the northwest-trending Chiwaukum graben, a structure that dominates the geology of central Washington (Figure 4). The Chiwaukum graben is bounded on the east by the Entiat fault and on the west by the Leavenworth fault zone. North and east of the Entiat fault, metamorphic rocks of uncertain age named the Swakane Gneiss by Waters (1930) are exposed. The Swakane Gneiss is also exposed within the graben north of Cashmere along a structural trend parallel to the Entiat fault named the Eagle Creek anticline (Figure 4). West of the Leavenworth fault zone, pre-Tertiary crystalline rocks of the Mount Stuart batholith and the Ingalls tectonic complex are exposed. The southern portion of the Chiwaukum graben is overlain by Miocene-aged Columbia River Basalt.

Tertiary Sedimentary Rocks

Early Eocene sedimentary rocks of the Swauk Formation are exposed southeast of the Leavenworth fault zone (Figure 4). The Swauk Formation consists mainly of lithic to feldspathic sandstone and pebble conglomerate, inferred to have been deposited in a fluvial environment (Gresens, 1983, p. 5). Lacustrine deposition of portions of the Swauk Formation is evidenced by a shaly facies that consists of evenly bedded alternating shale and sandstone (Gresens, 1983, p. 5). The Swauk is at least 2.3 km thick at the type locality along

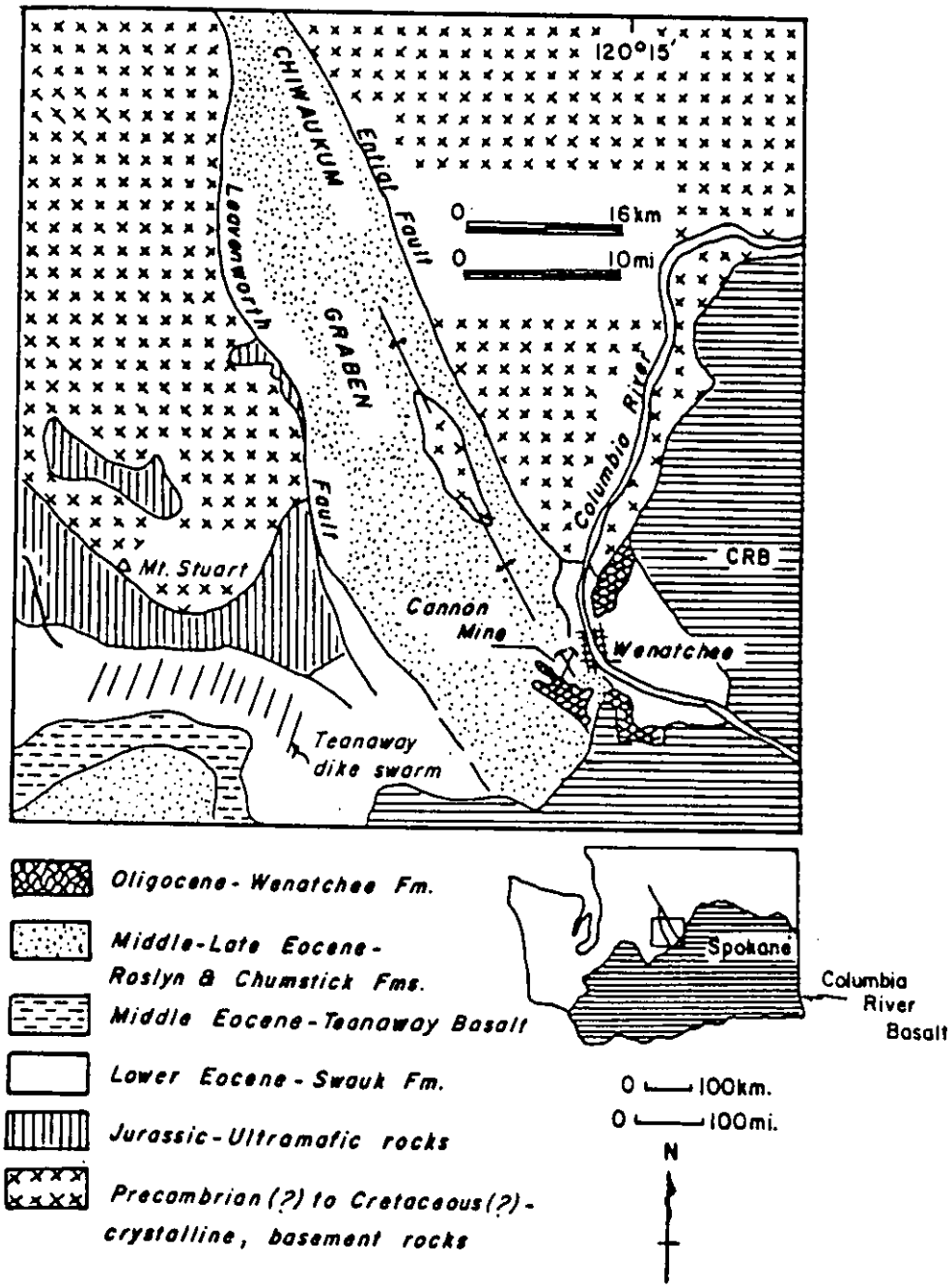

Figure 4. Regional geology of central Washington (modified from Gresens, 1983, Figure 2).

Swauk Creek in the Mount Stuart 15 minute quadrangle. Volcanic rocks interbedded with the top of the Swauk Formtaion give a K-Ar date of 51 m.y. (Gresens, 1982a).

Unconformably overlying the Swauk Formation southeast of the Leavenworth fault zone are volcanic rocks belonging to the the Teanaway Formation. The Teanaway Formation consists of basaltic, andesitic, and rhyolitic tuff, breccia, and flows, in addition to minor feldspathic sedimentary rocks. Whole rock K-Ar determinations indicate that the Teanaway Formation was deposited about 47 m.y. (Tabor and others, 1984, Table 1).

The Roslyn Formation conformably overlies the Teanaway Formation southeast of the Leavenworth zone. The Roslyn Formation is a thick-bedded arkose with interbedded coal and conglomerate beds, and is estimated to be about 2.6 km thick (Walker, 1980). Paleontological evidence indicates that the Roslyn is middle to late Eocene age (Tabor and others, 1984).

The Chiwaukum graben is infilled by Eocene sedimentary rocks of the Chumstick Formation. The Chumstick consists of a lower member of arkose, conglomerate, shale and local thin tuff beds and an upper siltstone member. Chumstick sediments were deposited between 46 and 42 m.y., based on radiometric dates from tuff beds within the formation, and are correlative to the Roslyn Formation (Gresens, 1983). Chumstick rocks are estimated to be between 6.0 and 6.7 km thick (Gresens, 1983).

The Chumstick Formation is unconformably overlain by the Oligocene-aged Wenatchee Formation. The Wenatchee Formation, as originally described by Gresens and others (1981) is about

255 m thick and consists of a lower sandstone and shale member and an upper conglomerate member.

Tertiary Igneous Rocks

Two distinct Tertiary igneous episodes are important regionally. During middle Eocene time, volcanic and hypabyssal intrusive rocks were emplaced southwest of the Chiwaukum graben to make up the greater part of the Teanaway Formation. These rocks range in composition from basalt to rhyolite. At the same time, and continuing into late Eocene time, andesitic, dacitic, and rhyolitic volcanic and hypabyssal rocks were emplaced within the Chiwaukum graben, in and near the present-day Wenatchee district. These middle to late Eocene rocks are part of the Challis magmatic arc, that extends from southern British Columbia into southern Idaho (Armstrong, 1978, p. 271).

The second igneous event occurred during Miocene time when hypabyssal andesite intrusions were emplaced throughout the southern Chiwaukum graben. These rocks are best exposed in the vicinity of Horse Lake Mountain (Figure 1) where they form a large stock and sill complex (Bayley, 1965).

Structural Geology

Regional Cenozoic structural events pre-dating the formation of the Chiwaukum graben include folding of the Swauk Formation about east to east-northeast-trending hinges prior

to Teanaway deposition (Gresens, 1982a, p. 220) and regional northwest-southeast extension represented by emplacement of the Teanaway dikes and flows (Foster,1958).

The Chiwaukum graben began forming in middle Eocene time. Using radiometric dates on tuff beds within the Chumstick Formation, Gresens (1982b) determined that the main period of graben faulting was between 46 and 40 m.y. Evans (1987) in a complex graben formation scenario, determined that initial graben formation began as early as 48 m.y. Various authors (Evans, 1987, Gresens, 1982a, 1982b, 1983, Johnson, 1983) cite several lines of evidence for graben formation by right-lateral, transtensile movement (combined translation and extension, see Harland, 1971) on the Entiat and Leavenworth faults. These lines of evidence include: 1) the dissimilarity of lithologies and structural domains on either side of the graben, 2) the linearity of the Entiat fault in contrast with the irregular strike of the Leavenworth fault zone (Figure 5), and 3) evidence of syndepositional deformation of the Chumstick Formation.

Gresens(1982b) has proposed that the graben may have formed as a result of right-lateral movement across a deflection in the strike of the proto-Entiat/Leavenworth fault (Figure 5). This concept has been further advanced by Johnson (1983) and Evans (1987). However, intragraben structures, principally the Eagle Creek anticline, indicate that the graben is more complex than many transtensile strike-slip basins as described by Reading (1980), Rodgers (1980), and

Mann and others (1983). The Eagle Creek structure (Figure 4) appears to be an intragraben horst whose long axis is parallel to the Entiat fault (Gresens, 1983, Silling, 1979). In a simple strike-slip basin, such a structure would theoretically develop oblique to, rather than parallel to, the basin boundary or master faults (Reading, 1980). Thus, although there is ample evidence for graben formation by a regionally compressive stress regime, the exact mechanics of graben development remain poorly defined.

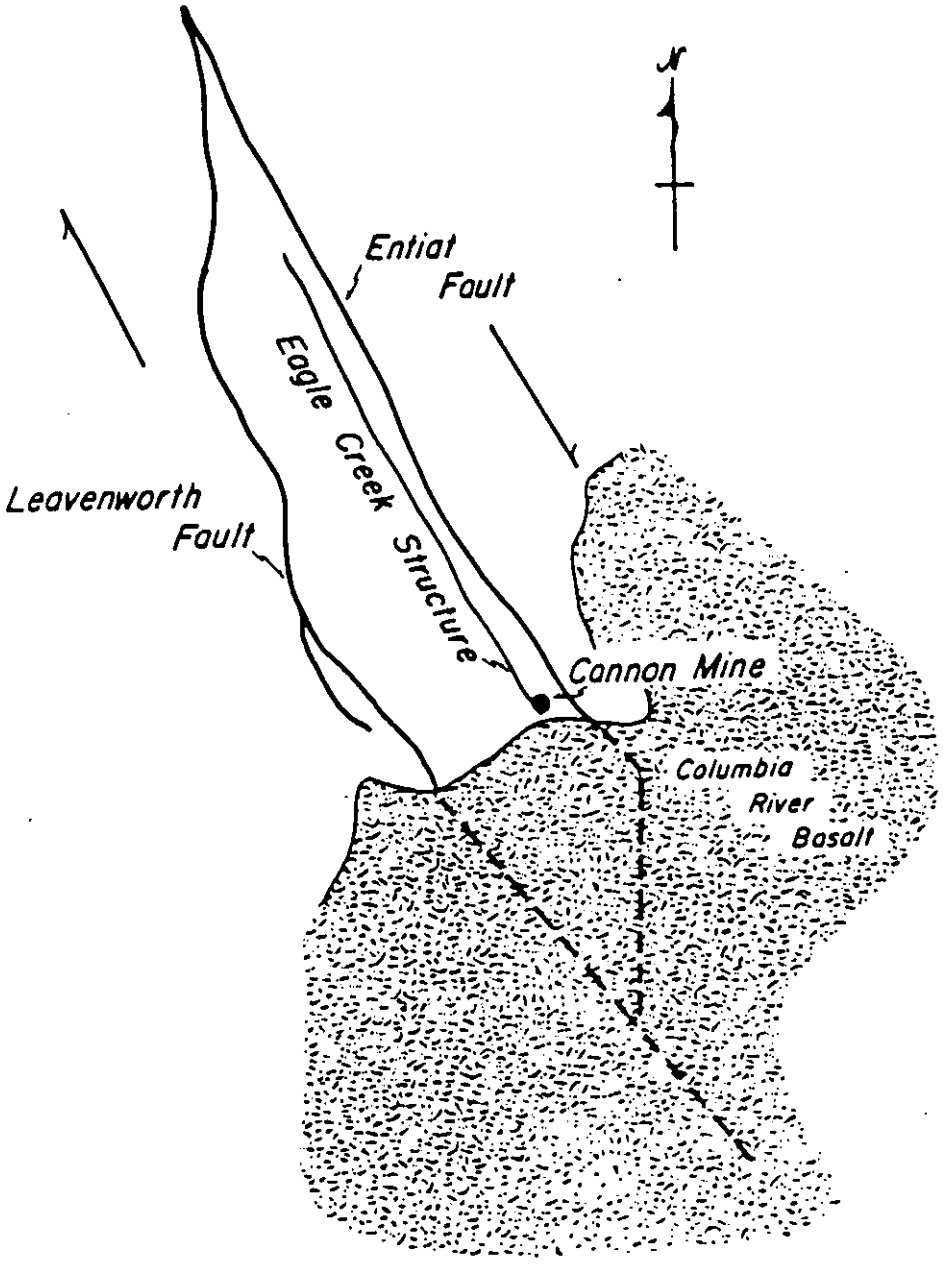

Figure 5. Schematic diagram of graben formation by dextral strike-slip movement on the Entiat and Leavenworth faults (modified from Gresens, 1983, Figure 7).

DISTRICT GEOLOGY

The Wenatchee district is located in the southeast part of the Chiwaukum graben in a structurally complex sequence of Eocene and Oligocene non-marine sedimentary rocks and Eocene hypabyssal intrusions and volcanic rocks. The district-wide structural trend of both igneous and sedimentary rocks is N20° - 40°W and steeply dipping, parallel to the structural grain of the graben. Plates 1 and 2 show the relationship of rocks in the district and the reader is encouraged to have these maps in hand while reading this section.

Sedimentary Rocks

Most of the rocks in the Wenatchee district are Eocene-aged continental sedimentary rocks. These rocks are generally poorly exposed on the surface owing to their low resistance to weathering. Consequently, most of the information collected for this report has come from underground workings and drill core. Three distinct sedimentary packages are exposed in the Wenatchee area. The oldest sedimentary rocks, of uncertain age, are exposed in the central portion of the district as a northwest-trending belt of complexly deformed feldspathic sandstones, siltstones, claystones, and local conglomerate beds. These rocks host all known mineralization and alteration north of Squilchuck Canyon (Plate 1). East of this complexly deformed belt of older rocks is a distinctive package of conglomerates overlain by feldspathic sandstone and

siltstone. Sedimentary rocks in this eastern package belong to the middle Eocene Chumstick Formation and are generally less deformed than the rocks in the central portion of the district. The third distinct sedimentary package is the Oligocene-aged Wenatchee Formation which unconformably overlies the western flank of the complexly deformed central package.

Sedimentary rocks of uncertain age

There is disagreement regarding the age and correlation of the principal ore host in the Wenatchee district. Gresens (1975, 1983, Plate 1) interpreted these rocks to represent the erosionally breached core of the Eagle Creek anticline (Figure 4) and tentatively mapped the central package of sedimentary rocks in the district as the lower Eocene Swauk Formation. Gresens (1983, p. 15) described rocks in the central part of the district as light- to dark-gray, well-lithified, evenly bedded arkose, in 0.5 to 2 meter-thick beds, with 15 to 25 centimeter-thick shale and siltstone interbeds. In contrast, the Chumstick Formation consists of tan to light-gray, poorly indurated arkose in 5 to 15 meter-thick beds that commonly contain large-scale fluvial cross-beds, and occasionally contain cut and fill structures and rip up clasts of shale (Gresens, 1983, Table 1). Gresens (1983, Table 1) also recognized a structural discordance between rocks that he mapped as Swauk(?) and the Chumstick Formation (Figure 6), but the contact between the two sedimentary sequences is not

exposed. Tabor and others (1982, p. 10) were unable to distinguish significant differences between the Chumstick Formation and the belt of rocks mapped by Gresens as the Swauk; they mapped both the complexly deformed central portion of the district and the eastern package of sedimentary rocks as the Chumstick Formation.

The ore-hosting sediments consist of feldspathic sandstone, siltstone, and claystone, with local pebble conglomerate beds and epiclastic tuffs and breccias. Plagioclase, K-feldspar, quartz, and biotite are the most common grains in the feldspathic sandstone beds. Lithic fragments, chlorite, muscovite, and epidote make up most of the minor clast content. Leaf fragments and other carbonaceous material are common and become increasingly abundant in finer-grained sediments. There is very little compositional variation between individual sandstone intervals. Clastic grains are angular to subangular and poorly sorted. Unaltered feldspathic sandstones near the "B" reef complex have an average porosity of 13.65%, which is average for most Phanerozoic sandstones (Pettijohn and others, 1972, p. 94).

The rocks are generally evenly bedded where exposed in the "B" reef complex. Siltstone and claystone beds are commonly 0.5 to 15 cm thick, and sandstone beds rarely exceed 2 meters in thickness. Cross-bedding is not common in thicker feldspathic sandstone intervals but is characteristic of thin siltstone and silty sandstone beds. Flame structures, load

Figure 6. Complexly deformed Eocene-aged sedimentary rocks in the central portion of the district as exposed in the highwall excavated during preparation of the mill site at the Cannon mine. Photograph courtesy of Eric McCulloch of Asamera Minerals.

casts, rip-ups, and graded bedding are common.

At "D" reef, exposed in the underground workings of the L-D mine, the rocks contain a greater proportion of thicker feldspathic sandstone beds. Individual sandstone beds are commonly 3 to 5 meters thick; siltstone and claystone beds average about 0.5 meters thick.

Elsewhere in the central portion of the district, these older rocks are either poorly exposed or sufficiently altered by hydrothermal activity so that their original character is not evident. Drilling has identified two minor but significant lithotypes in the complexly deformed package. A distinctive clayey hematitic horizon is consistently intercepted by drill holes on the eastern margin of the package. This bed (or beds) is commonly magnetic, 25 - 30 cm thick, and consists of hematite, magnetite and unidentified clay minerals. It has been intercepted by drilling east of Wenatchee dome and exposed by trenching west of Rooster Comb (Plate 1). Red magnetic soil can be traced along the drainage east of "D" reef (Plate 1). The origin of this lithotype is uncertain. Superficially, it resembles a paleo-soil horizon, but there are no rock types in sufficient volume nearby which would weather to such a material.

South of Wenatchee Dome and west of Rooster Comb, a distinctive sequence of heterolithic epiclastic breccia has been intercepted by drilling. This interval consists of angular fragments of argillized volcanic rock, up to 5 cm in diameter, and smaller fragments of black chert, in a matrix of

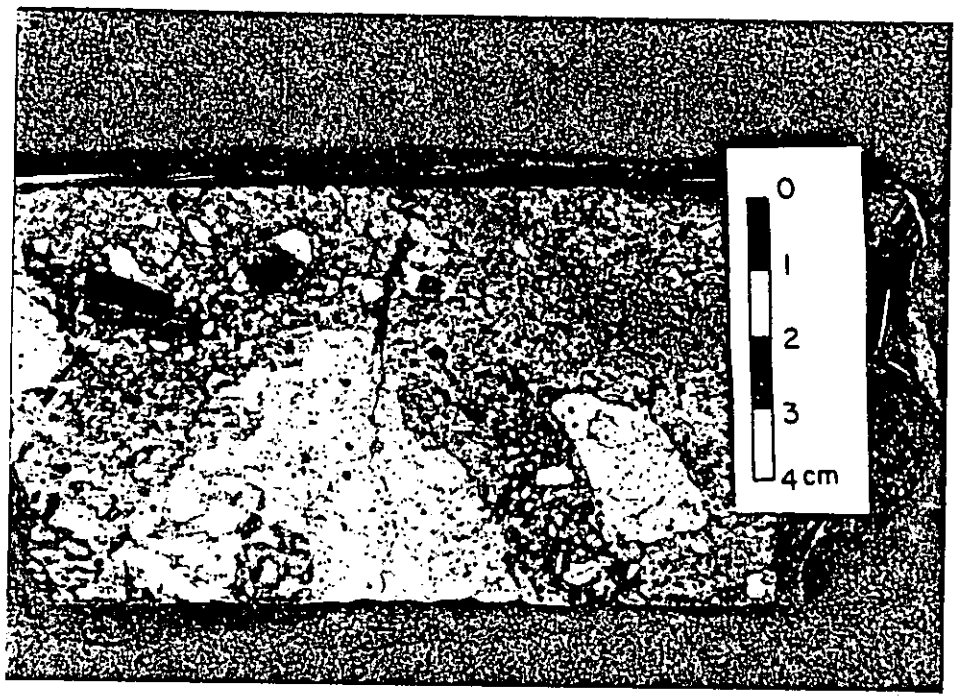

Figure 7. Heterolithic epiclastic breccia west of Rooster Comb. Drill Hole ASH-70A, 602 ft. down hole.

green to greenish-gray volcanic sand (Figure 7). These breccias occur repetitively as stratiform lenses averaging 10 cm thick, interbedded with medium to fine-grained green volcanic sandstone beds which are 15 - 25 cm thick. The overall thickness of the unit has not been determined, but is in excess of 30 meters. This unit may represent a sequence of distal, water-lain volcanic breccias. The green coloration is suggestive of zeolitic alteration; however, no x-ray diffractive work has been done to identify the mineral phase responsible for the green color.

Chumstick Formation

For district-wide correlation, the most useful sedimentary section is a sequence of conglomerate beds with interbedded feldspathic sandstone referred to as the Chumstick Formation. Conglomerate outcrop and float occurs on a small ridge east of "A" reef, east of Wenatchee dome, west of Rooster Comb, and east of the 1250 portal at "D" reef (Plate 1). Drill holes have intercepted this conglomeratic sequence at points between these surface exposures, and provide confirmation of the implied surface trend. The conglomerates are polymictic with clasts of felsic volcanic rocks, vein quartz, granitic rocks, and biotite gneiss occurring in variable amounts in individual conglomerate beds. Clast size generally increases to the south indicating a southerly source area. Overlying this northwest-dipping conglomerate package, with apparent conformity, is a repetitive sequence of thick-

bedded feldspathic sandstone with interbedded siltstone and shale. Gresens (1983, plate 1) mapped the conglomerates as the base of the Chumstick Formation, in fault contact with the complexly deformed rocks in the central portion of the district.

Of the criteria used by Gresens (1983, Table 1) to distinguish Chumstick rocks from those of the Swauk(?) Formation, only the style of bedding, and, to a certain extent, the degree of calcite veining and cement were found to be valid field criteria during this study. Bedding style in the feldspathic sandstone and siltstone overlying the conglomerate package is notably different than the bedding style of rocks exposed in the "B" reef complex workings. As noted by Gresens (1983, Table 1) individual beds in the Chumstick Formation tend to be thicker than those in the central belt of more complexly deformed rocks. There is clearly a structural discordance between the conglomerate package and overlying rocks and the belt of rocks mapped by Gresens as the Swauk(?). The belt of sedimentary rocks in the central portion of the district has been folded and faulted by at least two deformation events (see structural geology section) but the Chumstick Formation, as exposed east of Wenatchee Dome and Rooster Comb, shows evidence of only one deformation event.

Radiometric age determinations by Ott and others (1986, Table 2) indicate that andesitic igneous rocks intruding the central belt of ore hosting sedimentary rocks are about 51

m.y. old. This date would require the sediments into which these rocks intruded to pre-date the earliest stages of graben formation determined by Gresens (1983) and Evans (1987), and would support Gresens' choice of the Swauk Formation. Margolis (1987) correctly points out that the relatively broad error limits on the date published by Ott and others would permit the ore hosting rocks to have beeen very early graben-fill sediments. Subsequent radiometric age determinations indicate that the 51 m.y. age may be anomalously old (see section on igneous rocks). However, this date, when combined with differences in bedding style and tectonic history, presents a strong argument that the ore-hosting sedimentary rocks may be older than the Chumstick Formation. Also, the belt of altered and mineralized sedimentary rocks which constitute the Wenatchee district is directly on trend with the Eagle Creek anticline (Figure 4) a known structural high within the Chiwaukum graben, where the presence of pre-graben rocks would be most likely to be expected.

Wenatchee Formation

West of "D" reef, "C" reef and Saddle Rock, ore-hosting sedimentary rocks are overlain by the Oligocene-aged Wenatchee Formation (Plate 1). The Wenatchee Formation consists of non-marine sediments and has been fully described by Gresens (1976a).

Igneous Rocks

Three compositional varieties of Eocene igneous rocks occur in the Wenatchee district, two of which are spatially related to gold mineralization. Biotite rhyodacite porphyry associated with perlite is present along the eastern margin of the known mineralization trend. Hornblende andesite porphyry occurs along the general western margin of mineralization, although hydrothermal alteration and weak gold mineralization are present west of the andesite in the northern part of the district (Plate 1). Amygdaloidal basalt has been intercepted by drilling at various locations in the district and is exposed on the northern side of Dry Gulch at the base of Saddle Rock (Plate 1). The relation of this basalt to mineralization or other intrusions in the district is poorly understood. Extensive outcrops of the Oligocene-aged Horse Lake Mountain hornblende andesite dike and sill complex (Bayley, 1965) are located a few hundred meters northwest of the present study area, but are exposed only in minor amounts in the Wenatchee district (Plate 1).

Major oxide and normative mineral contents of rhyodacite, perlite, and andesite are shown in Table 2. Ternary diagrams in Figure 8 show Na_2O - K_2O - CaO content and normative orthoclase - quartz - plagioclase content of these rock types. Amygdaloidal basalt samples obtained during this investigation were too altered to provide meaningful chemical analysis.

Amygdaloidal basalt

Amygdaloidal basalt has been encountered by drilling approximately 150 meters east of Wenatchee dome, and about 200 meters west of Rooster Comb (Plate 2). It also occurs in surface exposure south of Rooster Comb. In hand specimen, the rock is very dark green, strongly magnetic, and commonly amygdaloidal. Amygdules are filled with calcite. In thin section, the rock contains phenocrysts up to 1.5 mm in diameter which have the shape of olivine crystals, but which are completely altered to calcite. The groundmass consists of plagioclase partially altered to brown smectitic clays and glass in approximately equal proportions (Fischer, 1986).

Chappell (1936, p. 123) identified the central portion of Saddle Rock as hypersthene basalt porphyry. Although the exact location of samples collected by Chappell to make this determination is not certain, a strongly magnetic outcrop of basalt, easily distinguished from the typical flow-banded andesite that makes up the greater part of Saddle Rock, is present at the base of Saddle Rock in Dry Gulch. This rock type has also been encountered in considerable volume by drilling in the vicinity of Saddle Rock and appears to partially underlie the main mass of andesite. In drill core, the basalt is commonly amygdaloidal, similar in appearance to the basalt encountered east of Wenatchee Dome.

The relationship of the basalt to other intrusive rocks in the district is not well understood. The greatest volume of basalt appears to be spatially and genetically related to

Table 2. Major oxide and normative mineral content of hypabyssal intrusive rocks in the Wenatchee district.

Rock Type*	HA	HA	RD	RD	RD	RD	RD	P	P
Oxide Percentages (Normalized):									
SiO_2	65.81	66.58	70.27	70.19	71.47	75.71	74.47	71.87	69.36
Al_2O_3	16.22	15.54	14.65	16.14	14.60	11.95	12.66	16.10	19.02
Fe_2O_3	1.46	1.36	1.12	1.15	0.87	0.91	1.01	1.26	1.25
FeO	3.27	1.59	0.01	0.01	0.01	0.01	0.01	1.42	1.42
MgO	3.44	2.34	0.17	0.50	0.28	0.34	0.26	2.04	2.24
CaO	3.57	3.21	0.79	1.44	1.03	0.81	0.89	2.33	2.35
Na_2O	3.83	7.45	7.49	7.58	9.29	5.61	6.42	4.38	4.12
K_2O	1.96	1.53	5.35	2.87	2.33	4.52	4.16	0.42	0.07
TiO_2	0.31	0.30	0.06	0.04	0.03	0.10	0.10	0.12	0.05
P_2O_5	0.07	0.05	0.06	0.05	0.07	0.01	0.01	0.01	0.08
MnO	0.07	0.05	0.03	0.04	0.03	0.02	0.02	0.04	0.04
Normative Mineral Percentages:									
Q	38.49	33.17	32.28	37.29	36.83	45.85	43.14	50.71	48.68
C	6.42	0.55	0.73	5.28	2.08	0.39	0.59	11.46	17.43
Or	9.77	7.75	26.50	13.87	11.48	22.10	20.37	1.99	0.31
Ab	17.95	35.47	34.96	34.55	43.24	25.86	29.68	19.32	17.72
An	17.19	15.82	3.46	6.59	4.53	3.91	4.30	10.86	10.08
Hy	6.12	3.41	0.20	0.57	0.33	0.40	0.31	2.88	3.07
Il	0.85	0.82	0.11	0.10	0.08	0.08	0.06	0.31	0.12
Ap	0.19	0.14	0.16	0.13	0.18	0.02	0.02	0.02	0.21
Mt	3.02	2.86	----	0.05	0.05	----	----	2.46	2.39
Hm	----	----	1.59	1.56	1.20	1.28	1.43	----	----
Ru	----	----	0.02	----	----	0.10	0.11	----	----

* HA - Saddle Rock Andesite, RD - Biotite Rhyodacite Porphyry from Wenatchee Dome, P - Perlite from Wenatchee Dome.

Note- Initial analyses reported total iron as Fe_2O_3. The percentages of FeO and Fe_2O_3 shown above were calculated from the total iron as Fe_2O_3 as specified by Irving and Baragar (1971, p. 525). Analyses by Chemex Labs, Ltd., North Vancouver, British Columbia.

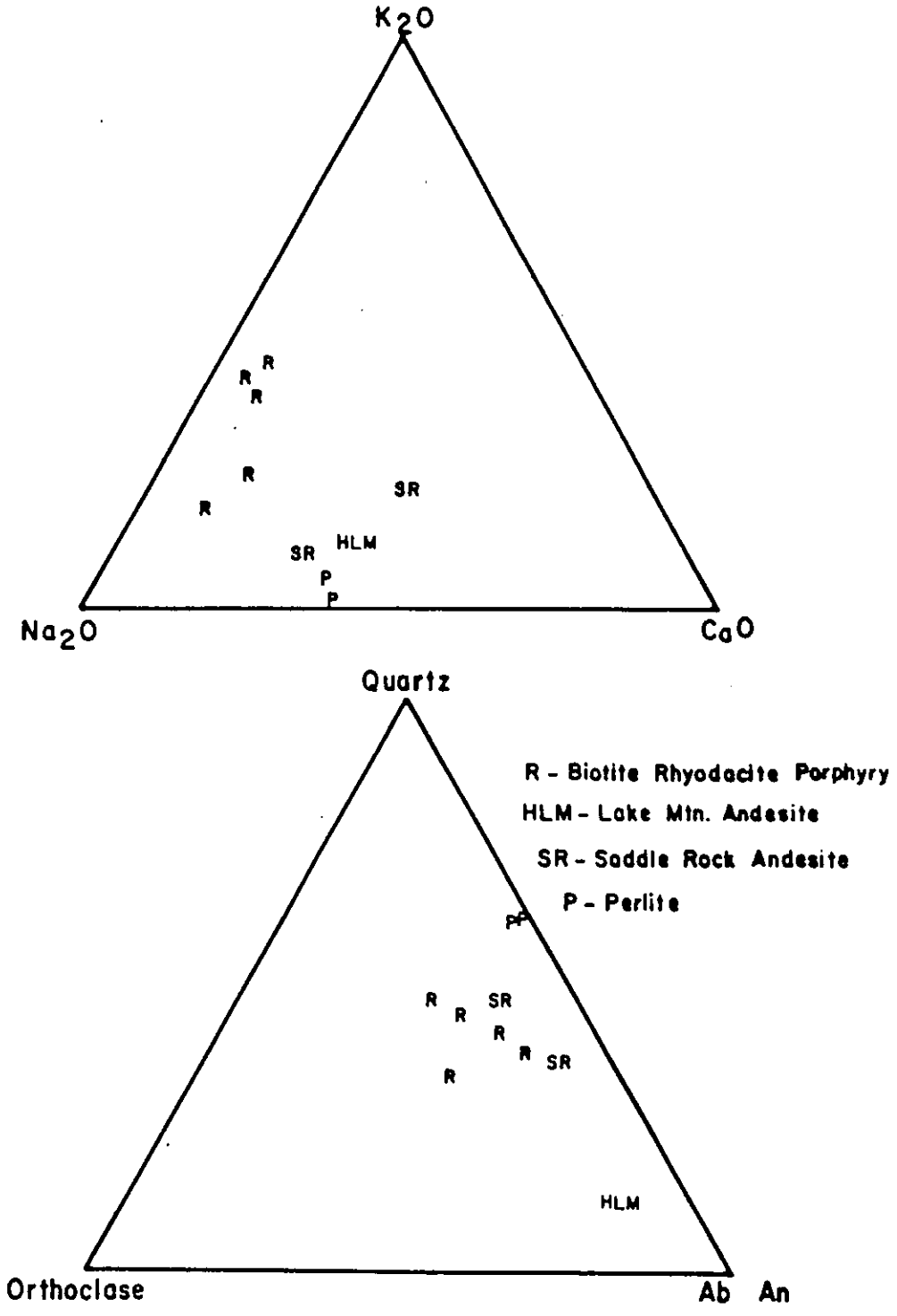

Figure 8. Ternary diagrams showing Na_2O - K_2O - CaO content, and normative quartz - orthoclase - plagioclase in hypabyssal intrusive rocks in the Wenatchee district.

the andesite of Saddle Rock. However, occurrences of basalt east of Wenatchee dome and west and south of Rooster Comb suggests that the rock may represent a separate intrusive event.

Saddle Rock andesite

Hornblende andesite porphyry forms conspicuous outcrops at Old Butte, Saddle Rock, and west of "C" reef (Figure 9). This andesite, herein referred to as the Saddle Rock andesite, has been traced below the surface by drilling, and is present along the general western boundary of the "B" reef (Plates 1 and 2).

The andesite is green to greenish-gray, and consists of hornblende and biotite phenocrysts, 1-4 mm in width, with fine-grained plagioclase in a glassy groundmass. Gresens (1983, p. 40) noted that samples of the Saddle Rock andesite appeared to contain quartz phenocrysts by hand lens examination, but that petrographic examination of the samples revealed these phenocrysts to be untwinned or poorly twinned plagioclase.

At Old Butte, Saddle Rock, and the exposure west of "C" reef, the andesite displays a well developed flow layering, particularly on the west side of these outcrops (Figure 9). Gresens (1983, p. 38) noted that the outcrop pattern of the hornblende andesite forms a continuous northwest-trending belt with a pinch and swell structure. Mapping of the flow layering shows that it conforms to this pinch and swell

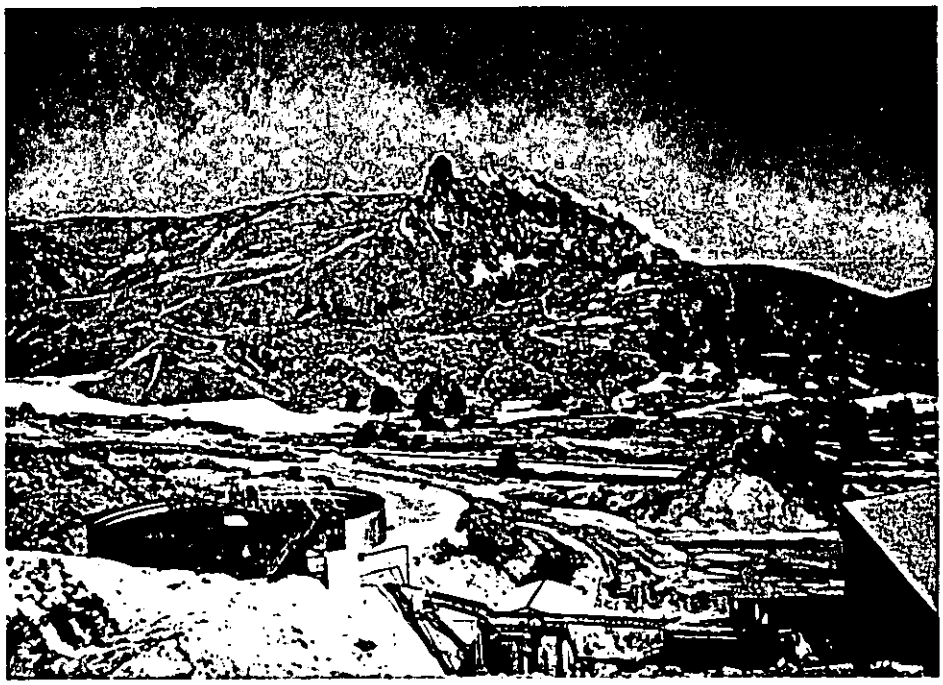

Figure 9. View of the Saddle Rock andesite, looking northwest from Wenatchee Dome. "B" reef is in the foreground, "A" reef is in the middle distance as the bleached rock on the old mine dump.

outcrop pattern, but that, without drill hole information, individual outcrops cannot be confidently inferred as belonging to the same intrusive body. Two examples are flow layering at the southeast extensions of the Old Butte exposure and the Saddle Rock exposure. In both these instances, the strike of flow layering swings abruptly from the dominant northwest trend, through east-west, to a northeast trend. The andesite contact between Old Butte and Saddle Rock is concealed by a landslide deposit, and between Saddle Rock and the exposure west of "C" reef, the contact is concealed by alluvial deposits in Dry Gulch (Plate 1). The flow layering pattern, however, suggests the possibility that each of the andesite exposures may be separate entities, similar to the rhyodacite at Wenatchee Dome and Rooster Comb.

At Saddle Rock and the exposure west of "C" reef, drill hole information indicates that the eastern margin of the andesite dips 40° to 70° to the east. West of Saddle Rock, the andesite contact dips 70° to 85° to the east, and locally is vertical.

Chappell (1936, p. 139) interpreted the Saddle Rock andesite to be a dike that was emplaced in the axial region of a large anticline. However, many aspects of the andesite are indicative of extrusive emplacement. The eastern portion of Saddle Rock is a lithoclastic breccia that consists of angular fragments of flow-layered andesite in a matrix of dense, dark-gray silty material. A section through the Saddle Rock andesite, based a drill hole north of "A" reef that passed

through the igneous body, is shown in Figure 10. The contact between the andesite and overlying sedimentary rocks is conformable to sedimentary layering, as far as can be determined in drill core. The upper 20 meters of andesite consists of a lithoclastic breccia. At the top of the andesite, this breccia consists of angular fragments of flow banded andesite supported by a matrix of dense, dark-gray siltstone. The rims of the angular fragments are bleached, and the breccia is cut by thin hematite-chalcedony veinlets. This material grades downward into a clast-supported breccia of similar fragments and a matrix of granular, comminuted andesitic material. Underlying the breccia zone is flow banded andesite (Figure 10).

In the drill hole that completely penetrated the andesite, two intervals of the brecciated andesite - flow banded andesite sequence were penetrated. These intervals are separated by an apparently conformable sequence of sedimentary rocks (Figure 10).

Two possible origins of these features in the andesite are (1) the andesite was emplaced as a sill by multiple intrusions, with later injections disrupting partially cooled early injections, and (2) the andesite was extruded as a viscous, possibly subaqueous flow and the upper zone is a result of autobrecciation.

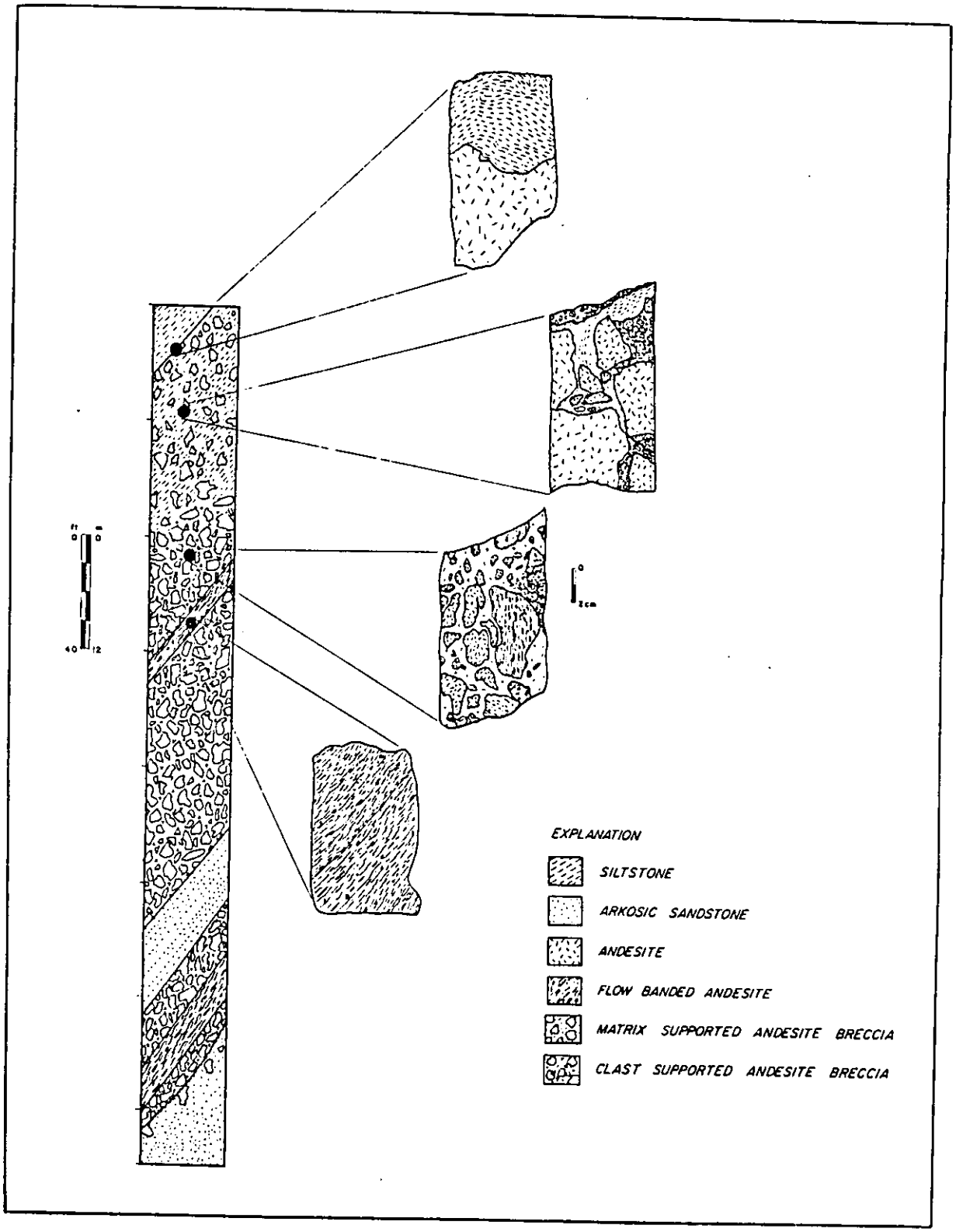

Figure 10. Section of the Saddle Rock andesite, based on DDH B87-6B.

Biotite rhyodacite porphyry

Biotite rhyodacite porphyry intrusions form a small dome-shaped geographic feature locally referred to as the Wenatchee Dome, and a prominent pinnacle shown on the Wenatchee 7.5' quadrangle as Rooster Comb (Figure 11). The Wenatchee Dome has been described in detail by Coombs (1950, 1952). Rhyodacite at Wenatchee Dome and Rooster Comb is light gray in fresh exposure, and consists of millimeter-size quartz and plagioclase phenocrysts in an aphanitic to glassy groundmass. Quartz phenocrysts make up about 15 percent of the rhyodacite; zoned plagioclase phenocrysts with sodic rims are less abundant than quartz. Biotite and green hornblende are present in small amounts (Coombs, 1952, p. 198). In places, the rocks of both Wenatchee Dome and Rooster Comb consist almost entirely of spherulites.

A border phase of perlite is associated with the rhyodacite at both Wenatchee Dome and Rooster Comb. The perlite consists of more than 90 percent glass with characteristic perlitic cracks, and less than 10 percent phenocrysts. Chappell (1936, p. 123) noted that the perlite at Wenatchee Dome is mineralogically dacite, based on phenocryst composition, but that the glassy phase is unusually high in silica for dacite as determined by the index of refraction method. Major oxide analysis (Table 2) indicates that the perlite is depleted in SiO_2 and K_2O and enriched in CaO relative to the adjacent rhyodacite; however, normative mineral calculations (Table 2 and Figure 8) do show the

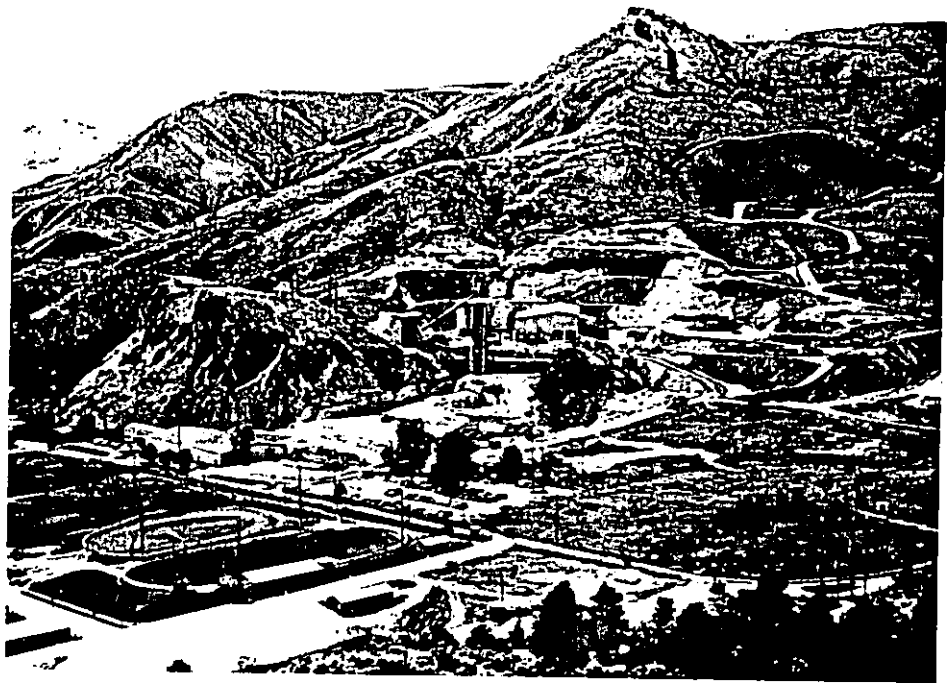

Figure 11. View of Wenatchee Dome and Rooster Comb looking southeast.

perlite to contain more quartz than the rhyodacite.

Perlite is exposed at the surface on the south and west sides of Wenatchee Dome and is present in underground workings as a shell encasing the western and northern borders of rhyodacite. Holes drilled through the rhyodacite to its eastern margin have also penetrated perlite. On the south and west sides of Wenatchee Dome, the perlite has an abrupt contact with rhyodacite (Figure 12); it is 5 to 15 meters wide on the west side of the rhyodacite, and up to 60 meters wide on the south side. On the east side of Wenatchee Dome, the contact between rhyodacite and perlite is gradational over a width of about 3 meters.

The rhyodacite at Wenatchee Dome and Rooster Comb has a pronounced flow layering due to alternating layers of aphanitic and glassy material. Flow foliation is enhanced by weathering, but is also evident in underground workings and drill core. Flow foliation is parallel to the surface form of Wenatchee Dome on the western side and on top of the body. On the eastern side of Wenatchee Dome, foliation dips about 65° to 70° to the west, parallel to the contact between the intrusion and adjacent sedimentary rocks.

Gresens (1983, p. 39) has suggested that Wenatchee Dome and Rooster Comb may have been emplaced as a single intrusion and subsequently offset by a northwest-trending dextral strike-slip fault. Gresens' interpretation was based on an apparent lack of perlite on the west side of Rooster Comb and the east side of Wenatchee Dome, and the apparent truncation

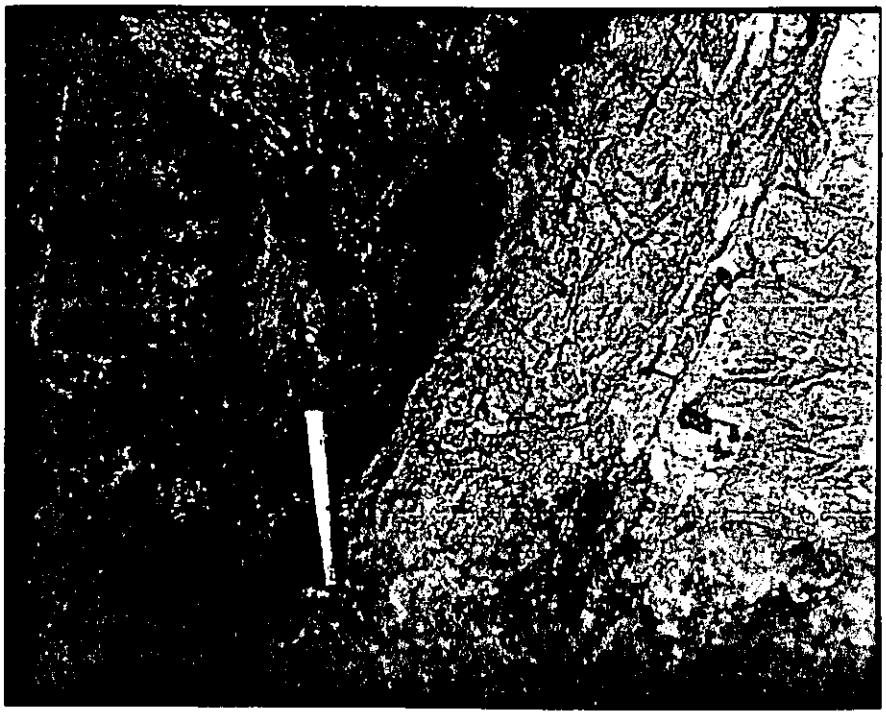

Figure 12. Contact between perlite (on the left) and rhyodacite (on the right) on the west side of Wenatchee Dome. Photographed on the 690 level access drift into the "B" North ore body. Note flow layering in the rhyodacite. Hammer is 45 cm long, view is to the north.

of flow foliation on the east side of Wenatchee Dome.

Detailed mapping, coupled with drill core information, indicates that perlite completely surrounds the Wenatchee Dome intrusion, and is present on both the east and west sides of the Rooster Comb intrusion. The apparent truncation of flow foliation on the east side of Wenatchee Dome appears to be related to intrusion morphology and erosion rather than faulting. This evidence suggests that Rooster Comb and Wenatchee Dome are, in fact, separate intrusions.

Rhyodacite at Wenatchee Dome and Rooster Comb is also locally brecciated. At Wenatchee Dome, brecciation of the rhyodacite is largely confined to flow layers and is evidently flow related. At Rooster Comb, brecciation is more extensive and consists of angular fragments of flow-layered rhyodacite in a glassy matrix.

Ore bodies of the "B" reef complex are in fault contact with the perlite at Wenatchee Dome. The width of the fault zone separating the ore bodies from intrusive rocks varies from a few centimeters up to 30 meters. Neither rhyodacite nor perlite show any visible signs of hydrothermal alteration, although the perlite is depleted in Na_2O and K_2O relative to rhyodacite (Table 2). This depletion of alkalis is probably a result of normal devitrification rather than hydrothermal alteration associated with gold-silver mineralization in the adjacent "B" reef complex.

Other occurrences of rhyodacite and perlite include flow-layered rhyodacite bordered by perlite east of Saddle Rock

(intercepted by drilling) and perlite in drill core and rhyodacite "float" east of Block 1 at "D" reef (Plates 1 and 2). Rhyodacitic intrusive and extrusive rocks have been penetrated by drilling southeast of "D" reef under the area shown in Figure 1 as Wenatchee Heights. These rocks, which are discussed by Margolis (1987), occur southeast of and along the trend of alteration and mineralization defined by exposures of silicified sedimentary rocks extending from "G" reef to "D" reef.

Andesite of the Horse Lake Mountain Complex

Oligocene-aged dikes and sills of hornblende andesite porphyry are well exposed a few hundred meters northwest of the present study area. These rocks have been described by Bayley (1965) and Gresens (1983). They are mentioned here because, prior to this study, it was uncertain whether the hornblende andesite of Saddle Rock was genetically related to the Horse Lake Mountain Complex. Gresens (1983, p. 40) in summing up the uncertain age and correlation of the "mafic rocks of the Wenatchee Pinnacles" (Saddle Rock andesite) with respect to both the Horse Lake Mountain Complex and "felsic rocks of the Wenatchee Pinnacles" (Wenatchee Dome and Rooster Comb rhyodacite) states:

> "On the one hand, the mafic rocks are most similar in composition to hornblende andesite of the Horse Lake Mountain intrusive complex prior to alteration. On the other hand, they occur in proximity to the felsic rocks with similar alignment (similar structural control), and they may contain minor amounts of dacite (that is, compositionally more akin to rhyodacite)."

Chemical analyses and radiometric age determinations obtained during this study indicate that the Saddle Rock andesite is not related to the Horse Lake Mountain Complex (see Figure 8 and the next section).

Age of emplacement

Prior to this investigation, the Saddle Rock andesite and amygdaloidal basalt had not been dated. Published radiometric dates for rhyodacite and perlite at Wenatchee dome include K-Ar ages averaging 42.3 m.y.b.p. and fission track ages for zircon averaging 49.2 m.y.b.p. (Gresens, 1983, p. 39), and an average age of 29.3 m.y.b.p. from five K-Ar determinations on hornblende from andesites of the Horse Lake Mountain Complex (Gresens, 1983, Table 3). During this investigation, one additional K-Ar date for rhyodacite intercepted by drilling east of Saddle Rock, seven K-Ar dates on the Saddle Rock andesite, and one K-Ar date on amygdaloidal basalt intercepted by drilling east of Wenatchee dome have been obtained by written communication (1987) from R. Gill of Asamera Minerals (Table 3).

Radiometric dates for the Saddle Rock andesite vary widely depending on the material tested. The oldest date, 73.6 $\pm$ 5.8 m.y.b.p., is from hornblende (Table 3). A whole rock determination of 50.9 m.y.b.p. was obtained from one sample. Five plagioclase determinations average 37.5 m.y.b.p. Disregarding the anomalously old hornblende determination, but including the whole rock determination, the average K-Ar age

Table 3. Summary of age determinations on igneous rocks in and near the Wenatchee district and adularia from the "B" North ore body.

Rock Type	Location	Material	Method	Age	Source
Rhyodacite	East of Saddle Rock, DDH G3-83 760′	Biotite	K-Ar	45.0±1.8	1
Rhyodacite	Wenatchee Dome	Biotite	K-Ar	43.2±0.4	2
Rhyodacite	Wenatchee Dome	Zircon	Fisson Track	47.0±2.7	2
Rhyodacite	Wenatchee Dome	Zircon	Fisson Track	51.4±2.8	2
Perlite	Wenatchee Dome	Biotite	K-Ar	41.4±1.6	2
Andesite	Saddle Rock DDH CC-3, 475′	Plagio-clase	K-Ar	38.5±2.5	1
Andesite	Saddle Rock DDH CC-3, 475′	Whole Rock	K-Ar	50.9±3.5	1
Andesite	Saddle Rock DDH TW-353, 645′	Plagio-clase	K-Ar	33.5±2.0	1
Andesite	Saddle Rock DDH SR-9B, 482′	Plagio-clase	K-Ar	38.1±2.4	1
Andesite	Saddle Rock DDH G2-82, 742′	Horn-blende	K-Ar	73.6±5.8	1
Andesite	Saddle Rock DDH G2-82, 742′	Plagio-clase	K-Ar	37.5±4.1	1
Andesite	"C" Reef DDH LV-3, 330′	Plagio-clase	K-Ar	40.1±2.5	1
Alkali Basalt	East of Wenatchee Dome, DDH FA-1A, 577′	Whole Rock	K-Ar	42.9±1.9	1
Andesite	Average of five samples from the Horse Lake Mountain complex	Horn-blende	K-Ar	29.0	2
Quartz-adularia vein	700 level, "B" North ore body	Adularia	K-Ar	44.2±1.9	1

Sources: 1) Asamera Minerals (US) Inc
2) Gresens, 1983, Table 3

for the Saddle Rock andesite is 39.8 m.y.b.p.

The K-Ar age of rhyodacite east of Saddle Rock, when combined with published K-Ar dates from Wenatchee dome gives an average age of emplacement for the rhyodacite of 43.3 m.y.b.p. A single whole rock age from amygdaloidal basalt east of Wenatchee dome yielded an age of 42.9±1.9 m.y.b.p.

Structural Geology

Two well-defined structural orientations are present in the Wenatchee district: A dominant, northwest structural trend that is parallel to the Chiwaukum graben, and a superimposed north-south fault set (Figure 13). In this section, structures that display continuity on a district scale will be described, but in order to fully develop the relationship between these and smaller-scale structures related to mineralization, a brief mention of mine-scale structures is included: These are fully described in the following economic geology section.

The district is located on the southeastern extension of the Eagle Creek anticline, a major northwest-trending, intragraben structure that is parallel to the Entiat fault (Figure 4). Determination of the exact timing of deformation events is hindered by the uncertain age of sedimentary rocks in the district, and this problem is exacerbated by the poorly understood deformation mechanics of graben formation. Observational data are presented here, interpretations and speculations are reserved for a later section.

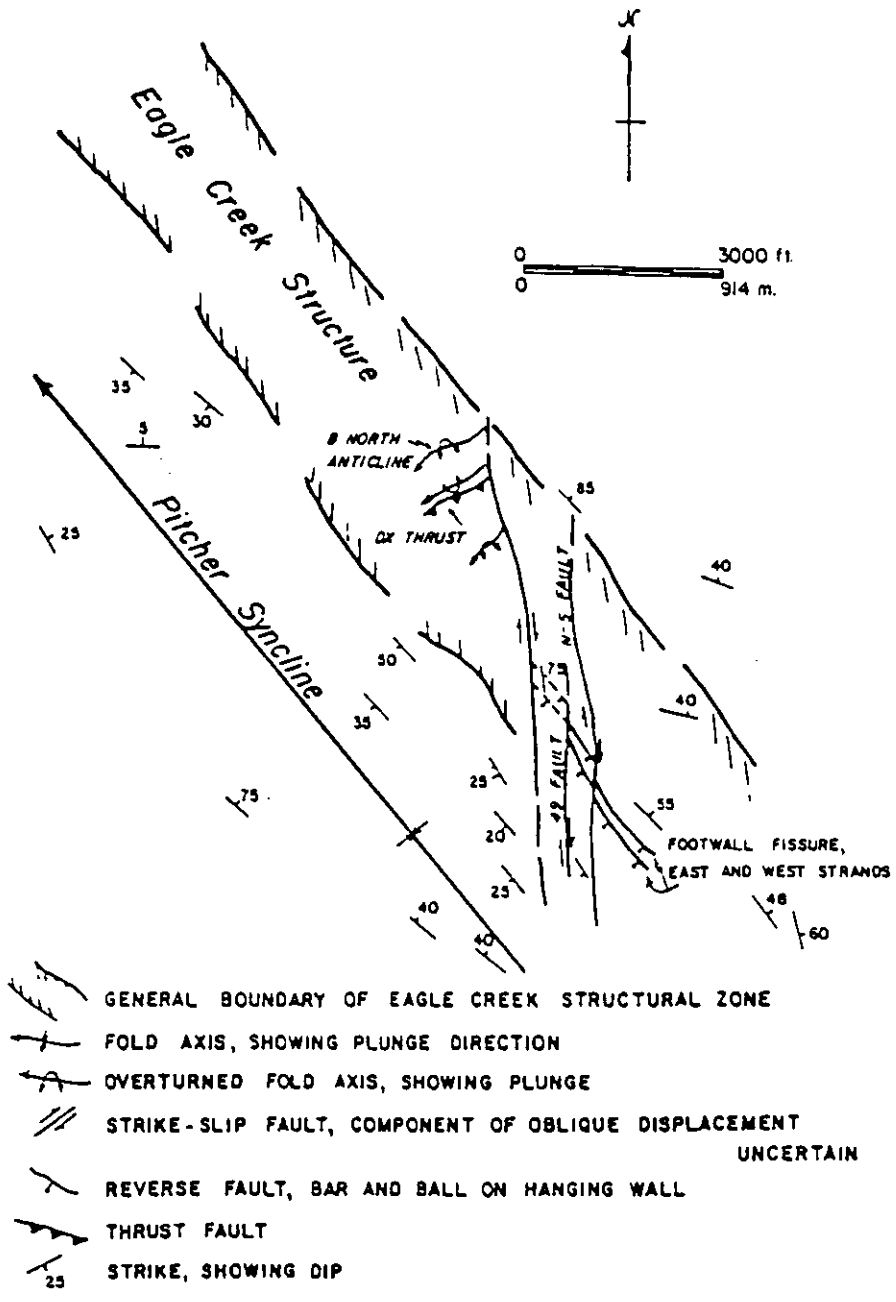

Figure 13. Principal structural features in the Wenatchee district.

Eagle Creek Structure

As originally defined by Willis (1953, P. 794) the Eagle Creek anticline extends from Little Chumstick Creek in the northern part of the graben, southeastward beyond the city of Wenatchee, a distance of over 55 km. Gresens (1983, p. 55) has suggested that this structure may not be an anticline in the normal sense of the term, but may have formed in response to fault-generated drape folding during extension and infilling of the graben. Given this hypothesis (an alternative to shortening perpendicular to the axial plane) the structure will be referred to as the Eagle Creek structure to avoid genetic implications.

In the Wenatchee district, the overall northwest structural trend appears to be related to the Eagle Creek structure. Rocks of uncertain age in the central portion of the district generally strike northwest with variable, but commonly near-vertical dips. This observation is true for most surface exposures of these rocks, and for underground exposures at "D" reef, "B" reef, and the "B" West ore body. Conglomerates and feldspathic sandstones of the Chumstick Formation on the eastern flank of the district also have an overall northwest strike, and dip uniformly to the northeast at 50° to 60°. The emplacement of the Saddle Rock andesite and rhyodacite at Wenatchee Dome and Rooster Comb also appears to be a manifestation of the Eagle Creek structure (Chappell, 1936, p. 139). The overall trend of hydrothermally altered and mineralized zones in the district is parallel to this

northwest trend, as is the Pitcher syncline in the Oligocene Wenatchee Formation (Figure 14), and the Footwall Fissure (Lovitt and McDowall, 1954; Lovitt and Skerl, 1958; Patton, 1967; Patton and Cheney, 1971) at "D" reef (Figure 13). The Footwall Fissure is a northwest-trending, southwest-dipping high angle reverse fault that is present on the eastern margin of "D" reef.

Gresens (1983, plate 1) mapped a northwest-trending fault between rocks of the Chumstick Formation on the eastern flank of the district and rocks of uncertain age in the central portion of the district. There is a distinct discontinuity between these two sedimentary packages, but data collected during this investigation were inconclusive as to whether the two sedimentary packages are unconformable or in fault contact. This contact is also parallel to the grain of the Eagle Creek structure.

From the above observations, it can be seen that the orientation of sedimentary rocks of all ages in the district, the location of intrusive rocks, and the general trend of hydrothermally altered and mineralized rocks all seem to be a product of, or are influenced by the Eagle Creek structural trend. The Eagle Creek structure is therefore considered to be the most important structural feature in the Wenatchee district.

North-trending faults

Early workers (Lovitt and McDowall, 1954; Lovitt and Skerl, 1958; Patton, 1967; Patton and Cheney, 1971) recognized a prominent post-mineralization north-trending fault pattern in the L-D mine at "D" reef. These faults are near vertical and have dextrally offset the silicified lens that constitutes "D" reef into a series of partially and completely detached blocks. Three main faults have been identified at "D" reef: The North-South fault, the 49 fault, and an unnamed fault that defines the northwestern boundary of "D" reef (Plate 1). The North-South fault has been traced by drilling and geophysical data, and forms the western margin of the rhyodacite at Rooster Comb. The unnamed fault on the the western boundary of Block 3 has been traced by drilling to the western margin of Wenatchee Dome. There, it defines the boundary between the "B" reef complex and the perlite and rhyodacite of Wenatchee dome (Plate 1).

Other north-trending faults are shown on Plate 1. These include the fault between Old Butte and Saddle Rock, and a fault west of the andesite outcrop adjacent to "C" reef. The location of these structures is based largely on inference from very limited drill-hole information. Lovitt and Skerl (1958, p. 966) show ten north- to northwest-trending faults in a zone extending from "D" reef to "G" reef, a remarkably perceptive interpretation, considering the limited amount of subsurface data at that time.

The north-trending fault pattern appears to be confined to rocks of uncertain age in the central portion of the district. This may merely reflect either the benefits of underground exposures and detailed drill-hole information in these rocks, in contrast with the paucity of outcrops elsewhere in the district, or it may represent a more complex tectonic history for rocks in the central portion of the district.

Pitcher syncline

Sedimentary beds of the Oligocene-aged Wenatchee Formation have been folded into a northwest-trending syncline in the western part of the district. This structure is well exposed on the north side of Squilchuck Canyon where the fold profile has continuous curvature and a well defined vertical axial plane (Figure 14). The axis of the Pitcher syncline plunges gently to the northwest, but becomes poorly defined at Dry Gulch. Where it crosses Dry Gulch, the fold profile is defined by a broad, flat-lying central area with sharply upturned edges at the eastern and western borders (Gresens, 1983, p. 55). Northwest of Dry Gulch the Pitcher syncline becomes even broader, but the structure cannot be traced beyond the northwesternmost exposure of the Wenatchee Formation.

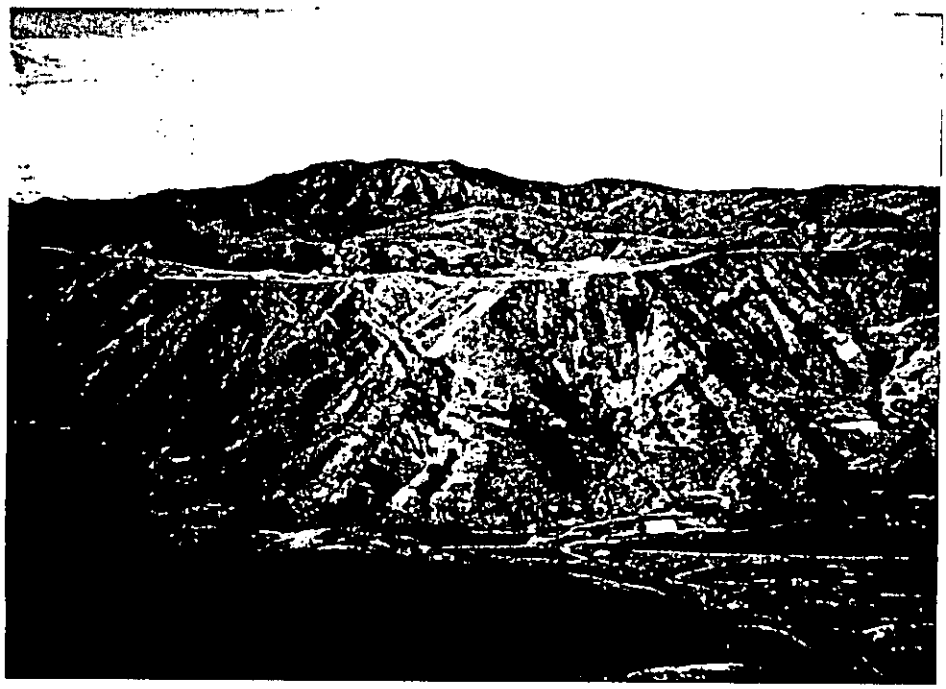

Figure 14. View of the Pitcher syncline in beds of the Wenatchee Formation, looking northwest across Squilchuck Canyon. The western edge of "D" reef is located on the right margin (east side) of the photograph. Horse Lake Mountain defines the far horizon in the center of the photograph.

Structures Associated with Mineralization

Asymmetric folds with west- to southwest-trending fold axes and axial planes that dip 30° to 50° to the south are present in the "B" reef complex. Folds with a similar orientation are exposed in the highwall excavated during preparation of the mill site at the Cannon mine (Plate 1 and Figure 6). In the "B" North ore body, the dominant vein set appears to be related to these folds as filled a-c extension joints (that is, dilatant joints formed in response to elongation parallel to the fold axes). This relationship will be demonstrated in the economic geology section of the report. Additionally, a south-dipping thrust fault, that has the same strike, but a less variable and somewhat steeper dip than the axial plane than the asymmetric folds, separates the major ore bodies of the "B" reef complex.

Two prominent vein orientations are present at "D" reef. Both vein sets strike N60°E to N80°E; one set dips 60° to 80°NW and is cross-cut by the second set, which dips 80° to 85°SE. Veins with a similar orientation are present at "A" reef, but temporal relationships there have not been worked out. The Saddle Rock andesite is cut by thin, unmineralized hematite-chalcedony veinlets that also strike N60°E to N80°E and dip 60°NW (Plate 1).

Interpretation of District Structural History and its Relation to Mineralization

Two levels of structural control of mineralization in the Wenatchee district are evident: (1) The confinement of all known mineralization and alteration to a narrow, northwest-trending belt of complexly deformed rocks in the central portion of the district implies a fundamental pre-mineralization structural control, and (2) displacement and truncation of mineralized rocks by north-trending dextral strike-slip faults, and northwest-trending reverse faults clearly represents post-mineralization structural control of ore location. Furthermore, the relationship between vein and fold orientations at the "B" reef complex suggests that intra-mineralization deformation may have been important in localizing economic concentrations of gold.

Structural interpretations made by previous workers are shown in Figure 15. These workers have relied primarily on observed and presumed structural aspects of the "D" reef. All of the structures shown in Figure 15 have post-mineralization displacement, and they can all be ascribed to southwest to northeast contractional strain on a district scale. Similarly, dextral strike-slip movement on the north-trending fault set can be interpreted as tear faults under conditions of southwest to northeast regional shortening; and these structures also post-date mineralization. Finally, the dominant vein orientation at "D" reef (both barren and auriferous veins), "A" reef, and the orientation of chalcedony

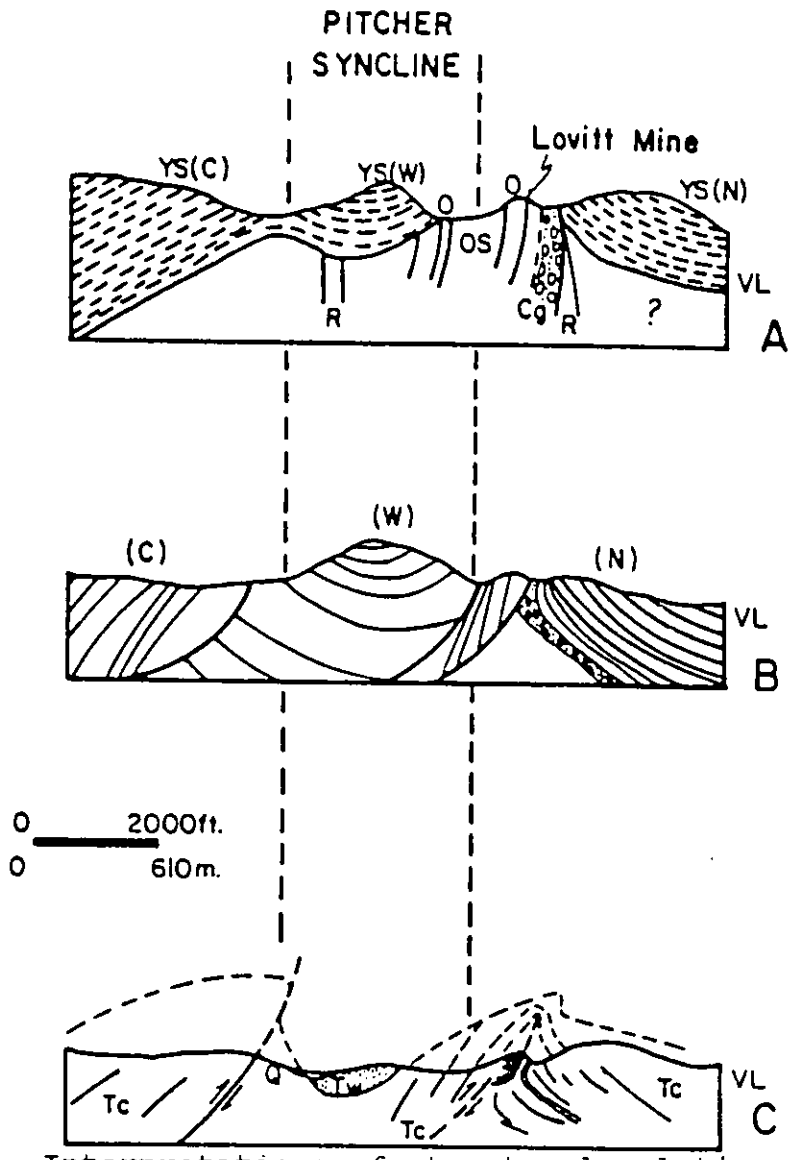

Figure 15. Interpretations of structural relations at the Pitcher syncline and "D" reef made by previous workers. All three cross sections are viewed to the northwest. (A) cross section of Lovitt and Skerl (1958): Cg- conglomerate, Os- Old Sandstone, Ys- young sandstone, R- rhyolite, O- ore zone. Lithological interpretation of Gresens (1983) is shown in parentheses: (w)- Wenatchee Formation, (c)- Chumstick Formation, (n)- Nahahum Canyon Member of the Chumstick Formation. Gresens mapped both Cg and Os as the Swauk(?) Formation. (B) is the interpretation of Patton and Cheney (1971), who mapped all sedimentary rocks as the Swauk Formation. (C) is the interpretation of Margolis (1987), and is essentially the same as (B) except for two modifications: The Footwall Fissure (thrust fault in the Lovitt Mine area) is shown as an axial plane structure, and the lithological interpretation that no Swauk Formation is present. VL is valley level. A and B from Gresens (1983, fig. 9, p. 57) C from Margolis (1987, fig. 4, p. 11).

veinlets that cut the Saddle Rock andesite averages N70°E with dips ranging from 60°NW through vertical, to 70°SE. These vein structures represent northwest to southeast elongation, which is compatible with the shortening orientation indicated by faults and folds in the district.

If simultaneous mineralization at "D" reef, the "B" reef complex, and "A" reef is assumed, and the vein orientations at "D" reef and "A" reef are interpreted to be products of the same regional strain that produced post-mineralization structures in the district, then the fold, thrust fault, and vein orientations at the "B" reef complex can readily be ascribed to strain from initial displacement on the north-south faults. Thus, within the constraints of the above assumptions, all of the observed structures in the Wenatchee district can be attributed to a protracted deformation period that involved southwest-northeast shortening, accompanied by minor northwest-southeast elongation.

This interpretation poses a fundamental problem in the context of the temporal relationship of district-scale deformation with regional structural development. The strain axes indicated by deformation features in the Wenatchee district are opposite, or oblique to, the predicted strain axes that would develop during graben formation. If the graben formed as a dextral strike-slip basin, as is well established in recent literature (Gresens, 1983; Johnson, 1983; Johnson, 1985), predicted regional strain axes would be oriented approximately north-south for shortening, and east-

west for elongation. In the case of graben formation by regional northeast-southwest extension, elongation and shortening directions would theoretically be exactly opposite of the southeast to northwest shortening and northwest to southeast elongation directions observed in the Wenatchee district. Finally, the limited stratigraphic and radiometric dating information available in the Wenatchee district requires deformation periods to be related to the known episodes of sedimentation, igneous activity, hydrothermal activity, and periods of tectonic quiescence and erosion unless there is definite evidence to the contrary.

Timing and type of deformation

The northwest orientation of the Saddle Rock andesite, and its linear arrangement with crystalline rocks at the core of the Eagle Creek structure northwest of the Wenatchee district (Figure 4), indicates that the Eagle Creek structure was well developed by at least middle Eocene time, and possibly by early Eocene time (Table 3). This age temporally relates the development of the Eagle Creek structure to the earliest stages of graben formation (Gresens, 1983; Evans, 1987). It is possible that the Eagle Creek structure could have initially developed at an oblique orientation to the Entiat fault and then rotated to its present position by subsequent deformation events, but the kinematics of rotating such a large linear feature intact are difficult to envision without significant internal strain, for which there is no

evidence.

Buza (1977, p. 14) has used paleocurrent data to show that the Eagle Creek structure was a positive topographic feature during the period of Chumstick deposition. This implies that the Chiwaukum graben developed as two northwest-trending basins bounding the Eagle Creek structure. If the Chiwaukum graben formed as a dextral strike-slip basin, it is not likely that the Eagle Creek structure formed as an intra-graben horst as proposed by Gresens (1983, p. 55). Alternatively, the Eagle Creek structure may be a dextral shear zone, and could conceivably be the principal displacement zone within the Chiwaukum graben.

Syndepositional deformation of the Chumstick Formation is one of the criteria used by Evans (1987) as evidence that the Chiwaukum graben formed as a strike-slip basin. This suggests that a regional, northerly-directed, subhorizontal compressive stress environment encompassed the Wenatchee district through at least part, and possibly most, of the Chumstick depositional period, from about 49 m.y.b.p. to 42 m.y.b.p. Mineralization and alteration occurred in the Wenatchee district near the end of this period of time, based on a single K-Ar determination (Table 3). Theoretically, strain features from this deformation period would display north-south shortening, and east-west elongation. With the exception of the fold and thrust arrangement in the "B" reef complex, strain of this orientation is nowhere evident in the Wenatchee district. One possibility is that all strain within

the dextral Eagle Creek structure has been rotated by simple shear into parallelism with the principal displacement zone. The orientation of foliation in the Swakane gneiss in the core of the Eagle Creek structure northwest of Cashmere supports the concept of rotational strain during dextral deformation on the Eagle Creek structure. In the Entiat Mountains, east of the Entiat fault, foliation in the Swakane gneiss defines an antiform, the axis of which is oriented approximately N65^{o}W, oblique to the trace of the Entiat fault. However, foliation in the Swakane gneiss where exposed in the core of the Eagle Creek structure, is parallel to the Eagle Creek fault (see figure 1 of Willis, 1958), which indicates a reorientation of foliation as a result of graben formation. Rotational strain would explain both the northwest alignment of mineralization in the district, and the evident discordance in structural complexity between rocks in the central portion of the district, and those that appear to be less deformed on the eastern and western flanks of the district. This interpretation detracts from the argument that the structural complexity of rocks in the central portion of the district can be used as evidence that they are older than Chumstick sediments on the eastern flank of the district.

Deformation continued beyond the final deposition of the Chumstick Formation, and was followed by a period of tectonic quiescence and erosion prior to deposition of the Wenatchee Formation. This is indicated by the angular unconformity between these two Formations.

Folding of the Wenatchee Formation into the Pitcher syncline requires this structure to be post-Oligocene. Deformation capable of creating the Pitcher syncline may have been coeval with the Miocene uplift of the Cascade Range west of the Wenatchee district. The Footwall Fissure at "D" reef is strain coaxial with the Pitcher Syncline that post-dates mineralization; although Patton and Cheney (1971, p. 8) interpreted it to be a pre-mineralization structure. However, it clearly truncates mineralized veins at "D" reef, and, since both the Footwall Fissure and the Pitcher syncline represent southwest to northeast shortening, the most recent movement on the Footwall Fissure is interpreted to post-date mineralization and to be contemporaneous with the formation of the Pitcher syncline.

Parallelism of post-, intra-, and pre-mineralization strain in the Wenatchee district may appear to be somewhat fortuitous. However, initial deformation evidently produced a sufficient northwest-trending, near vertical planar anisotropy in the rocks to force later, west-to-east directed deformation to conform to the existing planes of weakness.

Patton and Cheney (1971) interpreted the Footwall Fissure at "D" reef to be part of a northwest-trending imbricate thrust fault. They extrapolated the Footwall Fissure from "D" reef to the northwest, and their Figure 2 (Patton and Cheney, 1971, p. 8) shows a northwest-striking thrust fault separating the "B" reef from Wenatchee Dome. In this investigation, the unnamed north-trending fault on the

western margin of "D" reef was traced by drill holes and found to extend from "D" reef to Wenatchee Dome, juxtaposing the rhyodacite intrusion and the "B" reef complex. Minor folds in the fault between the Wenatchee Dome and the "B" reef complex have near-vertical axes, and lineations in the gouge are subhorizontal. These features indicate strike-slip, rather than dip-slip displacement. The Footwall Fissure has been offset by the North-South and 49 faults, and cannot be confidently located beyond the northwesternmost extent of "D" reef (Figure 13). Latest movement on the north-trending fault set post-dates development of northwest-trending structures, and on a detailed scale, the overall northwest structural grain of the district is locally subordinate to the north trend.

The timing of earliest movement on the north-trending faults is not certain. Since they offset mineralization, the maximum age for most recent movement on the north-trending faults is 44 m.y.b.p. (Table 3). If these faults formed in response to dextral displacement on the Eagle Creek structure, their initial development could theoretically have been either as dilatant features or as Reidel shears. However, evidence for this is lacking, and since the north-trending faults offset all other structures that have district-scale continuity, they presumably are the most recent structures in the district. For this reason, they are interpreted as tear faults related to deformation responsible for the Pitcher syncline and the Footwall Fissure.

West-trending, north-verging folds at the "B" reef complex are the only features in the district that clearly imply north-south shortening. These structures, and the west-trending, south-dipping thrust fault at the "B" reef complex (Figure 15), have two possible origins. As previously discussed, these structures may be the products of resolved stresses from dextral displacement on the north-trending faults. However, the north-south faults appear to be related to post-Oligocene deformation that produced the Pitcher syncline, and the folds at the "B" reef complex appear to be contemporaneous with mineralization. Thus, a temporal problem is posed by this interpretation. An alternative interpretation is that the fold-thrust arrangement at the "B" reef complex is the product of strain developed late during the period of dextral shear on the Eagle Creek structure. Fold axis orientation and transport direction indicated by vergence is compatible with this interpretation.

The east-northeast strike and steep dip of veins at the "D" reef, "A" reef and veinlets in the Saddle Rock andesite remain somewhat enigmatic. One possibility is that these structures represent post-deformation relaxation strain within the Eagle Creek structure. The age of mineralization at the "B" reef complex is close to the end of graben development as determined by Gresens (1983). Removal of northerly directed, subhorizontal compressive stress would possibly result in a limited amount of north-south elongation (release joints). Development of these structures would account for the observed

orientation of the "D" reef veins, and would be temporally compatible with the age of mineralization at "B" reef.

In summary, the Pitcher syncline, Footwall Fissure, and north-south faults all represent west-southwest to east-northeast contraction that post-dates mineralization. These structures are the basis for interpretations made by previous workers in the district. Mineralization in the Wenatchee district occurred near the end of, or shortly after, a period of dextral displacement on the Eagle Creek structure; deformation that was contemporaneous with development of the Chiwaukum graben. Fold and vein orientation, and the age of mineralization at the "B" reef complex, supports this interpretation. Veins at the "D" reef, "A" reef, and in the Saddle Rock andesite may represent relaxation strain that developed immediately after termination of dextral deformation on the Eagle Creek structure. A significant component of rotational strain occurred in the deformation of the Eagle Creek structure, and developed a strong northwest-trending regional anisotropy in the rocks. This anisotropy, in turn, controlled the orientation of younger structures.

INTRODUCTION TO THE ECONOMIC GEOLOGY OF THE WENATCHEE DISTRICT

The Wenatchee mining district is an unusual example of epithermal gold-silver mineralization in respect to the host lithology, tectonic setting, ore mineralogy, and style of mineralization. Shortly before its closure in 1967, the L-D mine was the 13th largest gold producer and 6th largest gold mine in the United States (Patton and Cheney, 1971, p. 9). Past and present proven reserves in the district total approximately 1.5 million ounces (46.7 metric tons) of gold, and nearly 2.25 million ounces (70.7 metric tons) of silver at an average grade of about 0.25 oz/ton (8.6 g/mt) Au, and 0.37 oz/ton (12.7 g/mt) Ag. Individual ore bodies in the Wenatchee district are described in the following sections of this thesis, with an emphasis on the recently discovered Cannon mine. The general characteristics of hydrothermally altered rocks in the Wenatchee district as exposed at the surface are described in this section to provide a background for later, more detailed discussions of the ore bodies.

Hydrothermally altered rocks that host gold and silver mineralization in the Wenatchee district are resistant to weathering and generally form rugged outcrops that contrast sharply with the surrounding colluvial slopes. Early prospectors in the district referred to these outcrops as "reefs", a term that is still used in the Wenatchee district, but one that is not intended to imply any systematic, geometric relationship between the location of hydrothermally altered rocks and district-scale structures. Various reefs,

which have alphabetic designations, are shown on Plate 1 and in Figure 2. Except for "A" reef, all exposures of silicified rock in the Wenatchee district consist of tan to very light-gray, iron-stained, and brecciated sedimentary rocks that are cross-cut by quartz veins and veinlets. The matrix of feldspathic sandstone beds is replaced by fine-grained quartz, and this replacement process has produced a very competent rock that has a plutonic appearance. Early miners referred to "D" reef as the "bastard granite" in allusion to its plutonic appearance (Patton and Cheney, 1971, p. 8).

"A" reef, located on the north side of Dry Gulch (Plate 1) is distinctive in that it is the only place in the area under consideration that good underground and surface exposures of intensively silicified and veined Saddle Rock andesite occur. On the 1250 level of "A" reef, an exploration adit developed by Anaconda, the Saddle Rock andesite is strongly silicified and argillized, and cut by a northeast-trending vein set. Locally, these veins contain up to 0.2 oz./ton (6.9 g/mt) gold. Diamond drilling information indicates that the Saddle Rock andesite is also altered west of the "B" reef complex.

"F" and "G" reefs are the only zones of alteration on Plate 1 that are west of the Saddle Rock andesite. These reefs are poorly exposed except for several small trenches excavated by early prospectors. "E" reef, located about 150 meters west of "D" reef (Plate 1), may also be west of andesite equivalent to the Saddle Rock andesite, but current

information is insufficient to make this determination.

"C" reef is located between "D" reef and "B" reef along the main trend of mineralization extending from "D" reef to "A" reef. "C" reef forms a small but distinct ridge, but does not crop out well. A small exploration adit was driven on the 1575-foot level at "C" reef but was not accessible during the course of this investigation. Geologic and assay maps of the adit indicate that sedimentary rocks at "C" reef are extensively silicified, but not well mineralized. A jagged outcrop of hornblende andesite cut by small northeast-striking hematite-chalcedony veins is located immediately west of "C" reef (Plate 1). The andesite does not appear to be appreciably altered, and the hematite-chalcedony veinlets are not mineralized with gold.

Economic mineralization has been identified only at "D" reef and the "B" reef complex (Plate 1). "D" reef is the best surface exposure of hydrothermally altered rocks in the district as it forms a rugged outcrop of silicified coarse-grained feldspathic sandstone on the north side of Squilchuck Canyon (Plate 1). Northwest-striking quartz veins are well-developed in the "D" reef outcrop, and stand out as 0.5 to 1 meter-thick quartz-filled fractures cutting the silicified and oxidized cliffs (Figure 16). Surface exposures of silicified sedimentary rocks at "D" reef extend continuously to the northwest from the contact of undifferentiated alluvial sediment at Methow Street to about the 1800-foot elevation (Plate 1). Above this elevation, outcrops are sparse, but

Figure 16. Silicified, veined sedimentary rocks at the "D" reef. View is looking west. Note the well developed north and south-dipping veins.

exposures in road cuts indicate that the sedimentary rocks are argillized (Plate 1).

"B" reef forms a small outcrop of silicified sedimentary rocks west of Wenatchee Dome on the south side of Dry Gulch (Figure 17). The surface exposure of "B" reef contains few quartz veins and is only weakly mineralized with gold. Other ore bodies at the "B" reef complex are overlain by up to 100 meters of surficial deposits, such that, there is no surface exposure of ore-grade rock. Ore bodies of the "B" reef complex will be discussed in the next section.

Mineralization at "D" reef and the "B" reef complex is both disseminated and vein and veinlet controlled. Ore bodies at both reefs consist of widely spaced quartz-adularia veins in pervasively mineralized and silicified wall-rock. The southeasternmost part of "D" reef contains veins that are wide enough that they could be mined as separate entities. However, most of the economic mineralization at "D" reef, and all of the ore bodies in the "B" reef complex require employment of bulk mining techniques, as mineralized veins, although they may be very high grade, are small and discontinous. Wallrock between the veins contains lower grades of disseminated mineralization. Local hydrothermal breccias and quartz-veinlet stockworks are also mineralized at both "D" reef and in ore bodies of the "B" reef complex.

Both pre-mineralization and post-mineralization faulting and folding are important in localizing these bodies of alteration and mineralization. On a district scale,

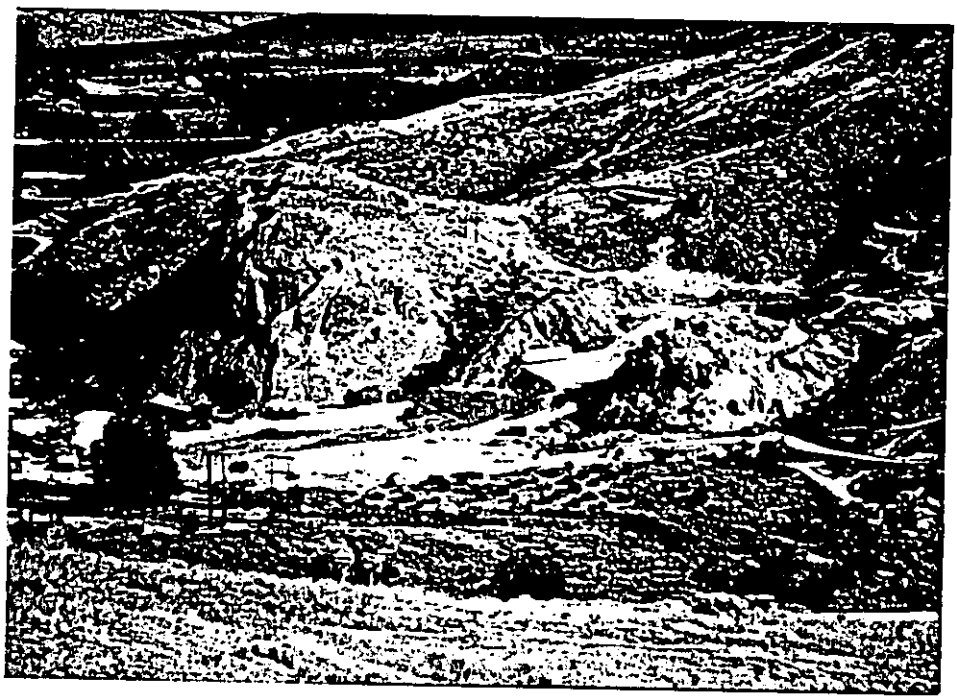

Figure 17. Surface outcrop of "B" reef prior to development of the Cannon mine. View is looking east, Wenatchee Dome is located about 50 meters east of the "B" reef outcrop.

stratigraphy appears to exert little control over the location of altered and mineralized zones, except that most, if not all, hydrothermal activity was apparently confined to the belt of complexly deformed sedimentary rocks in the central portion of the district. On a more detailed scale, individual stratigraphic horizons do exert significant local control over the boundaries of alteration and mineralization. Rhyodacite and andesite intrusions have a close spatial relationship with hydrothermally altered rocks; radiometric dating indicates a close temporal relationship as well (Table 3).

GEOLOGY OF THE "B" REEF COMPLEX

The "B" reef complex consists of four distinct bodies of altered and mineralized rock; the "B", "B" West, "B" Neath, and "B" North bodies. The "B-4" ore body appears to be an extension of the "B" North ore body, and, unless otherwise noted, further references to the "B" North ore body will imply the "B-4" ore body as well. Terminology employed in naming various ore bodies in the "B" reef complex is somewhat less than desirable when attempting a concise description of the deposit. Frequent reference to Figure 18 may help to alleviate any sense of "B" -wilderment the reader may experience while reading in this section. The "B" North ore body is the largest of the four ore bodies, the "B" Neath is the highest grade. Proven and probable reserves and average grade of each of the ore bodies is shown in Table 4.

Distribution and Morphology of Ore Bodies

Vertically, mineralization extends from about the 100 foot elevation in the lower part of the "B" Neath ore body to about the 1000 foot elevation at "B" reef. Each ore body is morphologically distinctive. The "B" Neath ore body is a pipe-like body, shaped like an upward-flaring cone. The "B" North ore body closely parallels the fold geometry of the sedimentary host rocks. The "B" reef and the southern portion of the "B" West ore body have northwest-trending, steeply dipping, tabular to lense-shaped configurations that may also

Table 4. Proven and probable ore reserves at the Cannon mine by ore body, in ounces per short ton*.

	"B" North and "B-4"	"B" Neath	"B" West and "B" Reef
Short tons	2,435,000	929,000	1,134,000
Grade:			
Au	0.251	0.331	0.222
Ag**	0.338	0.528	0.299

Total Proven and Probable Short Tons: 4,498,000

Average Grade: Au** - 0.260 oz/short ton
Ag** - 0.367 oz/short ton

* Based on January, 1988 Annual Report by Asamera Minerals (US) Inc. to Securities and Exchange Commission.

** Silver grades not reported but were calculated from silver-gold ratios indicated by grade-control drill hole assays as follows:

"B" North, "B-4", "B", and "B" West Ag:Au ratio - 1.346
"B" Neath Ag:Au ratio - 1.596

Overall Ag:Au ratio (all ore bodies) - 1.413

be parallel to a fold orientation, but exposures are insufficient to make this determination. The northwestern extension of the "B" West ore body appears to be pipe-shaped and plunges toward the "B" Neath ore body. A zone of sheared, unaltered sedimentary rocks separates the northwestern extension of the "B" West ore body from the "B" Neath ore body (Figure 18).

Most of the ore bodies are bounded by sheared and unaltered or weakly altered sedimentary rocks; however, the boundary between the "B" Neath and "B" North ore bodies is somewhat arbitrarily set at the 500 level (Figure 18). Much of the mineralization in the "B" North ore body is contained within the south-dipping limb of an asymmetric anticline. This portion of the "B" North body extends from the 500 level to the 785 level at the anticline axis, and is mined by north-south-trending stopes, designated as D stopes (Figures 19 - 21). The southern boundary of the D stope portion of the "B" North ore body is defined by an east-west-trending, south-dipping thrust fault (Figure 18). South of this thrust fault, mineralized sedimentary rocks strike north to northwest and are nearly vertical, an orientation that requires stopes to be oriented east-west to reduce chances of failure along bedding planes. This part of the "B" North ore body has been designated as the X stope area (Figures 21 - 25). From a structural standpoint, the thrust fault that separates the D stope area from the X stope area, referred to as the DX thrust, is the natural boundary between the "B" Neath and "B"

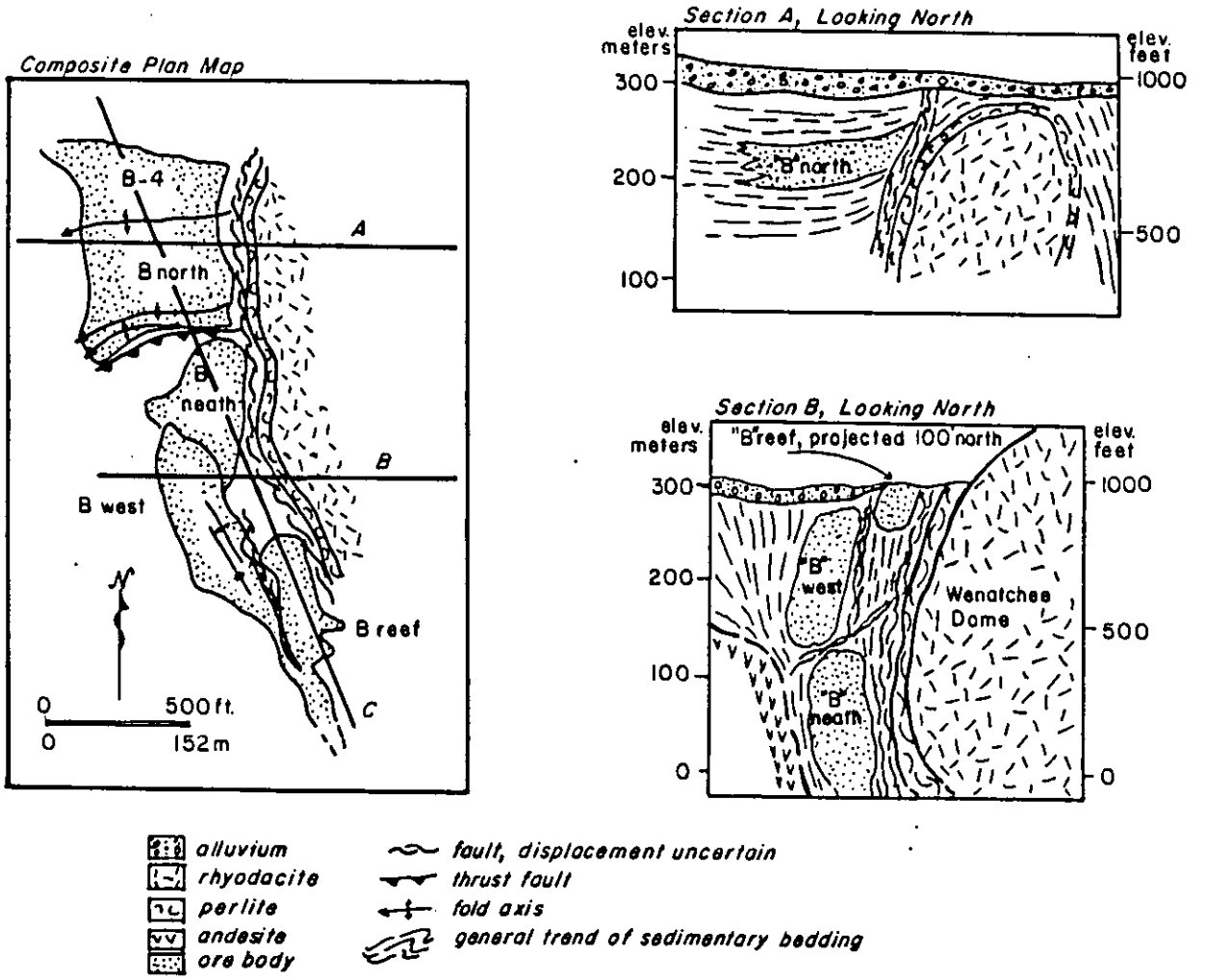

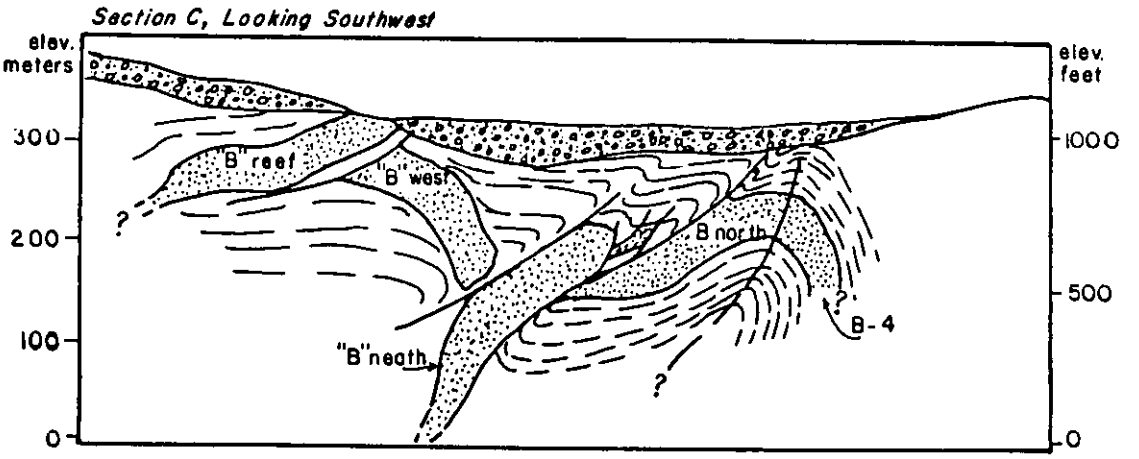

Figure 18. Generalized plan view, cross sections, and long section through the "B" reef complex.

North ore bodies.

Figures 19 through 29 show 50-foot level plans, cross sections and long sections through the currently developed part of the "B" reef ore bodies.

Mineralization and alteration are bounded on the east by a north-trending fault that separates the ore bodies from the perlite and rhyodacite of the Wenatchee Dome (Figure 18). Weakly altered hornblende andesite marks the western boundary of the "B" Neath and lower part of the "B" West ore bodies. In most cases, alteration intensity and gold content decrease significantly in sedimentary rocks near the contact with andesite, such that, the andesite is never in direct contact with ore-grade rock. In the D stope area of the "B" North ore body, the frequency of veins and amount of wallrock alteration decreases gradually to the west, and the ore boundary is represented by an assay wall. The nature of the western boundary of the "B-4" ore body has not yet been determined. The western boundaries of the "B" reef, the upper part of the "B" West ore body, and the X stope area of the "B" North ore body are evidently fault controlled. The southern boundaries of the "B" and "B" West ore bodies have not yet been defined (Figure 18).

Structural Framework

There are two well-defined structural trends in the "B" reef complex. The structural framework of the "B" North ore body is dominated by asymmetric folds with west to southwest-

trending axes. In the "B" reef and "B" West ore body, northwest-trending folds are the dominant structural feature. Northwest-trending folds are also present in the X stope area of the "B" North ore body, but development is currently insufficient to determine if this trend continues into the "B" Neath ore body.

The D stope area of the "B" North and the "B-4" ore bodies are partially stratabound within an asymmetric anticline, referred to here as the "B" North anticline. In the eastern part of the "B" North ore body, the axis of the "B" North anticline plunges about 20° to the southwest. To the west, in the vicinity of the 7-8 ramp (Figure 19 - 21) the fold axis plunges about 15° to the east. It is not certain if the reversal in plunge of the fold axis is due to a later folding event or simply a result of irregularities developed from a single folding event. The axial plane of the "B" North anticline dips about 60° to the south (Figures 27 and 28).

The axis of the "B" North anticline trends N70°E to N90°E where it is best exposed on the 700 level (Figure 21). Statistical analysis of bedding orientations shows the fold axis to plunge about 30°, S40°W (Figure 29). This discrepancy from the observed east-west trend may indicate that an insufficient sample population was used in the stereogram analysis. Alternatively, statistical data may approximate the true fold orientation that may not be evident at the detailed scale of observation within the mine.

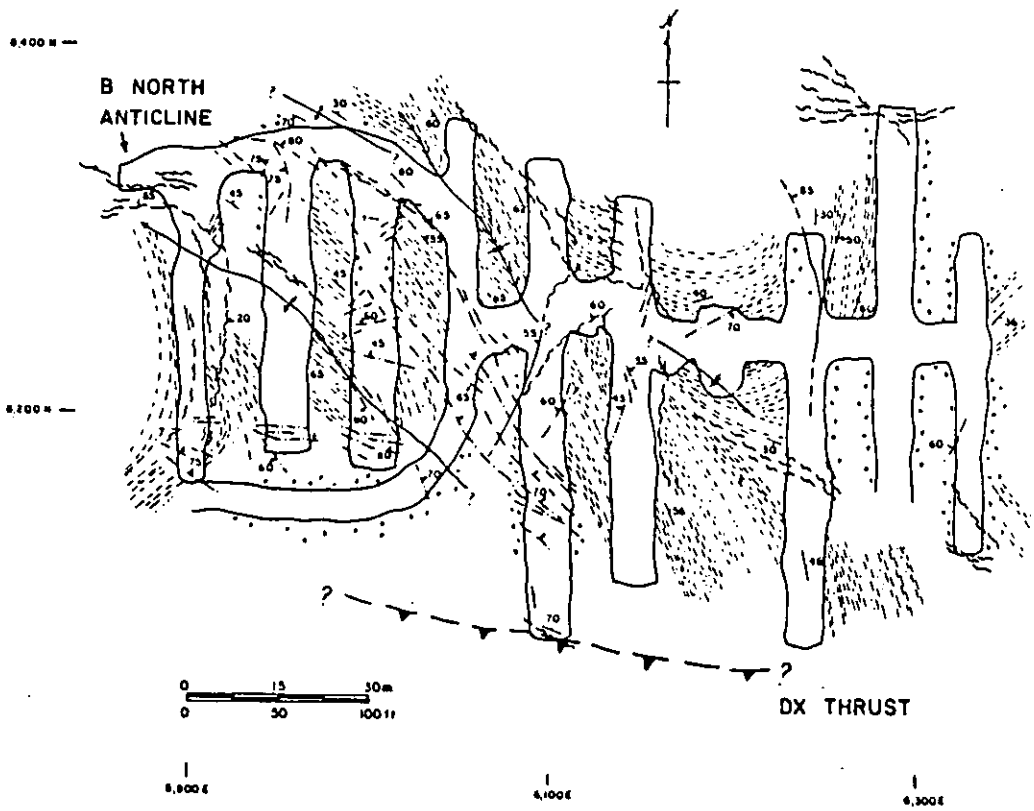

EXPLANATION OF PLAN MAPS

- BEDDED SILTSTONE AND SANDSTONE
- BRECCIATED, SILICIFIED SEDIMENTARY ROCKS
- QUARTZ VEINS
- STRIKE SHOWING DIP
- OVERTURNED BEDS
- JOINTS
- FAULT, DISPLACEMENT UNCERTAIN
- SHEAR ZONE
- THRUST
- ANTICLINE, SHOWING PLUNGE DIRECTION
- SYNCLINE, SHOWING PLUNGE DIRECTION
- OVERTURNED FOLD

Figure 19. Geology of the "B" North ore body, 785 level, Cannon mine. Mapped by D. Groody and L. Ott. Explanation applies to Figures 20 through 28.

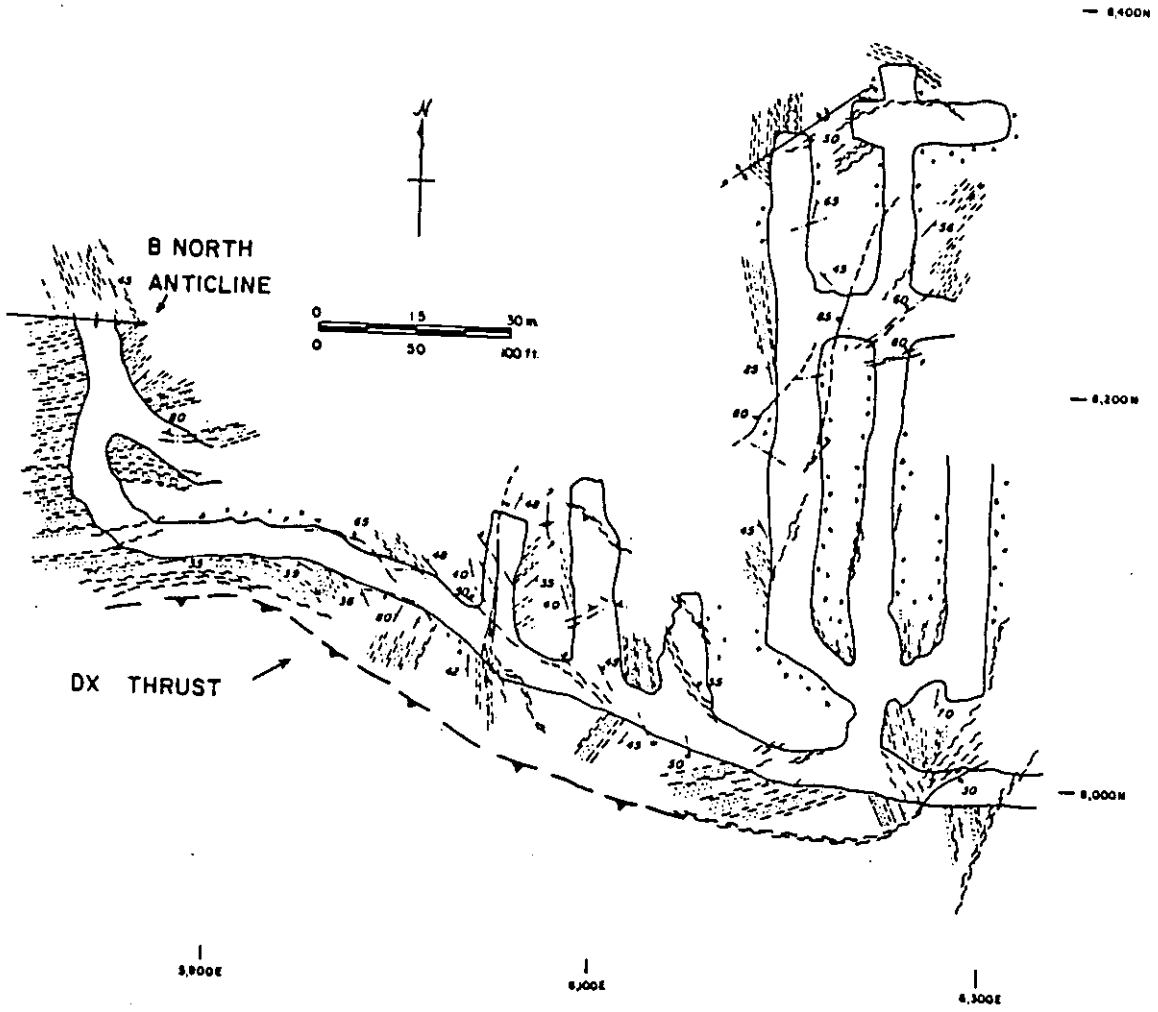

Figure 20. Geology of the "B" North ore body, 755 level, Cannon mine. Mapped by D. Groody and L. Ott. Refer to Figure 19 for explanation of symbols.

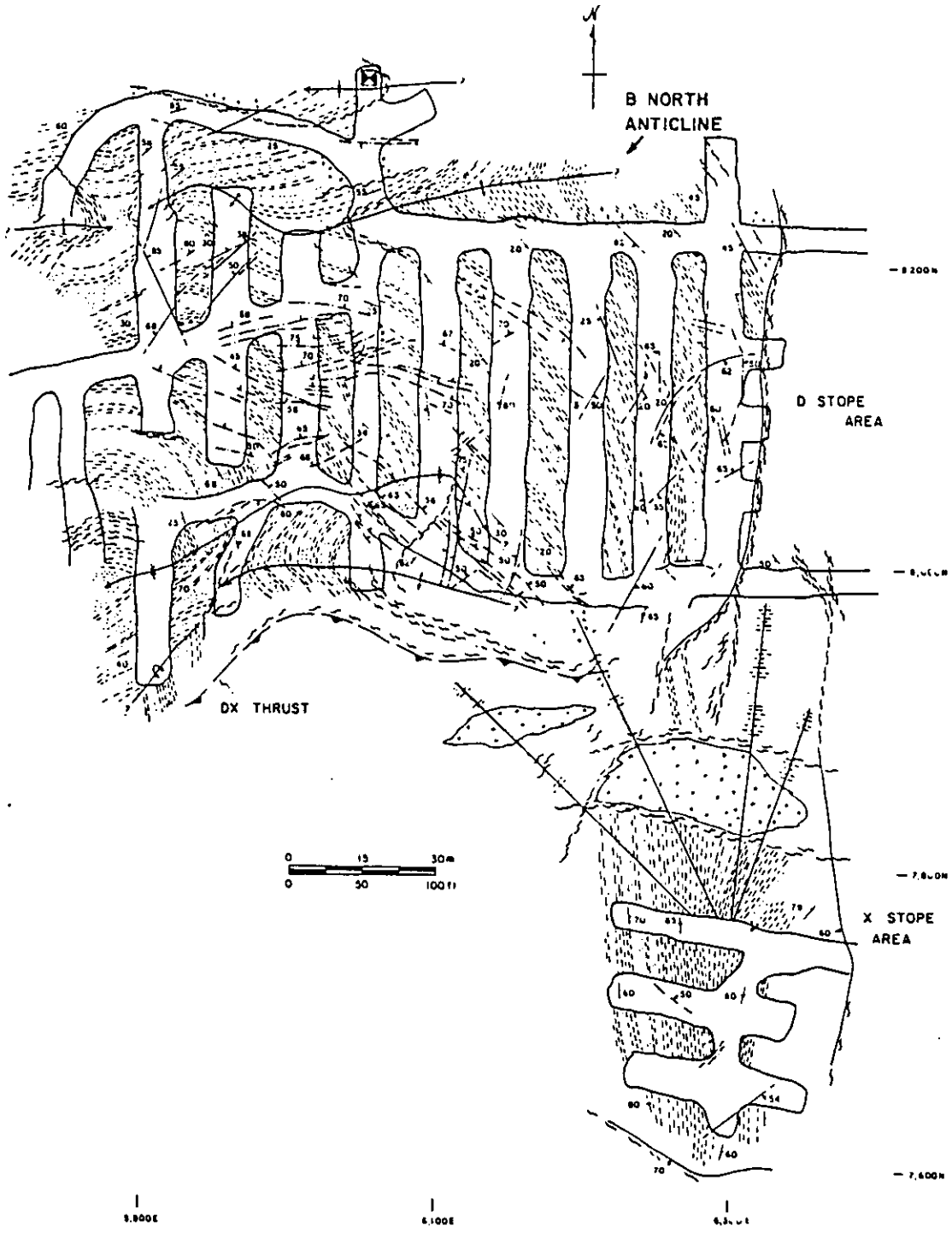

Figure 21. Geology of the "B" North ore body, 700 level, Cannon mine. Mapped by D. Groody and L. Ott. Refer to Figure 19 for explanation of symbols.

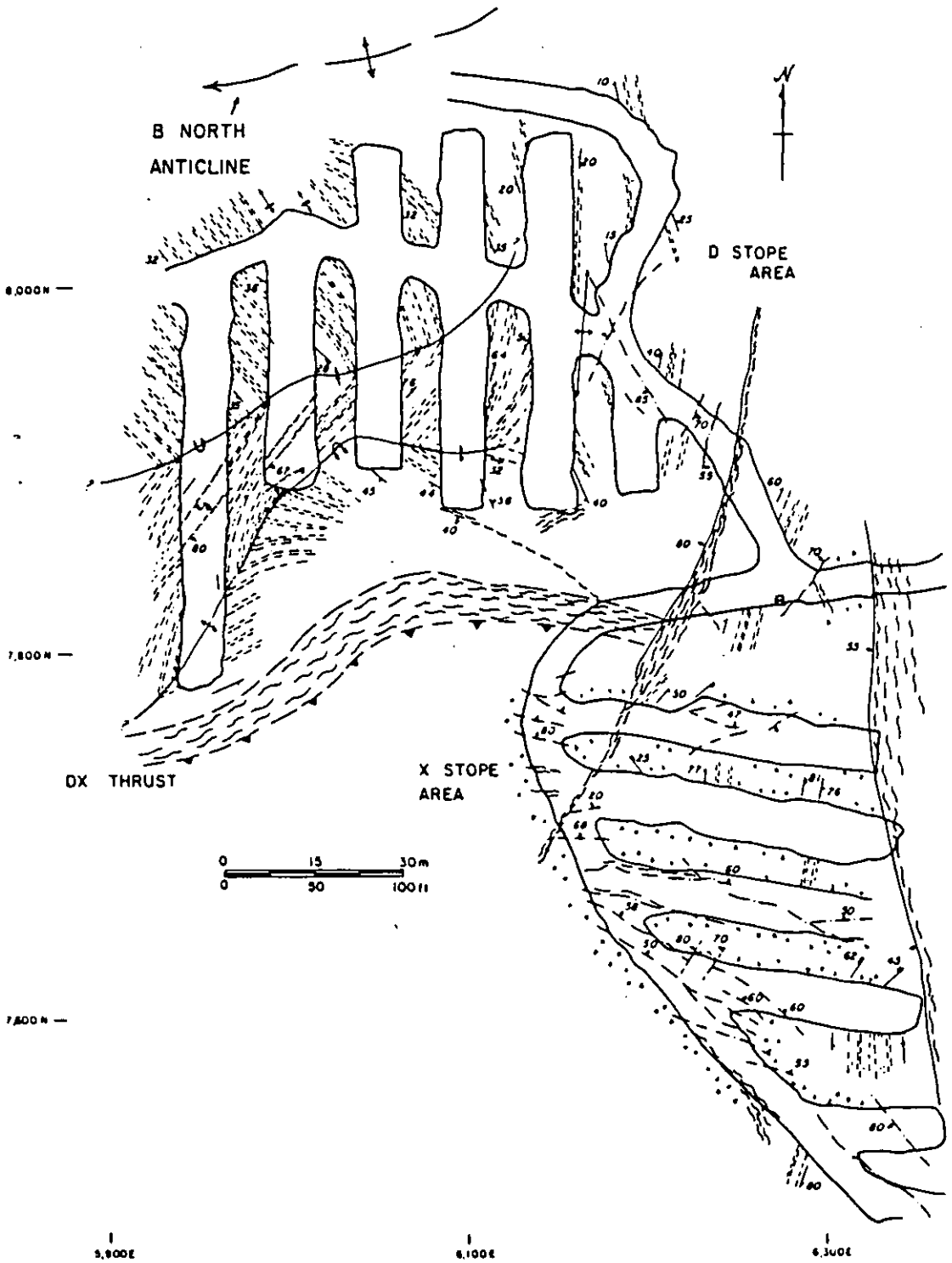

Figure 22. Geology of the "B" North ore body, 650 level, Cannon mine. Mapped by D. Groody and L. Ott. Refer to Figure 19 for explanation of symbols.

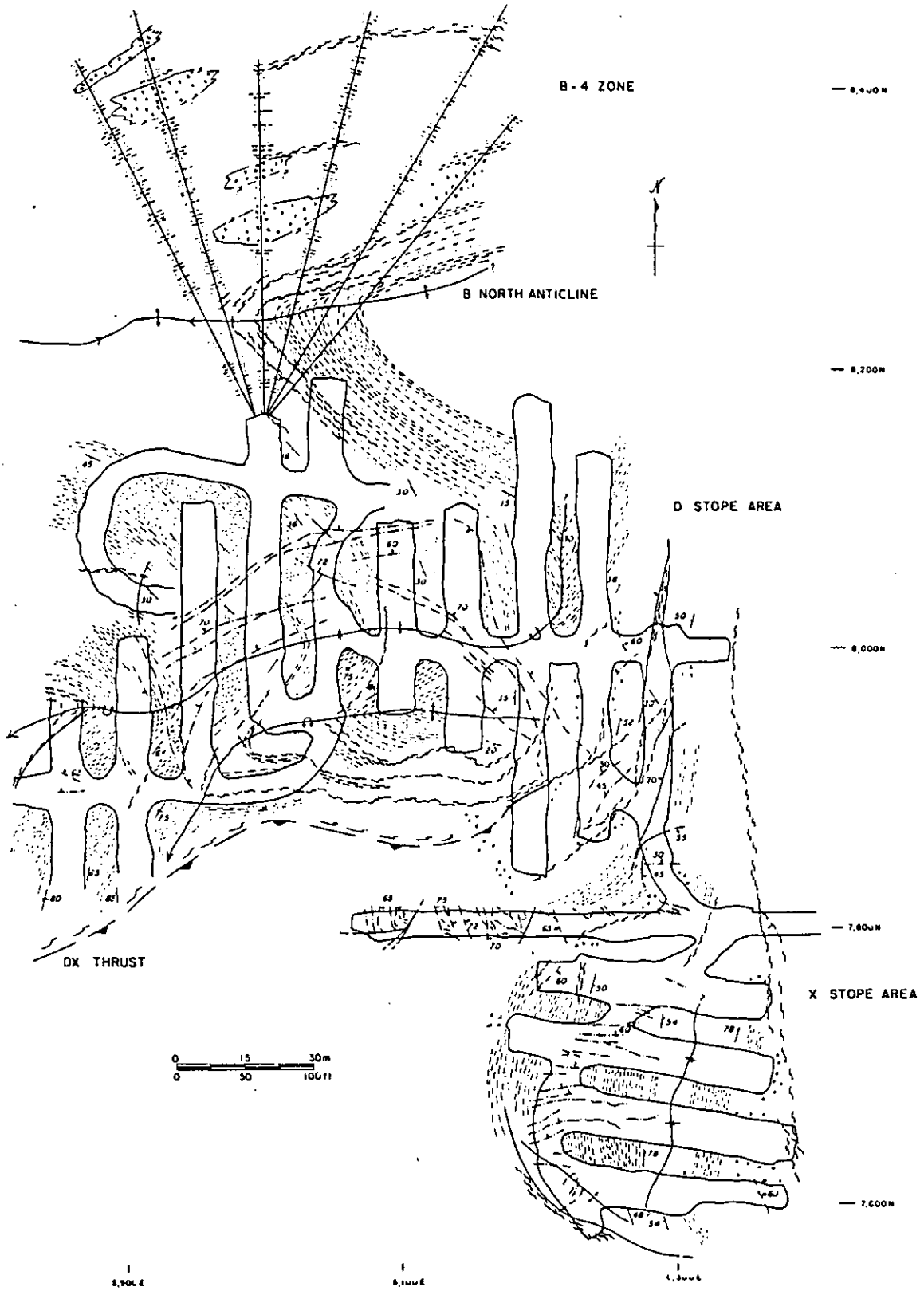

Figure 23. Geology of the "B" North ore body, 600 level, Cannon mine. Mapped by D. Groody, T. Alexander, and L. Ott. Refer to Figure 19 for explanation of symbols.

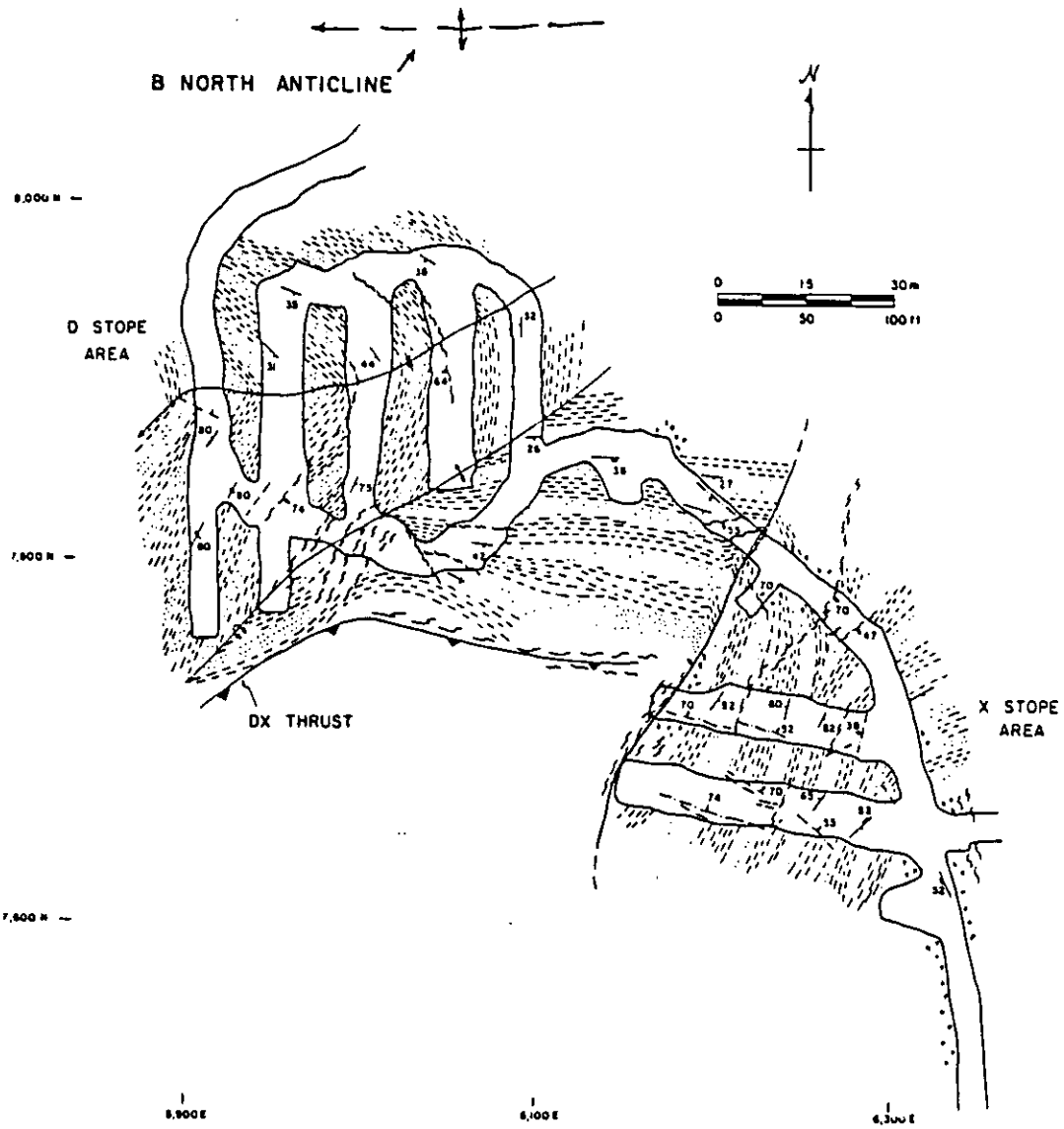

Figure 24. Geology of the "B" North ore body, 550 level, Cannon mine. Mapped by T. Alexander and L. Ott. Refer to Figure 19 for explanation of symbols.

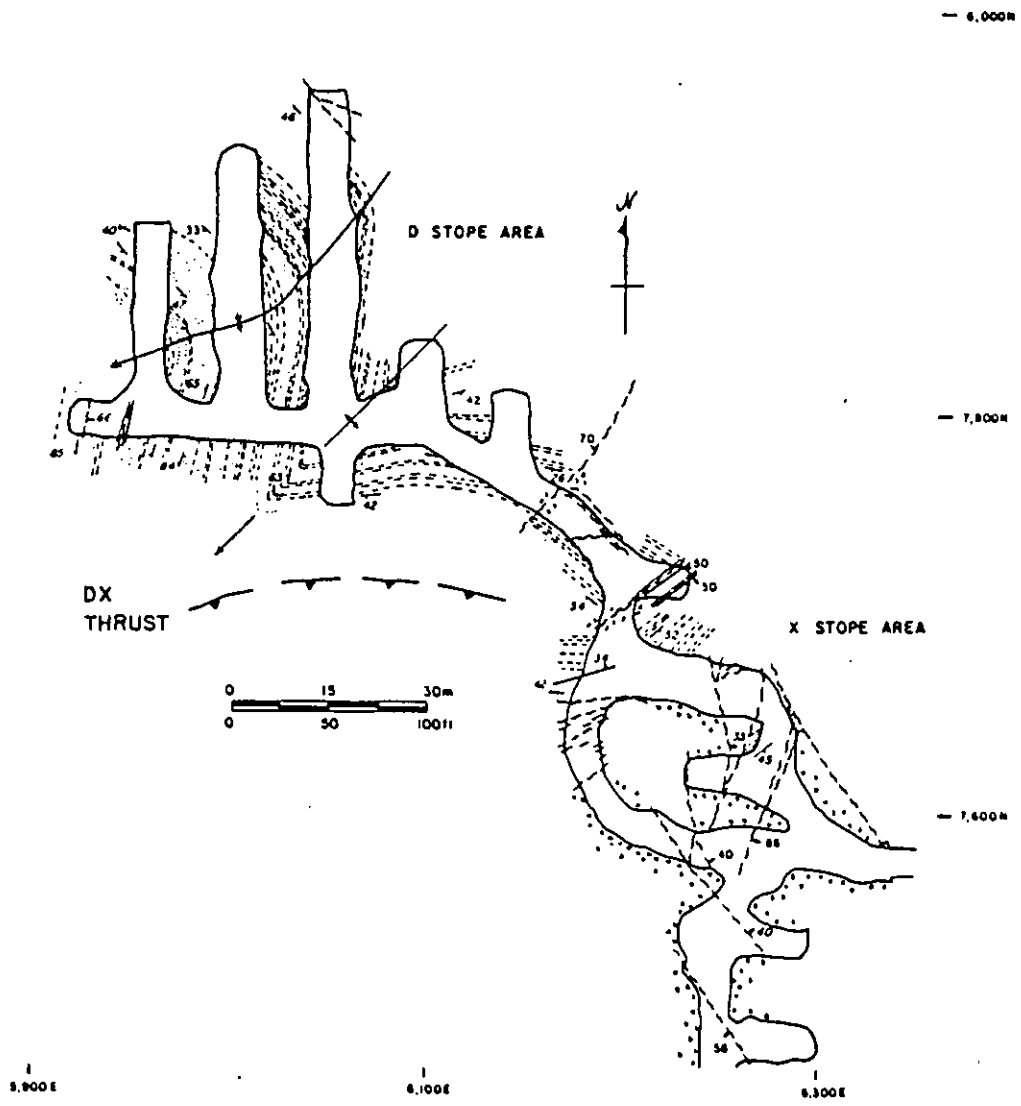

Figure 25. Geology of the "B" North ore body, 500 level, Cannon mine. Mapped by T. Alexander and L. Ott. Refer to Figure 19 for explanation of symbols.

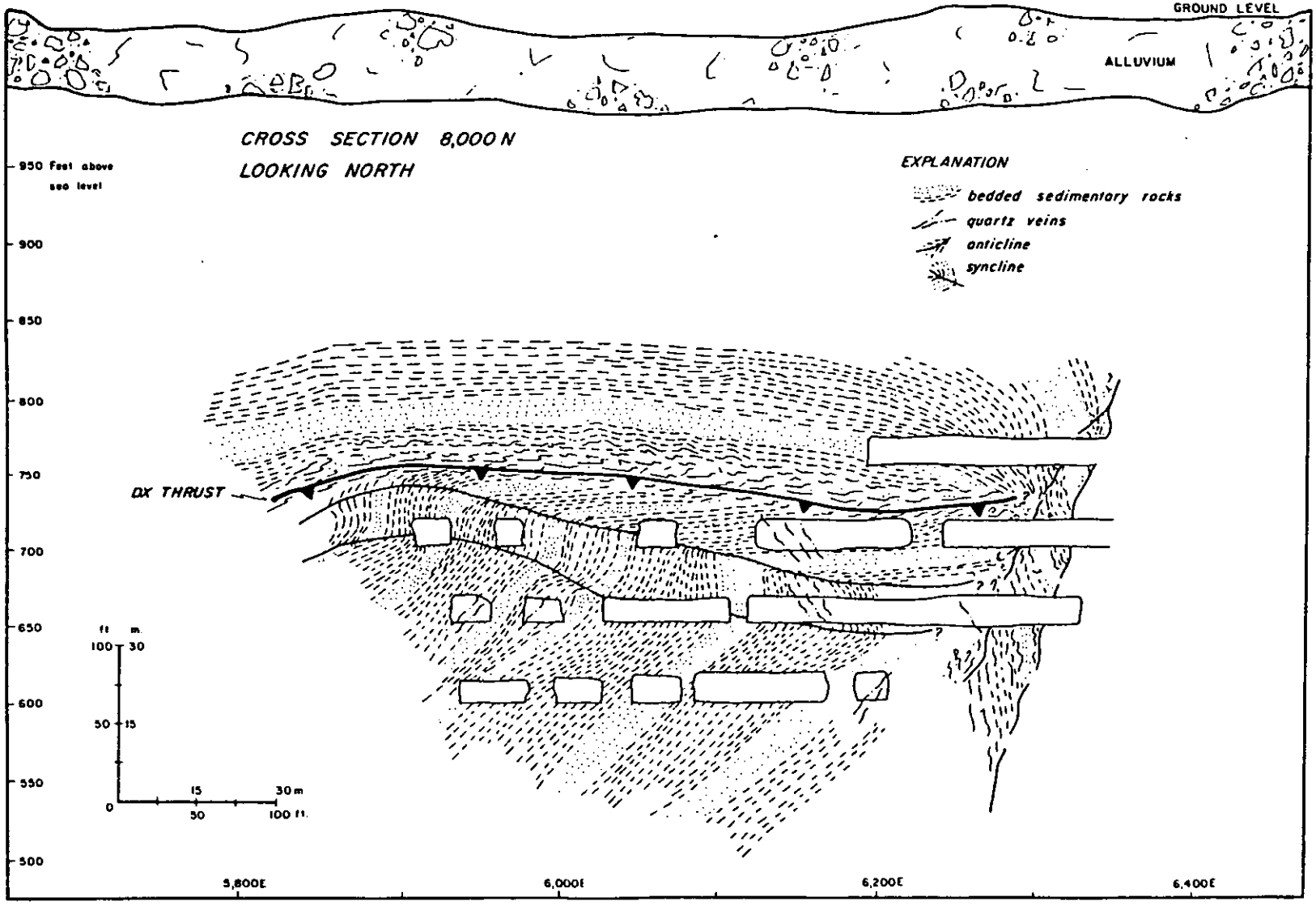

Figure 26. East-West cross section 8000 N through the D stope area of the "B" North ore body, looking north.

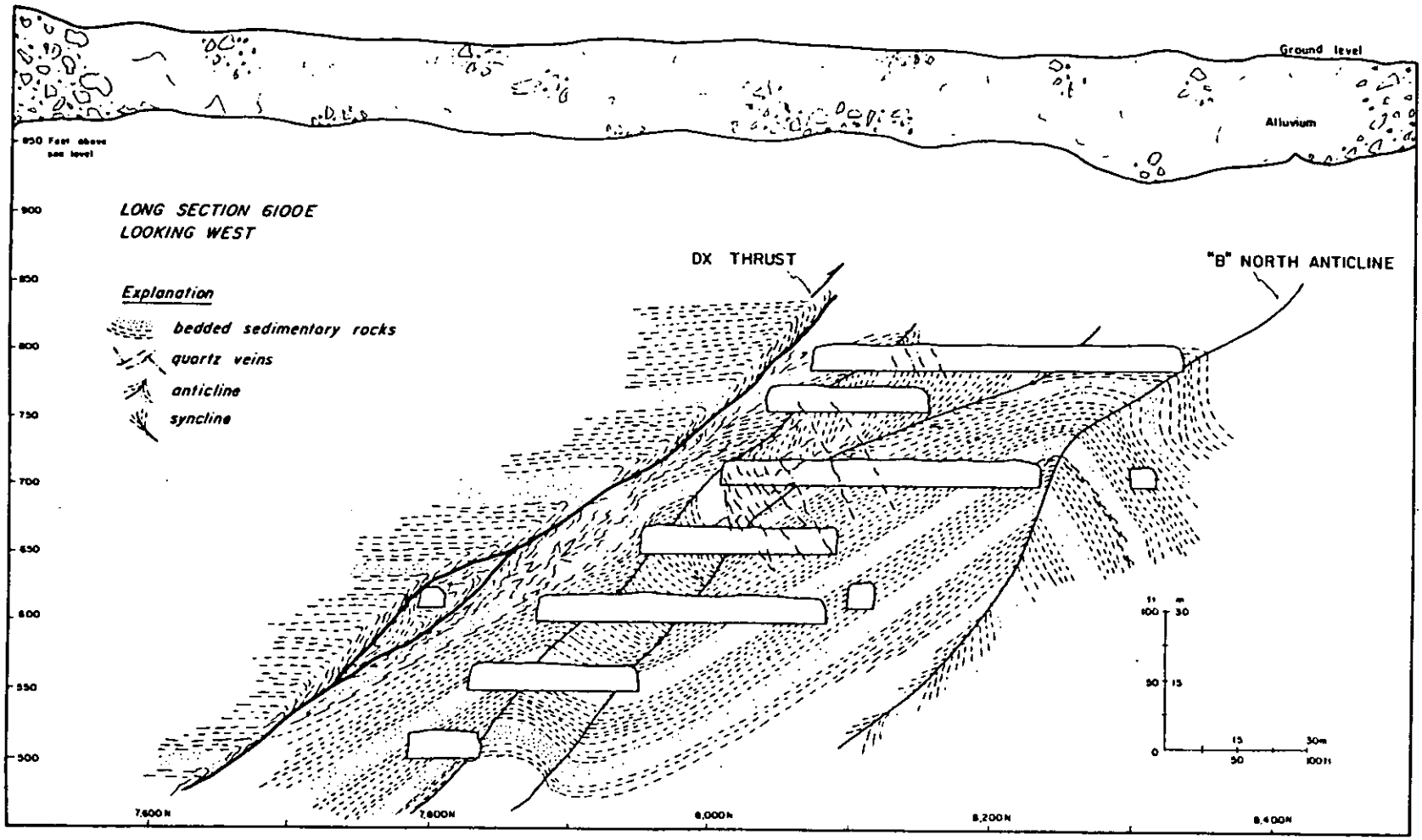

Figure 27. North-south long section 6100 E through the "B" North ore body, Cannon mine, looking west.

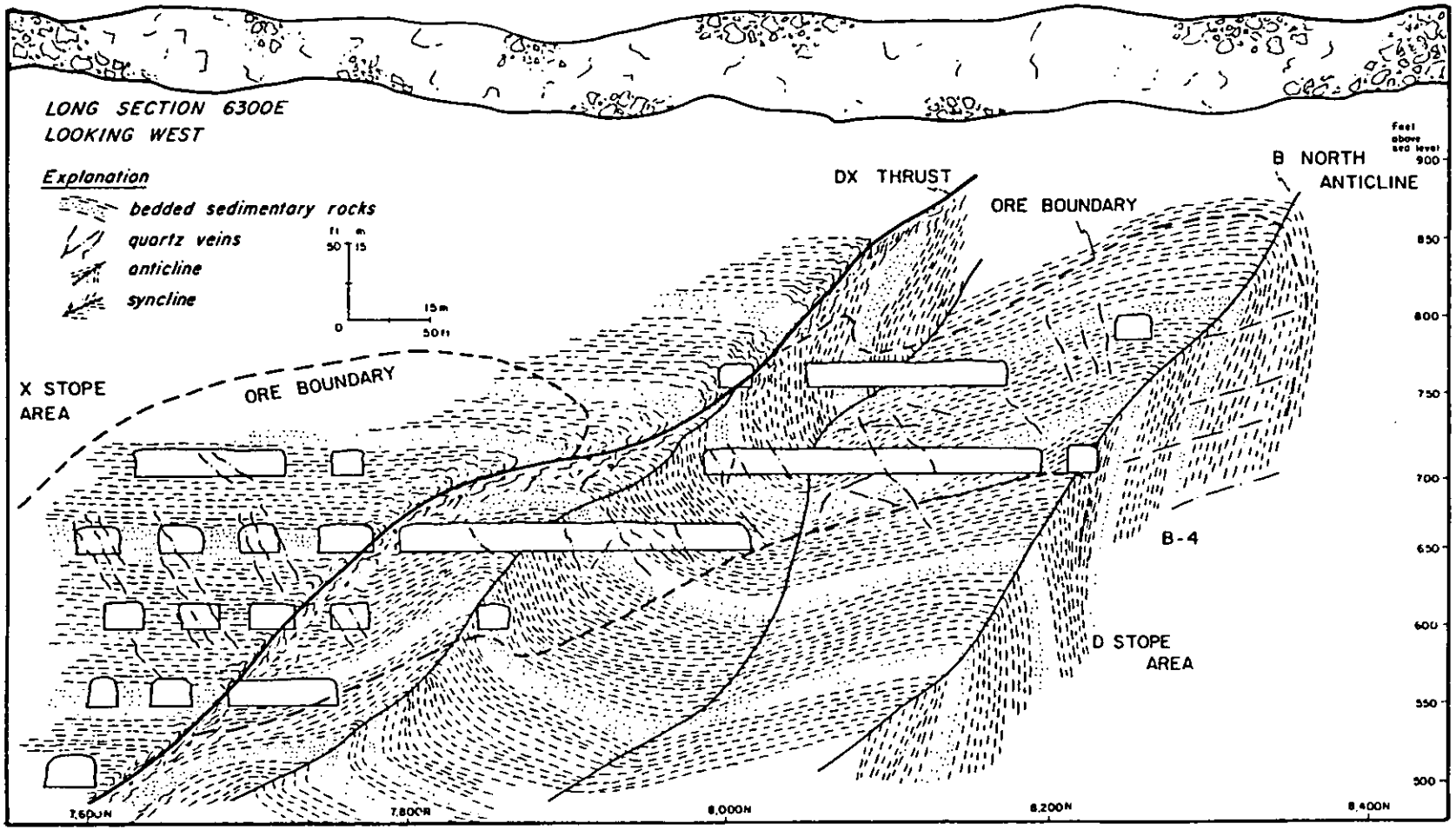

Figure 28. North-south long section 6300 E through the "B" North ore body, Cannon mine, looking west. The X stope area can be considered as the upper portion of the "B" Neath ore body.

The sedimentary host rocks were deformed by both layer-parallel slip and layer-parallel flow during folding. Carbonaceous siltstone and claystone beds flowed plastically into the hinge regions of the folds (Figure 30). Feldspathic sandstone and silty sandstone beds have well developed shear surfaces on many bedding planes.

The geometry of northwest-trending folds in the X stope area of the "B" North ore body and in the "B" West and "B" ore bodies are poorly defined. On the 690 level (Figure 21) sedimentary rocks hosting ore are folded into a tight anticline with a near-vertical axial plane and a north-trending axis. In the "B" reef, folds with northwest-trending axes are present (Figure 18). The relationship of these folds with respect to the "B" North anticline is uncertain.

There are at least two generations of pre- or intra-mineralization fractures in the "B" reef complex. In the "B" North ore body, an early, minor vein set occupies fractures distributed radially about fold hinges. These fractures strike subparallel to fold axes and dip perpendicular to bedding. The majority of veins in the "B" North ore body occupy northwest-trending normal faults. Details of vein orientations are shown in Figures 19 through 25; a generalized composite map which illustrates vein attitude trends is shown in Figure 32. Vein-filled faults generally trend north to northwest in the D stope area of the "B" North ore body; in the X stope area, the majority of vein-filled fractures trend near N90^{o}W (Figure 32).

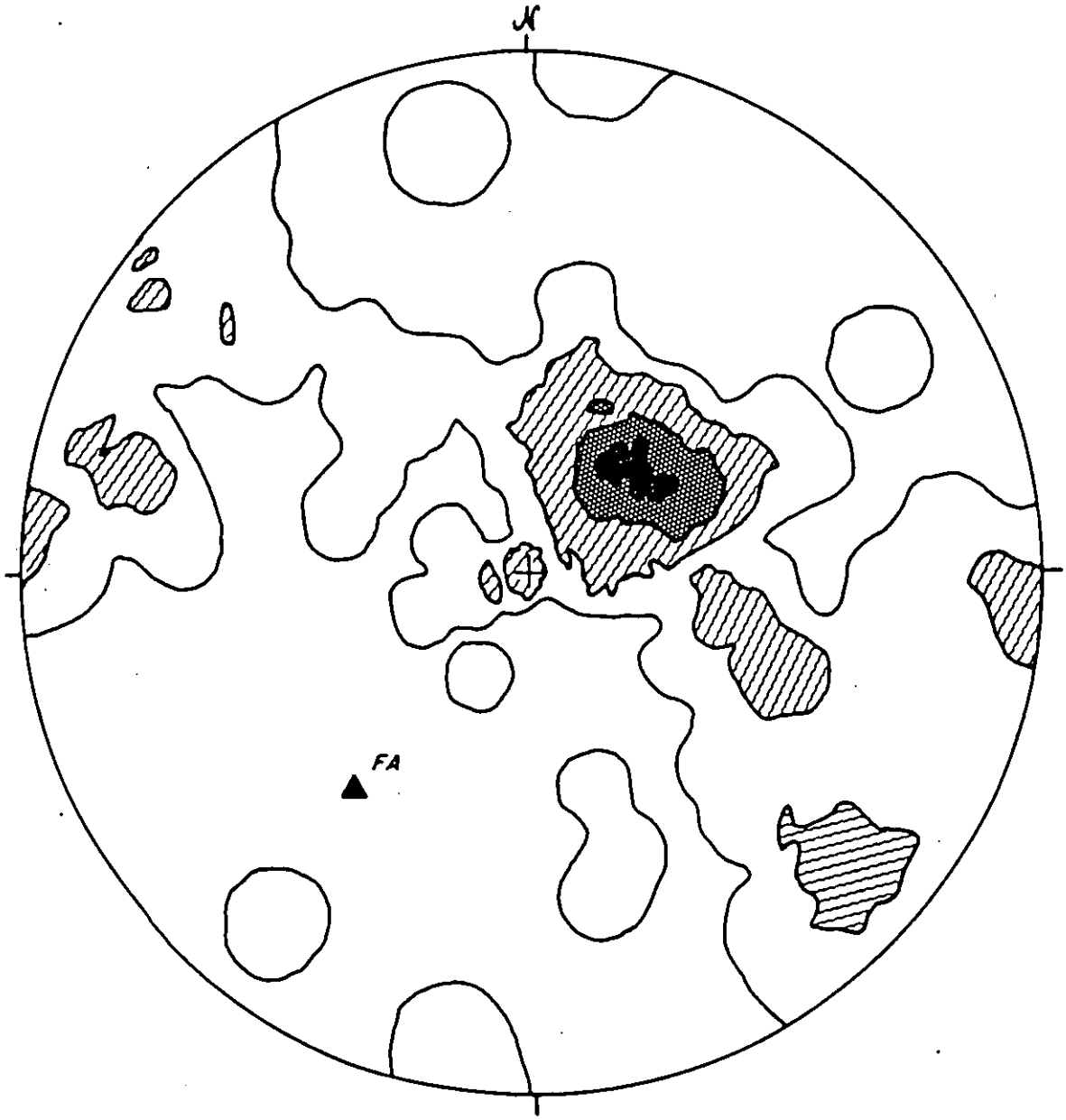

Figure 29. Equal area plot of bedding poles from the the "B" North anticline in the D stope area of the "B" North ore body. Contours at 1%, 5%, and 9% per 1% area, 196 observations. Maximum concentration is 13% per 1% area. The statistical fold axis defined by bedding poles is plotted as FA.

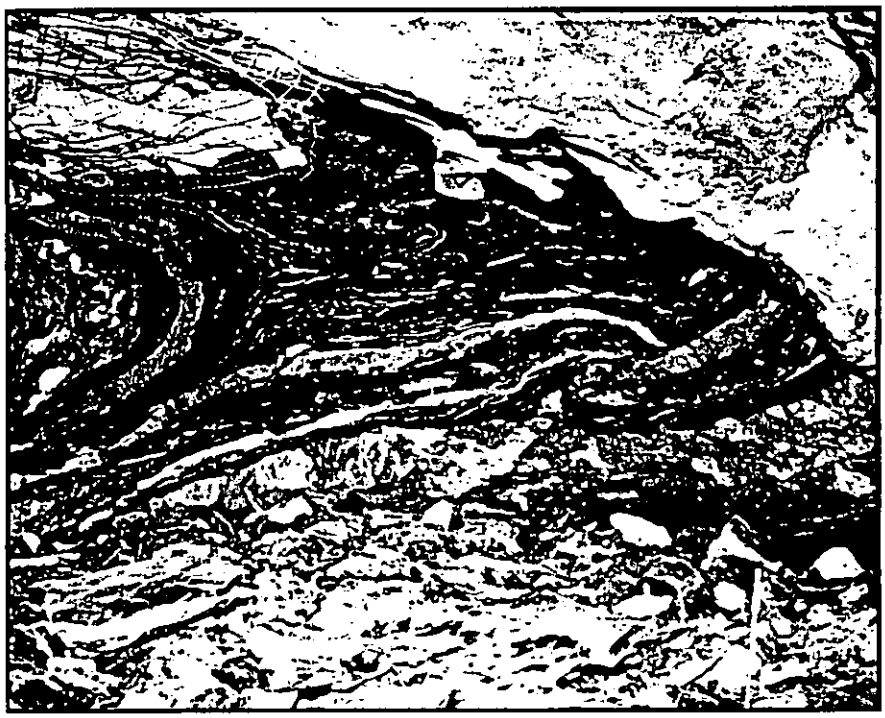

Figure 30. Southeast-trending asymmetric syncline in the D 36 stope on the 650 level of the "B" North ore body. Note ductile flow of carbonaceous silty claystone beds into the hinge area. Viewed to the north, stake on muck pile in lower right part of photograph is about 1 meter long.

Analysis of vein orientations in the D stope area of the "B" North ore body shows that they are related to fold geometry of the "B" North anticline (Figure 33). Vein poles from this part of the ore body cluster around the statistical fold axis defined by bedding poles (Figure 29), and indicate that the fractures hosting veins were generated by extension parallel to the fold axis (a-c extension, refer to Hobbs and others, 1976, p. 294). Fractures hosting veins in other parts of the "B" reef complex have not been thoroughly investigated. The change in vein orientation from northwest to east-west passing from the D stope area to the X stope area is accompanied by a change in fold axis orientation from nearly east-west to northwest. This suggests that a similar arrangement between fracture orientations and folding may exist in the "B" Neath and "B" West ore bodies.

The structural behavior of sandstone and siltstone beds in the "B" reef complex in response to pre- and intra-mineralization deformation events is interpreted to be transitional between brittle and ductile. The rocks were sufficiently competent to fail by brittle fracture as is indicated by open-space-filled veins. However, isolated fragments of dismembered veins are common in the "B" reef complex, and occur in many localities where primary sedimentary layering does not appear to be significantly disturbed (Figure 31). The ability of detrital grains to flow around disjointed vein fragments is interpreted to be a significant reflection of fluid pressure during the period of pervasive alteration and

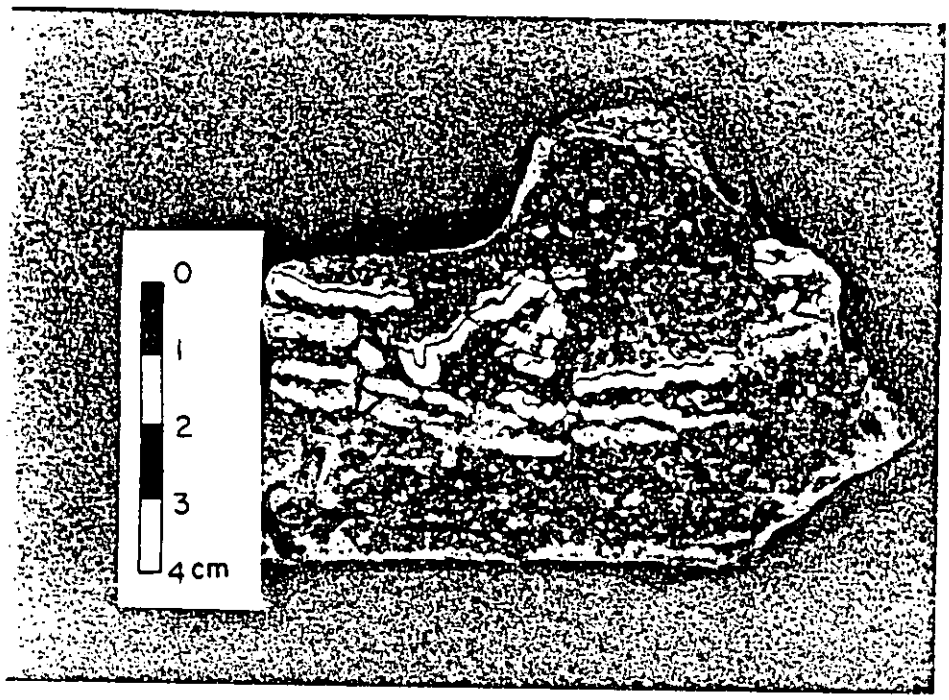

Figure 31. Dismembered quartz-adularia veinlet in medium-grained feldspathic sandstone from the 700 level of the "B" North ore body. Vein has been stained with sodium cobaltinitrate to show potassium feldspar content. Significant ductility, enabling detrital grains to flow around vein fragments is implied by this texture.

mineralization; the rocks evidently responded in a ductile manner to intra-mineralization deformation. The presence of both brittle and ductile deformation features in individual sedimentary beds may indicate variations in strain rates during the period of mineralization; brittle fractures, now filled with crustified quartz-adularia veins, may have developed during periods of accelerated strain, whereas vein dismemberment and ductile flow of detrital grains around dismembered vein fragments may have occurred during periods of reduced strain rate.

The principal post-mineralization structure at the "B" reef complex is a fault that marks the eastern boundary of the ore bodies. This north-south trending fault separates the ore bodies from intrusive rocks of the Wenatchee Dome (Figure 18). Minor folds in this fault zone have near-vertical axes, and lineations in carbonaceous gouge material are subhorizontal. These features indicate that displacement on the fault was strike-slip, rather than dip-slip. In most exposures, the fault between Wenatchee Dome and the "B" reef complex is 10 to 30 meters in width. However, on the 590 level (Figure 23), the fault narrows to about 25 cm. Here, although the perlite margin of the Wenatchee Dome intrusion is only a few centimeters from the intensively silicified and mineralized sedimentary rocks of the X stope area, perlite is not altered or devitrified. Fold axes of the "B" North anticline and related folds are truncated by this fault. Ott and others (1986, p. 432) interpreted this relationship to indicate that

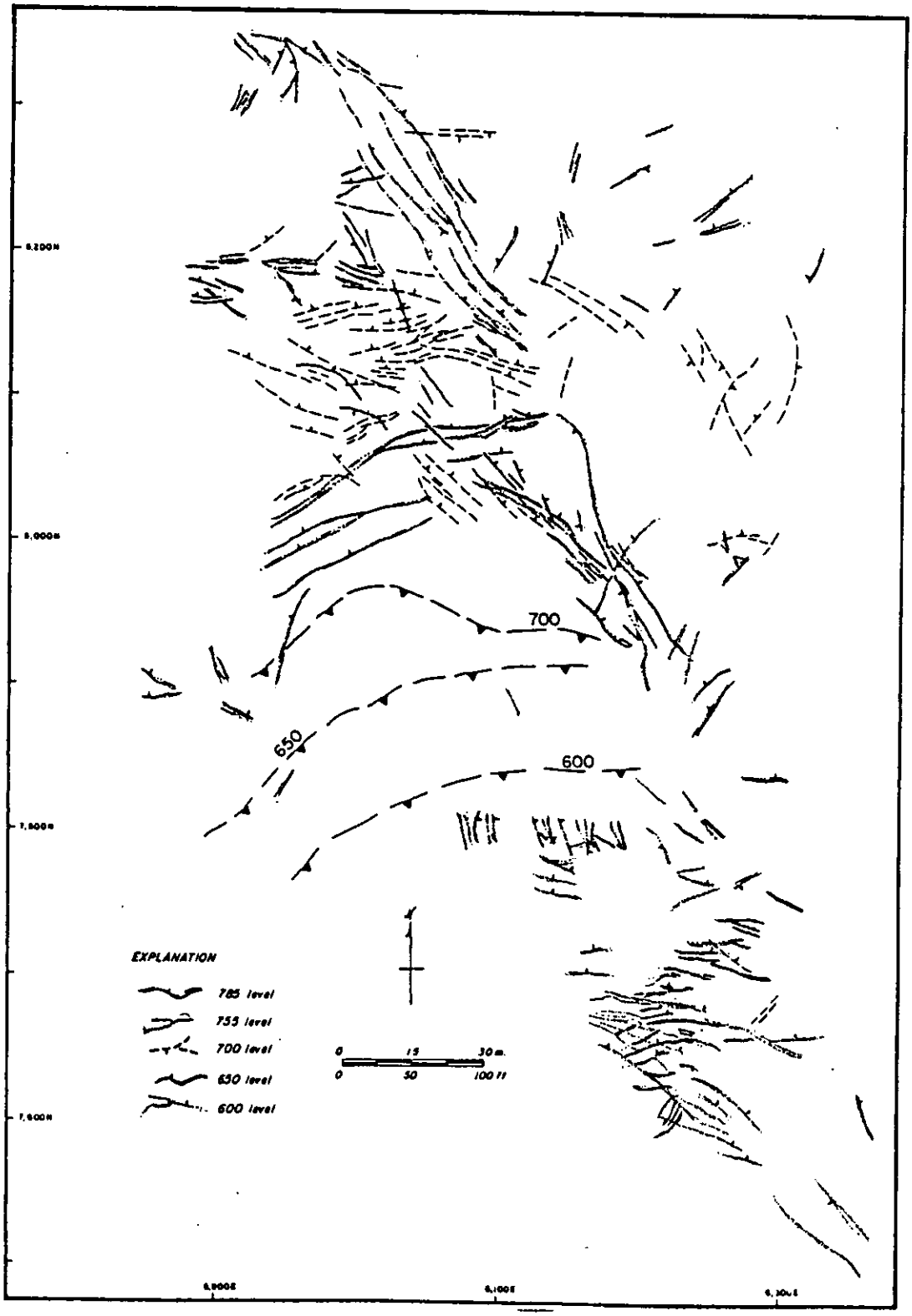

Figure 32. Composite map of vein orientations in the "B" North ore body, including the D stope and X stope areas. Note the abrupt change in vein orientations across the DX thrust. The location of the DX thrust on the 700, 650, and 600 levels is indicated.

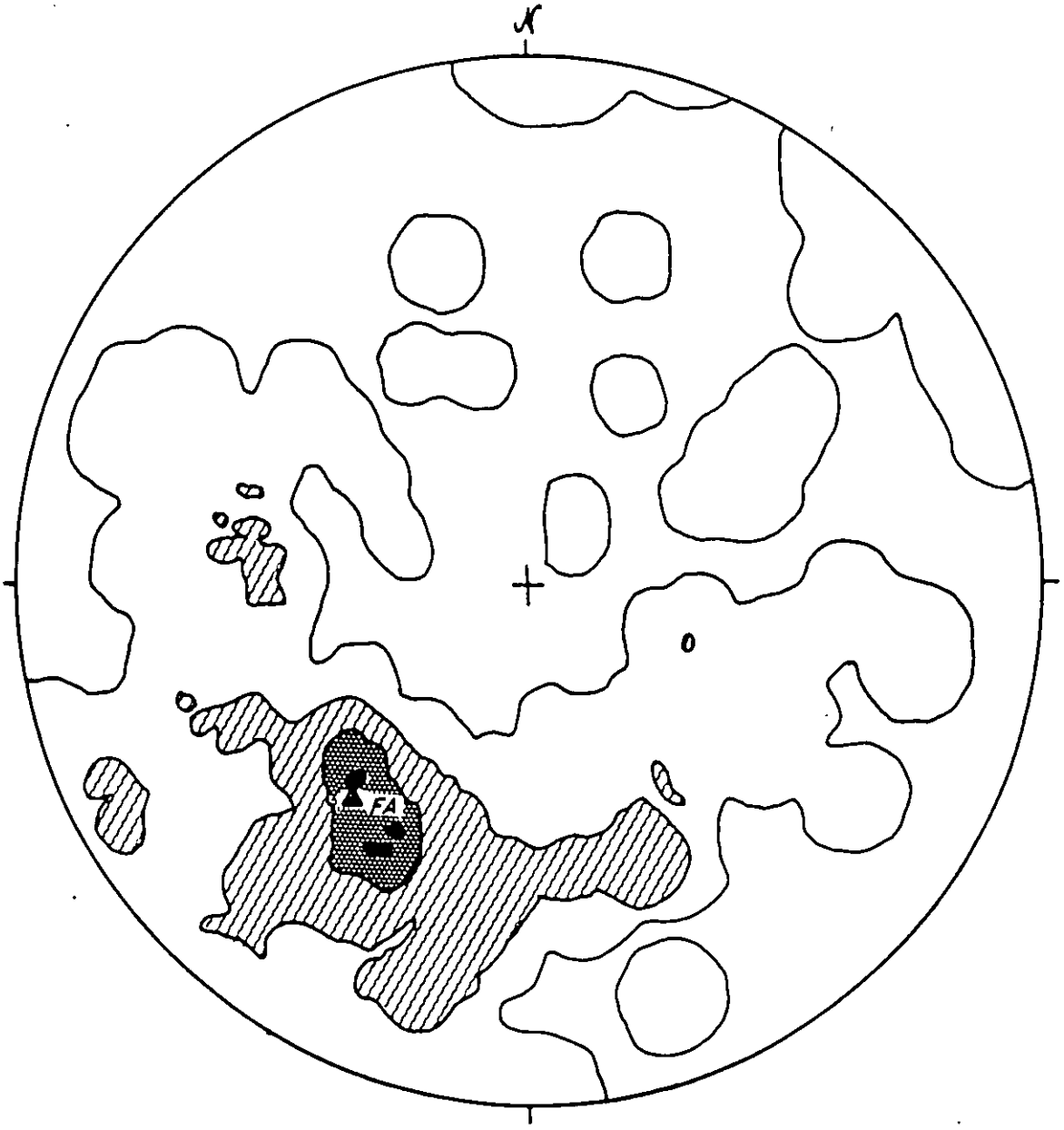

Figure 33. Equal area plot of vein poles from the D stope area of the "B" North ore body. Contours at 1%, 5%, and 9% per 1% area. Maximum concentration is 15% per 1% area. Most vein poles lie near the statistical fold axis derived from bedding poles (plotted as FA). 165 observations.

post-mineralization emplacement of the Wenatchee Dome rhyolite was responsible for development of the fault zone between the intrusion and ore bodies. Alternatively, the fault may post-date both the mineralization event and emplacement of the Wenatchee Dome intrusion.

Final movement on the DX thrust also appears to post-date mineralization. The DX thrust is essentially coplanar with the axial plane of the "B" North anticline (Figure 27), which may indicate that this fault was initially developed during folding. However, the "B" Neath ore body and the X stope area of the "B" North ore body appear to have been thrust over the D stope area, which attests to final post-mineralization movement.

Other post-mineralization structures include a northeast-trending fault present in the eastern part of the "B" North ore body (Figures 18 to 26), and fault zones that separate the "B" reef, "B" West and "B" Neath ore bodies. The orientation and nature of movement on these structures remain poorly defined.

Stratigraphy

Gold mineralization in the "B" reef complex is hosted by a repetitive sequence of interbedded sandstone, sandy siltstone, siltstone, and claystone. No marker bed or sequence of beds common to all ore bodies has been identified. Details of the stratigraphy in the "B" Neath and "B" West ore bodies have not been investigated as yet, owing to limited exposure.

Stratigraphic information for the "B" Neath and "B" West ore bodies is restricted to drill core information and exposures in a limited amount of development drifts. The "B" Neath ore body, based on drill core information, appeared to consist largely of brecciated feldspathic sandstone, to the extent that the original stratigraphy may not be preserved. However, exposures in the initial development drifts on the 440, 360, and 200 levels have revealed that much of the original stratigraphy is preserved, and that breccia constitutes less than half of the "B" Neath ore body (D. Groody, oral communication, 1988).

The relative competency of various sedimentary lithologies during the period of deformation responsible for development of the "B" North anticline partially controlled the location of mineralization and alteration in the "B" reef complex. Feldspathic sandstones and sandy siltstones are apparently favorable ore hosts because they failed by fracture during the folding event. The dilatant openings that resulted are radial to fold hinges (radial joints) and perpendicular to fold axes (a-c joints). Carbonaceous siltstone and mudstone beds deformed in a ductile manner during the folding event and developed no dilatant openings (Figures 30 and 34). This control of stratigraphy over ore boundaries has only been identified to a significant extent in the D stope area of the "B" North ore body, but has been observed locally throughout the "B" reef complex (Figure 34).

Figure 34. Local stratigraphic control of ore boundaries in the "B" North ore body. Quartz-adularia-gold vein is well developed in pervasively silicified feldspathic sandstone in the lower half of the photograph. The vein terminates abruptly against unaltered carbonaceous silty claystone beds in the upper part of the photograph. Photograph location is the X-21 stope of the "B" North ore body on the 650 level, viewed to the west. Hammer is 45 cm long.

The D stope area of the "B" North ore body, as well as the "B-4" ore body, is partially stratabound within a 40 meter-thick section of sandstone, sandy siltstone, siltstone, and mudstone. Sandstone and sandy siltstone beds in the mineralized section are light-gray and feldspathic. Detrital grains are angular to subangular and poorly sorted, and consist primarily of quartz, K-feldspar, and plagioclase, with lesser amounts of chlorite (after biotite), muscovite, zircon, and epidote. The matrix of these sandy beds, which normally consists of clays, disaggregated lithic fragments, and calcite, is completely replaced by quartz, adularia(?), and pyrite in the mineralized section. Siltstone and mudstone beds are generally dark-brown to dark-gray and carbonaceous. Carbonized plant material is common on many bedding surfaces, and fragments of coal-like material have been observed in drill core from above the "B-4" ore body. Thin, intensively altered tuff(?) beds are present locally within the mineralized section, and generally have a blue-gray to green-gray waxy appearance. These tuff(?) beds do not appear to have extensive lateral continuity. Less altered tuff beds, 3 to 5 centimeters thick, have been identified in drill core west of the "B" Neath and "B" West ore bodies, but their potential usefulness in deciphering the stratigraphic section has not been investigated.

Ott and others (1986, p. 428) divided the 40 meter-thick mineralized section in the D stope area into four units (Figure 35). Their description of these units, in descending

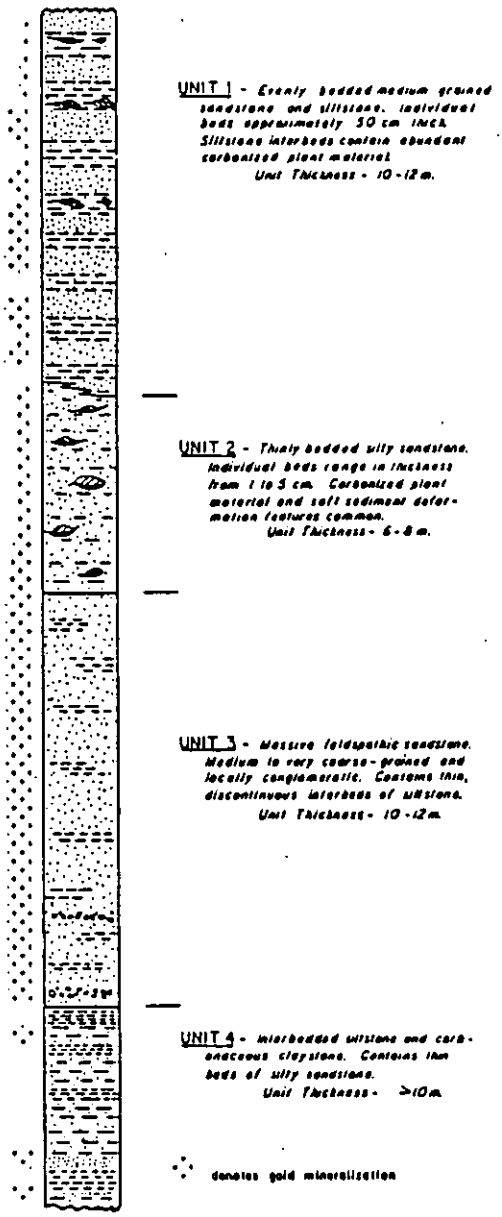

Figure 35. Generalized stratigraphic column showing mineralized sedimentary rocks in the D stope area of the "B" North ore body. Gold mineralization occurs as 0.1 to 0.5 millimeter grains of electrum, associated with pyrite, tetrahedrite(?), and pyrargyrite(?) in the silicified matrix of the rocks (from Ott and others, 1986, fig. 5).

order, is reproduced here with additional details.

Unit 1 consists of approximately 12 meters of evenly-bedded sandstone and siltstone. Beds are generally 15 to 50 centimeters thick. The sandstone interbeds of this unit are gray, medium-grained, and feldspathic. Clastic grains are angular to subangular and poorly sorted. The siltstone interbeds are medium- to dark-gray, and contain laminae and lenses of carbonaceous plant material. Siltstone becomes increasingly abundant, finer grained, and more carbonaceous at the top of unit 1, and this clay-rich, carbonaceous layer is the upper boundary of economic mineralization in the D stope area. Ductile flow of the fine-grained upper portion of unit 1 into the hinge region of an overturned syncline is well displayed in Figure 30. A typical example of the appearance of unit 1 is shown in Figure 36. Note the fragmented appearance of the medium-gray sandstone in the center of Figure 36, and the well-preserved continuity of dark siltstone beds above and below the sandstone bed. This apparent <u>in situ</u> brecciation of medium- to coarse-grained feldspathic sandstone beds is common in the "B" North ore body, and is interpreted to be a result of tectonic adjustments during the period of pervasive silicification, when the sandstone beds were saturated with hydrothermal fluids.

Unit 2 is approximately 6 meters thick and consists of thin interbeds of silty sandstone and carbonaceous siltstone (Figure 37). Vein development in this unit is generally not as good as in units 1 and 3, possibly due to the more finely

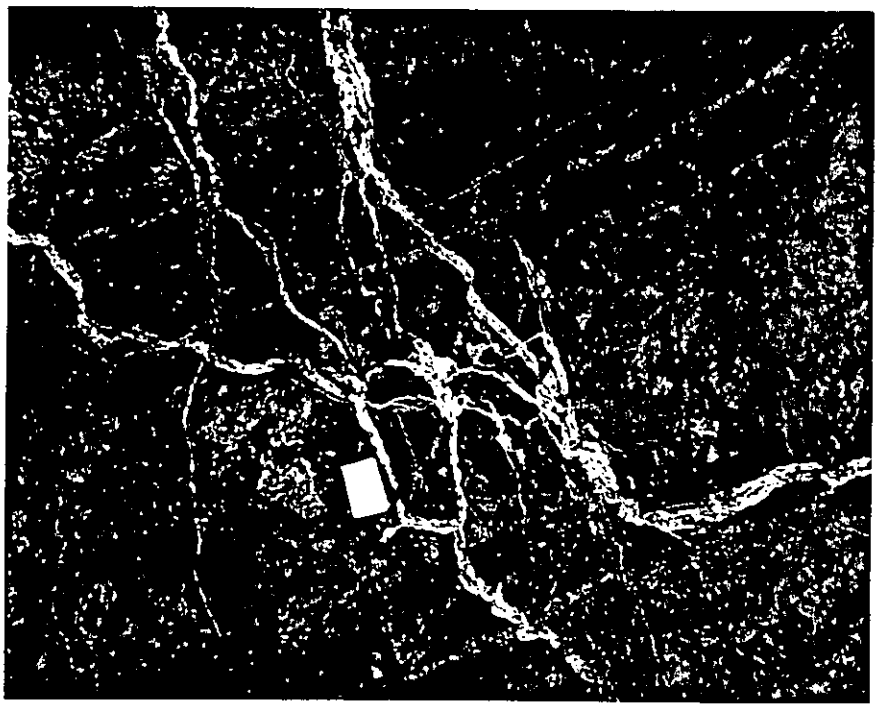

Figure 36. Typical exposure of unit 1 on the 700 level of the "B" North ore body. The brecciated appearance of the medium-gray sandstone bed in the center of the photograph contrasts with the well-preserved continuity of bedding planes in dark-gray siltstone beds above and below the sandstone bed. Note the bulbous nature of the veins, and the non-parallel nature of the vein walls, features that may indicate that the behavior of these sedimentary rocks during deformation periods was intermediate between brittle and ductile. Also note the tendency of quartz veins to follow bedding planes. Field book for scale is 18 cm long.

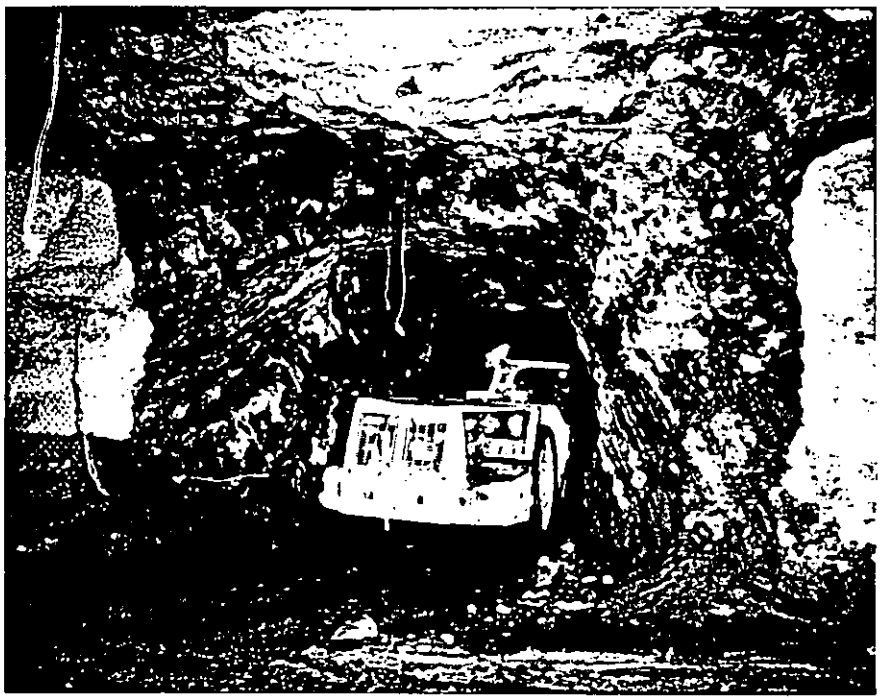

Figure 37. Thinly laminated siltstone and sandy siltstone beds of unit 2 as exposed on the 500 level. Vein development in this unit is generally poor, owing to the less massive nature of individual beds. Note the cement-backfilled stopes on both sides of the pillar being mined. Photograph courtesy of J. Baz Dresch, Asamera Minerals (US) Inc.

laminated, less massive nature of individual beds. Carbonaceous plant material and pyrite occur as lenses and laminae throughout this unit, and well-preserved plant fossils are common on many bedding surfaces. Unit 2 is particularly useful in determining locations where the sediments have been overturned because it contains an abundance of well-preserved sedimentary structures. Soft sediment deformation features, in the form of load casts, rip-up clasts, and flame structures are present, and wisp-like cross bedding is commonly well-preserved in the more sandy interbeds of this unit.

Unit 3 consists of 10 to 12 meters of massive feldspathic sandstone with minor lenses of siltstone. The unit is medium- to very coarse-grained, and locally pebbly. Detrital grains are angular and poorly sorted (Figure 41). Fractures that host veins are particularly well-developed in this unit, and finer-grained sediments above and below unit 3 have accommodated much layer-parallel deformation as a result of folding of the sedimentary package. These structural features related to unit 3 are interpreted to be a reflection of the relatively competent nature of the massive sandstone in respect to the surrounding silty beds. Primary sedimentary structures are not well-preserved in unit 3, and, like the sandy beds in unit 1, the initial physical characteristics of this unit may have been internally reorganized as a result of the replacement of the original sandstone matrix by hydrothermal quartz. The exact nature of this reorganization is uncertain; however, in many instances, fragments of vein

material are isolated in altered, but otherwise apparently undisturbed sandstone beds. This suggests that these beds were sufficiently fluidized at the time of vein formation and mineralization to allow detrital grains to flow in response to intra-mineralization structural adjustments (Figure 32).

Unit 4 is a dark-brown, medium- to very fine-grained sandy siltstone with interbeds of carbonaceous claystone. This unit is at least 10 meters thick, and marks the lower boundary of alteration and mineralization in the D stope area of the "B" North ore body. Carbonaceous claystone beds in unit 4 deformed in a ductile manner during deformation events, and, like equivalent beds in unit 1, appear to have restricted infiltrational flow hydrothermal fluids, and would have provided an effective stratigraphic control over mineralization (Figure 38).

From the above descriptions, it is evident that, on the limited scale of observation within the "B" reef complex, stratigraphy is an important factor in both the location of ore boundaries and variations in the style of veining within the mineralized section. However, when considered in view of the fact that at least several thousand meters of similar-appearing sedimentary rocks are present in the Wenatchee district that are not mineralized, very little is presently known about the influence that stratigraphy has had on the localization of mineralization on a district scale.

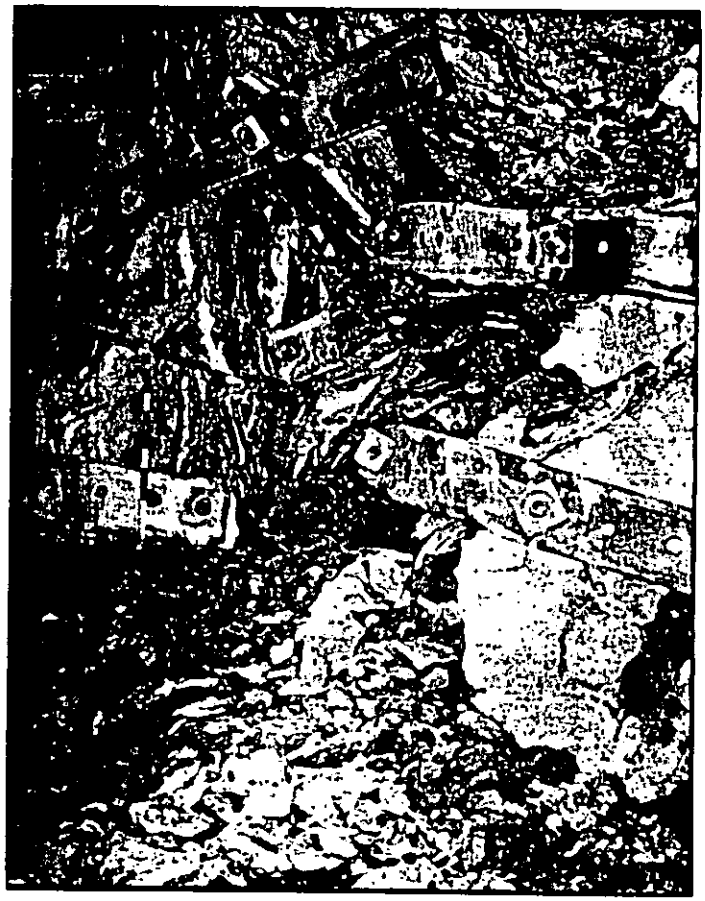

Figure 38. Carbonaceous siltstone beds of unit 4 that have been squeezed into the hinge of an anticline adjacent to the DX thrust on the 650 level, D stope area, "B" North ore body. These fine-grained siltstone and claystone beds mark the lower boundary of mineralization in the south-dipping limb of the "B" North anticline. The stake in the left-center of the photograph is approximately 1 meter long, view is to the northeast.

Wall-Rock Alteration and Mineralization

Mineralization in the "B" reef complex consists of widely spaced veins in silicified and mineralized feldspathic sandstone and sandy siltstone. The highest grades of mineralization are confined to quartz-adularia veins which range in width from less than 25 mm to greater than 50 cm. Gold and silver values are also present in locally developed hydrothermal breccias and quartz-veinlet stockworks. Lower grades of mineralization are present in feldspathic sandstone and sandy siltstone beds that have been subjected to selectively pervasive silicification and pyritization.

Alteration types associated with mineralization at the "B" reef complex include argillic alteration, silicification, potassium silicate alteration, carbonate alteration, pyritic alteration, and possible weak sericitic alteration. Argillic alteration, silicification, and pyritic alteration have a selectively pervasive character; potassium silicate alteration and carbonate alteration are mostly confined to veins and veinlets. This study concentrated primarily on changes in the host rock that were brought about by selectively pervasive silicification, and on the nature and paragenesis of adularia, calcite, and quartz in veins in the "B" North ore body. The nature of the argillic zone has not been studied in great detail, other than to note the location of "clay altered" rocks in drill logs, and x-ray identification of clays in five samples of these "clay altered" rocks. Sericite has been noted as a minor constituent which has selectively altered

detrital plagioclase grains in all feldspathic sandstone samples that were petrographically examined; it is not certain to what extent the presence of sericite can be attributed to hydrothermal alteration.

Alteration zoning

Argillically altered feldspathic sandstones are present as a relatively thin halo capping the silicified zones that constitute the "B" reef complex. Most of the silicified rocks of the "B" reef complex underlie the valley floor of Dry Gulch, and a zone of argillic alteration extends from the base of alluvial fill in Dry Gulch downward, to the upper contact of the silicified zone (Figure 39). Southeast of the "B" reef complex, patchy zones of argillized sedimentary rocks have been encountered in drill holes between "C" reef and Rooster Comb. The extent of argillic alteration in this area has not been fully delineated, but unaltered rocks are present above argillically altered rocks. This indicates that the argillic zone did not extend everywhere to the paleo-surface.

Selectively pervasive silicification, potassium silicate alteration, and selectively pervasive sericitic alteration (assuming that sericite is a result of hydrothermal alteration, and not a product sedimentary processes) are present in a single mixed zone that underlies the argillic cap. The contact between silicified rocks and argillized rocks is commonly a fault boundary, a result of post-mineralization structural adjustments, and is therefore abrupt.

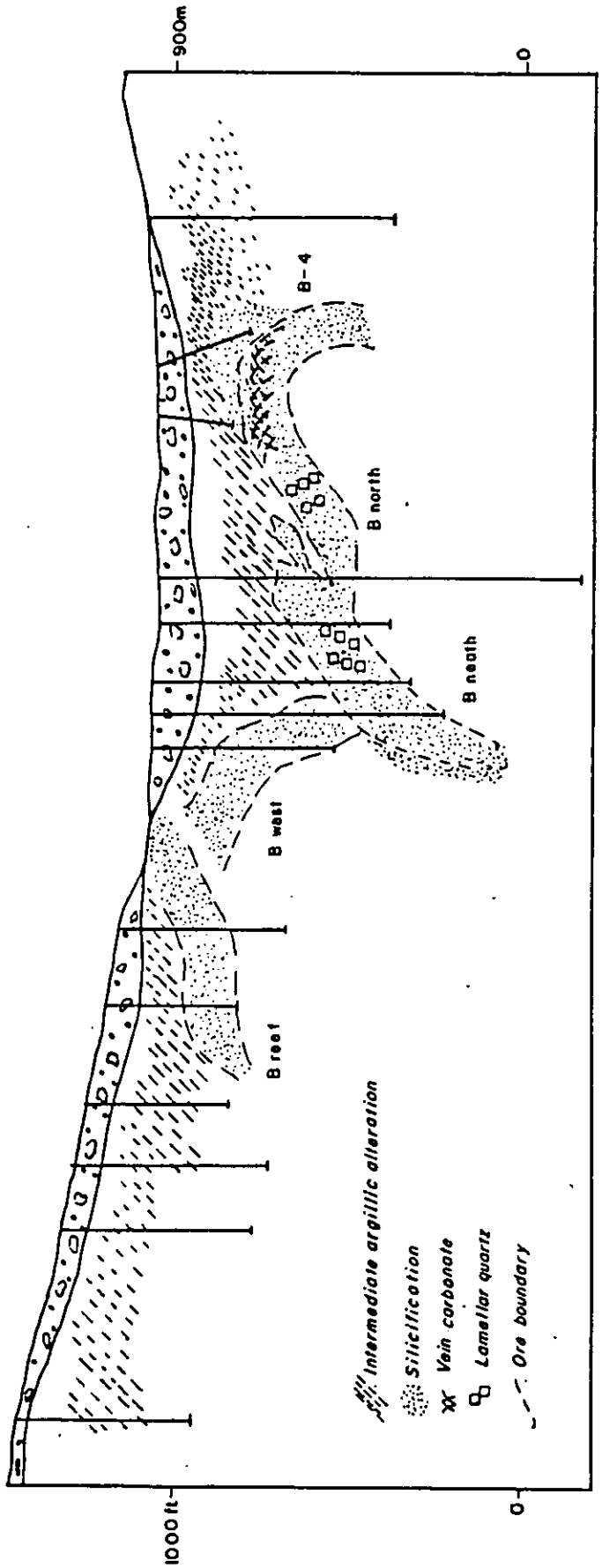

Figure 39. Vertical distribution of alteration zones at the "B" reef complex.

Margolis (1987, p. 47) recognized a widely dispersed zone of propylitic alteration in the Wenatchee Heights area. Criteria used by Margolis to recognize propylitically altered rocks include the presence of chlorite, brown biotite, pink albite, and epidote. In this study, chlorite and brown biotite were found to be ubiquitous, and, like sericite, could not be definitely attributed to hydrothermal processes. Epidote is a common detrital grain present as a minor constituent in the feldspathic sandstones of both the Chumstick Formation, and the rocks of uncertain age in the central portion of the district. Pink albite was not recognized in altered rocks at the "B" reef complex; however, weakly altered rocks were not examined in detail, and the presence of pink albite, and epidote, as a replacement of plagioclase, is not discounted or verified by this study.

Carbonate alteration is essentially restricted to veins and veinlets in the "B" reef complex, and the zonation of carbonate-bearing veins will be discussed in a later section. Pyrite is common to all alteration zones at the "B" reef complex.

Intermediate argillic alteration

Intermediate argillic alteration is well developed only in feldspathic sandstone beds, and is both selectively pervasive and pervasive in style; the intensity of argillic alteration varies from weak to strong. Strongly argillized sedimentary rocks do not crop out owing to their lack of

resistance to weathering. Weakly to moderately argillized sedimentary rocks are exposed in road cuts on the ridge between "D" reef and "B" reef, and along a jeep trail west of Saddle Rock (Plate 1). These rocks are bleached and overprinted by the affects of supergene alteration; gypsum veinlets are characteristic of surface exposures of argillized rocks. The Saddle Rock andesite is moderately argillized east of "F" reef (Plate 1) and has a distinctive mottled green and light-gray color. In hand sample, chlorite and smectite(?) can be recognized in argillized andesite.

The first indication of argillic alteration in drill core is the appearance of small discontinuous fractures and veinlets filled with dark-yellow to pale-gray smectite(?). In some instances these clay-filled veinlets appear to be a stockwork, but they most commonly occur as planar fractures in the core. Disseminated, very fine-grained pyrite is generally present in the matrix of rocks that are cut by clay-filled fractures, and indicates incipient pervasive alteration. With increasing intensity of alteration, biotite and feldspar grains are altered to chlorite and smectite(?) respectively. In moderately argillized sandstone beds, biotite is not recognizable, but detrital quartz, and the outline of detrital feldspar grains that have been altered to smectite(?) can be identified. Strongly argillized feldspathic sandstone beds in drill core samples are a pale green-gray color and commonly contain up to 2% pyrite as fine disseminations and irregular clots up to 3 cm in diameter. The rocks are very soft and NX-

size core can easily be split with a knife blade. The core decrepitates to scaly and powdery clay with interspersed granular quartz grains after 2 - 3 days of exposure to air. An example of feldspathic sandstone that has been intensively argillized is shown in Figure 40.

Clay minerals in the argillic zone were identified by x-ray diffraction in five samples from the argillic cap above the "B" North ore body. In each case, smectite was the principal clay mineral, and small kaolinite peaks were present. Pyrite is invariably present as clots and disseminations, and attests to the hypogene origin of the intermediate argillic zone.

The restriction of strong argillic alteration to feldspathic sandstone beds suggests that permeability and porosity were important factors in controlling the location of this alteration type. Fine-grained, carbonaceous siltstone and claystone beds are not appreciably altered, and commonly mark the upper boundary of intermediate argillic alteration in the area southeast of the "B" reef complex. These fine-grained beds evidently acted as barriers to fluid migration.

Weakly argillized rocks have not been examined in sufficient detail to recognize clay mineral paragenesis. Similarly, neither the lateral distribution of argillically altered rocks, in respect to silicification, nor the variation in clay mineral types within the intermediate argillic zone have been studied to the extent required for meaningful interpretation.

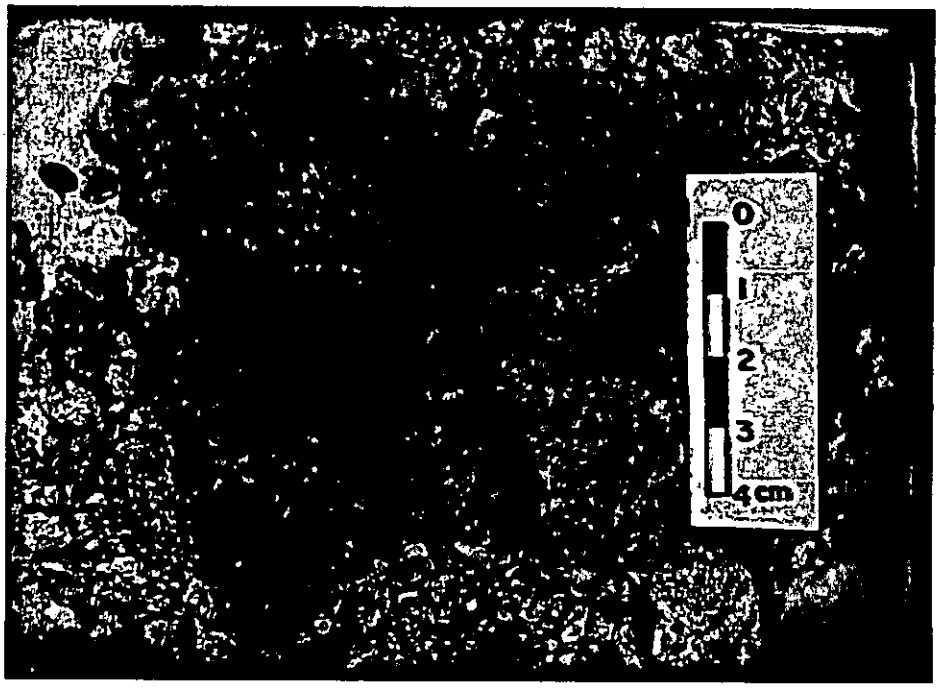

Figure 40. Strong intermediate argillic alteration in feldspathic sandstone, drill hole B87-7B, 118 feet down hole.

Silicification

Introduction of hydrothermal quartz in sedimentary rocks at the "B" reef complex has significantly changed the physical characteristics of the rocks. Unaltered feldspathic sandstones near the "B" reef complex are poorly indurated and friable. In thin section, these unaltered rocks have a matrix of fine-grained clay minerals, and disaggregated lithic fragments. The matrix material has been replaced by hydrothermal quartz and pyrite in silicified sandstone beds, a process that has resulted in a thoroughly indurated rock.

The intensity of silicification ranges from weak to very strong; weakly to moderately silicified beds are not always obvious as hydrothermally altered rocks, but strongly silicified rocks are generally accompanied by breccias and quartz veins. In drill core, weakly to moderately silicified sandstone beds have the appearance of a well-lithified feldspathic sandstone. Detrital feldspars, quartz, and lithic fragments are recognizable, and, except for the presence of pyrite and the more competent nature of beds, silicification, as such, is not readily evident. With increasing intensity of silicification, millimeter-wide dark-gray quartz veinlets may appear, both as stockworks, and as planar fractures filled with very fine-grained quartz. Strongly silicified sandstone beds are generally cross-cut by multiple generations of quartz veins and commonly contain local hydrothermal breccias.

Petrographic examination of samples of silicified sandstone and silty sandstone beds, primarily from the 600,

650, and 700 levels of the "B" North ore body reveal that mineralogical changes due to silicification are minor. The most pronounced change is replacement of the matrix of sandstones by fine-grained quartz and pyrite, possibly associated with adularia. The matrix of unaltered sandstone beds consists of calcite + various clay minerals + dissaggregated lithic fragments. These have been replaced by very fine-grained quartz + pyrite + chlorite + adularia(?) + sericite(?) + ore minerals. The ore minerals in silicified wall rock will be discussed in a later section. Detrital quartz and feldspar grains are rimmed with hydrothermal quartz and pyrite, but only weakly altered to sericite (Figure 41). The alteration style is therefore selectively pervasive. Adularia has not been confidently identified in thin section; the matrix of silicified sandstone beds takes a faint sodium cobaltinitrate stain that can be seen in thin section, but the material that stains is too fine grained to be positively identified. Detrital biotite grains are altered to both pyrite + quartz, and chlorite in silicified sandstone beds.

The most apparent effect of silicification is a pronounced decrease in the porosity and permeability of the host rocks. Preliminary tests, based on 10 samples, indicate that medium- to coarse-grained silicified feldspathic sandstone beds from units 2 and 3 have porosities and permeabilities near 9.5% and 4.9 millidarcies, respectively. Unaltered feldspathic sandstone porosities average 13.65%. Permeability tests on unaltered sandstone samples were

(A)

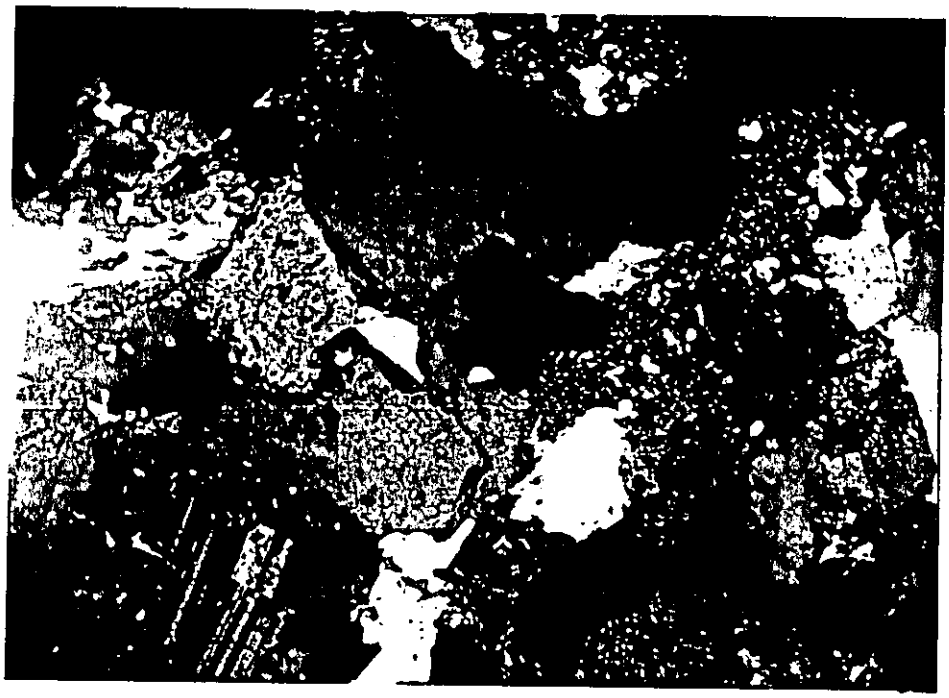

(B)

Figure 41. Photomicrographs of feldspathic sandstone from unit 3 in the "B" North ore body. (A) unaltered, note micaceous matrix clays and angular detrital grains, (B) silicified, showing fine-grained quartz that has replaced matrix. Horizontal field of view is 2 mm.

unsuccessful, but the decrease in porosity resulting from silicification presumably causes a decrease in permeability. Incipient alteration was evidently not an important factor in ground preparation with respect to the development of permeability, although early silicification may have sufficiently modified the physical characteristics of the ore host to enable it to maintain dilatant openings during periods of intra-mineralization fracturing.

Weakly silicified and pyritized claystones of unit 1, sampled at the upper boundary of alteration on the 700 level (Figure 21) have a measured porosity of about 11% and an average permeability of about 0.18 millidarcies. Unaltered claystone porosity measurements range from 16.0% to 18.0%, which indicates that the process of alteration may have decreased porosity by 30% to 35%. A corresponding change in permeability would require the claystone to have an initial permeability of approximately 0.5 millidarcies.

Gold and silver values generally increase with increasing intensity of silicification and potassium silicate alteration. In part because of this association, and in part due to the mining method employed at the Cannon mine, the boundary of material to be extracted, in general, corresponds to the outer limit of silicification. Two exceptions to this are the crest of the "B" reef anticline, where silicification continues upward beyond the limit of economic mineralization, and the deeper portions of the "B" Neath ore body, where silicification and gold mineralization continue downward

beyond the currently planned lowest mining level. The boundary between silicification and unaltered wall rock is generally a structural boundary, and therefore abrupt. However, the western boundary of silicification and potassium silicate alteration in the D stope area of the "B" North ore body is gradational over approximately 20 meters, and evidently represents the boundary of fluid migration.

Sericitic alteration

Sericitic alteration is confined to feldspar grains within the envelope of silicification that constitutes the "B" reef complex. Sericite is minor as an alteration product, and consists of ragged wisps and shreds of sericite that have formed along plagioclase twin planes (Figure 42) and partially replaced orthoclase and microcline grains. It is estimated that about 15% of the detrital plagioclase grains have been weakly sericitized. Unaltered(?) sandstone beds near the "B" reef complex also exhibit weak sericite development in plagioclase, such that, the extent to which sericitization can be attributed to hydrothermal alteration is uncertain. Sericite is not intimately mixed with quartz and pyrite as a sandstone matrix replacement, but since feldspar grains in silicified rocks are weakly sericitized, much of the silicified zone may be viewed as a quartz + sericite + pyrite zone.

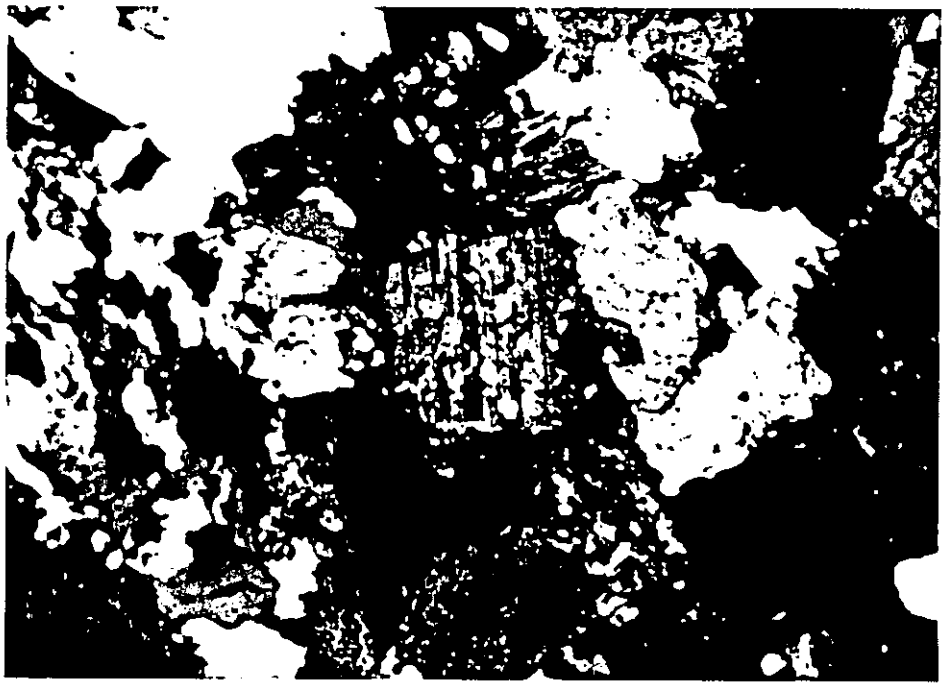

Figure 42. Weakly sericitized plagioclase grain in feldspathic sandstone from the 755 level of the "B" North ore body. Horizontal field of view is 1.25 mm.

Wall-rock mineralization

Gold - silver mineralization in the wall rock of the "B" reef complex is generally low grade and would be subeconomic in the absence of high-grade veins. The highest grades of mineralization, in the absence of veins, occur in locally developed hydrothermal breccias. These breccias have irregular geometries, and range in size from discontinuous 5 to 10 centimeter-wide lenses adjacent to quartz-adularia veins, to 15 to 20 meter diameter bodies with indistinct boundaries that grade into bedded, silicified sedimentary rocks. Hydrothermal breccias are best developed adjacent to the faulted eastern contact of the "B" reef complex. Hydrothermal breccias consist of crustified vein material and silicified wall rock as clasts in a poorly consolidated matrix of clay, quartz, and carbonaceous debris (Figure 43). Crustified quartz-adularia veins also cross-cut many of the hydrothermal breccia zones, and these, together with breccia clasts of similar vein material, indicate multiple periods of veining and brecciation. Detrital grains in patchy zones adjacent to veins are commonly well-rounded and spherical, in contrast to the poorly sorted and angular detrital grains in the host rock (compare Figures 44 and 37). These rounded, spherical grains in the breccias consist of mono- and polycrystalline quartz, microcline, plagioclase, and lithic fragments. The grains are not embayed or preferentially altered along twin planes, which suggests that they attained their present shape by abrasion rather than chemical activity.

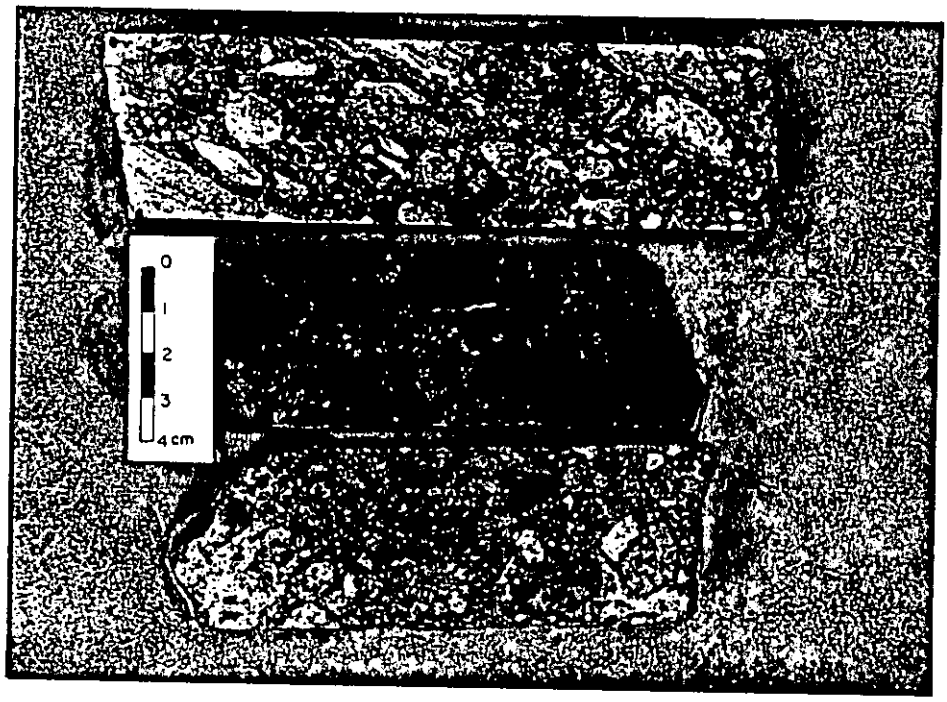

Figure 43. Core samples of hydrothermal breccia from about the 650 level of the "B" North ore body. Note the small fragment of quartz vein material contained within a large fragment of carbonaceous siltstone in the center sample.

Figure 44. Well rounded, spherical detrital grains of polycrystalline quartz, monocrystalline quartz, and microcline in a breccia from the "B" Neath ore body. Drill Hole TAD-10E, 48 feet down hole. Horizontal field of view is 2.3 mm.

Ore minerals in pervasively silicified sandstones and siltstones are sparsely distributed and very fine grained. In rare instances, minute grains of electrum(?) and tetrahedrite(?), associated with disseminated pyrite, can be recognized in polished sections of silicified wall rock. However, only three polished sections of silicified wall rock were examined in this study, all from the 700 level of the "B" North ore body, and the ore minerals in these samples were not analyzed by microprobe. A more detailed study might yield further significant petrographic information.

Vein-Controlled Alteration and Mineralization

The majority of gold and silver mineralization at the "B" reef complex occurs in crustified quartz-chalcedony-adularia-calcite veins that range in width from less than 25 mm to greater than 50 cm. These veins are discontinuous along strike and dip and seldom can be traced more than 10 meters in any direction, although some veins in the X stope area and on the 650 level of the D stope area can be traced up to 60 meters along strike and 20 meters along dip (Figures 22 and 31). Two generations of veins have been recognized in the "B" North ore body, based on structural relations: An early vein set occupies joints that are radial to fold hinges, and these veins are offset by vein-filled a-c extension fractures, perpendicular to the fold hinge line. The mineralogy and textures of the two veins sets appear to be identical.

The general character of all veins in the "B" reef

complex is similar; the outer margins of the veins are delicately layered with encrustations of quartz, chalcedony, and adularia, and the interior portions of the veins contain breccia. Vein calcite occurs on all levels of the Cannon mine, but on the 755 and 785 levels (the uppermost levels of economic mineralization), it is particularly abundant, and occurs as distinctive brown and pink calcite in the vein interiors. On the lower and intermediate levels of the Cannon mine, calcite has been replaced by lamellar quartz, a process that has produced a distinctive quartz boxwork texture (Figure 51).

Quartz-adularia veins

Quartz-adularia veins in the "B" reef complex display remarkably well-developed open-space filling textures. The outer portions of veins are finely crustified, with symmetric layers of crystalline quartz, chalcedony, and adularia. Calcite may be present as crustifications or as relic lamellar blades, partially or completely replaced by lamellar quartz. Inspection of cut and polished vein specimens has revealed that multiple stages of fracturing and ore and gangue mineral precipitation have occurred. The interior portions of most veins contain breccia that consists of clasts of crustified vein material from the vein walls, and detrital grains and lithic fragments from the sedimentary host rocks. Ore minerals are commonly concentrated on or near the vein walls. Non-ore sulfide minerals are concentrated near the vein walls,

and in the brecciated interior portions of the veins.

Representative samples from various levels of the "B" reef complex are shown in Figures 45 through 51, and they help to illustrate many of the mesoscopic textures discussed in this section. No effort is made to describe in detail each individual episode of mineral precipitation within the veins, because some of the wider veins show more than 50 mineral and textural layers from the vein wall to the interior. Additional layers become apparent when vein specimens are stained for potassium feldspar. However, on a general scale, many of the veins have similar characteristics.

Vein content and textures change notably from the upper levels of the "B" North ore body to the deeper portions of the "B" Neath ore body, such that, vein samples from the D stope area of the "B" North ore body are readily distinguishable from veins from the X stope area and other areas of the "B" Neath ore body. Sulfide minerals constitute less than 10% of the vein mineralogy in all veins of the "B" reef complex. Veins from the "B" Neath ore body, contain characteristic pyrite layers, 5 to 15 millimeters-thick, that are not common in veins in the upper levels of the mine. In the X stope area, on the 550 and 600 levels of the "B" North ore body, over 60% of the sulfide mineral content consists of pyrite, and pyrargyrite constitutes over half of the remaining sulfides. In the main part of the D stope area, electrum is more common than pyrargyrite. On the 600, 650, and 700 levels of the "B" North ore body, veins are characterized by the

presence of lamellar quartz boxwork textures, and on the 755 and 780 levels, pink and brown calcite veins are common.

Typical examples of veins from the "B" Neath ore body are shown in Figures 45, 46, and 47. The outer portions of these veins consist of dense, medium- to dark-gray, very fine-grained quartz, which is best displayed in Figure 45. Progressing toward the vein interior, the next feature that is consistent in all three specimens is a zone of delicately crustified milky white chalcedony, fine-grained quartz, and adularia. In Figure 45, the milky white vein material is in direct contact with the dark-gray quartz on the vein margin. In Figure 46, a zone of brecciated vein and wall-rock material separates the milky white quartz-adularia from the dark gray quartz, and in Figure 47, a layer of pale-red quartz is present between the two zones.

The final open-space filling prior to breccia-filling of the interior portions of the veins was precipitation of pyrite. Symmetric layers of pyrite, partially brecciated, but for the most part, in contact with the milky quartz-adularia stage, is shown in Figure 46. Pyrite is ubiquitous in veins and altered wall-rock of the "B" reef complex; however, crusts of pyrite are common only in veins from the "B" Neath ore body and the lower part of the X stope area of the "B" North ore body.

Three distinct breccias are recognizable in the vein specimens from the "B" Neath ore body: Brecciated wall rock that hosts the veins in Figure 47, a thin zone of breccia,

that consists of dark-gray quartz and silicified lithic fragments, is present between the dark-gray quartz stage and the milky quartz-adularia stage in Figure 47, and breccia-filled vein interiors are present in all three samples. Brecciated wall-rock is cross-cut by the vein in Figure 47, and therefore represents a period of fracturing that pre-dates vein formation. Wall-rock brecciation is discussed above in the section on wall-rock mineralization.

The breccia between the dark-gray quartz and milky quartz-adularia stages consists primarily of fragments of dark-gray quartz from the outer crustification stage. It is not certain whether this breccia resulted from increased fluid activity, or coeval tectonic deformation during the period of vein filling.

Breccia in the vein interiors is characteristic of veins throughout the "B" reef complex, and may represent relatively violent fluid activity during the final stages of vein formation.

Features that are characteristic of veins from the "B" Neath ore body are shown as a composite drawing in Figure 48. Not all the features shown in Figure 48 occur in every vein in the "B" Neath ore body, and many veins show a much more intricate depositional history. However, the stages shown in Figure 48 are the most consistent features in veins from the lower part of the "B" reef complex.

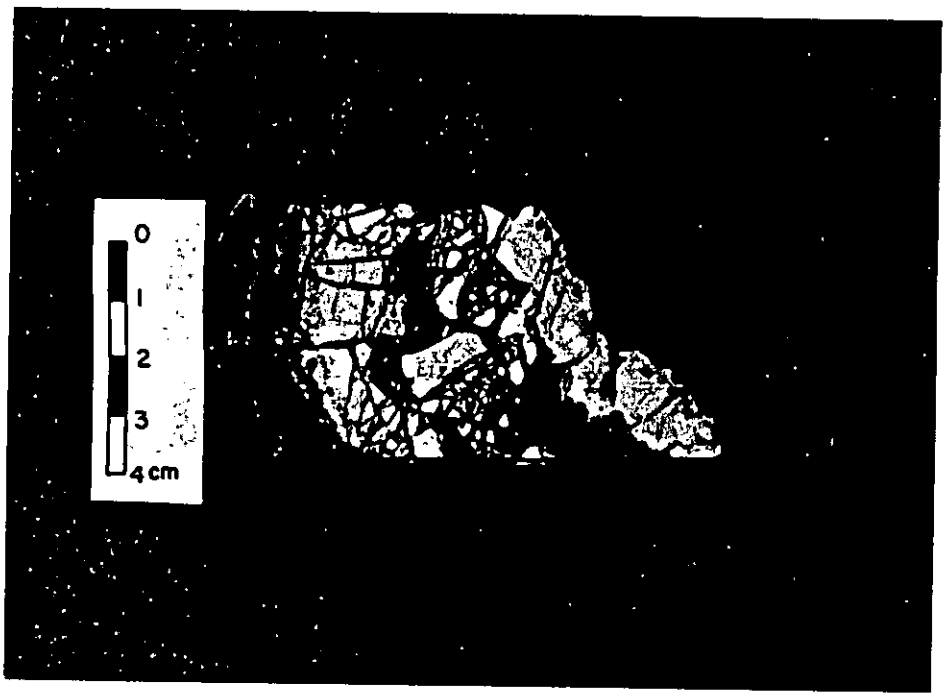

(A)

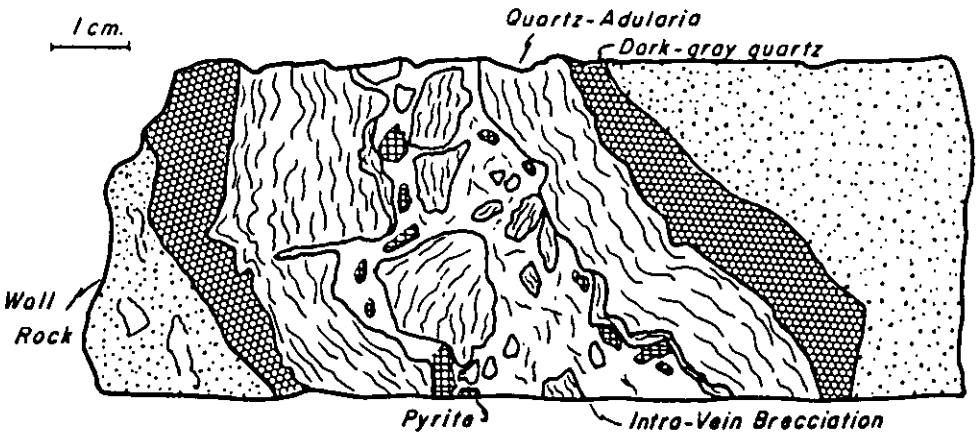

(B)

Figure 45. Photograph (A) and sketch (B) of a vein sample from the "B" Neath ore body. Drill hole TAD-7A, 38 ft.

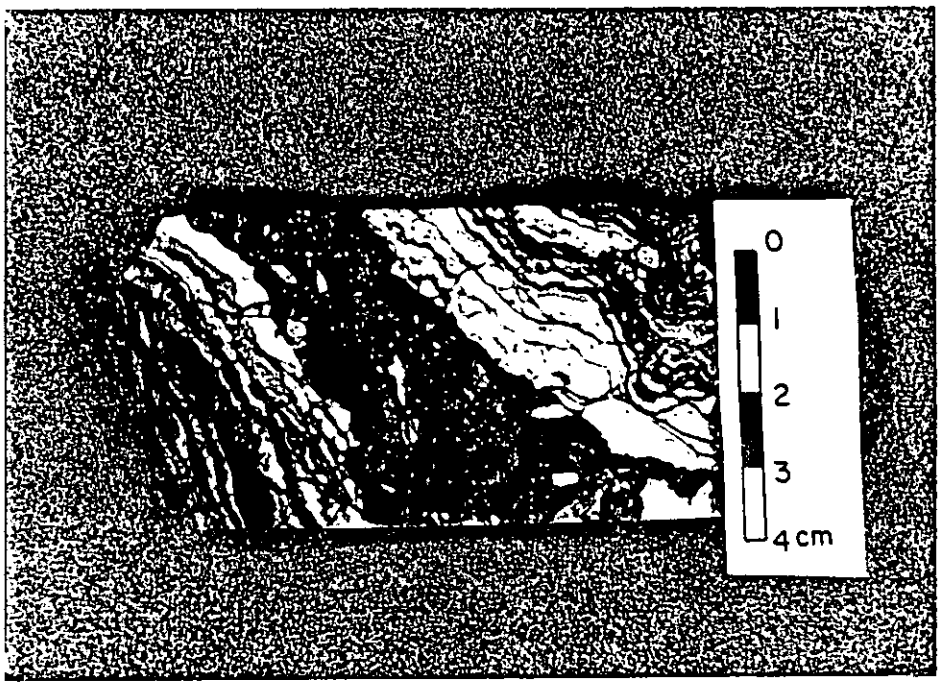

(A)

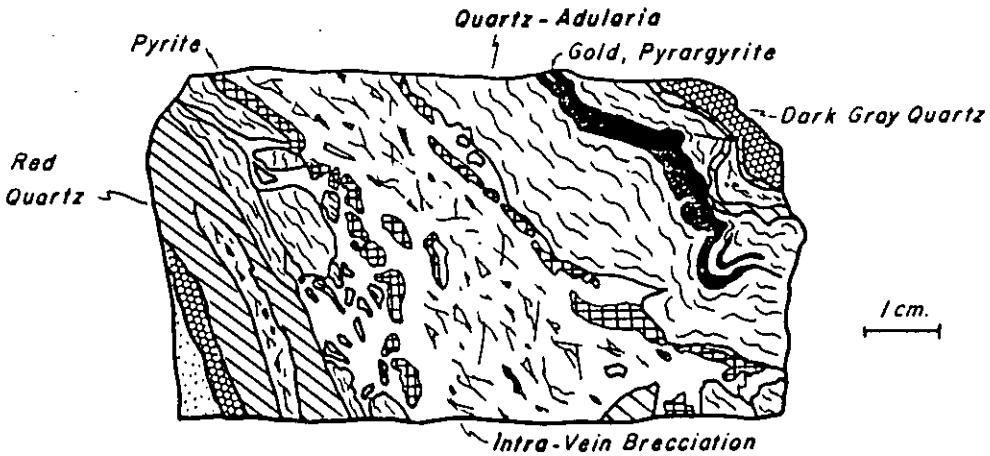

(B)

Figure 46. Photograph (A) and sketch (B) of a vein sample from the "B" Neath ore body, showing thin pyrite layers. Drill hole TAD-11D, 63 ft.

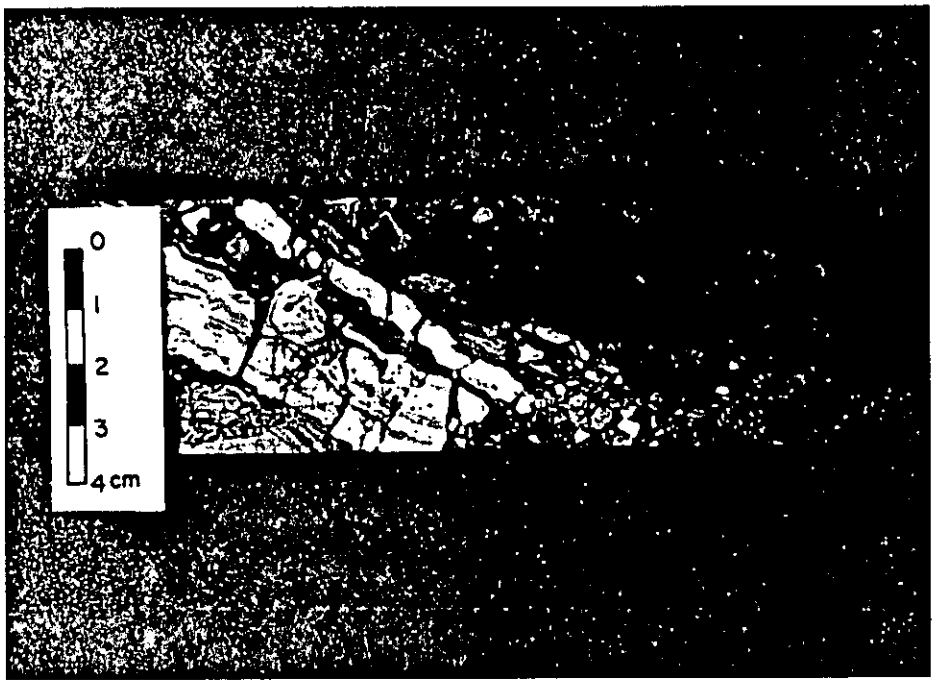

(A)

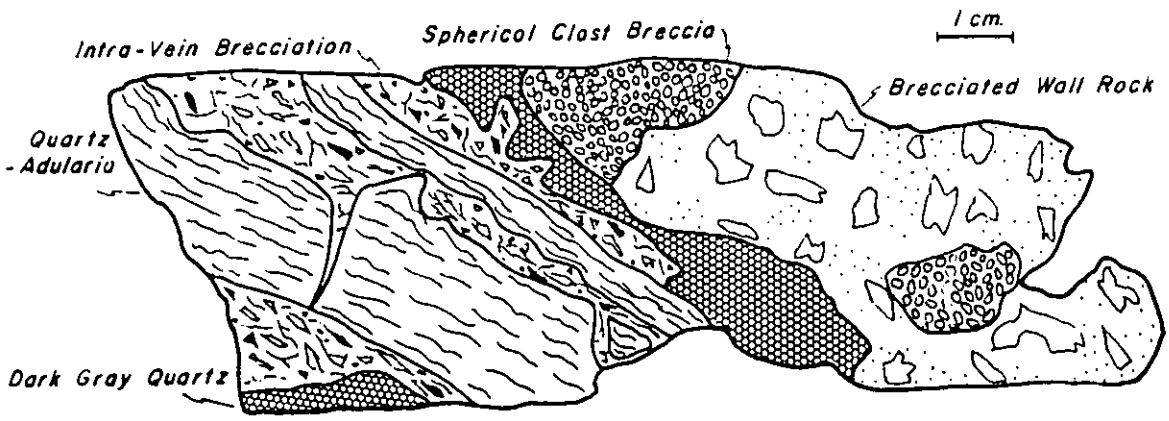

(B)

Figure 47. Photograph (A) and sketch (B) of vein sample from the "B" Neath ore body showing brecciated wall rock as vein host. Drill hole TAD-11A, 49 ft.

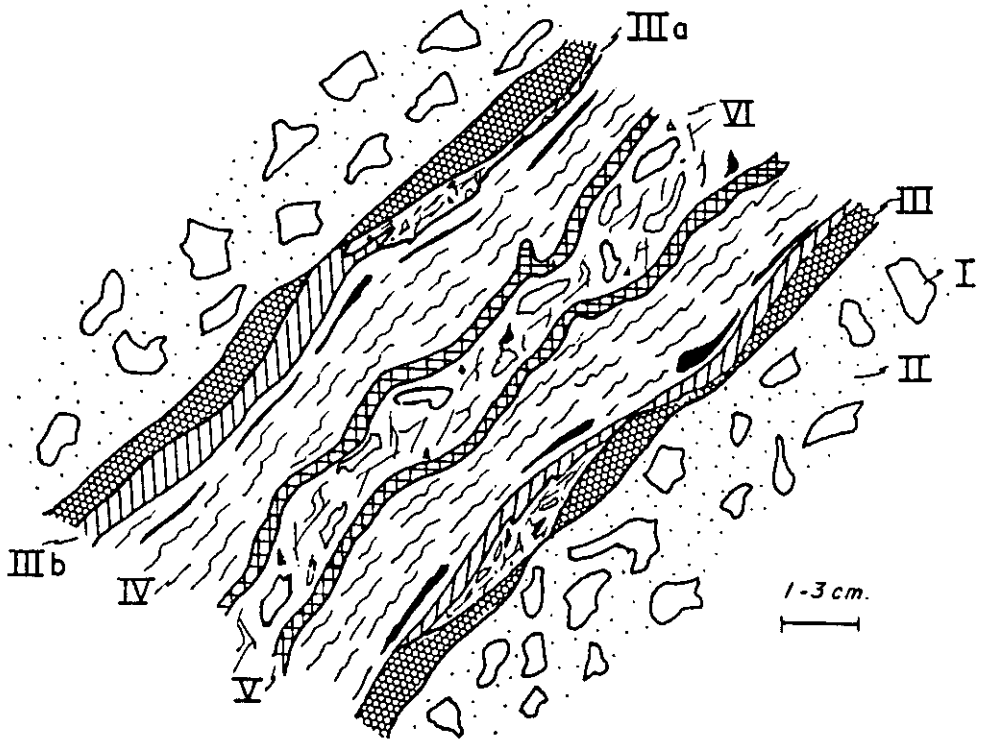

Figure 48. Schematic drawing showing characteristic features of veins in the "B" Neath ore body. Six stages of hydrothermal activity and deformation are recognizable: (1) Incipient silicification of wall rock, (2) fracturing and brecciation of silicified wall rock, possibly coeval with opening of fractures hosting major veins, (3) precipitation of dark-gray, fine-grained quartz, (4) precipitation of delicately crustified milky white quartz and adularia. Mesoscopically visible gold and pyrargyrite is commonly near the outer margin of this stage. (5) Precipitation of massive pyrite, and (6) development of breccia in vein interior. Two minor stages are commonly observed in many veins in the "B" Neath ore body: (3A) brecciation of dark-gray quartz and silicified wall rock in thin, discontinuous zones adjacent to the dark-gray quartz stage, and (3B) precipitation of pale-red quartz.

Vein samples from the D stope area of the "B" North ore body are shown in Figures 49, 50, and 51. These samples represent vein textures in the intermediate and upper portions of the "B" reef complex. The most common vein textures in the D stope area are shown in Figures 49 and 50. Like the veins from the "B" Neath ore body, these veins are finely crustified on their outer margins, and have interior portions consisting of breccia. Unlike the veins in the "B" Neath ore body, there are no pyrite layers present, and the dark-gray quartz stage is absent or poorly developed. Mesoscopically visible precious metal mineralization is most commonly observed near the vein margins, similar to the "B" Neath veins.

Quartz that has replaced calcite has resulted in a lamellar boxwork texture that is characteristic of veins on the 650 level of the "B" North ore body (Figure 51). Microscopic examination of veins that display lamellar boxwork textures has revealed that fine-grained quartz, chalcedony, and possibly opal has replaced calcite to produce the boxwork texture. Shreds and wisps of calcite remain, and the rhombohedral outline of pre-existing calcite crystals has been preserved in the replacement process (Figure 51). The presence of amorphous silica is suspected but has not been verified; a small percentage of quartz(?) associated with lamellar quartz and chalcedony is very fine grained and appears to be isotropic in cross-polarized light. However, this material is clouded with abundant, disseminated inclusions of carbonaceous(?) debris, and these inclusions may

be responsible for the apparent isotropic character.

Analysis of fluid inclusions in veins from the "B" North ore body was unsuccessful. Samples from 20 veins were prepared for fluid inclusion analysis, but only six inclusions were identified in all samples. The inclusions are less than 10 microns in diameter and contain both a liquid and vapor phase. Due to the small size of the inclusions, they could not be positively identified as primary or secondary, and homogenization temperatures could not be measured with confidence. The largest of these inclusions was homogenized through 10 heating and cooling cycles and yielded an average homogenization temperature of 165^{o}C, but temperatures ranged from 135^{o}C to 215^{o}C in the 10 cycles. This inclusion was contained in very fine-grained quartz near the interior of a 12 centimeter-wide, northwest-trending vein on the 700 level of the "B" North ore body.

Stockwork veining

Stockwork veining occurs in intensively silicified feldspathic sandstone near the eastern boundary of mineralization. The stockwork (Figure 52) consists of dark-gray, fine-grained quartz veinlets, 3 - 5 mm in width. The type of quartz in the stockwork veinlets is similar in appearance to the early dark-gray quartz stage of the "B" Neath veins. If the two dark-gray quartz occurrences are, in fact, paragenetically equivalent, then the stockwork veining would represent a relatively early hydrothermal stage.

Figure 49. Typical crustified quartz-adularia vein on the 700 level of the "B" North ore body. View is to the west, note the symmetric layers and intra-vein breccias.

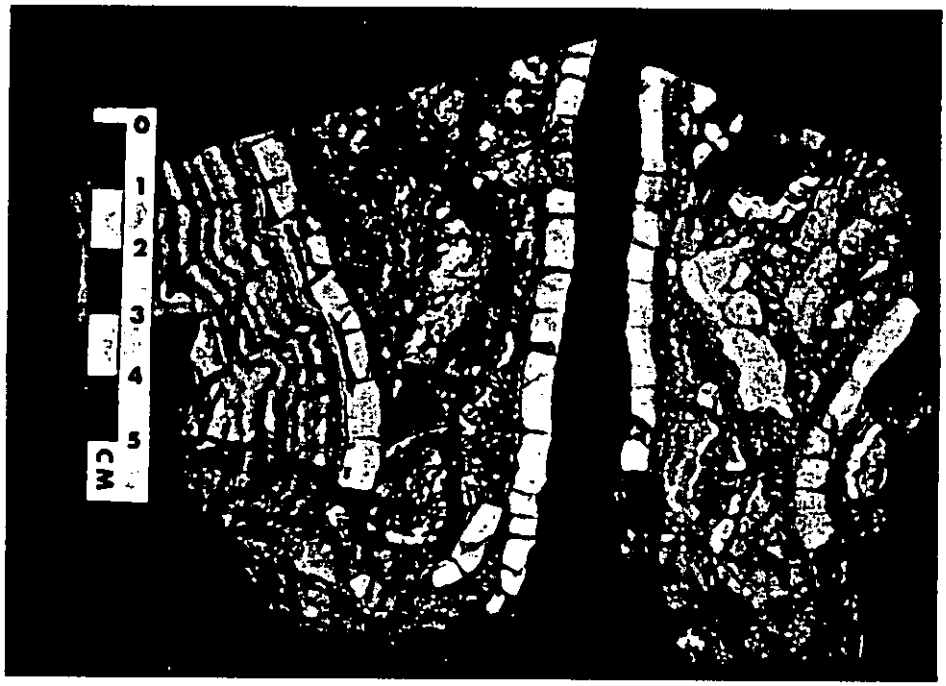

Figure 50. Vein sample from the 700 level of the "B" North ore body, showing adularia layers (stained yellow), and breccia-filled vein interior.

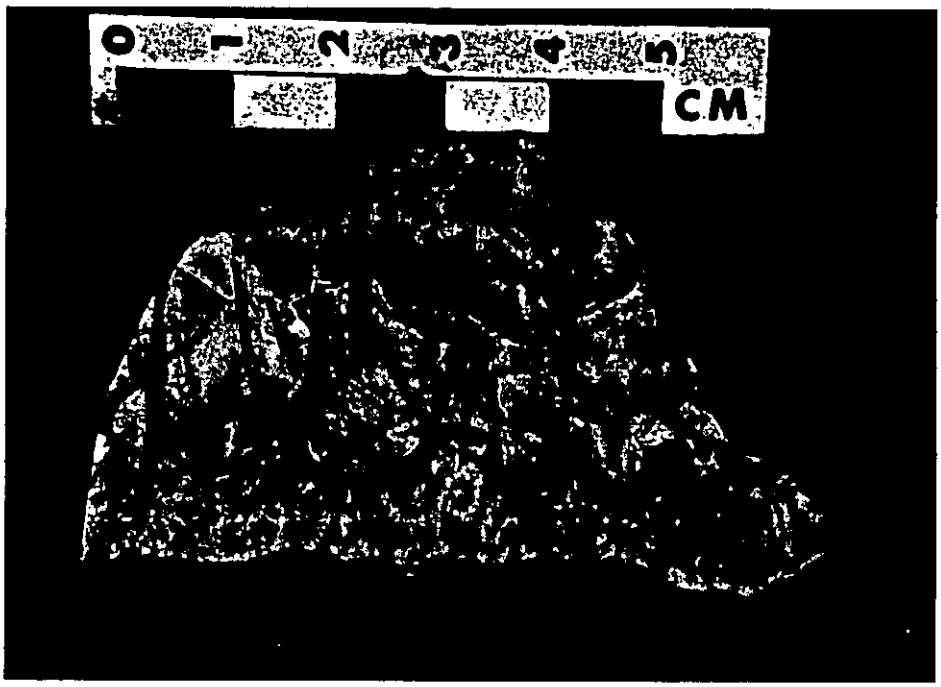

(A)

(B)

Figure 51. Hand sample (A) and photomicrograph (B) of lamellar boxwork texture developed from the replacement of calcite by quartz and chalcedony. Sample is from the 650 level of the "B" North ore body. Horizontal field of view in photomicrograph is 2.3 mm.

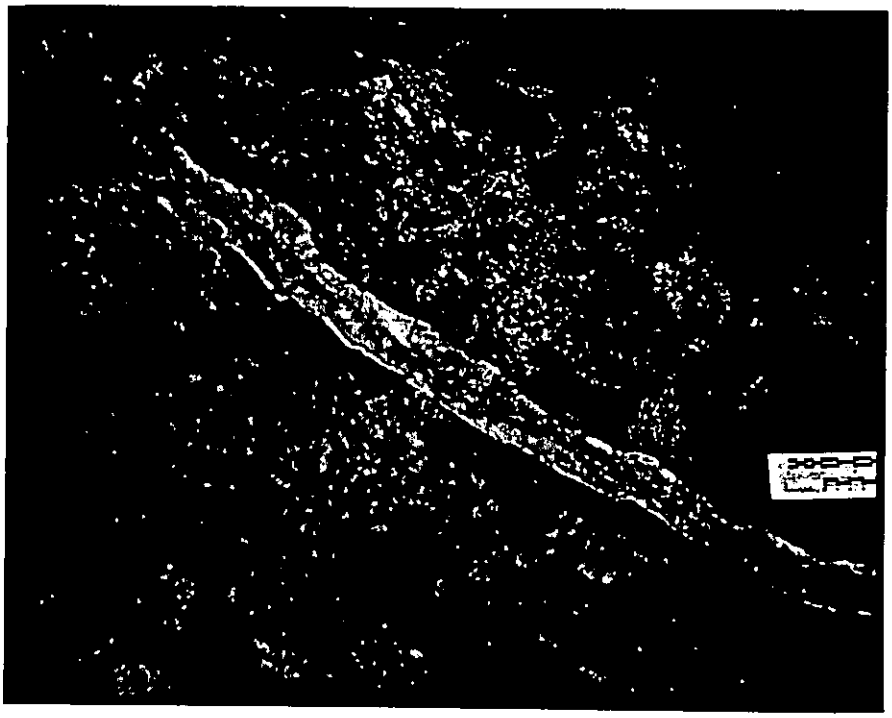

Figure 52. Stockwork veining on the 650 level of the "B" North ore body. Silicified, medium-grained feldspathic sandstone is cross-cut by 1 - 3 cm dark-gray quartz veinlets. A east-striking, south dipping quartz-adularia vein cuts the silicified sandstone. Note the dark-gray quartz layer in the footwall of the vein. Veiw is to the east, the lower part of the scale is in centimeters, the upper part is in 1/4 and 1 inch graduations.

Calcite veins

Calcite occurs in veins at all levels of the "B" reef complex, but is most prevalent in the upper levels. On the 755 and 785 levels of the "B" North ore body, pink and brown calcite commonly fills the interior portions of veins that have outer encrustations of quartz and adularia (Figure 53). On the 700, 600, and 500 levels, white calcite generally occurs by itself in small veinlets, or as relic grains in quartz-adularia veins. The reason for color variation in calcite is not known.

Ore mineralogy

Ore minerals in the "B" reef complex consist of electrum, pyrargyrite, tetrahedrite, and very minor acanthite, associated with ubiquitous pyrite and minor chalcopyrite. Naumannite, the silver selenide, was an important ore mineral at the L-D mine (Guilbert, 1963). A selenium geochemical anomaly overprints the "B" reef ore bodies (see trace element geochemistry section), but no selenide-bearing minerals have been identified from the Cannon mine. In the Wenatchee Heights area, southeast of the L-D mine, Margolis (1987, p. 61) identified arsenopyrite, marcasite, stibnite, sphalerite, galena, and hessite in silicified arkose and quartz vein samples from drill core. None of these minerals have been identified in the "B" reef complex, and no anomalous concentrations of tellurium or zinc have been detected in trace element analysis of altered rocks in the Cannon mine

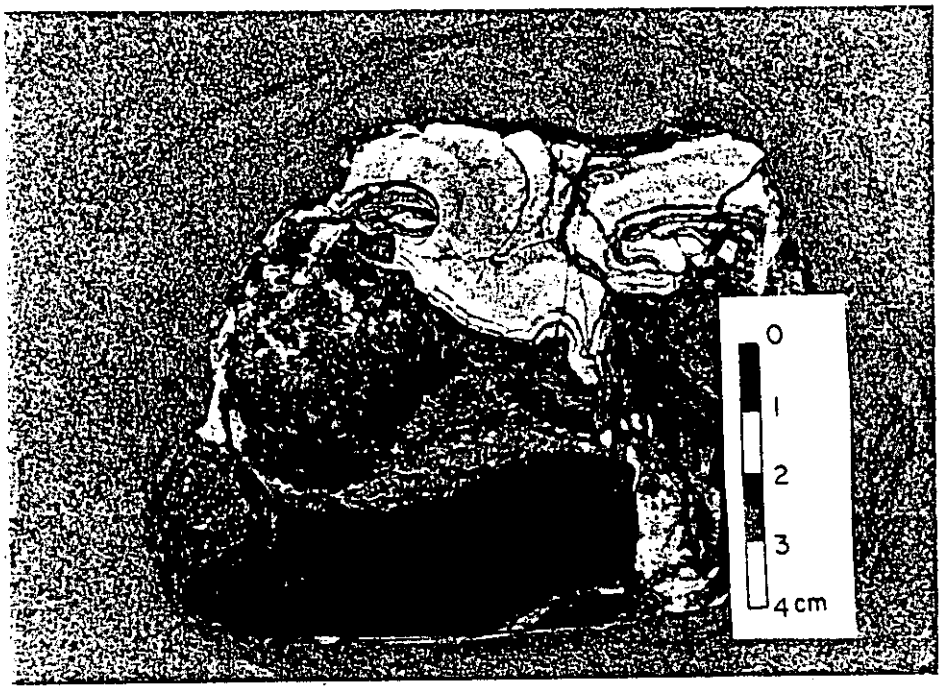

(A)

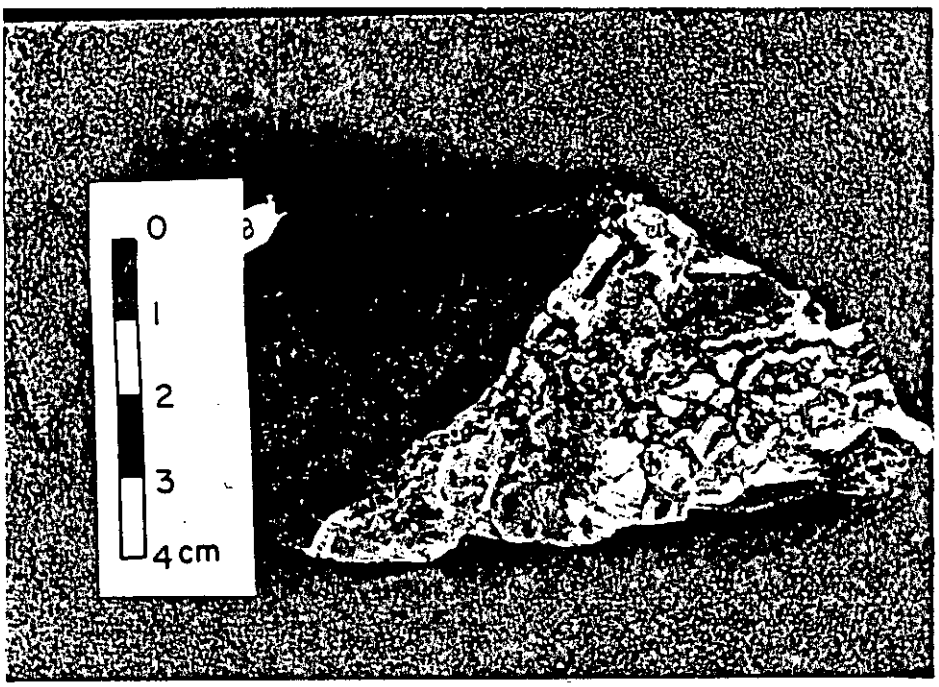

(B)

Figure 53. Vein calcite from the "B" North ore body. (A) Brown and pink calcite with a small layer of fine-grained milky-white quartz from the 755 level, (B) pink calcite in the interior of a vein from the 785 level. Note the broken crusts of quartz and adularia.

area. There is a substantial mercury geochemical anomaly associated with the "B" reef complex, but no mercury minerals were identified during this investigation. Mercury could be present as mercurian tetrahedrite. Arsenic and antimony anomalies are also associated with mineralization; tetrahedrite and pyrargyrite are the only minerals identified so far that contain these elements.

The highest concentration of ore minerals is in quartz-adularia veins, and, within these veins, the ore minerals are commonly concentrated near the margins of the veins. In this study, 20 polished specimens were examined in reflected light to establish the identity and paragenetic relations of the ore minerals. From these 20 samples, five were selected for microprobe analysis to quantitatively establish the composition of electrum and pyrargyrite, the most abundant ore minerals in the "B" reef complex. The following characterizations of the ore minerals can therefore be considered preliminary.

Pyrargyrite is the principal silver mineral in the "B" reef complex, and occurs in veins on every level of the Cannon mine. However, it is most abundant in the intermediate and deep levels of the mine; many veins on the 550 and 600 levels, in the X stope area, are speckled with the characteristic purple-red of pyrargyrite on fresh exposure. The pyrargyrite in these veins generally oxidizes to dull-gray within 5 - 6 hours after the samples are brought to the surface. The largest crystals of pyrargyrite are about 0.5 mm in length,

and occur in vugs, but pyrargyrite most commonly occurs as subhedral to anhedral grains and grain aggregates, less than 0.1 mm in diameter. Pyrite, chalcopyrite, and electrum may be intergrown with pyrargyrite, but in many cases, the sulfosalt occurs only with electrum.

No arsenic is detected in microprobe analysis of pyrargyrite grains. Where pyrargyrite is intergrown with, or has common grain boundaries with chalcopyrite, 3 - 5% iron and copper were detected in the sulfosalt. Presumably, there is a limited amount of substitution by these elements for silver.

Electrum occurs as isolated grains, arborescent grain aggregates intergrown with pyrargyrite, as acicular needles a few tens of microns in diameter and up to 1 mm in length, and in quartz-adularia veins throughout the Cannon mine. It occurs sporadically in the veins, commonly as lenticular pods that vary in length from 1 to 2 cm and in width from 0.5 to 1 cm. In hand sample, the electrum is bronze to brown, and difficult to distinguish from fine-grained pyrite. On cut surfaces, however, electrum "smears" are easily recognized. The color of electrum grains is more yellow with decreasing silver content. Microprobe analysis of electrum has shown that silver content varies from 30% to 50%. Higher percentages occur where electrum is isolated and not in contact with pyrargyrite. The lowest silver percentages in electrum occur where it is in contact with the sulfosalt (Figures 54 and 55).

Acanthite was identified by microprobe analysis of vein samples from the 600 and 700 levels of the "B" North ore body

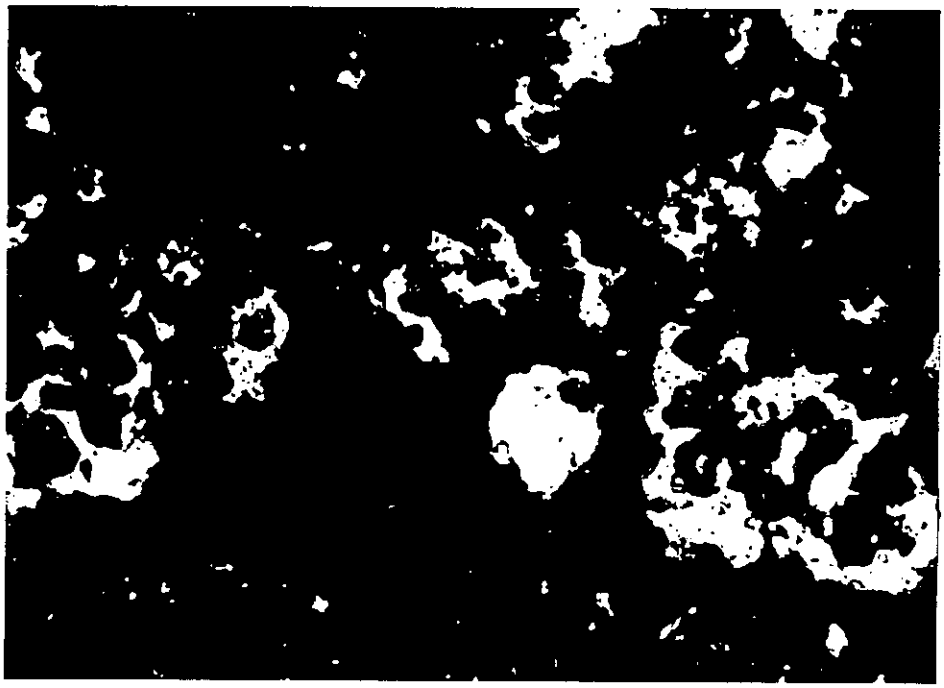

Figure 54. Electrum grains encapsulated in fine-grained quartz. Note the small euhedral grains of pyrite within the anhedral electrum grains. Silver content of isolated electrum grains is about 50 percent. Sample from the 700 level. Horizontal field of view is 1.25 mm.

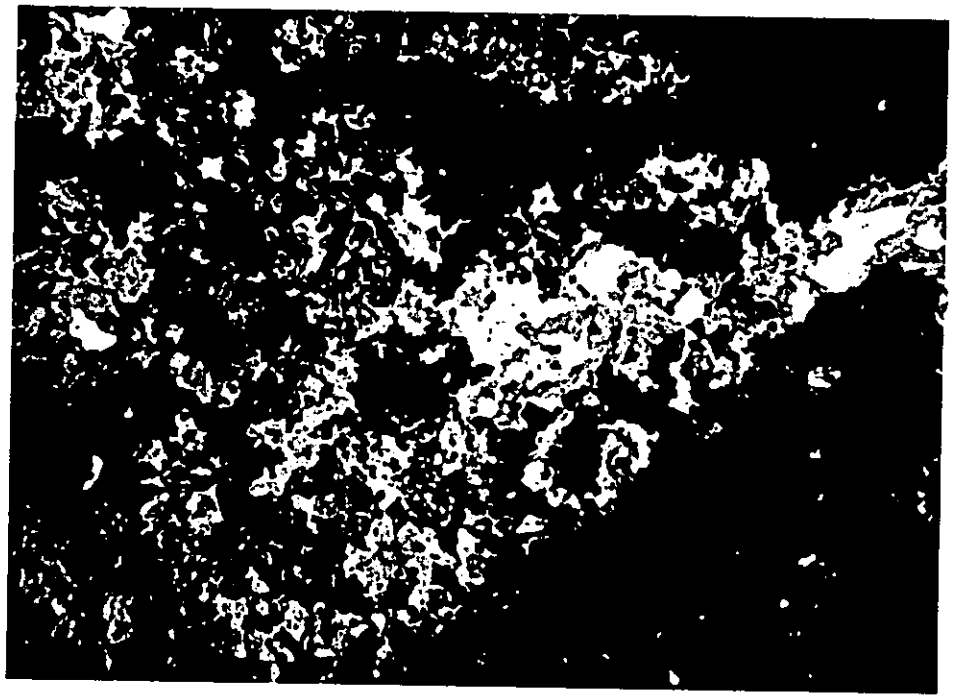

Figure 55. Photomicrograph of electrum, pyrargyrite, and pyrite from the X stope area of the "B" North ore body on the 650 level. Acanthite occurs on grain boundaries between electrum (medium-yellow color) and pyrargyrite (blue-gray color) but has only been identified by microprobe analysis. Horizontal field of view is 2.0 mm.

in this study only along grain boundaries between electrum and pyrargyrite. Roderick (1986) identified 1 - 5 micron-size grains of acanthite by microprobe analysis of mill-feed ore. Ott and others (1986, p. 424) interpreted the occurrence of acanthite to be a transitional phase in the sulfidation of electrum to form pyrargyrite. Subsequent reflected-light petrographic work has indicated that electrum may be a later phase, formed in part at the expense of pyrargyrite, and that acanthite may be a transitional phase precipitated as a result of decreasing sulfur activity in the hydrothermal system (Figure 56).

Tetrahedrite has not been recognized in polished specimens analyzed by the writer, Roderick (1986) Williams (1986) and Hazen and Hazen (1986) have reported tetrahedrite in mill-feed ore and concentrate samples from the "B" North ore body. The nature of tetrahedrite in mineralized veins and wall-rock at the "B" reef complex is therefore unknown.

Timing of Mineralization and Alteration

A single K-Ar date on adularia from the 700 level of the "B" North ore body indicates that mineralization occurred about 44 m.y.b.p., during the main period of graben formation as determined by Gresens (1983, p. 53), and near the end of graben formation as determined by Evans (1987). Based on textural and spatial relations, ore and gangue mineral deposition occurred in three stages at the "B" reef complex: (1) Pre-main stage silicification, (2) main-stage vein

formation with attendant potassium silicate, carbonate, sericitic(?), and silicic alteration, and (3) late-stage brecciation, possibly coeval with argillic alteration. Intra-vein breccias, and alternating layers of quartz, chalcedony, and adularia indicate that deformation and possible decompressional boiling occurred intermittently through all stages, and, coupled with the paragenetic sequence, influenced the overall texture and form of the mineralized veins and rocks.

Major quartz-adularia veins commonly transect irregular bodies of hydrothermal breccia. Lithic fragments in the hydrothermal breccias are strongly silicified, and commonly contain quartz veinlets. The wall rock therefore appears to have been silicified prior to brecciation, and brecciation appears to have occurred prior to main-stage vein formation. Alternatively, incipient silicification, brecciation, and vein formation may have been coeval, or developed as a single continuous process. Pre-main stage hydrothermal silicification as a distinct paragenetic event is therefore largely interpretative.

Main-stage veins are hosted by a-c extension fractures that cross-cut early-formed breccia zones. Whether folding and development of a-c fractures pre-dated hydrothermal activity entirely or was coeval with main-stage vein formation is uncertain. The poorly indurated nature of sedimentary rocks in the district that were not altered makes it seem unlikely that dilatant opening generated during the period of

folding could have been maintained for any length of time without substantial fluid pressure. It therefore seems probable that main-stage vein formation and folding may have a close temporal relationship.

Late-stage brecciation in any single vein is exhibited by brecciated vein interiors, and crustified vein fragments as breccia clasts. Poorly cemented vein and wall rock breccias indicate that the fluids involved in this stage were relatively barren, and well-rounded, spherical detrital grains associated with many breccias in the mine indicate that abrasion of grains and breccia fragments, possibly by violent release of a gas-rich phase, may have been important in the formation of these late breccias.

Initial silicification was accompanied by pervasive dissemination of pyrite and, possibly, a limited amount of adularia. Sericitization of plagioclase grains and chloritization of biotite grains may have been initiated in this stage. Low-grade gold and silver values indicate a limited amount of precious metal deposition of electrum, tetrahedrite(?), and pyrargyrite(?)in wall rocks prior to, or coeval with main stage vein formation.

Main stage veins are characterized by episodic deposition of quartz and adularia. Calcite was deposited relatively early in the crustification sequence, and later replaced by chalcedony, quartz, and possibly opal. The presence of calcite in veins in the upper levels of the Cannon mine, and lamellar quartz boxwork textures in the intermediate and

deeper levels of the mine may indicate that calcite deposition and replacement was a continuous, upward-migrating process, possibly controlled by an advancing level of hydrothermal fluid boiling.

A preliminary inspection of ore mineral textures indicates that the sequence of metallic mineral precipitation was early pyrite + pyrargyrite + chalcopyrite, followed by electrum + acanthite + late pyrite, and finally pyrite only. The exact paragenetic position of tetrahedrite is not certain. This interpretation of the temporal relationship between electrum and pyrargyrite is opposite of the interpretation of Ott and others (1986, p. 424) and is based on compelling textural evidence from more recent petrographic work (Figure 56).

The exact paragenetic position of montmorillonite and kaolinite is not certain. Late-stage vein breccias and evidence of liberation of gases from hydrothermal fluids in the form of abraded detrital grains indicate possible late fluid boiling. Condensation of liberated gases may have caused the moderately acidic alteration assemblage capping silicified rocks of the "B" reef complex. These minerals have therefore been tentatively placed in the late-stage of hydrothermal mineral deposition (Figure 57).

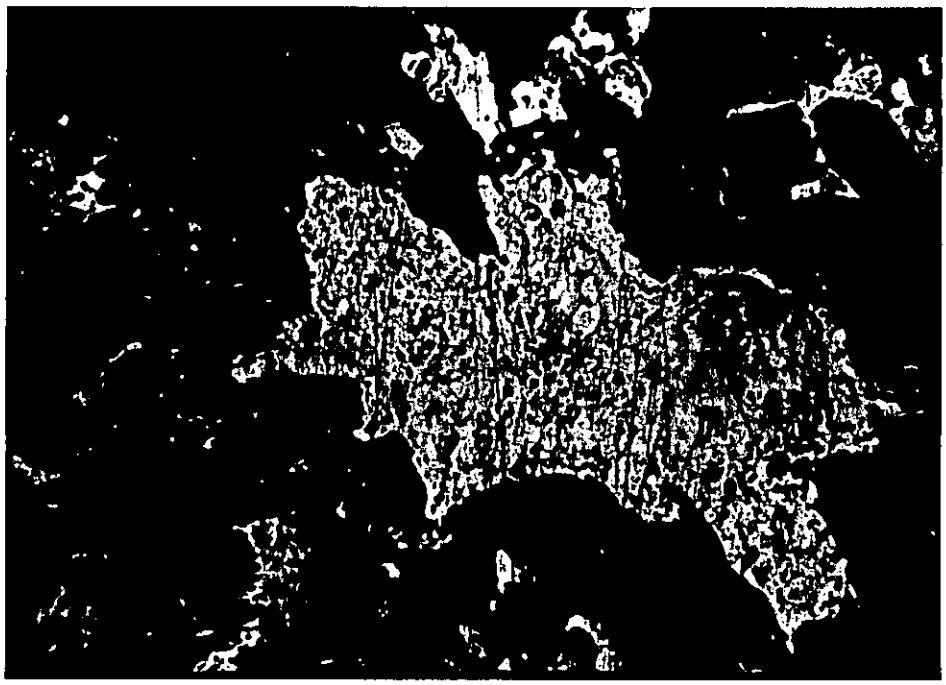

Figure 56. Pyrargyrite grain (medium gray) engulfed and partially replaced by electrum (yellow). This texture is significant in that it may indicate that sulfur activity in the ore-forming solutions decreased with time. Horizontal field of view is 2.0 mm.

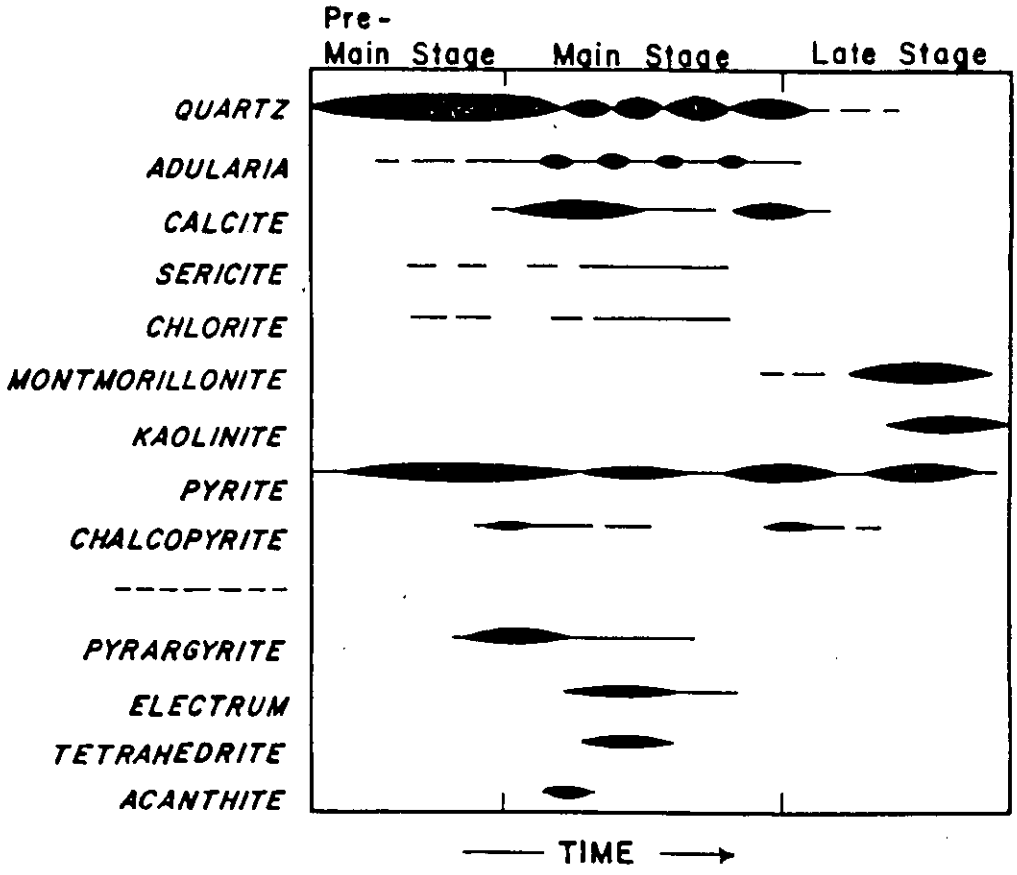

Figure 57. Generalized paragenetic diagram showing the interpreted sequence of ore and gangue mineral deposition at the "B" reef complex.

GEOLOGY OF THE "D" REEF

The geology of the L-D mine at "D" reef has been described by Lovitt and McDowall (1954), Lovitt and Skerl (1958), Patton (1967), and Patton and Cheney (1971). Moody (1958), and Guilbert (1963) investigated the ore and gangue mineralogy at the L-D mine. Geologic investigations subsequent to these publications include an extensive diamond and rotary drilling program by Cyprus Mines Corporation, diamond drilling and geophysical investigations by Lovitt Mining Company (Folk, 1987), and surface mapping and drilling by Asamera Minerals Company and Breakwater Resources. During this investigation, the 1250 level of the L-D mine was rehabilitated and Block 1 was mapped in detail; a cursory examination of Blocks 2 and 3 was also made.

Distribution of Mineralized Rocks

"D" reef consists of an elongate lens of hydrothermally altered and mineralized sedimentary rocks. This lens of altered rock strikes northwest and dips 60° to 80° southwest, approximately parallel to the orientation of the sedimentary host rocks. A regular pattern of north-trending dextral strike-slip faults have offset the mineralized rocks, and produced en echelon of blocks of ore, shown in Figure 58 as Blocks 1, 2, and 3. Ore was mined at "D" reef between the elevations of 850 and 1600 feet; mineralization and alteration have been identified as deep as the 750-foot elevation.

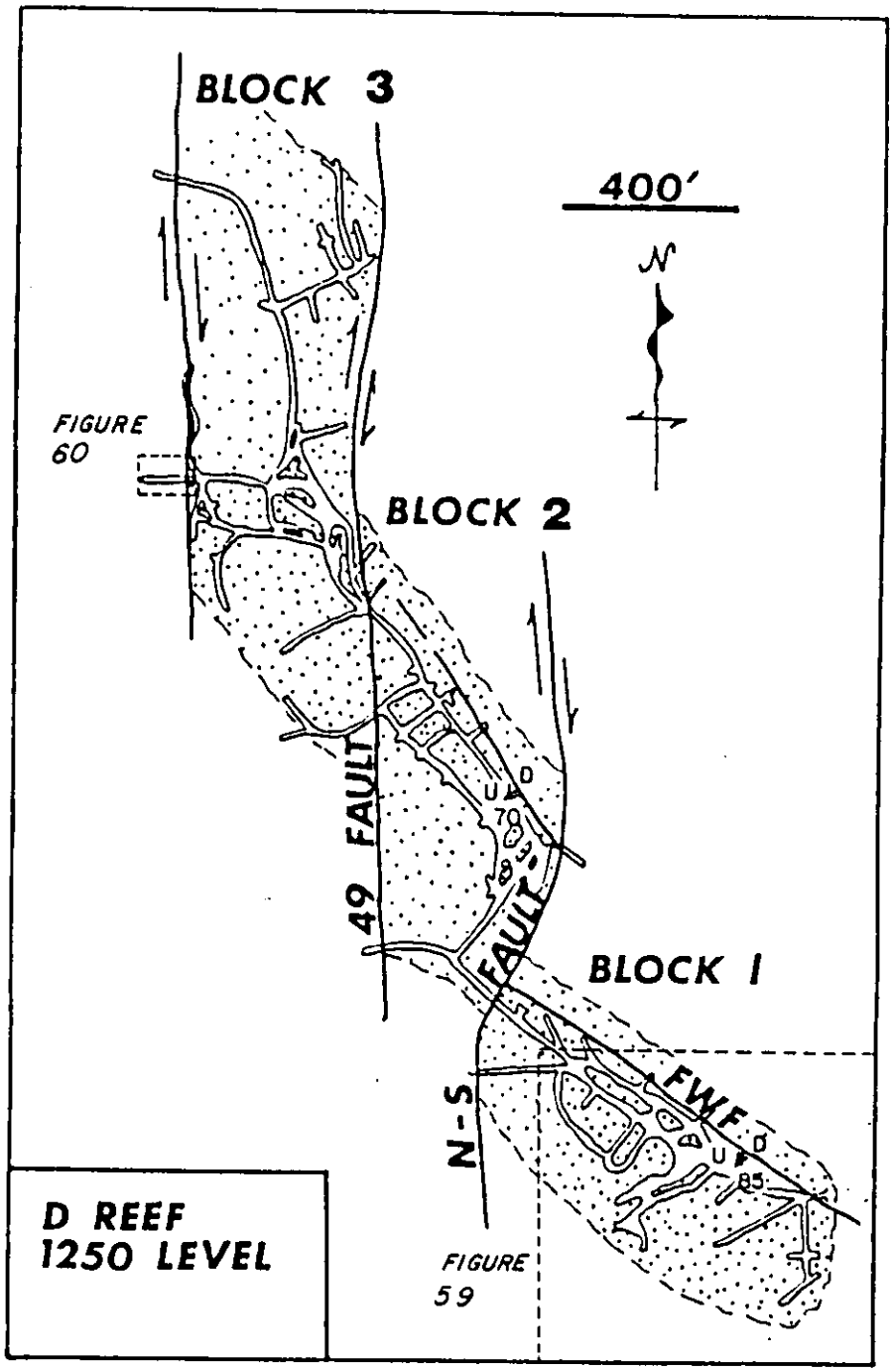

Figure 58. Plan map of the 1250 level of the L-D mine at "D" reef. FWF is the Footwall Fissure, stippled pattern indicates limit of silicification. Locations of Figures 59 and 60 indicated. Modified from Patton and Cheney (1971, figure 4).

Sructural Framework

The main structural feature in Blocks 1 and 2 is a northwest-striking, reverse fault known as the Footwall Fissure (Lovitt and Skerl, 1958, p. 966). The Footwall Fissure consists of two strands that dip steeply to the southwest, and are variably separated by 50 to 75 feet of intensively silicified and broken sedimentary rocks, the original character of which are not recognizable (Figure 58). Patton and Cheney (1971, p. 9) state that alteration and mineralization are restricted to the hangingwall side of the western strand. However, in Block 1 of the 1250 level, the section of rocks between the east and west strands of the Footwall Fissure is intensively silicified and weakly mineralized with gold. Also, the main access drift on the 1250 level of Block 1 was developed in silicified sedimentary rocks on the footwall side of the west strand (Figure 59, and Plate 8 of Patton, 1967). Patton and Cheney (1971, p. 7) also suggest that the Footwall Fissure is a pre-mineralization structure; however, the most recent movement on the Footwall Fissure post-dates mineralization, as is evidenced by the abrupt termination of northeast-trending veins in Block 1 (Figure 59). Sedimentary beds in the hangingwall of the west strand dip 75° to 85° to the southwest, approximately parallel to the plane of the fault. Progressing west into the hanging-wall, the dip of bedding gradually decreases 50° to 60° (Figure 59). Sedimentary beds are poorly defined between the east and west strands, but where bedding can be recognized, it

8,900 E

se grained feldspathic sandstone

ceous claystone

dip

ement uncertain

re

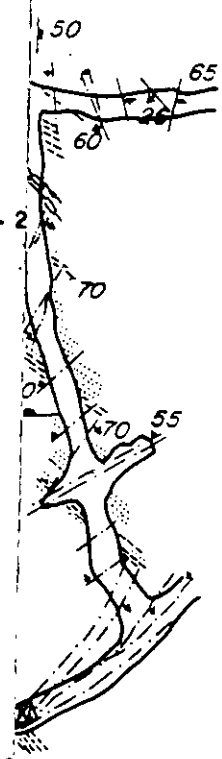

dips steeply to the northeast.

The Footwall Fissure has been offset by three north-trending strike-slip faults that separate Blocks 1, 2, and 3. The North-South fault has laterally displaced mineralization as much as 300 feet and separates Blocks 1 and 2 (Figure 58). The amount of displacement on the 49 fault that separates Blocks 2 and 3, has not been determined, but is less than the displacement on the North-South fault. An unnamed north-trending strike-slip fault marks the western boundary of Block 3 (Figure 58). These three north-trending strike-slip faults also appear to have a component of oblique reverse displacement of undetermined magnitude. Minor folds in carbonaceous gouge of the unnamed fault on the western margin of Block 3 indicate a hangingwall movement direction of N20°E to N40°E (Figure 60). Patton and Cheney (1971, p. 9) cite several interpretive lines of evidence for oblique reverse movement on the north-trending faults.

At least three generations of vein development have been observed in Block 1, and presumably correspond to intra-mineralization fracturing. Early veins are developed along fractures parallel to bedding, and are cut by later northeast-trending vein filled fractures that dip 60° to 80° to the northwest (Figure 61). These northwest-dipping fractures are offset by northeast-striking veins that dip 80° to 85° to the south (Figure 59). Both the bedding-plane veins, and the northwest-dipping veins are mineralized, but the south-dipping veins are barren. The northeast-trending vein pattern is

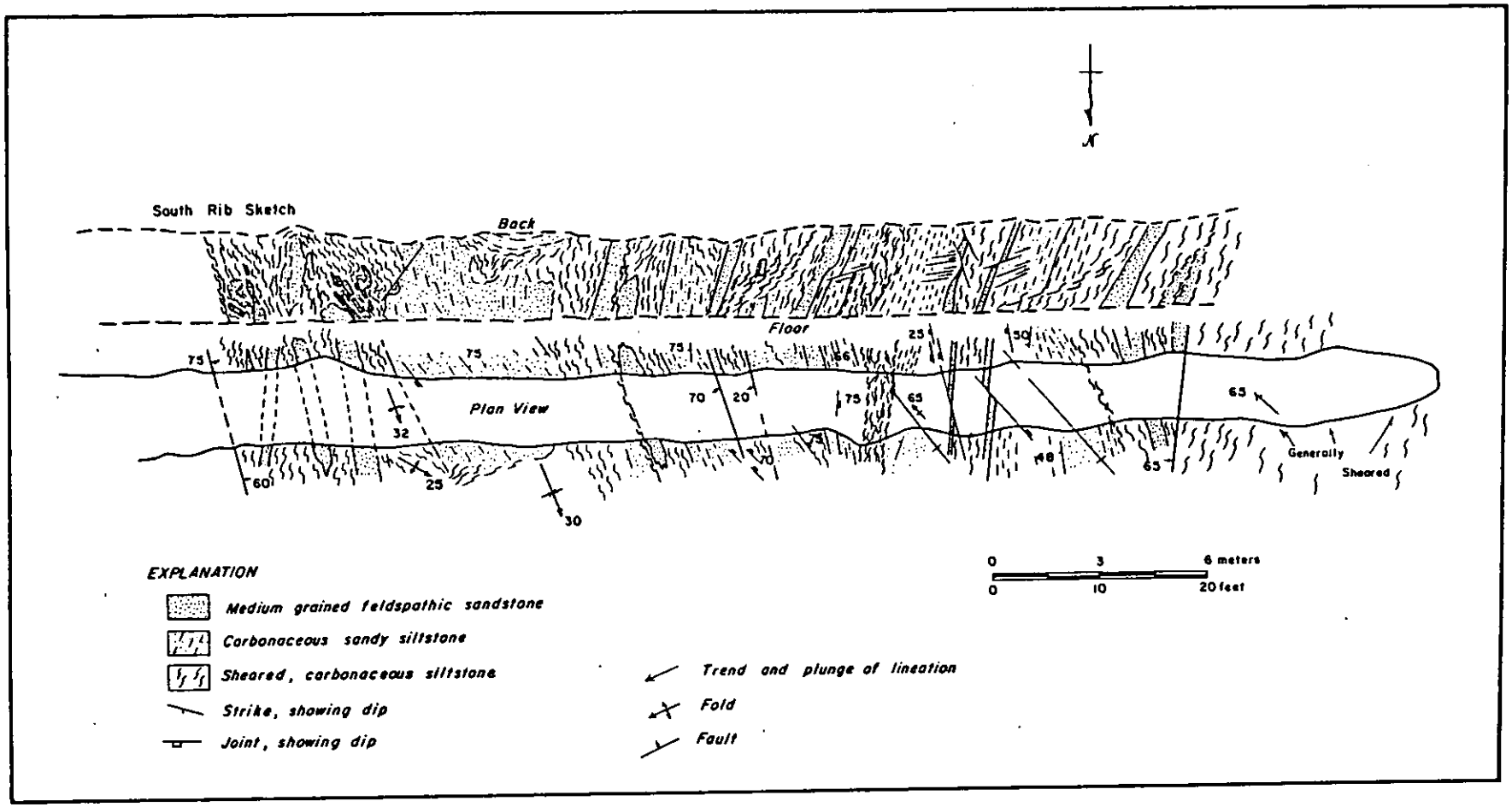

Figure 60. Detailed geologic map of carbonaceous gouge zone in unnamed fault on the western boundary of Block 3 on the 1250 level. Minor structures indicate that the slip direction is to the northeast.

consistent throughout Block 1, but it is only in the southeast portion of Block 1 that the width of the veins is sufficiently developed that they could be individually stoped (Figure 59). In Blocks 2 and 3, based on a brief examination, the pattern of veins approaches a stockwork, although the northeast strike remains the dominant orientation.

Detailed mapping in Block 1 has identified a series of regularly spaced, small thrust faults that offset both mineralized and barren quartz veins. These faults are typically less than 2 cm in width, they strike northwest and generally dip less than 20^{o} to the southwest. Displacement is commonly on the order of 2 to 5 meters and the vertical spacing between thrust planes is commonly 1 to 5 meters (Figure 59). Patton (1967, Plate 7) noted a well-developed low-angle fault on the 1100 level in Block 2, which he referred to as the "Flat Fault".

Patton and Cheney (1971, p. 7) interpreted the Footwall Fissure to be part of an imbricate thrust zone. They correctly identified the structure as a reverse fault, and indicated that the dip of the Footwall Fissure decreased in the lower levels of the mine. An earlier observation by Patton (1967) is inconsistent with the latter observation. Patton's map of the 850 level, the deepest level in the mine, shows the Footwall Fissure to dip 75^{o} to 85^{o} to the southwest, essentially parallel to the dip of this structure on all levels of the mine (Patton, 1967, Plate 4). The decrease in dip on the Footwall Fissure suggested by Patton and Cheney

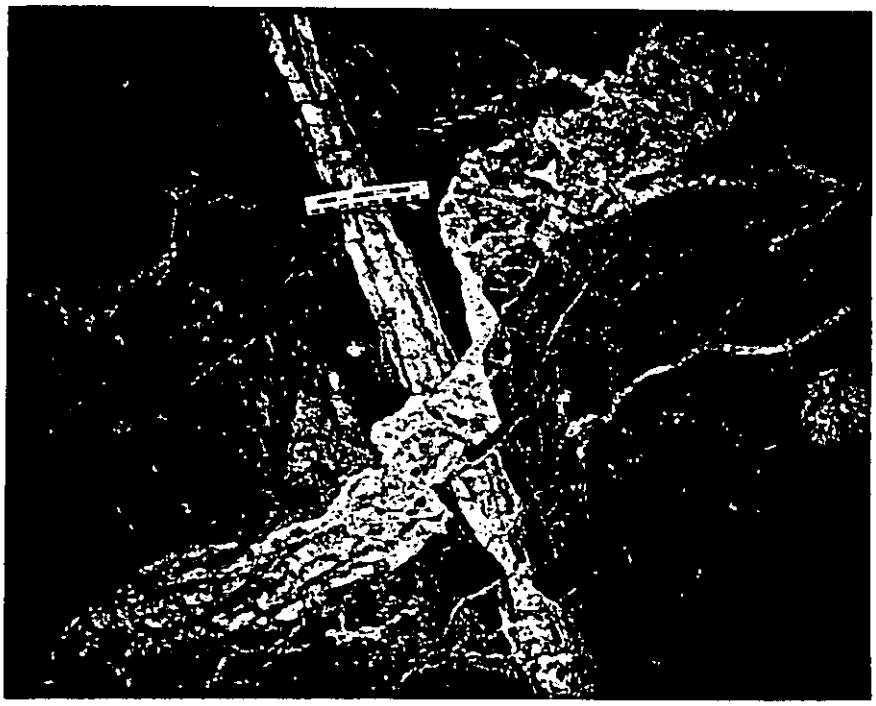

Figure 61. Bedding-plane vein crosscut by northeast-striking, north-dipping vein in Block 1. A later structural adjustment has offset the northeast trending vein. Viewed to the southeast, scale is in inches and centimeters.

(1971) is based on their interpretation that the Footwall Fissure is the same structure as the Flat Fault. The lower levels were not accessible during the course of this study, and this relationship could not be confirmed.

Stratigraphy of the Mineralized Section

Rocks in the footwall portion of the east strand of the Footwall Fissure consist of a cobble to boulder conglomerate at least 200 feet thick. Patton (1967) and Patton and Cheney (1971) correlated this conglomerate with conglomerates exposed on the western side of Rooster Comb. Where exposed east of the 1250 level portal (Plate 1) the conglomerate consists of cobbles and small boulders of volcanic rocks, quartz, and some biotite gneiss that are stained with red and yellow iron oxide minerals, in a weakly argillized matrix of feldspathic sandstone.

The stratigraphy between the east and west strands of the Footwall Fissure is not well defined due to intensive silicification and brecciation. Breccia fragments commonly consist of medium to coarse-grained feldspathic sandstone. Pebble conglomerate and laminated silty beds occur locally.

Three stratigraphic sections were measured in Block 1 in the hangingwall portion of the west strand and are shown in Figure 62. The hangingwall section of Block 1 consists largely of feldspathic sandstone beds, 0.5 to 1 meter thick, with thin interbeds of carbonaceous clayey siltstone. Distinctive pebble conglomerate beds that consists of 1 - 3

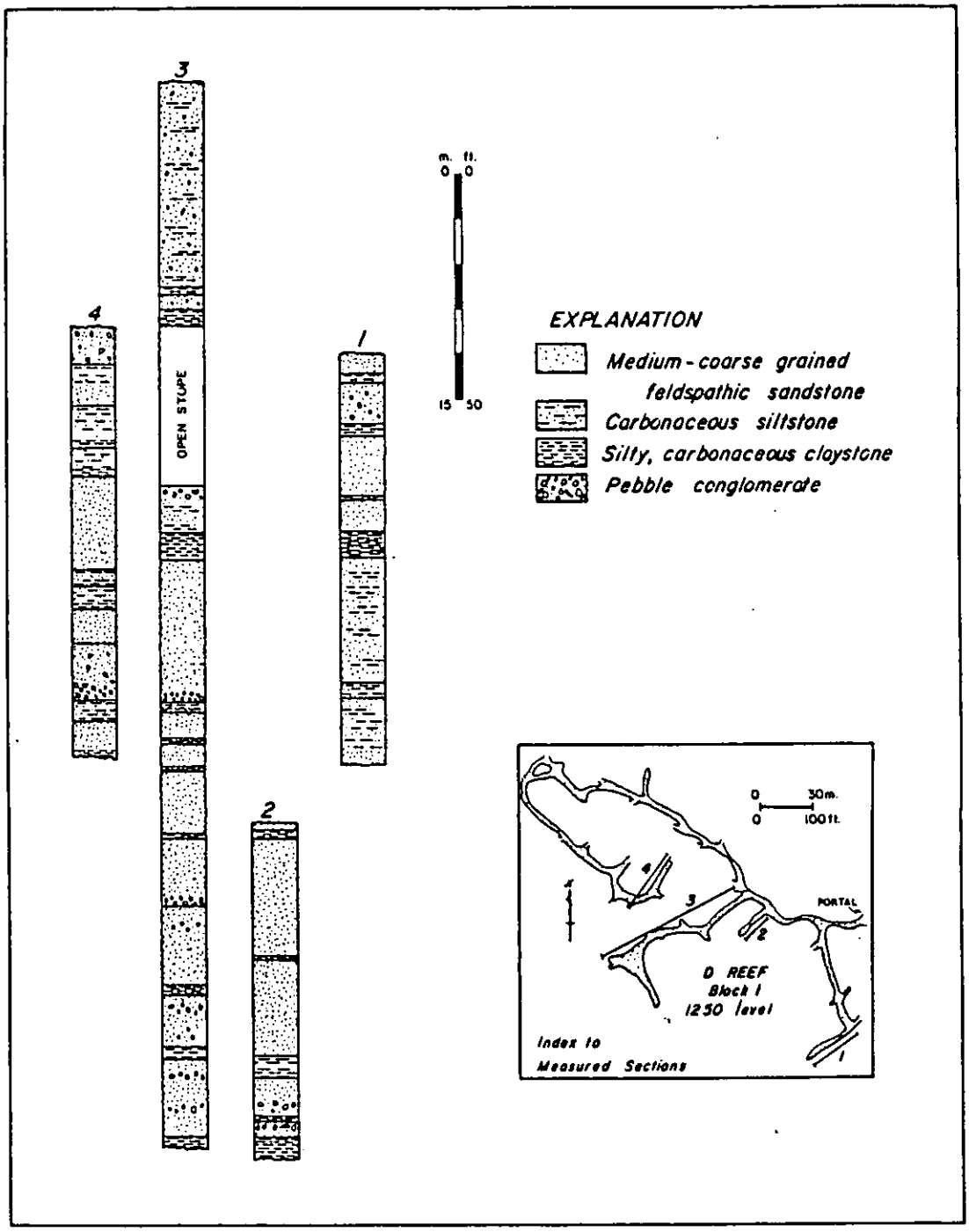

Figure 62. Measured stratigraphic sections in Block 1 of the 1250 level of the L-D mine. Measured by T. Roberts M. Klisch, and L. Ott.

centimeter diameter pebbles of biotite gneiss, granite, and volcanic rock supported by a feldspathic sandstone matrix, are locally useful for correlation purposes (Figure 62). Carbonized plant remains are common in all of the sedimentary beds and abundant in siltstone horizons.

The stratigraphic section in Blocks 2 and 3 has not been closely inspected. In general, Block 2 appears to contain more silty carbonaceous rocks than are present in Block 1. However, the intensity of silicification and veining in Block 2 is greater than in Block 1, and the original character of the sedimentary host rock is not as evident. Thickly bedded feldspathic sandstones are the principal rock type in Block 3; cross bedding and other useful sedimentary structures can be observed in the northwestern portion of this area of the 1250 level, where the intensity of alteration diminishes.

Sedimentary beds at "D" reef are thicker and contain a greater portion of medium- to coarse-grained feldspathic sandstone beds than the beds at the "B" reef complex. The thinly laminated interbeds of carbonaceous siltstone that are prevalent in units 1 and 2 in the "B" North ore body are not evident at "D" reef, and the distinctive pebble conglomerate beds in coarse-grained sandstones at "D" reef are not evident in the "B" reef complex. The two sequences of mineralized sedimentary rocks therefore cannot be directly correlated.

Mineralization and Hydrothermal Alteration

With the exception of the southeast part of Block 1, the style of mineralization at "D" reef is generally similar to the "B" reef complex. In Blocks 2 and 3, ore-grade rock consisted of discontinuous high-grade veins and veinlets in pervasively silicified feldspathic sandstone (Figure 63). In the southeast portion of Block 1, northeast-trending veins, up to 2 meters in width, were mined as separate entities. In Blocks 2 and 3, multiple periods of fracturing are manifest by complex cross-cutting vein relationships; however, the paragenesis of veining, particularly with regard to gold deposition, has not been deciphered. In Block 1, there are fewer veins, and the veins have greater continuity, enabling early workers to recognize a temporal relationship between mineralized and barren veins. Lovitt and Skerl (1958, p. 966) note that auriferous veins in Block 1 always dip 60^{o} to 80^{o} to the north, and are offset by barren south-dipping to near-vertical quartz veins.

Guilbert (1963) examined 23 ore specimens for Day Mines Co. and his work revealed that the principal ore minerals at "D" reef are electrum, native gold, and naumannite (Ag_2Se). Other sulfide minerals reported by Guilbert are pyrite, marcasite, chalcopyrite, and minor tetrahedrite, sphalerite, and stibnite. Moody (1958) unsuccessfully searched for the presence of telluride minerals. Neither stibnite nor any selenide minerals have been identified at the "B" reef complex.

Figure 63. Style of veining in the northeast part of the 1250 level of Block 1. Note the sinuous discontinuity of veins in the right portion of the photograph. The vein in the back, above the miner, is gold-bearing and dips steeply to the north. The south-dipping vein in the lower left part of the photograph is barren and offsets the north-dipping vein.

Guilbert (1963, p. 24) noted that precious metals were deposited in veins early during the period of fracture filling. Gold, electrum and naummanite were localized within approximately a millimeter of the vein wall in all the samples studied by Guilbert. Traces of chalcopyrite occurred between the vein wall and ore minerals in only a single specimen.

Non-sulfide gangue minerals identified by Guilbert include quartz, and calcite. Chappell (1936, p. 131) recognized adularia in an outcrop sample of vein material from the "D" reef. Guilbert (1963) identified three modes of silicification in samples from the L-D mine: (1) quartz flooding in feldspathic sandstone, (2) gray to milky white fine-grained, vuggy vein quartz, and (3) coarse-grained, clear coxcomb quartz. Guilbert emphasized that the flood silica and milky quartz modes are not necessarily representative of sequential silicification stages, and suggested that the two may be contemporaneous (Guilbert, 1963, p. 23).

Lamellar quartz with attendant calcite is common in veins at the L-D mine, particularly in Block 2. The lamellar quartz with infilling calcite is commonly in the inner portion of the veins, but some veins display this structure across the entire vein width. Only minor amounts of sericite and kaolinite are present in wall rocks of Blocks 1 and 2 of the 1250 level. Feldspathic sandstones in the northwest portion of Block 3 are argillized but still contain auriferous veins. Sedimentary rocks exposed in road cuts at the ridge crest between "D" reef and the "B" reef complex are moderately argillized.

OTHER MINERALIZED AREAS

No economic mineralization has been identified at "E" reef, "C" reef, "A" reef, "F" reef, or "G" reef, although each of these exposures has been prospected in varying degrees of detail. "A" reef is the largest of the subeconomic outcrops of mineralized rock and has been prospected thoroughly since 1952, when Anaconda drove approximately 500 feet of exploratory drifts at the 1250 foot elevation. A short exploration drift was also driven into the "C" reef outcrop, and numerous trenches and small pits have been excavated in the vicinity of "F" and "G" reefs. Subsequent to these early exploration efforts, intensive diamond drilling has been conducted at "A" reef and "C" reef by Cyprus Mines Corporation and Asamera Minerals and Breakwater Resources. To date, none of these efforts have been successful in locating any ore grade material in sufficient tonnage to be economic.

With the exception of "A" reef, all of the peripheral reef consist of silicified, veined sedimentary rocks, generally similar in appearance to the "B" reef and "D" reef. At "A" reef, the Saddle Rock andesite has been altered and weakly mineralized with gold. Figure 64 is a map of the 1250 exploration drift at "A" reef. Sedimentary rocks east of the andesite have been extensively brecciated, and bedding attitudes are not recognizable. The andesite is intensively silicified and not recognizable as andesite, except for a few relict hornblende "ghosts" in thin section. Petrographic examination of silicified andesite sampled from surface

exposures at "A" reef reveal that the rock is pervasively silicified and argillized in a selectively pervasive style. Plagioclase grains are altered to pale-brown clay that has been tentatively identified by x-ray diffraction as kaolinite (R. Ashley, written communication, 1986). Hornblende phenocrysts are altered to pale-brown kaolinite(?) and pyrite. The groundmass of the andesite is completely altered to fine-grained quartz, and millimeter-size quartz veinlets cross-cut this pervasively silicified groundmass.

The highest grades of gold mineralization at "A" reef occur in quartz veins in the altered andesite. These veins have a dominant northeast strike, and dip 50^{o} to 60^{o} to the southeast (Figure 64). In contrast to veins in the "B" reef complex, the quartz veins at "A" reef do not have a crustified appearance, and consist mainly of white drusy quartz.

North of the "A" reef outcrop, two isolated blocks of silicified, veined feldspathic sandstone are exposed. Drilling and trenching indicate that these blocks are not connected to each other or to the "A" reef outcrop. Numerous drill holes in the vicinity of "A" reef indicate that alteration and veining do not persist below approximately the 950-foot elevation, and that the silicified zone is underlain by sheared carbonaceous claystone beds or gouge material. For this reason, "A" reef, and the blocks of mineralized rock to the north are interpreted to be down-dropped from "F" reef (Plate 2).

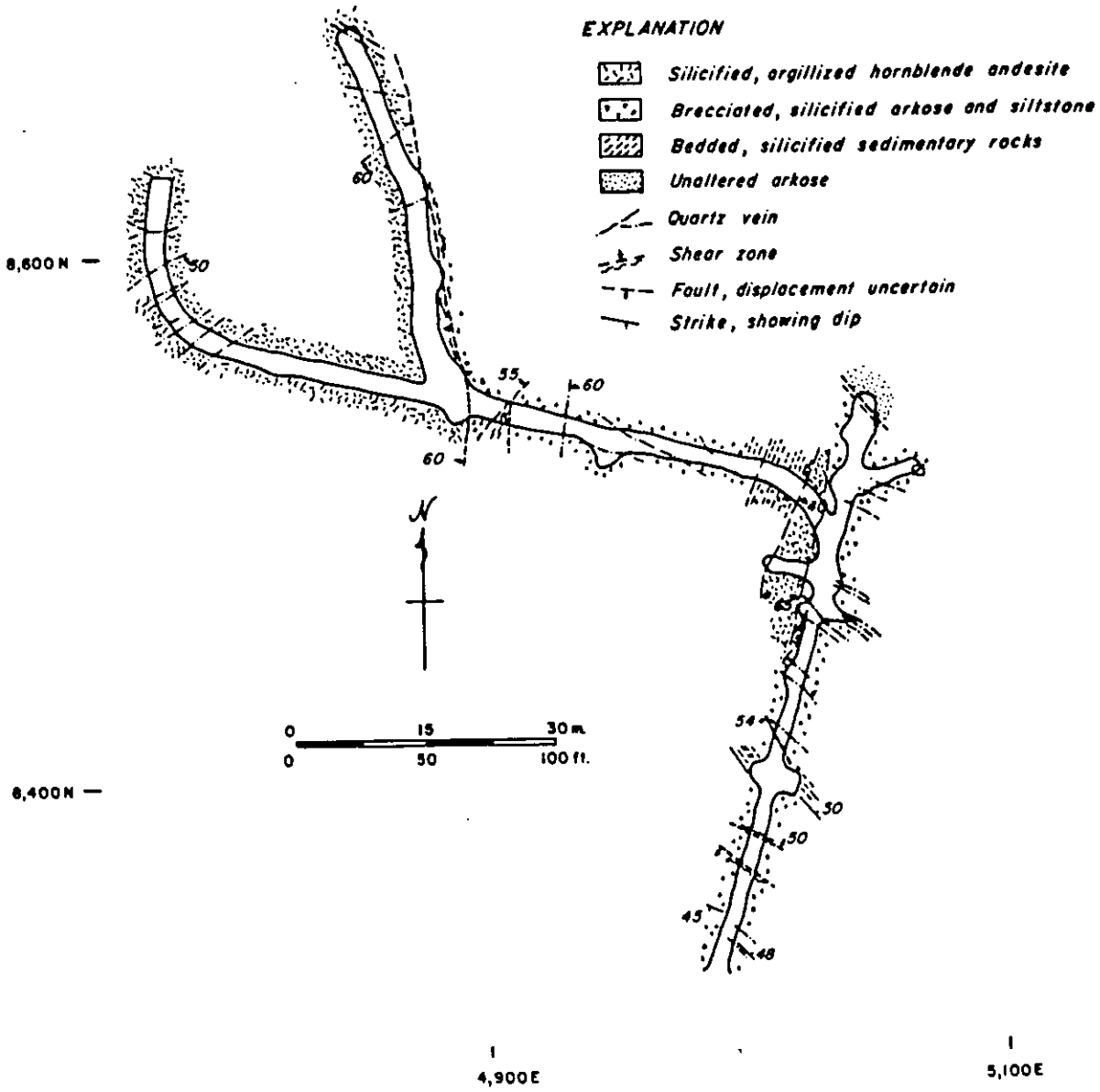

Figure 64. Geologic map of the 1250 level at "A" reef.

"F" and "G" reefs are of interest because they are the only zones of altered sedimentary rocks west of the Saddle Rock andesite. Unfortunately, there is a paucity of outcrop in the area and drilling is not extensive enough to make a very detailed interpretation of the subsurface. From the drill hole information available, there appears to be a diffuse zone of weakly to moderately argillized sedimentary rocks west of the Saddle Rock outcrop, extending from nearly the bottom of Dry Gulch, northwest to "G" reef. Within this zone of argillization are sparse zones of more intensively argillized and, uncommonly, silicified sedimentary rocks. Gold values are generally low, but some intercepts of silicified rock have produced assays in excess of 0.20 oz/ton over a five foot core run. "F" and "G" reefs are apparently larger silicified zones within the northwest-trending argillic zone, but an assessment of the full mineralization potential in this area will require additional subsurface information.

"C" reef appears to be a weakly mineralized extension of "D" reef, and can possibly be considered as Block 4 in the en echelon series (Plate 1). The exploratory drift into the "C" reef was not accessible during this investigation, but existing assay and geologic maps show low grades of gold in silicified, brecciated sedimentary rocks. The southernmost limit of drift at "C" reef is approximately 250 west and 350 feet above the northwesternmost limit of drifting in Block 3 of the 1250 level. This amount of displacement is within range of estimated displacement on the North South fault

which separates Blocks 1 and 2.

Hornblende andesite, compositionally equivalent to, and on strike with the Saddle Rock andesite crops out immediately west of "C" reef. In surface exposure, this andesite exposure is not appreciably altered, but drilling shows the andesite to be weakly argillized at depth, similar to andesite intercepted by drilling along the western margin of the "B" reef complex. No drilling has been conducted west of the andesite exposure adjacent to "C" reef to investigate the potential presence of mineralized and altered rocks similar to the trend west of the Saddle Rock exposure.

"E" reef forms a small topographic high in the mouth of the drainage west of "D" reef (Plate 1). A limited amount of drilling has been conducted at "E" reef by Cyprus and, more recently, by the Lovitt Mining Company (Folk, 1987). Data are not sufficient to determine the relationship of "E" reef to "D" reef. "E" reef may be a structurally detached block that was initially part of "D" reef, but the required displacement would be inconsistent with known fault patterns in the district. Hornblende andesite has been encountered by drilling west of the "D" reef outcrop, between "E" reef and "C" reef and may continue southeast between "E" reef and "D" reef (Plates 1 and 2). "E" reef may represent a southeastern extension of the trend of altered sedimentary rocks extending from "G" reef to the bottom of Dry Gulch.

DISCUSSION

The mineralogical and textural characteristics of ore deposits in the Wenatchee district are typical of those found in epithermal precious metal deposits worldwide. The principal characteristics and occurrences of epithermal systems as well as conceptual models of the genesis of epithermal precious metal deposits, are reviewed in recent literature by Berger and Eimon (1983), Buchanan (1981), Durning and Buchanan (1981), Hayba and others (1985), and Heald and others (1987). Such models are either based on, or substantiated by, studies of active geothermal systems (Weissberg and others, 1979; White, 1981; Henley and Ellis, 1983), some of which are currently depositing ore-grade concentrations of gold and silver (Weissberg, 1969; Krupp and Seward, 1987; Hedenquist and Henley, 1985).

Ore deposits in the Wenatchee district can be classified in the gold-selenide category of epithermal deposits as proposed by Lindgren (1933). Other selenide-bearing epithermal precious metal deposits include Knob Hill, Golden Promise, and Seattle deposits in the Republic district of Washington (Dixon and Brackney, 1986; T. Devoe and R. Tschauder, oral communication 1988), the De Lamar-Silver City district, Idaho (Barrett, 1985; Bonnichsen, 1983; Pansze, 1975; Lindgren, 1900), the Hishikari gold deposit in Japan (Abe and Kawasaki, 1987), and Guanajuato, Mexico (Gross, 1975). The most common selenide minerals at these localities are aguilarite and naummanite, which were important ore minerals at the L-D mine.

Fluid inclusion analyses of veins from the "B" reef complex were unsuccessful, and light stable isotopes have not been investigated in the Wenatchee district; therefore, there is no quantitative data on the original chemistry of hydrothermal fluids responsible for mineralization. In this discussion, it is assumed that the general chemical characteristics of the mineralizing fluids were similar to other epithermal fluids, and fluids in active geothermal systems, that have been extensively analyzed. The fluids were probably dilute (Nash, 1972; Hayba, 1983), of meteoric origin (O'Neil and Silberman, 1974), temperatures ranged from 300^0C to 100^0C (Hayba, 1983), the principal solutes were SiO_2, Na, K, Ca, Cl, CO_2, H_2S, and CH_4 (Ellis, 1979), the pH range was slightly acidic to slightly alkaline (Henley, 1985), and gold transport was by means of either chloride or bisulfide and thiosulfide complexes (Seward, 1973, 1984; Cole and Drummond, 1986). Furthermore, sulfide and gangue mineral precipitation may have resulted from either fluid boiling or mixing with oxygenated waters (Buchanan, 1981; Berger and Eimon 1983; Drummond and Ohmoto, 1985; Reed and Spycher, 1985; Cole and Drummond, 1986).

Within these constraints, an interpretation of the geochemistry of the hydrothermal system responsible for mineralization in the Wenatchee district will be made. This interpretation will be based on ore and gangue mineralogy, vein and breccia textures, alteration patterns, trace element assemblage, and comparison of these data with similar

characteristics in other epithermal deposits.

Davidson (1960) investigated the occurrence of selenium in some epithermal deposits hosted by volcanic rocks, and has suggested that selenium concentrations may be influenced by the degree of crystallinity of extrusive rocks. Davidson (1960, p. 14) has proposed that selenium is lost in the process of crystallization, and that rapidly cooled, noncrystalline volcanic rocks retain their selenium content. Coleman and Delevaux (1957, p. 525) have proposed that selenium enrichment in sedimentary rocks is suggestive of a volcanic provenance.

Similar ionic charge and radii permit ready substitution of selenium for sulfur in many common sulfide minerals, and Coleman and Delevaux (1957, p. 522) have proposed that a complete isomorphous series FeS_2-$FeSe_2$ may exist at moderately high temperatures. Isomorphous series for PbS-PbSe have been produced experimentally by Earley (1950, p. 356) and identified in nature by Coleman (1958, p. 1679). Wright and others (1965, p. 1814) produced continuous solid solutions for PbS and PbSe, and for ZnS and ZnSe at temperatures as low as 300^0C. Davidson (1960, p. 3) has proposed that a similar system may exist for Ag_2S-Ag_2Se. Petruk and others (1974, p. 369) determined from specimens from Guanajuato, Mexico and Silver City, Idaho, that acanthite composition can vary from Ag_2S to $Ag_2S_{0.85}Se_{0.15}$, aguilarite composition from $Ag_4S_{0.95}Se_{1.05}$ to $Ag_4S_{1.10}Se_{0.90}$, and naummanite composition from Ag_2Se to $Ag_2S_{0.12}Se_{0.88}$. They assumed a complete solid

solution between argentite and naummanite above 176^{0}C (Petruk and others, 1974, p. 368). No naturally occurring gold selenide minerals have been reported, although various forms of AuSe have been produced experimentally (Cranton and Heyding, 1968), and fishchesserite (Ag_3AuSe_2) the selenium analog of petzite, has been reported in carbonate veins at Predborice, Czechoslovakia associated with native gold, naumannite, and clausthalite (Zdenek and others, 1972, p. 1554).

Trace amounts of Se associated with mineralization at the "B" reef complex are possibly an indication of limited substitution of Se for S in one or more of the sulfides present. However, microprobe analysis of these pyrargyrite, acanthite, and electrum did not detect any selenium.

Pyrargyrite and electrum are the principal ore minerals in the "B" reef complex. Most experimental studies on the stability of pyrargyrite have focused on its phase relations with other sulfosalts and argentite (Chang, 1963; Craig and Barton, 1973; Keighin and Honea, 1969). Barton and Skinner (1979, p. 383) point out that sulfosalts are not particularly good indicators of physical conditions of ore formation, as they represent a diverse group of minerals that require sophisticated analytical techniques for positive identification. Barton and Skinner also point out that sulfosalts are difficult to synthesize experimentally as they have undesirable quenching properties, and are compositionally complex.

Textural relations indicate that pyrargyrite has been partially replaced by electrum in vein samples from the "B" North ore body. This may indicate that sulfur activity decreased during the period of ore mineral deposition. Margolis (1987, p. 78) interpreted the paragenetic sequence of arsenopyrite to stibnite to native antimony in vein samples from the Wenatchee Heights area to be indicative of decreasing sulfur activity with time.

The nature of precious metal transport in solutions from which ore bodies in the Wenatchee district were deposited is uncertain. Experimental work by Cole and Drummond (1986, p. 53) indicates that $Au(HS)_2^-$ (and presumably similar sulfide complexes) is more stable than chloride complexes at relatively low temperatures (less than 250^0C), high pH (>5) and high total H_2S concentrations, and that the ratio of silver to gold in solution in these solutions is generally less than 10. Their work also predicts that deposits precipitated from solutions that transport gold as bisulfide complexes will contain argentite as the dominant silver mineral with subordinant native silver (and presumably silver as electrum), and that these deposits will have low Ag/Au ratios provided that the Ag/Au ratio in solution is not significantly changed during mineral precipitation (Cole and Drummond, 1986, p. 58). Solutions in which $AuCl_2^-$ is stable are characterized by relatively high temperatures ($>250^0C$), low pH (<5), lower H_2S concentration, and higher chloride concentration (Cole and Drummond, 1986, p. 53), and that the

dominant silver mineral deposited from these solutions will be native silver, with subordinant argentite. Ag/Au ratios in solutions in which chloride complexes are dominant tend to be greater than 10 and typically are greater than 100.

The silver/gold ratio at both "D" reef and the "B" reef complex is between 1 and 2, and this may indicate metal transport as bisulfide complexes, and would be compatible with observed metal complexes in active geothermal systems (Seward, 1973; Krupp and Seward, 1987, p. 1127). Acanthite is not abundant, as would be expected in hydrothermal environments in which gold is transported as a bisulfide complex (Cole and Drummond, 1986, figure 3), but pyrargyrite, paragenetically earlier than electrum, may indicate comparatively high total H_2S concentrations. Precipitation of silver as electrum later in the period of ore deposition reflects decreasing sulfur activity, but does not necessarily suggest precious metal transport by chloride complexes (Cole and Drummond, 1986, p. 53).

The reasons for episodic variation in fluid chemistry, indicated by symmetric encrustations of quartz, chalcedony, and adularia, are not fully understood, but fluid boiling is a possibility. No direct evidence of fluid boiling was found in this investigation. Criteria described by Buchanan (1981) as evidence for fluid boiling include fluid inclusion data, the presence of very fine-grained quartz, ore shoots with flat bottoms, and the presence of a low-pH alteration assemblage overlying ore. The lower boundary of mineralization in the

"B" North and "B-4" zones is stratigraphically controlled but the nature of the lower boundary has not been identified in the "B" Neath zone. Elswhere in the district, the bottom of mineralization appears to be controlled by post-mineralization faults. Fine-grained quartz is abundant in all ore bodies in the district, and rocks overlying the "B" reef complex are argillized and wall-rock and vein breccias, and stockwork veining in massive feldspathic sandstone beds indicate excessive fluid pressures, and local, violent pressure release, with attendant boiling. Also, the spherical-clast breccias associated with many veins and breccia zones are indicative of grain abrasion in a vapor-dominated environment.

Numerous workers have cited evidence of fluid boiling in epithermal systems (Buchanan, 1981; Berger and Eimon, 1983). Drummond and Ohmoto (1985) and Reed and Spycher (1985) discuss important changes in fluid chemistry that are caused by boiling. Silicate precipitation, particularly quartz, is primarily a function of temperature in near-surface hydrothermal systems (Fournier, 1985, p. 55). Of particular interest is the work by Reed and Spycher (1985) on the stability of potassium silicate minerals in a boiling epithermal solution. Reed and Spycher (1985, p. 258) have shown that muscovite and K-feldspar precipitate because Al is liberated from $Al(OH)_4^-$ as temperature decreases. These silicate minerals, therefore, are not precipitated as a result of boiling. However, K-feldspar is more stable than muscovite in high pH solutions, as is indicated by the following

reaction of Reed and Spycher (1985, p. 258):

$$6SiO_2 + KAl_3Si_3O_{10}(OH)_2 + 2K^+ = 3KAlSi_3O_8 + 2H^+$$

In dilute, near-surface hydrothermal solutions, such as the solutions in active geothermal systems, the most significant chemical difference between solutions that boil and solutions that cool without boiling is the change in pH. In boiling solutions, pH increases as a consequence of rapid liberation of acid volatile phases, primarily CO_2, but also H_2S and HCl (Reed and Spycher, 1985, p. 253). In solutions that cool without boiling, pH decreases from the dissociation of weak acids (H_2CO_3, HCl, HSO_4^-) (Reed and Spycher, 1985, p. 252).

In the reaction shown above, decreasing pH would tend to drive the reaction to the left, producing sericite at the expense of K-feldspar. Abundant adularia in veins and, possibly, the matrix of silicified wall-rocks, and unaltered detrital grains of orthoclase and microcline in the mineralized wall-rocks, together with the paucity of sericite in altered rocks of the "B" reef complex, attest to the relatively alkaline pH of the mineralizing fluids.

Quartz is present as fine-grained quartz, chalcedony, and possibly, opal in the "B" reef complex. Fournier (1985, p. 46) states that the amount of dissolved silica in geothermal well waters is a function of the solubility of quartz at temperatures over 180^0C and a function of the solubility of chalcedony at temperatures below about 140^0C. The possible presence of opal is significant because amorphous silica has

the same solubility at 100^{0}C as quartz at about 220^{0}C (Fournier, 1985, figure 3.2); therefore, considerable cooling of the solution is required to precipitate opal. In veins in the "B" North ore body, opal(?) is minor, and occurs most commonly paragenetically late, associated with fine-grained quartz and chalcedony in lamellar boxworks, where quartz has replaced calcite. Chalcedony generally occurs as discontinuous bands and lenses on the borders of fine-grained quartz bands. Slight silica supersaturation with respect to quartz is required for chalcedony to precipitate (Fourneir, 1985, p. 55).

Fournier (1985, p. 71) has shown that, in most natural geothermal waters, calcite can be precipitated by heating or boiling, and that simple cooling of solutions, without decompressional boiling, tends to increase calcite solubility. Where vein calcite is abundant in the "B" reef complex, it commonly fills the interior portions of veins; elsewhere, the interior portion of veins are filled with hydrothermal breccia and lamellar boxworks of quartz. One possible interpretation of this relationship is that vein carbonate was precipitated at various stages of boiling in the mineralizing fluids, but that, with a general cooling of the hydrothermal system, calcite solubilities increased, and quartz solubilities decreased, resulting in the replacement textures observed.

Alteration patterns at the "B" reef complex are characteristic of alteration patterns associated with adularia-sericite-type epithermal deposits as described by

Heald and others (1987). In these deposit types, a clay-rich cap, generally consisting of sericite or mixed layer illite-smectite clays, commonly forms over the ore body, due to condensation of acid volatiles released during boiling (Heald and others, 1987, p. 8). The most abundant clay mineral in the argillic zone at the Cannon mine is smectite, but additional XRD work is needed to fully appreciate the spatial distribution of clay species within this zone.

Reed and Spycher (1985, p. 265) show that oxidation of H_2S by ground waters containing Fe concentrations in the tens of ppm range is sufficient to produce pyrite in excess of that produced by sulfidation of iron originally present in the host rock, by the following reaction:

$$4Fe^{2+} + 7H_2S + SO_4^{=} = 4FeS_2 + 4H_2O + 6H^{+}$$

Abundant pyrite in the argillic cap over ore bodies in the Wenatchee district may indicate mixing of condensed acidic volatile phases with oxygenated meteoric ground waters. The above reaction would also contribute to the development of acid-stable minerals in the argillic cap as a result of increased hydrogen ion concentration.

TRACE ELEMENT GEOCHEMISTRY

Trace element geochemical trends were investigated in three interrelated studies at the "B" reef complex during the course of this research. As a preliminary investigation, a suite of mineralized wall rock and vein samples, collected by D. Groody of Asamera Minerals, were submitted to Bondar-Clegg and Company of North Vancouver, B. C. for instrumental neutron activation analysis (NAA). The purpose of this investigation was to rapidly determine the content and variability of a broad spectrum of trace elements within the "B" North ore body. Elements included in the NAA package were Au, Sb, As, Ba, Cd, Cr, Co, Hf, Ir, Fe, La, Mo, Ni, Se, Ag, Na, Ta, Th, W, U, and Zn. In a closely related study, a separate suite of vein samples from the "B" North and "B" Neath ore bodies was submitted to Bondar-Clegg for directly coupled plasma emission spectrographic analysis (DCP) to determine if a vertical zonation of trace elements could be detected within the veins.

The second geochemical study was designed to determine if there were any significant trends in trace element content across the contacts between ore and intrusive rocks of the Wenatchee Dome, and ore and hornblende andesite on the eastern and western boundaries of mineralization, respectively. Continuous chip samples, divided into five-foot intervals, were taken across the fault zone separating ore from perlite on the 755, 700, and 550 levels. The chip sample lines extended a minimum of 50 feet to the east, and to the west of the contact. Also included in this sampling program were core

samples, divided into five-foot intervals, from a single drill hole that passed through mineralization into andesite west of the "B" Neath ore body. These samples were submitted to Chemex Labs of Vancouver, B. C. for semi-quantitative emission spectrographic analysis.

The third geochemical investigation was designed to evaluate zonal trends in trace elements vertically above and below the "B" reef complex. A fifty-foot-wide vertical corridor, oriented $N25^{0}W$, was selected as a long section through the various ore bodies of the "B" reef complex from which to collect samples for this program. This corridor was subdivided into 50-foot cubes, and drill core samples were composited for each cube. The sample point was selected as the center of each cube, regardless of drill hole orientation or the position of the core interval within the cube. Samples composited for this investigation were crushed to -1/8 inch mesh, split, and submitted to Silver Valley Labs of Kellogg, Idaho for atomic absorption (AA), and fire assay analysis. These samples were analyzed for Au, Ag, As, Sb, Se, Hg, Te, Cu, and Pb.

Instrumental Neutron Activation Analytical Data

Wall-Rock Samples

NAA geochemical data for mineralized wall-rock samples were treated separately from vein sample data. Analytical results for 78 wall-rock samples are shown in Appendix A. Pertinent statistical information for these data is shown in

Table 5. Results for Ir, Se, and Ta are omitted from Appendix A because all samples are below the detection limits of 100 ppb, 10 ppm, and 1 ppm, respectively. Zn is omitted because of the insensitive lower detection limit of the analytical technique (200 ppm).

Information on trace element content of unmineralized sedimentary rocks in the Wenatchee district does not exist, so the data in Appendix A and Table 5 cannot be compared with "background" element contents. However, for the sake of comparison, Table 6 shows the average values of elements in Appendix A and average values for the same elements in "normal" shale, sandstone, and granite. Average trace element values in unmineralized feldspathic sandstone and shale beds in the Wenatchee district may deviate from average sandstone and shale in the following respects: (1) feldspathic sandstone beds in the Wenatchee district consists of very angular grains of feldspar, quartz, and lithic fragments. This feature, coupled with the depositional setting, indicates that element content of the sandstones may be closer to the igneous and metamorphic parent rocks than to worldwide sandstone averages. (2) the Ingalls ultramafic complex on the western margin of the Chiwaukum graben (Figure 4) contributed to sediments in the region during Eocene sedimentation. For this reason, sedimentary rocks in the mine area may contain elevated concentrations of Co, Fe, and Cr. With these cautions in mind, it can be seen from Table 6 that mineralized wall rocks in the "B" North ore body contain noticeably

Table 5. Statistical summary of instrumental neutron activation analyses for Au, Sb, As, Ag, Na, Cr, Fe, Ba, Hf, La, Mo, Cd, Co, Th, W, and U in wall rock samples from the "B" North ore body. 78 samples.

Element	Maximum Value	Minimum Value	Average Value	Standard Deviation	Detection Limit
Au ppb	9780	1	937	1783	2
Sb ppm	29	0.3	4.4	4.1	0.1
As ppm	611	2	93	110	0.5
Ag ppm	9	1	1.3	1.4	2
Na %	4.6	0.8	2.5	0.6	0.02
Cr ppm	350	53	162	68	20
Fe %	6	0.5	2.7	1.2	0.2
Hf ppm	9	1	3.8	1.2	1
La ppm	55	12	21.2	6.3	2
Mo ppm	95	1	9.2	11.6	1
Cd ppm	3	1	1.1	0.3	1
Co ppm	29	5	7.7	4.2	5
Th ppm	12	2.4	4.7	1.8	0.2
W ppm	6	1	2.4	1.2	1
U ppm	14	0.7	2.2	1.8	0.2
Ba ppm	2200	370	895	326	50

Correlation Coefficients:

	Sb	As	Ag	Na	Cr	Fe	Hf	La	Mo
Au	.36*	.53*	.76*	-.21	.38*	.04	-.31	-.34	.16
Sb	1	.59*	.13	-.53*	.31	.13	-.41	-.26	.09
As		1	.30	-.13	.24	.46	-.42	-.20	.04
Ag			1	-.09	.23	-.08	-.23	-.25	.15
Na				1	-.14	.12	.50	.44	-.03
Cr					1	-.02	-.42	-.46	.33
Fe						1	.20	.34	-.26
Hf							1	.73	-.22
La								1	-.23
Mo									1

* - denotes element pairs for which scatter diagrams are shown in Appendix E.

Table 6. Comparison of average concentrations of trace elements in mineralized wall rock samples from the "B" North ore body with worldwide averages for sandstone, shale, and granite.

Element	Average Shale*	Average Sandstone*	Average Granite**	Mineralized Wall Rock
Sb ppm	1.50	0.0X+	0.20	4.40
As ppm	13.00	1.00+	1.50	93.00
Ag ppm	0.07	0.0X+	0.04	1.30
Na %	0.96	0.33	2.80	2.50
Cr ppm	90.00	35.00	20.00	162.00
Fe %	4.72	0.98	2.70	2.70
Hf ppm	2.80	3.90	4.00	3.80
La ppm	92.00	30.00	55.00	21.20
Mo ppm	2.60	0.20+	1.50	9.20
Cd ppm	0.30	0.0X+	0.10	1.10
Co ppm	19.00	0.30	3.00	7.70
Th ppm	12.00	1.70	20.00	4.70
W ppm	1.80	1.60	1.50	2.40
U ppm	3.70	0.45+	4.00	2.20
Ba ppm	580.00	X0.00+	700.00	895.00

* From Mason, 1966, p. 181.
** From Krauskopf, 1979, p. 544.
\+ Variable concentration, shown as order of magnitude estimate.

elevated levels of Ag, Sb, As, Mo, and Cd, and possible enrichments of Ba, W, Cr, and Co, relative to "normal" sandstones and shales.

The primary objective of this investigation is to determine if any of the elements in the NAA package had a linear correlation with gold. Values for many of the elements (La, Hf, W, U, Co) show little variation; other elements (Ag, Cd) are present in concentrations below the analytical detection limit in over 90% of the samples. Elements showing the best correlation with gold are silver ($r = 0.76$) and arsenic ($r = 0.53$). Because silver concentrations in most samples are below the instrumental detection limit, the high correlation between gold and silver is considered dubious.

Other significant correlations in element values include Sb and As ($r = 0.59$), As and Fe ($r = 0.46$), and a negative correlation for Sb and Na ($r = -0.53$) (Table 5).

Vein samples

NAA data for 62 vein samples from the "B" North ore body are shown in Appendix B. Table 7 shows a statistical summary of the NAA data for vein samples. Compared with wall rocks, veins in the "B" North ore body are strongly enriched in Au, Ag, Sb, and Cd. As, Cr, Mo, and W are moderately enriched, and Na, Fe, La, Th, and Ba are comparatively depleted in the veins. U, Co, and Hf concentrations are comparatively unchanged.

Gold does not correlate well with other trace elements in veins, and the best correlation coefficients are all negative (Table 6). Arsenic, which correlates relatively well with gold in wall rock samples, shows a moderately negative correlation with gold in vein samples. The doubtful correlation between gold and silver in wall rock samples is not evident in vein samples. This is surprising, as electrum is a major ore mineral in the "B" North ore body. The poor correlation between gold and silver may be attributed to the fact that the maximum reported gold concentration is >30,000 ppb; therefore, the sample population is artificially restricted from high gold concentrations. However, many of the gold values that exceed the upper detection range contain relatively low silver concentrations (Appendix E), and this indicates that gold, without silver is present in many samples.

There is a strong correlation between silver and antimony, silver and cadmium, silver and hafnium, and silver and chromium. The silver-antimony correlation is a reflection of the presence of pyrargyrite as a major ore mineral. Since hafnium concentrations are essentially the same in vein and wall rock samples (compare average values in Tables 5 and 7), its correlation with silver in vein samples may be fortuitous. Arsenic, sodium, and iron values show good correlations with each other (Table 7).

Table 7. Statistical summary of instrumental neutron activation analyses for Au, Sb, As, Ag, Na, Cr, Fe, Ba, Hf, La, Mo, Cd, Co, Th, W, and U in vein samples from the "B" north ore body. 62 samples.

Element	Maximum Value	Minimum Value	Average Value	Standard Deviation	Detection Limit
Au ppb	49500	935	18090	12001.1	2
Sb ppm	1490	11	86	190.5	0.1
As ppm	515	37	130	99.1	0.5
Ag ppm	2210	1	97	301.1	2
Na %	2.16	0.05	0.34	0.44	0.02
Cr ppm	1300	160	428	151.9	20
Fe %	2.60	0.1	0.77	0.53	0.2
Hf ppm	28	1	2	3.81	1
La ppm	20	1	4	4.71	2
Mo ppm	93	1	24	17.1	1
Cd ppm	140	1	8	19.7	1
Co ppm	24	5	6	2.9	5
Th ppm	15	0.1	1.6	2.3	0.2
W ppm	61	1	4.4	8.4	1
U ppm	23	0.2	1.5	3.2	0.2
Ba ppm	1500	100	342	272	50

Correlation Coefficients:

	Sb	As	Ag	Na	Cr	Fe	Hf	La	Mo	Cd
Au	.25	-.42	.27*	-.39*	.34*	-.47*	.16	-.60	.38	.32
Sb	1.0	.08	.98*	.15	.75*	.05	.94	-.04	.58	.95*
As		1.0	.06	.60*	-.23	.73*	.17	.77	-.22	.05
Ag			1.0	.18	.72	.08	.96	-.04	.61	.98*
Na				1.0	-.07	.72*	.32	.75	-.30	.17
Cr					1.0	-.25	.63	-.38	.59	.69
Fe						1.0	.24	.86	-.39	.08
Hf							1.0	.12	.52	.97
La								1.0	-.49	-.06
Mo									1.0	.60
Cd										1.0

* - denotes element pairs for which scatter diagrams are shown in Appendix E.

Directly Coupled Emission Spectrographic Analytical Data

Summary statistics for 46 vein samples analyzed by directly coupled plasma emission spectroscopy are shown in Table 8, the specific data from this geochemical program are shown in Appendix C. In addition to the elements shown in Table 8, and Appendix C, the samples were analyzed for Mo, Co, Cd, Tl, V, and Te without significant results. DCP data cannot be compared directly with the NAA data because the sample digestion procedure for the DCP samples only allowed elements contained in minerals that are soluble in Aqua-Regia (HNO_3 - HCL) to be detected. The DCP analyses are therefore semi-quantitative.

Significant correlation coefficients in the DCP data set are noted in Table 8. Correlations of trace elements with silver are of limited value because silver analyses were reported in a range of 0.5 to 50 ppm, and four of the samples (8.7% of the total sample population) contain >50 ppm Ag. Despite this limitation, silver and antimony correlate reasonably well. Only ten of the 46 samples contained selenium concentrations above the 5 ppm detection limit, and correlations of various trace elements with selenium should therefore be viewed with skepticism.

Average trace element content in veins from various levels of the "B" North and "B" Neath ore bodies is shown in Table 9. The data set is small and not statistically significant; elements that show little or no variation in average value may be better represented than those that are

Table 8. Statistical summary of directly coupled plasma emission spectrographic analyses for Ag, As, Sb, Cu, Zn, Se, Fe, Mn, Cr, and Ni, and cold vapor atomic absorption analysis for Hg in vein samples from the "B" North ore body. 47 samples.

Element	Maximum Value	Minimum Value	Average Value	Standard Deviation	Detection Limit
Ag ppm	50	1	20	15	0.5
As ppm	1460	8	148	236	5
Sb ppm	2000	5	151	383	5
Hg ppb	5000	25	637	937	5
Cu ppm	18000	10	566	2581	1
Pb ppm	102	5	8	14	5
Zn ppm	78	1	15	14	1
Se ppm	461	5	22	71	5
Fe %	3.46	0.21	0.69	0.64	0.05
Mn ppm	5528	14	277	811	1
Cr ppm	171	50	110	29	1
Ni ppm	6	1	3	1	1

Correlation Coefficients:

	As	Sb	Hg	Cu	Pb	Zn	Se	Fe	Mn	Cr	Ni
Ag	.18	.50*	.08	.33	.35	.25	.44	-.17	-.09	-.34	-.26
As	1	.63*	.59*	.81*	.79*	.21	.76	.55	-.06	-.19	.02
Sb		1	.38	.76*	.76*	.15	.93	.06	-.03	-.12	-.04
Hg			1	.14	.14	-.02	.26	.81	-.12	.01	.14
Cu				1	.97*	.29	.94	.03	.02	-.22	-.14
Pb					1	.42	.93	.02	.02	-.24	-.18
Zn						1	.24	.01	-.04	-.33	.06
Se							1	.03	.01	-.19	-.10
Fe								1	-.12	.03	.30
Mn									1	-.25	-.37
Cr										1	.28
Ni											1

* - denotes element pairs for which scatter diagrams are shown in Appendix E.

Table 9. Average content of Cu, Pb, Zn, Ni, Cr, Mn, Ag, As, Sb, Se, Fe, and Hg in vein samples from the "B" North and "B" Neath ore bodies, by level. Semi-quantitative DCP emission spectrographic analysis.

Element	Level (Number of Samples) 755-780 (11)	700 (13)	600-650 (17)	450-500 (5)
Cu ppm	150	257	154	57
Pb ppm	5	7	5	5
Zn ppm	12	21	24	10
Ni ppm	3	3	3	4
Cr ppm	96	115	112	125
Mn ppm	651	230	130	72
Ag ppm	18	18	22	10
As ppm	115	78	119	262
Sb ppm	52	81	92	71
Se ppm	9	10	9	5
Fe %	0.59	0.40	0.70	1.60
Hg ppb	461	353	573	1350

highly variable on different levels. Concentrations of Pb, Zn, Ni, Cr, Sb, and Se do not change significantly from level to level. Fe and Hg concentrations appear to increase with depth, and Mn concentrations decrease with depth. Subsequent geochemical studies have shown that the apparent increase in mercury content with depth is the result of lateral zonation, and that, in general, elevated mercury concentrations overlie the "B" reef complex. Average Cu, Ag, and As concentrations in Table 9 appear to be too erratic to make a sensible interpretation, given the limited data base.

Trace Element Zonation

The most comprehensive geochemical investigation undertaken at the "B" reef complex was a sampling program designed to test for zonal distribution of trace elements. Samples for this investigation consisted of drill core composites representative of 50x50x50-foot cubes, each of which is contained within a N25^{0}W long section through the "B" reef complex (Figure 65). In contrast to the previous geochemical data, which evaluated vein and wall rock material separately, the samples for this data set are composites of all rock types encountered in the core interval, unaltered rock, altered rock, and vein material.

The N25^{0}W section was selected because it contains a sufficient density of drill holes, and provides a good transect through the D stope and X stope portions of the "B" North ore body, the upper part of the "B" Neath ore body, and

the "B" reef. The main drawback of the sample base is that the "B" West and lower part of the "B" Neath ore bodies are poorly represented. In compositing samples representative of each cube, drill core from both surface and underground drilling programs was utilized. Several hundred feet of drill core was available for some of the individual cubes; for instance, cubes which encompassed drill stations for underground grade-control drill hole fans. Other cubes, or sample points, contain less than 20 feet of drill core. On the average, each sample point is represented by approximately 50 feet of BX-size drill core. The entire core interval, or intervals, for each sample point was crushed, split, and submitted for analysis. These data are believed to represent global, rather than local or exotic trace element distributions.

The samples were analyzed by atomic absorption spectrophotometry for Cu, Pb, Sb, Hg, As, Se, Te, and Ag. Samples that contained greater than 25 ppm silver were fire assayed. All samples were fire assayed for gold. Table 10 summarizes the salient statistics of these analytical data, and Appendix D contains all analytical results. On a global basis, there is a very strong, positive correlation between Au, Ag, and Cu, and significant correlations of these elements with Sb.

The contoured distribution of gold, silver, copper, arsenic, mercury, antimony, and selenium is shown in Figures 66 - 69. At various parts of the long section, the lowest contour of each of these elements conforms to the limit of

Table 10. Statistical summary of atomic absorption analyses for Ag, Sb, As, Se, Te, Hg, Cu, and Pb, and fire assay analysis for Au in composite geochemical samples from the "B" reef complex. Silver values greater than 25 ppm obtained by fire assay. 197 samples.

Element	Maximum Value	Minimum Value	Average Value	Standard Deviation
Au ppb	59700	5	2109	5909
Ag ppm	182	0.1	5	18
Pb ppm	50	5	10	5
Cu ppm	219	1	17	25
Hg ppb	11643	16	617	1460
As ppm	608	5	145	134
Sb ppm	123	0.1	9	17
Se ppm	24	0.1	0.7	1.7
Te ppm	0.3	0.05	0.08	0.04

Correlation Coefficients:

	Ag	Pb	Cu	Hg	As	Sb	Se	Te
Au	.86*	-.07	.74*	-.10	.19	.35*	.01	.11
Ag	1.0	-.05	.84*	-.07	.12	.52*	.02	.08
Pb		1.0	.05	.11	.02	.03	-.02	.14
Cu			1.0	1.0	.15	.41*	.04	.23
Hg					.20	.10	.01	.02
As					1.0	.19	.14	.12
Sb						1.0	.02	-.01
Se							1.0	.10
Te								1.0

* - Denotes element pairs for which scatter plots are shown in Appendix E.

sample distribution. This indicates that the overall element distribution geometry would be modified if additional samples were available. This is particularly evident at the "B" reef ore body, and the "B-4" ore body (Figure 66).

The distribution of gold is reasonably well contained within the boundary of silicification (Figure 66). Gold concentrations appear to be uniformly distributed in the "B" North and upper part of the "B" Neath ore bodies, although moderately elevated values are concentrated on both the hangingwall and footwall of the DX thrust. There is a disparity between the southeastern boundary of economic mineralization in the lower part of the "B" Neath ore body, as defined by drilling, and the distribution of gold values (Figure 66). Detailed mapping of the "B" Neath ore body, when access becomes available, may prove that the ore body is somewhat larger in the southeast-northwest dimension than is currently indicated by drill hole information.

Silver, copper, and antimony values are elevated in the hangingwall of the DX thrust fault (Figures 67 and 68). Ott and others (1986, p. 432) noted that, qualitatively, there appeared to be an increase in pyrargyrite in the deeper levels (500 and 550 levels) of the mine. Geochemical information substantiates this observation, and indicates that the distribution of Ag, Cu, and Sb, and presumably therefore, the distribution of pyrargyrite and tetrahedrite, is structurally influenced. The reasons for this distribution are not clear. One possibility is that the original ore mineral zonation has

been transposed by post-mineralization displacement on the DX thrust fault. Small, detached, fault-bounded lenses of silicified and mineralized rock between the D stope and X stope areas of the "B" North ore body on the 700, and 650 levels support this interpretation.

The distribution of selenium values is contained within the bounds of silicification (Figure 68). There is a slight elevation in selenium concentration in the "B" North ore body, near the footwall of the DX thrust and at the crest of the "B" North anticline. As previously noted, no selenide minerals have been identified in the "B" reef complex, and none would be expected in view of the low selenium values.

Mercury is present as a halo that overlies the "B" North and "B" Neath ore bodies and is superimposed on the "B" reef (Figure 69). Arsenic is uniformly distributed throughout the "B" North and upper "B" Neath ore bodies and lower levels of arsenic also define an anomalous halo over these ore bodies (Figure 69). Mercury and arsenic appear to be the best geochemical exploration guides, as they define the broadest halo indicative of proximity to mineralization.

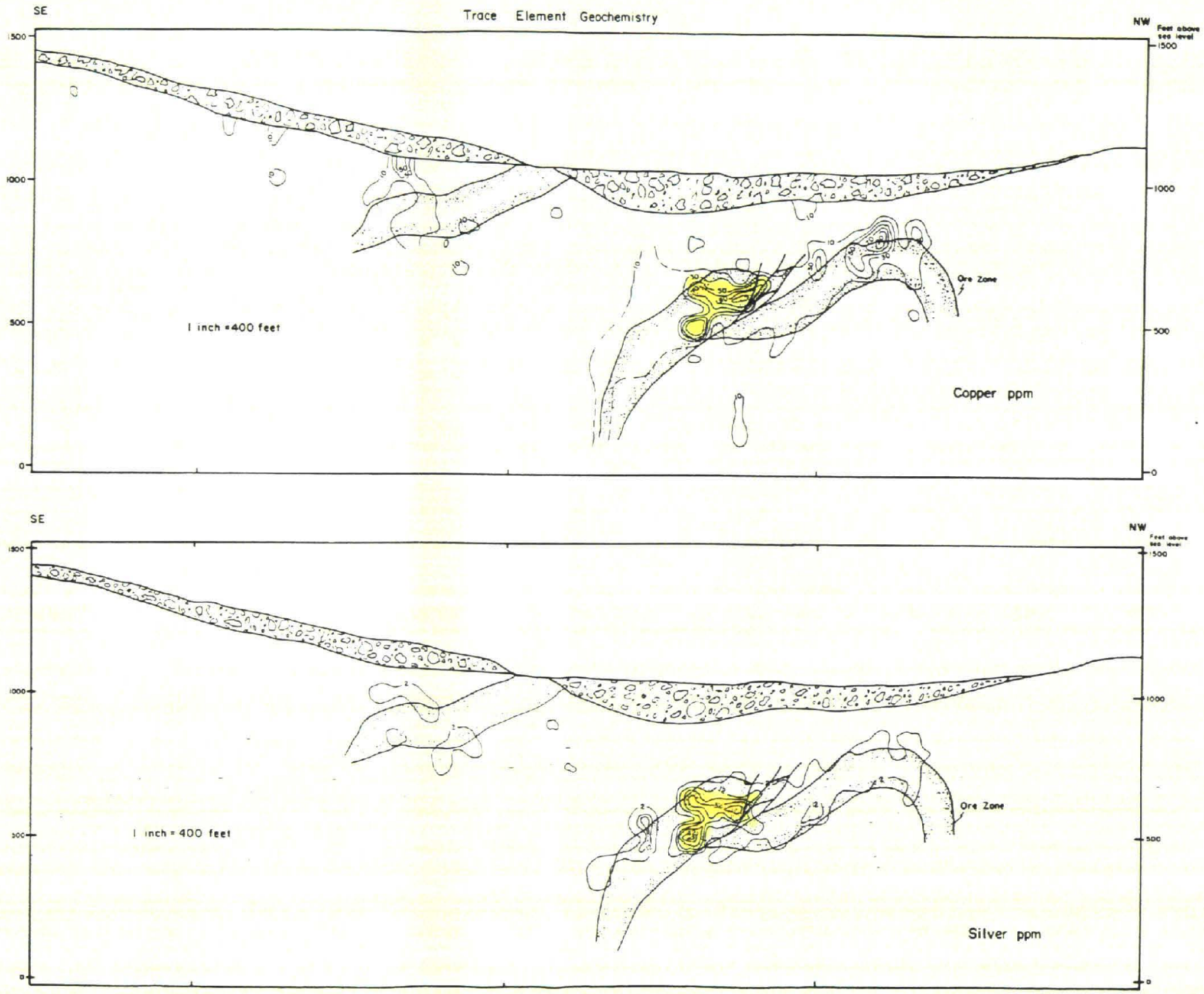

Figure 67. Copper and silver distribution.

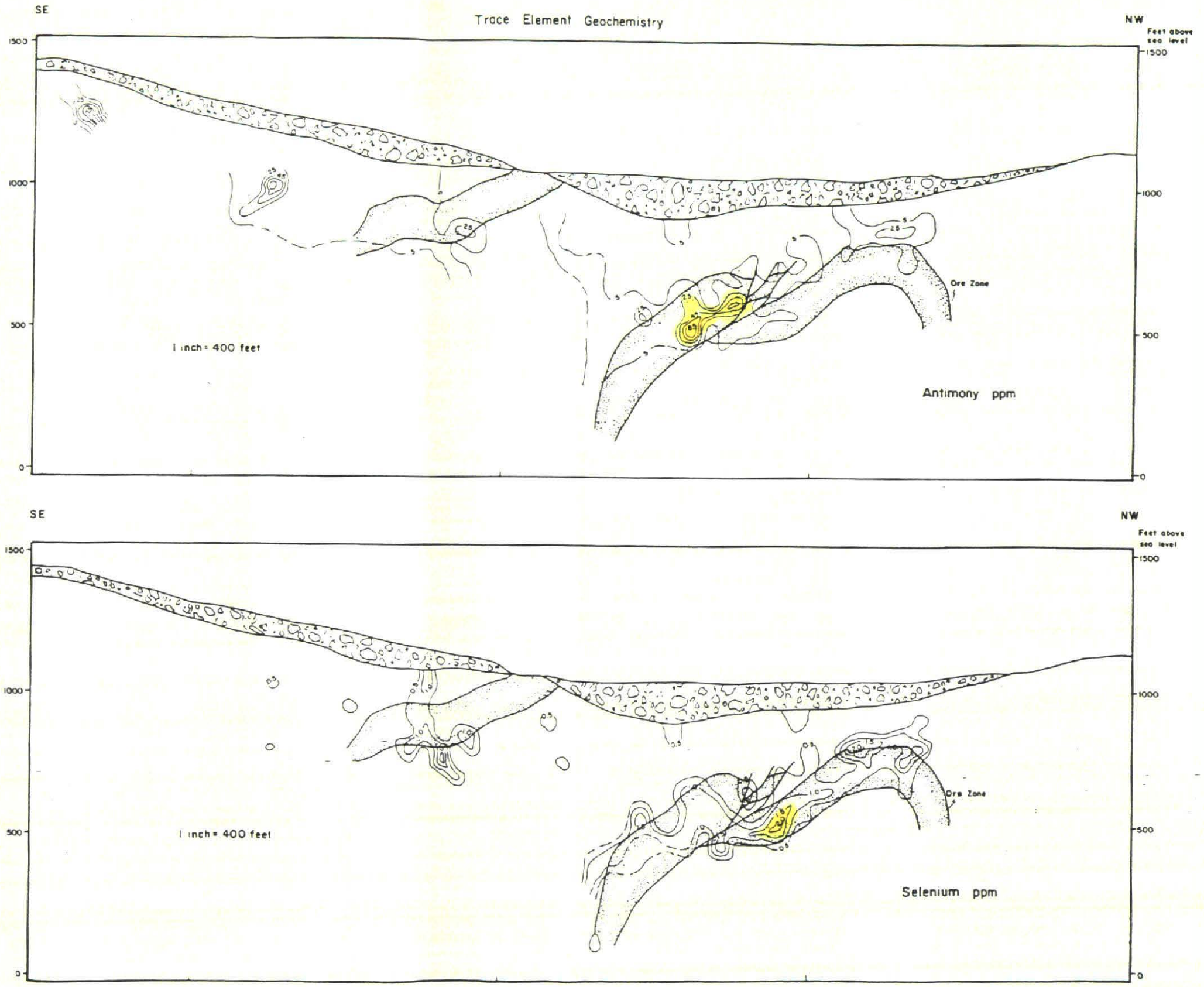

Figure 68. Selenium and antimony distribution.

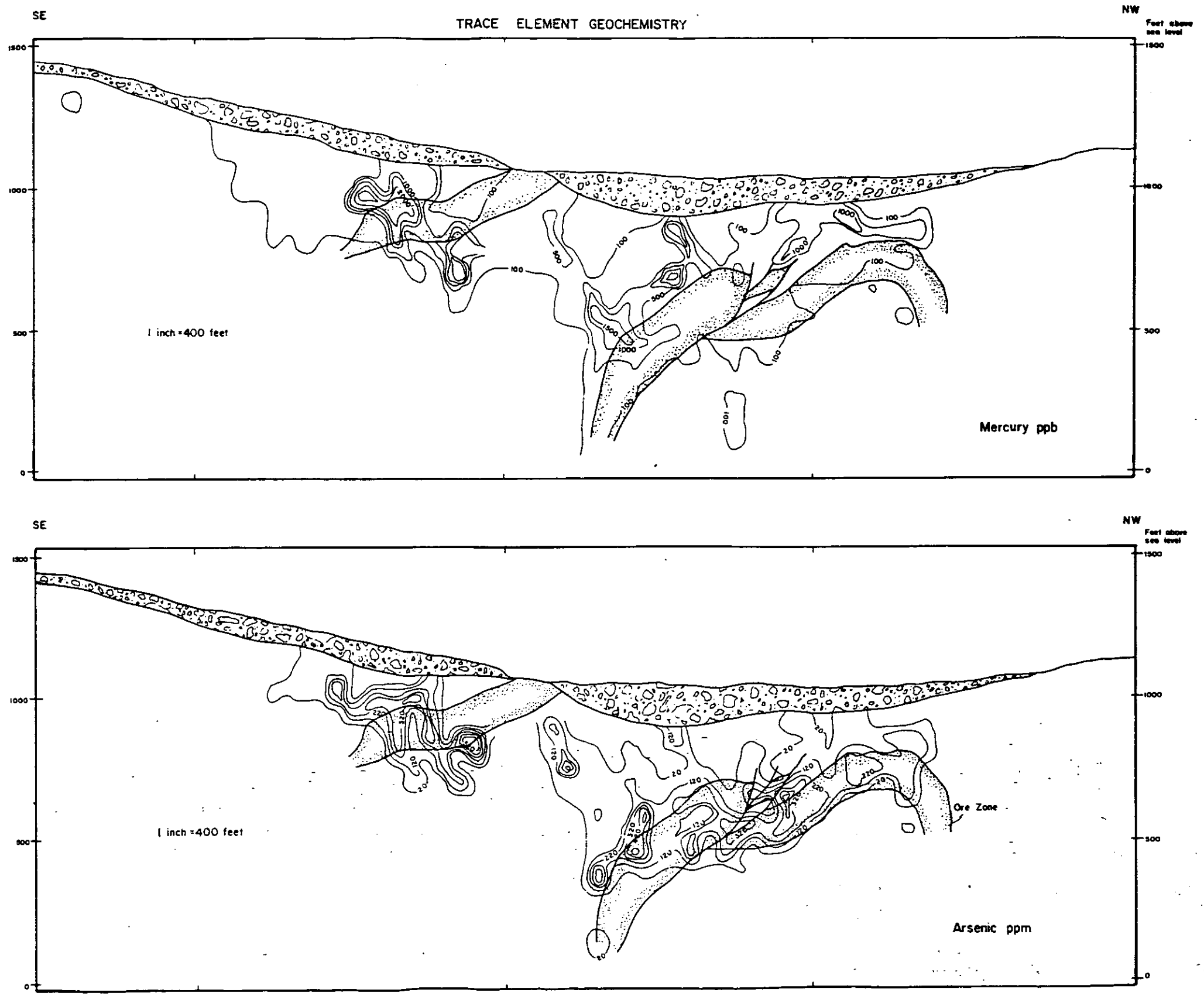

Figure 69. Arsenic and mercury distribution.

Trace Element Patterns at Ore Boundaries

Three suites of rock chip samples for were taken across the contact between intrusive rocks of the Wenatchee Dome and altered rocks of the "B" North ore body in this study. The samples were collected on the 755, 700, and 550 levels along sample lines that extended a minimum of 50 feet into mineralized and unmineralized rock on either side of the faulted contact (Figures 70, 71, and 72). The samples were submitted to Chemex Labs for semi-quantitative emission spectrographic analysis for As, Ba, Ca, Co, Cr, Cu, Fe, K, Mg, Mn, Na, Ni, Pb, Sb, and Zn. In a related study, a suite of core samples from a drill hole that passed through mineralization and into hornblende andesite on the southwestern margin of the "B" Neath ore body were geochemically tested for trace element variations. These drill core samples were submitted to Silver Valley Laboratories for atomic absorption analysis for Au, Ag, Pb, Cu, As, Sb, Hg, Se, and Te.

Analytical data for samples taken across the rhyodacite - ore contact on the eastern boundary of mineralization are shown in Appendix F. Trace element concentrations in rhyodacite and perlite are not influenced by concentrations in the mineralized sedimentary rocks. For each of the elements shown in Appendix F, there is an abrupt increase or decrease in concentration at the western margin of perlite. These patterns substantiate the interpretation that the "B" North ore body and intrusive rocks of the Wenatchee Dome attained

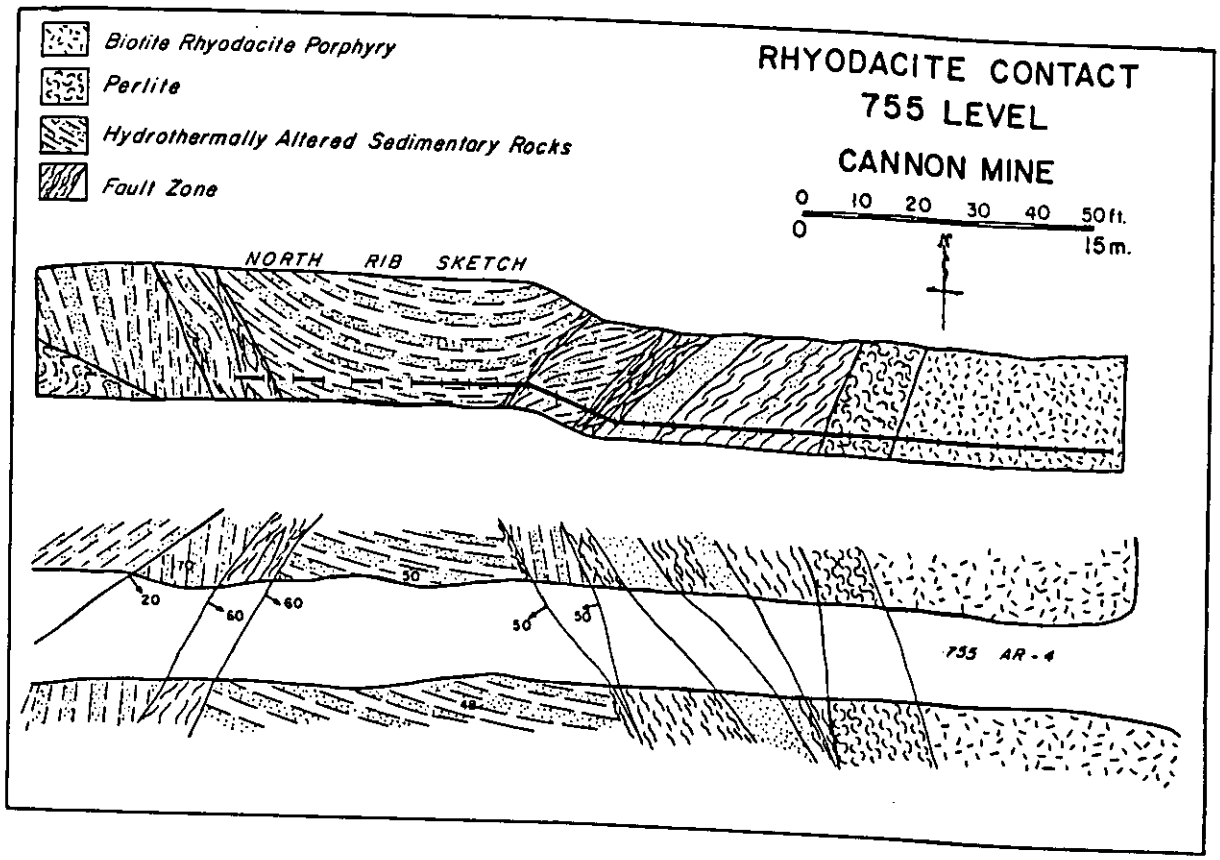

Figure 70. Plan map of rhyodacite-ore contact on the 755 level of the Cannon mine. Geochemical sample line is shown on the north rib sketch.

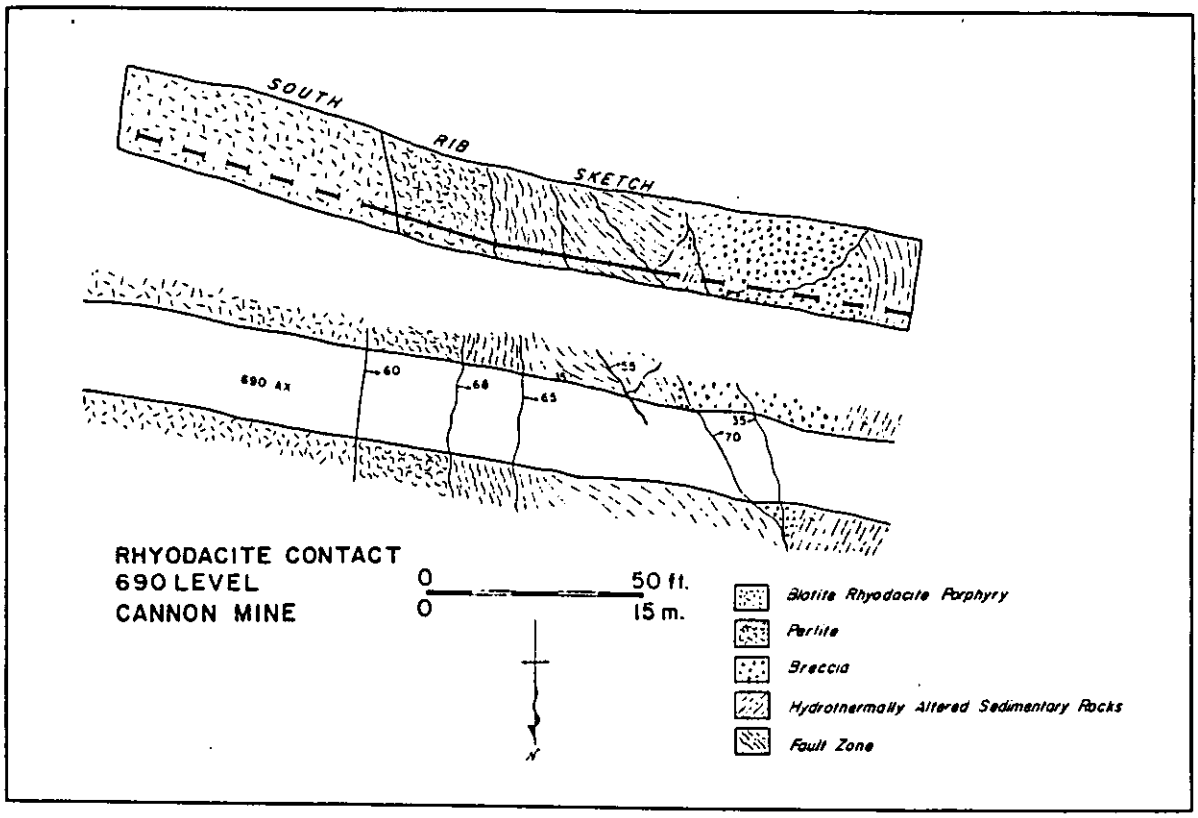

Figure 71. Plan map of rhyodacite-ore contact on the 700 level of the Cannon mine. Geochemical sample line is shown on the south rib sketch.

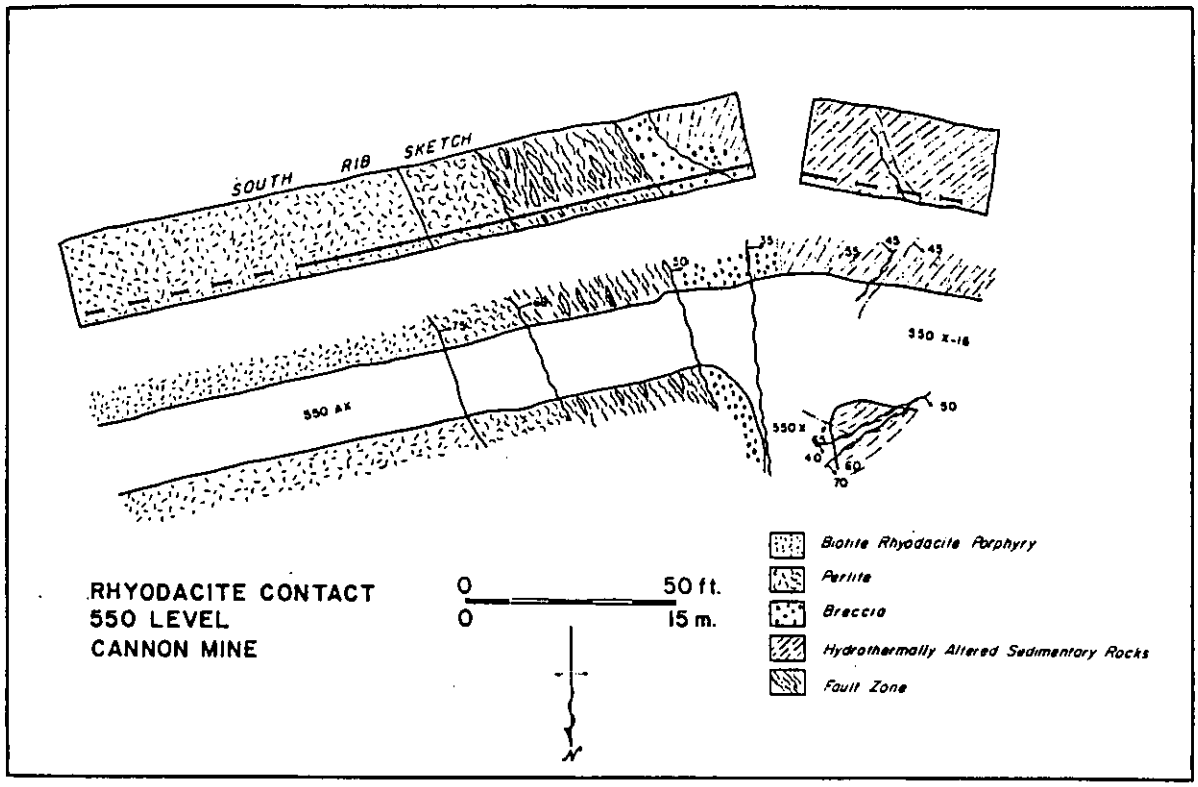

Figure 72. Plan map of rhyodacite-ore contact on the 550 level of the Cannon mine. Geochemical sample line is shown on the south rib sketch.

their present position sometime after the termination of hydrothermal activity.

Trace element patterns on the southwestern boundary of mineralization are similar to the patterns at the rhyodacite - ore contact on the eastern boundary of mineralization. Figure 73 shows Au, Ag, As, Sb, and Hg values in the lower part of drill hole TAD-10E. This hole was collared in the upper part of the "B" Neath ore body and drilled due south at an inclination of -68^{0}. The upper 245 feet of the hole consists of strongly silicified, well-mineralized, brecciated feldspathic sandstone and siltstone. From 245 feet to 270 feet downhole, an interval of weakly silicified, poorly mineralized sandstone and siltstone with intact bedding is present. The next 50 foot interval consists of moderately argillized hornblende andesite. The andesite is partly brecciated and partly flow layered, although the flow-layered portions of the core interval may be large breccia clasts. The bottom 35 feet of core consists of bedded sandstone and clayey siltstone that appear to be weakly silicified. Because this is one of the few holes drilled at the "B" reef complex that completely penetrated andesite, it was selected for trace element analysis.

The concentration of each of the elements shown in Figure 73 is reduced in the andesite, relative to the weakly altered sedimentary rocks above and below the interval. The andesite is altered, which attests to its pre-mineralization emplace-

ment, but the low levels of gold and attendant indicator elements suggest that it is not a particularly suitable host rock. The presence of weakly silicified sedimentary rocks, with increasing gold values below the andesite suggests that the area south and west of the andesite may warrant additional drilling.

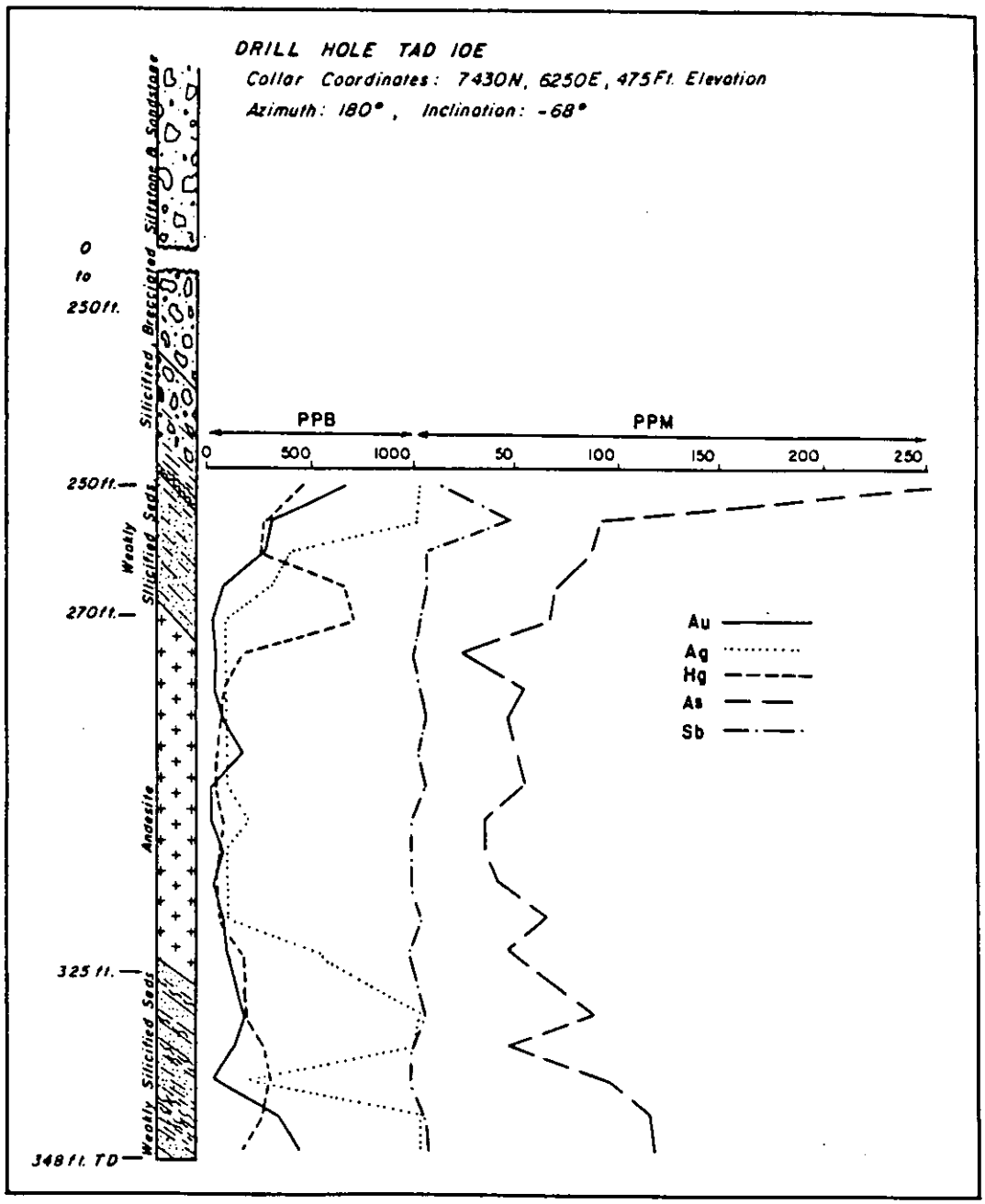

Figure 73. Graphic log of drill hole TAD-10E showing concentrations of Au, Ag, As, Sb, and Hg in the lower 105 feet of the hole. The core was sampled in 5-foot intervals.

SUMMARY

The purpose of this study is to describe the geology and gold occurrences in the Wenatchee mining district. A recapitulation of important observations made in the course of this research is provided below; conclusions drawn from the interpretation of these observations are outlined in the next section.

Gold mineralization in the Wenatchee district is hosted by a monotonous sequence of Eocene continental feldspathic sandstones and siltstones in the southeastern part of the Chiwaukum graben, a major northwest-trending structure in central Washington. The Chiwaukum graben formed between 49 m.y.b.p. and 42 m.y.b.p. as a dextral strike-slip basin that is bounded on the east by the Entiat fault, and on the west by the Leavenworth fault. The most important intragraben structure is the Eagle Creek fault zone, a structural high that is parallel to the Entiat fault in the eastern part of the graben.

The exact age and correlation of the host rocks is uncertain; they may be early Eocene sediments that were downdropped and deformed during the period of graben formation, or they may be middle Eocene graben-fill sediments that were syndepositionally deformed. Radiometric ages of andesitic rocks in the Wenatchee district favor the former hypothesis.

Eocene-aged hypabyssal intrusions and volcanic rocks of felsic to intermediate composition are also present in the district, and these rocks are spatially and temporally related

to gold mineralization. High-level domes of biotite rhyodacite porphyry with perlite borders are present on the eastern margin of a 500 meter-wide belt of known mineralization. Hornblende andesite porphyry occurs on the presently known western boundary of mineralization; although this boundary may be moved to the west in the future because weakly altered sedimentary rocks are present west of the andesite in the northern part of the district. Amygdaloidal basalt has been identified in drill core, and the greatest volume of this material is spatially associated with hornblende andesite. Average K-Ar ages for the rhyodacite (two biotite dates) and hornblende andesite (five plagioclase dates and one whole rock date) are 42.3 m.y.b.p. and 39.8 m.y.b.p., respectively. A single K-Ar determination on adularia from the "B" reef complex has yielded an age of 44.2 $\pm$ 1.9 m.y.b.p.

The structural geology of the district is dominated by northwest-trending folds and high-angle reverse faults, and north-south-trending dextral strike-slip faults. The most recent deformation on the faults post-dates mineralization. Structures that can be temporally related to hydrothermal activity are east-northeast-trending, steeply dipping veins at "A" reef and "D" reef, and east-northeast-trending, north-verging folds at the "B" reef complex. Veins at the "B" reef complex are filled radial and a-c extension joints formed when the host sediments were folded. The DX thrust fault is coplanar with the axial planes of folds at the "B" reef complex, and separates the "B" North ore body from the "B"

Neath, "B" West, and "B" ore bodies.

Mineralization at the "B" reef complex consists of widely spaced quartz-chalcedony-adularia-calcite veins in a pervasively mineralized section of feldspathic sandstone and siltstone. The highest grades of mineralization are contained within the veins; gold and silver values are also present in locally developed hydrothermal breccias and quartz-veinlet stockworks. Lower grades of mineralization are present in pervasively silicified and pyritized wall rock. Veins display well-developed open-space textures. The outer portion of the veins have symmetric encrustations of quartz, chalcedony, adularia, and calcite, and the interior portions of veins commonly contain breccia that consists of fragments of crustified vein material, and lithic fragments and detrital grains from the wall rock.

The principal ore minerals in the "B" reef ore bodies are electrum and pyrargyrite, minor ore minerals are tetrahedrite and acanthite. Other sulfide minerals are pyrite and chalcopyrite. Sulfide paragenesis is early pyrargyrite + pyrite + chalcopyrite, followed by electrum + acanthite + tetrahedrite + pyrite, and finally, pyrite only. At "D" reef, aguilarite and naummanite are important ore minerals, but no selenides have been identified at the "B" reef complex. With the exception of pyrite, sulfide minerals are generally sparse in all ore bodies in the Wenatchee district.

Silicification, potassium silicate alteration, sericitization, carbonate alteration, and intermediate argillic

alteration are associated with gold mineralization in the Wenatchee district. Argillic alteration is pervasive in character, potassium silicate alteration, as adularia, and carbonate alteration, as calcite, are vein-controlled. Silicification is both vein-controlled and pervasive. Sericitic alteration is very weak, and it is not certain whether the sericite that is present can be attributed to hydrothermal alteration, or was developed in the process of transport and deposition of detrital grains.

Argillized feldspathic sandstone overlies silicified, ore-grade rock at the "B" reef complex. The assemblage is intermediate argillic in character, as smectite is the principal alteration phase. Pervasive and vein-controlled silicification, vein-controlled potassium silicate alteration, and vein-controlled carbonate alteration are present as a single mixed alteration zone that constitutes the "B" reef complex. Vein carbonate is most abundant in the upper part of this zone, and lamellar boxwork textures, formed by the replacement of calcite by quartz and chalcedony, are common in the intermediate and deep levels of the ore body. The most profound affect that alteration has had on the wall rocks at the "B" reef complex is a marked reduction in porosity and permeability.

Trace element geochemical investigations at the "B" reef complex have shown a distinct vertical zonation of pathfinder elements commonly used in exploration for epithermal deposits. Mercury and arsenic define the broadest halo overlying

mineralization. Gold, silver, antimony, selenium, and copper are generally restricted to the silicified envelope that constitutes the "B" reef complex. Correlation of gold with other trace elements is dependent on the sample medium. In composite samples that consist of undifferentiated rocks, silver and copper correlate best with gold, and antimony correlates moderately well with gold. In silicified wall rock samples, silver shows a strong correlation with gold, and antimony, arsenic, and chromium show a weak correlation with gold. In vein samples from the "B" North ore body, no trace elements correlate well with gold, but iron, arsenic, and sodium show a weak to moderate negative correlation with gold. Trace element patterns on the eastern eastern boundary of the "B" reef complex indicate that the trace element assemblage in perlite and rhyodacite of the Wenatchee Dome is independent of the assemblage in the ore body. A similar pattern is observed in hornblende andesite on the southwestern boundary of the "B" Neath ore body, but the andesite has been hydrothermally altered and the values for gold and attendant pathfinder elements increase in sedimentary rocks west of the andesite.

CONCLUSIONS

The most significant interpretation made in this study has been a development of the structural relationship of mineralization in the Wenatchee district in respect to the formation of the Chiwaukum graben. Structural interpretations made by previous workers have been based on the orientation of faults and folds that post-date mineralization; these interpretations are useful in mine-site exploration, but they do not provide a satisfactory exploration guide that can be used on a district or regional scale. Recent work by Gresens (1983), Johnson (1985), and Evans (1987), provides compelling evidence that the graben formed by dextral strike-slip displacement on the Entiat fault. This implies that a regional, northerly-directed, subhorizontal compressive stress regime was in effect from early- to middle-Eocene time. The conclusion from this study is that the Eagle Creek structure was a zone of active dextral shear during the period of graben formation, and that igneous and hydrothermal activity were localized on this zone relatively late in the development of graben formation. Adularia from the "B" North ore body has yielded a K-Ar age of 44.2 $\pm$ 1.9 m.y.b.p., and this date indicates that the hydrothermal system responsible for mineralization was actively localizing gold and silver at the final stages of graben development as dated by Gresens (1983). The orientation and vergence of folds at the "B" reef complex is consistent with this interpretation. Veins at "D" reef and "A" reef can be ascribed to release strain at the end of

graben formation. Simple shear was important in the deformation of the Eagle Creek structure, as a strong, northwest-trending, steeply-dipping anisotropy was developed in the rocks. This anisotropy partially controlled the orientation of post-mineralization structures that offset mineralized rocks in the district.

Occurrence models that characterize deposits in the Wenatchee district include the gold-selenide (Lindgren, 1933) and adularia-sericite (Heald and others, 1987) categories of epithermal precious metal deposits. Vein and breccia textures, and alteration patterns indicate that ore and gangue minerals were deposited in response to chemical changes (mainly an increase in pH) in the mineralizing fluid invoked by boiling. Fluid inclusion data is not available to support this conclusion. Abundant pyrite in the argillic zone is an indication that mixing of ascending hydrothermal solutions with descending ground waters also may have been an important precipitation mechanism. Lack of siliceous sinter and presence of unaltered sandstones above the argillic cap at the "B" reef complex indicates that precious metal mineralization occurred in the subsurface, as opposed to surface hot-springs deposition; although surface sinter deposits may have been eroded prior to deposition of the Wenatchee Formation.

Extensive diamond drilling at "D" reef has shown that the lower boundaries of blocks 1, 2, and 3 are in fault contact with unaltered rocks. At the "B" reef complex, the "B" North and "B-4" ore bodies are stratabound within impermeable

mudstone beds above and below the mineralized section. These features, together with the lack of evidence for surface hot springs activity, may indicate that lateral fluid migration may have been more important than vertical fluid migration.

Lack of selenide minerals in ore bodies at the "B" reef complex, and their abundance in the "D" reef ore body provides evidence that the two area were not connected by the same hydrothermal system.

There is a close age relationship between adularia at the "B" reef complex and rhyodacite of the Wenatchee Dome, and this suggests that the onset of felsic igneous activity in middle to late Eocene time and the initiation of hydrothermal fluid circulation may have been coeval events. However, the Saddle Rock andesite is altered and mineralized and has a closer spatial relationship to mineralization, and may therefore be more closely related to the mineral genesis. More accurate radiometric age data on both the Saddle Rock andesite and mineralized rocks in the Wenatchee district, in addition to more detailed trace element data are necessary to resolve the relationsip between igneous and hydrothermal events in the district. The ultimate cause of both magmatic and hydrothermal activity was the formation of the Chiwaukum graben, and, specifically, deformation along the Eagle Creek fault zone.

RECOMMENDATIONS FOR FURTHER RESEARCH

This study represents a compilation and interpretation of information collected during the period of development and initial production at the Cannon mine. As such, the information contained herein can be viewed as an opportunity to assess what has been learned in the past four years and, more importantly, what critical information is lacking that is necessary for a better understanding of the nature and origin of mineralization in the Wenatchee district. Many of the interpretations made in the preceding pages are preliminary in the sense that the data base used is limited in both volume and the types of information available. The ensuing paragraphs outline what additional data, in the writer's view, are necessary to gain a better understanding of gold occurrences in the Wenatchee district.

The most significant shortcoming of this study has been the inability of the writer to put together a sufficiently detailed description of the Eocene stratigraphy in the Wenatchee district. A better understanding of district-scale variations in the stratigraphic section is necessary before a more complete understanding of lithologic and structural controls of mineralization can be made.

Trace element distribution has only been investigated at the "B" reef complex, and there, the data base is decidedly two dimensional, as only vertical zonation was investigated on a single long section through the "B" reef complex. Lateral distribution of trace elements has not been investigated.

Additionally, differences in ore mineral assemblages at "D" reef and the "B" reef complex may indicate that these deposits originated from separate, unique hydrothermal systems, or a possible district-scale zonation of trace elements.

A more thorough understanding of alteration assemblages in the Wenatchee district is necessary if alteration is to be better employed in exploration efforts. Information concerning the chemical evolution of the hydrothermal fluids responsible for mineralization might also result from more thorough alteration studies. Topics related to hydrothermal alteration that await further study range from a fundamental description of variations in alteration mineralogy within and away from ore bodies in the district, to investigations into subtle thermal effects caused by the passage of fluids through sedimentary rocks in the district.

Fluid inclusion and light-stable isotope information is completely lacking in the Wenatchee district, and would add substantially to a better understanding of the physical and chemical conditions of ore deposition, and the origin of ore fluids. Likewise, a more comprehensive investigation of ore and gangue mineral paragenesis at both the "D" reef and the "B" reef complex would shed additional light on the chemical conditions of mineral precipitation.

The configuration of most structural features in the district is only understood in small areas within a few hundred meters of the surface. Geophysical studies, such as gravity or seismic surveys, would be useful in defining the

geometry of district-scale structures at depth in order to better assess the importance of various faults and folds in ore localization.

In summary, it is hoped that the research that has been summarized in the preceding pages of this report will provide a fundamentally sound descriptive and conceptual base from which to generate much-needed future investigations. Ore deposits in the Wenatchee district represent an uncommon epithermal mineral occurrence in respect to the structural setting, and host lithology. For this reason, there are many geologic studies concerning the origin of mineralization, and mode of ore localization that warrant additional research.

REFERENCES

Abe, I., and Kawasaki, K., 1987, The Hishikari gold deposit, Kagoshima, Japan: Private Report for Sumitomo Metal Mining Company, Ltd., 13 p.

Anonymous, 1938a, Mining Journal, October edition.

Anonymous, 1938b, Spokane Spokesman-Review, October 16 edition.

Anonymous, 1953a, Wallace Miner, v. 47, no. 46, p. 4.

Anonymous, 1953b, Wallace Miner, v. 47, no. 3, p. 1.

Anonymous, 1962a, Wallace Miner, v. 56, no. 48, p. 1.

Anonymous, 1962b, Wenatchee World, July 4 edition.

Anonymous, 1965, Engineering and Mining Journal, v. 166, no. 12, p. 134.

Anonymous, 1967, Wallace Miner, v. 61, no. 7, p. 1.

Armstrong, R.L., 1978, Cenozoic igneous history of the U. S. Cordillera from Lat. 42 to 49 N., in Smith, R.B. and Eaton, G.P., eds., Cenozoic tectonics and regional geophysics of the western Cordillera: Geological Society of America Memoir 152, p. 265-282.

Barrett, R.A., 1985, The geology, mineralization, and geochemistry of the Milestone hot-spring silver-gold deposit near the Delamar silver mine, Owyhee County, Idaho: University of Idaho M.S. Thesis, 250 p.

Barton, P.B., Jr., and Skinner, B.J., 1979, Sulfide mineral stabilities, in Barnes, H.L., ed., Geochemistry of hydrothermal ore deposits, 2nd ed.: New York, John Wiley and Sons, p. 278-403.

Bayley, E.P., Jr., 1965, Bedrock geology of the Twin Peaks area, an intrusive complex near Wenatchee, Washington: University of Washington M. S. Thesis, 47 p.

Berger, B.R., and Eimon, P.I., 1983, Conceptual models of epithermal precious metal deposits, in Shanks, W.C., ed., Cameron volume on unconventional mineral deposits: New York, American Institute of Mining, Metallurgical, and Petroleum Engineers, p. 191-205.

Bingler, E.C., Trexler, D.T., Kemp, W.R., and Bohnam, H. F., Jr., 1976, Petcal: A BASIC language computer program for petrologic calculations: Nevada Bureau of Mines and Geology Report 28, 27 p.

Bonnichsen, B., 1983, Epithermal gold and silver deposits, Silver City - De Lamar district, Idaho: Idaho Bureau of Mines and Geology Open File Report 83-4, 29 p.

Buchanan, L.J., 1981, Precious metal deposits associated with volcanic environments in the southwest: Arizona Geological Society Digest, v. 14, p. 237-261.

Buza, J.W., 1977, Dispersal patterns of Lower and Middle Tertiary sedimentary rocks in portions of the Chiwaukum graben, east-central Cascade range, Washington: University of Washington M.S. Thesis, 40 p.

Chang, L.L., 1963, Dimorphic relations in Ag_3SbS_3: American Mineralogist, v. 48, p. 429-432.

Chappell, W.M., 1936, Geology of the Wenatchee quadrangle, Washington: University of Washington Ph.D. Thesis, 249 p.

Cole, D.R., and Drummond, S.E., 1986, The effect of transport and boiling on Ag/Au ratios in hydrothermal solutions: A preliminary assessment and possible implications for the formation of epithermal precious-metal ore deposits: Journal of Exploration Geochemistry, v. 25, p. 45-79.

Coleman, R.G., 1958, The natural occurrence of galena-clausthalite solid solution series (abstract): Geological Society of America Bulletin, v. 69, p. 1679.

Coleman, R.G., and Delevaux, M., 1957, Occurrence of selenium in sulfides from some sedimentary rocks of the western United States: Economic Geology, v. 52, p. 499-527.

Coombs, H.A., 1950, Granitization in the Swauk arkose near Wenatchee, Washington: American Journal of Science, v. 248, p. 369-377.

Coombs, H.A., 1952, Spherulitic breccias in a dome near Wenatchee, Washington: American Mineralogist, v. 37, p. 197-206.

Craig, J.R., and Barton, P.B., Jr., 1973, Thermochemical approximations for sulfosalts: Economic Geology, v. 69, p. 492-506.

Cranton, G.E., and Heyding, R.D., 1968, The gold/selenium system and some gold seleno-tellurides: Canadian Journal of Chemistry, v. 46, p. 2637-2640.

Davidson, D.F., 1960, Selenium in some epithermal deposits of antimony, mercury, silver, and gold: United States Geological Survey Bulletin 1112-A, 15p.

Dixon, J.B., and Brackney, K.M., 1986, Preliminary geology and development of the Seattle mine, Republic district, Ferry County, Washington: Northwest Mining Association 92nd Annual Convention reprint, 6 p.

Drummond, S.E., and Ohmoto, H., 1985, Chemical evolution and mineral deposition in boiling hydrothermal systems: Economic Geology, v. 80, p. 126-147.

Durning, W.P., and Buchanan, L.J., 1981, The geology and ore deposits of Oatman, Arizona: Arizona Geological Digest, no. 15, p. 141-158.

Earley, J.W., 1950, Descriptions and synthesis of the selenide minerals: American Mineralogist, v. 35, p. 337-364.

Ellis, A.J., 1979, Explored geothermal systems, in Barnes, H.L., ed., Geochemistry of hydrothermal ore deposits, 2nd ed., John Wiley and Sons, New York, p. 632-683.

Evans, J.E., 1987, Tectonic evolution of a Tertiary wrench-fault basin, Chumstick Formation, Cascade range, Washington: Geological Society of America Abstracts with Programs, v. 19, no. 6, p. 375-376.

Fischer, J.F., 1986, Petrographic report on five samples from the FA-1A core hole, Wenatchee gold district: Private Report for Asamera Minerals (US) Inc., 22 p.

Folk, P., 1987, Teck Resources (U.S.) 1983, Inc., summary report for 1986, Lovitt Mining Company - Asamera Inc. joint venture: Unpublished report for Asamera Minerals, Inc., Wenatchee, Washington, 15 p. 8 plates.

Foster, R.P., 1958, The Teanaway dike swarm of central Washington: American Journal of Science, v. 256, p. 644-653.

Geist, D.J., Baker, B.H., and McBirney, A.R., 1985, GPP A program package for creating and using geochemical data files: Center for Volcanology, University of Oregon, Eugene, Oregon, 33 p.

Gresens, R.L., 1975, Geologic mapping of the Wenatchee area: Washington Division of Mines and Geology Open-File Report 75-6, 2 sheets, scale 1:24,000.

-------- 1976a, A new Tertiary formation near Wenatchee, Washington: Geological Society of America Abstracts with Programs, v. 8, no. 3, p. 376-377.

-------- 1976b, Unusual structural features associated with mid-Tertiary deformation near Wenatchee, Washington: Geological Society of America Abstracts with Programs, v. 8, p. 892-893.

-------- 1980, Deformation of the Wenatchee Formation and its bearing on the tectonic history of the Chiwaukum graben, Washington during Cenozoic time, Summary: Geological Society of America Bulletin, v. 91, no. 1, pt. 1, p. 4-7.

-------- 1982a, Early Cenozoic geology of central Washington state: I. Summary of sedimentary, igneous, and tectonic events: Northwest Science, v.56, p. 218-229.

-------- 1982b, Early Cenozoic geology of central Washington state: II. Implications for plate tectonics and alternatives for the origin of the Chiwaukum graben: Northwest Science, v. 56, p. 259-264.

-------- 1983, Geology of the Wenatchee and Monitor quadrangles, Chelan and Douglas counties, Washington: Washington Division of Geology and Earth Resources Bulletin 75, 75 p.

Gresens, R.L., Whetten, J.T., Tabor, R.W., and Frizzell, V.A., Jr., 1977, Tertiary stratigraphy of the central Cascade mountains, Washington state, in Brown, E.H. and Ellis, R.C., eds., 1977, Geologic excursions in the Pacific Northwest: Western Washington University Press, Bellingham, Washington, p. 84-92.

Gresens, R.L., Naeser, C.W., and Whetten, J.T., 1981, Stratigraphy and age of the Chumstick and Wenatchee Formations, Tertiary fluvial and lacustrine rocks, Chiwaukum graben, Washington; Summary: Geological Society of America Bulletin, v. 92, no. 5, pt. 1, p. 233-236.

Gross, W.H., 1975, New ore discovery and source of silver-gold veins, Guanajuato, Mexico: Economic Geology, v. 70, p. 1175-1189.

Guilbert, J.M., 1963, Report on selected specimens form the Gold King mine, Wenatchee, Washington: Unpublished report for Day Mines, Inc., Wallace, Idaho, 27 p.

Harland, W.B., 1971, Tectonic transpression in Caledonian Spitzbergen: Geological Magazine, v. 108, p. 27-42.

Hayba, D.O., 1983, A compilation of fluid inclusion and stable isotope data on selected precious- and base-metal epithermal deposits: U. S. Geological Survey Open File Report 83-450, 24 p.

Hayba, D.O., Bethke, P.M., Heald, P., and Foley, N.K., 1985, Geologic, mineralogic, and geochemical characteristics of volcanic-hosted epithermal precious-metal deposits, in Berger, B.R., and Bethke, P.M., eds., Geology and geochemistry of epithermal systems: Reviews in Economic Geology, v. 2, p. 129-168.

Hazen and Hazen Research, Inc., 1986, Internal technical report on the ore mineralogy of the "B" North ore body for Asamera Minerals, Inc., Wenatchee, Washington.

Heald, P., Foley, N.K., and Hayba, D.O., 1987, Comparative anatomy of volcanic-hosted epithermal deposits: Acid-sulfate and adularia-sericite types: Economic Geology, v. 82, p. 1-26.

Hedenquist, J.W, and Henley, R.W., 1985, Hydrothermal eruptions in the Waiotapu geothermal system, New Zealand: Their origin, associated breccias, and relation to precious metal mineralization: Economic Geology, v. 80, p. 1640-1668.

Henley, R.D., and Ellis, A.J., 1983, Geothermal systems, ancient and modern: A geochemical review: Earth Science Reviews, v. 19, p. 1-50.

Hobbs, B.E., Means, W.D., and Williams, P.F., 1976, An outline of structural geology: J. Wiley and Sons, Inc., New York, N. Y., 571 p.

Irving, T.N., and Baragar, W.R.A., 1971, A guide to the chemical classification of igneous rocks: Canadian Journal of Earth Sciences, v. 8, no. 5, p. 523-548.

Johnson, P.E., 1983, The origin of the Chiwaukum graben, Chelan county, Washington: Washington State University M. S. Thesis, 96 p.

Johnson, S.Y., 1985, Eocene strike-slip faulting and non-marine basin formation in Washington, in Biddle, K.T., and Christie-Blick, N., eds., Strike-slip deformation, basin formation, and sedimentation: Society of Economic Paleontologists and Mineralogists Special Publication no. 37, p. 283-302.

Keighin, C.W., and Honea, R.M., 1969, The system Ag-Sb-S from 600°C to 200°C: Mineralium Deposita (Berlin), v.4, p. 153-171.

Krauskopf, K.B., 1979, Introduction to geochemistry, second edition: McGraw-Hill Company, New York, N. Y., 617 p.

Krupp, R.E., and Seward, T.M., 1987, The Rotokawa geothermal system, New Zealand: An active epithermal gold-depositing environment: Economic Geology, v. 82, p. 1109-1129.

Laravie, J.A., 1976, Geological field studies along the eastern border of the Chiwaukum graben, central Washington: University of Washington M. S. Thesis, 56 p.

Lindgren, W., 1900, The gold and silver veins of Silver City, De Lamar, and other mining districts in Idaho: United States Geological Survey, 20th Annual Report, Part III, p. 77-189.

--------, 1933, Mineral deposits, 4th ed.: New York, McGraw-Hill, 930 p.

Lovitt, E.H., and McDowall, V., 1954, The Gold King Mine: Western Miner, v. 27, no. 3, p. 37-39.

Lovitt, E.H., and Skerl, A.C., 1958, Geology of the Lovitt gold mine, Wenatchee, Washington: Mining Engineering, v. 10, p. 963-966.

Mann, P., Hempton, M.R., Bradley, D.C., and Burke, K., 1983, Development of pull-apart basins: Journal of Geology, v. 91, p. 529-554.

Margolis, J., 1987, Structure and hydrothermal alteration associated with epithermal Au-Ag mineralization, Wenatchee Heights, Washington: University of Washington M.S. Thesis, 90 p.

Mason, B.C., 1966, Principles of geochemistry, third edition: John Wiley and Sons, Inc., New York, N. Y., 329 p.

McClincey, M., 1986, Tephrostratigaphry of the Chumstick Formation: Portland State University M. S. Thesis, 122 p.

Moody, D.W., 1958, An examination of the ore minerals of the Lovitt mine, Wenatchee, Washington: University of Washington B. S. Thesis, 22 p.

Nash, J.J., 1972, Fluid inclusion studies of some gold deposits in Nevada: U. S. Geological Society Professional Paper 800-C, p. 15-19.

O'Neill, J.R., and Silberman, M.L., 1974, Stable isotope relations in epithermal Au-Ag deposits: Economic Geology, v. 69, p. 902-907.

Ott, L.E., Groody, D., Follis, E.L., and Siems, P.L., 1986, Stratigraphy, structural geology, ore mineralogy, and hydrothermal alteration at the Cannon mine, Chelan county, Washington, U.S.A., in Macdonald, A.J., ed., Proceedings, Gold '86, an international symposium on the geology of gold deposits: Toronto, Canada, p. 425-435.

Page, B.M. 1939, Geology of a part of the Chiwaukum quadrangle, Washington: Stanford University Ph.D. Thesis, 203 p.

Pansze, A.J., Jr., 1975, Geology and ore deposits of the Silver City - De Lamar - Flint region, Owyhee County, Idaho: Idaho Bureau of Mines and Geology Pamphlet 161, 79 p.

Patton, T.C., 1967, Economic geology of the L-D mine, Wenatchee, Washington: University of Washington M. S. Thesis, 29 p.

Patton, T.C., and Cheney, E.S., 1971, L-D gold mine, Wenatchee, Washington -- new structural interpretation and its utilization in future exploration: Society of Mining Engineers, American Institute of Mining Engineers, v. 250, p. 6-11.

Petruk, W., Owens, D.R., Stewart, J.M., and Murray, E.J., 1974, Observations on acanthite, aguilarite and naummanite: Canadian Mineralogist, v. 12, p. 365-369.

Pettijohn, F.J., Potter, P.E., and Siever, R., 1972, Sand and Sandstone: New York, Springer-Verlag Berlin, 618 p.

Reading, H.G., 1980, Characteristics and recognition of strike-slip fault systems, in Ballance, P.F., and Reading, H.G., eds., Sedimentation in oblique-slip mobile zones: International Association of Sedimentologists Special Publication Number 4, Blackwell Scientific Publications, Oxford, p. 7-26.

Reed, M.H., and Spycher, N.F., 1985, Boiling, cooling, and oxidation in epithermal systems: A numerical modeling approach, in Berger, B.R., and Bethke, P.M., eds., Geology and geochemistry of epithermal systems: Reviews in Economic Geology, v. 2, p. 249-272.

Roderick, S., 1986, Mineralogical report on the ore minerals of the "B" reef: Internal technical report for Asamera Minerals, Inc., Wenatchee, Washington by American Cyanimid Company.

Rodgers, D.A., 1980, Analysis of pull-apart basin development produced by en echelon strike-slip faults, in Ballance, P.F., and Reading, H.G., eds., Sedimentation in oblique-slip mobile zones: International Association of Sedimentologists Special Publication Number 4, Blackwell Scientific Publications, Oxford, p. 27-41.

Russell, I.C., 1900, A preliminary report on the geology of the Cascade Mountains in northern Washington: U. S. Geological Survey, 20th Annual Report, Part II, p. 85-210.

Silberman, M.L., and Berger, B.R., 1985, Relationships of trace-element patterns to alteration and morphology in epithermal precious-metal deposits, in Berger, B.R., and Bethke, P.M., eds., Geology and geochemistry of epithermal systems: Reviews in Economic Geology, v. 2, p. 203-232.

Silling, R.M., 1979, A gravity study of the Chiwaukum graben, Washington: University of Washington M. S. Thesis, 183 p.

Smith, G.O., and Calkins, F.C., 1904, A geological reconnaissance across the Cascade range near the 49th parallel: U. S. Geological Survey Bulletin, v. 235, p. 3-103.

Tabor, R.W., Waitt, R.B., Jr., Frizzell, V.A., Jr., Swanson, D.A., Byerly, G.R., and Bentley, R.D., 1982, Geologic map of the Wenatchee 1:100,000 quadrangle, central Washington: U. S. Geological Survey Miscellaneous Investigations Map 1-1311, 26 p., 1 plate.

Tabor, R.W., Frizzell, V.A., Jr., Vance, J.A., and Naeser, C.W., 1984, Ages and stratigraphy of lower and middle Tertiary sedimentary and volcanic rocks of the central Cascades, Washington: Application to the tectonic history of the Straight Creek fault: Geological Society of America Bulletin, v. 95, p. 26-44.

Walker, C.W., 1980, Geology and energy resources of the Roslyn-Cle Elum area, Kittitas County, Washington: Washington Department of Natural Resources, Division of Geology and Earth Resources Open-File Report 80-I, 59 p.

Waters, A.C., 1930, Geology of the southern half of the Chelan quadrangle, Washington: Yale University Ph.D. Thesis, 256 p.

Weissberg, B.G., 1969, Gold-silver ore-grade precipitates from New Zealand thermal waters: Economic Geology, v. 64, p. 95-108.

Weissberg, B.G., Browne, P.R.L., and Seward, T.M., 1979, Ore metals in active geothermal systems, in Barnes, H.L., ed., Geochemistry of hydrothermal ore deposits, 2nd ed.: John Wiley and Sons, New York, p. 738-780.

Whetten, J.T., 1976, Tertiary sedimentary rocks in the central part of the Chiwaukum graben, Washington: Geological Society of America Abstracts with Programs, v. 8, no. 3, p. 420.

White, D.E., 1981, Active geothermal systems and hydrothermal ore deposits: Economic Geology, 75th Anniversary volume, p. 392-423.

Willis, B., 1903, Physiography and deformation of the Wenatchee-Chelan district, Cascade range: U. S. Geological Survey Professional Paper 19, p.43-101.

Williams, S., 1986, Internal technical report on the ore mineralogy of the "B" reef ore bodies for Asamera Minerals, Inc., Wenatchee, Washington by Globo de Plomo Resources.

Willis, C.L., 1958, The Chiwaukum graben, a major structural feature of central Washington: American Journal of Science, v. 251, p. 789-797.

Wright, H.D., Walther, M.B., and Halbig, J.B., 1965, Solid solution in the systems ZnS-ZnSe and PbS-PbSe at 300°C and above: American Mineralogist, v. 50, p. 1802-1815.

Zdenek, J., Picot, P., Peirrot, R., and Kvacek, M., 1972, Fischesserite: American Mineralogist, v. 57, p. 1554.

APPENDIX A

INSTRUMENTAL NEUTRON ACTIVATION ANALYSIS DATA BY BONDAR-CLEGG AND COMPANY FOR WALL-ROCK SAMPLES FROM THE "B" NORTH ORE BODY.

Instrumental Neutron Activation Analysis For Au, Sb, As, Ag, Na, Cr, Fe, Ba, Wall Rock Samples from the "B" North Ore Body

SAMPLE NUMBER	Au ppb	Sb ppm	As ppm	Ag ppm	Na %	Cr ppm	Fe %	Ba ppm
10534	1370	8.1	204	1	2.30	210	2.0	1000
10535	360	3.7	68	1	2.20	120	4.4	700
10536	2500	7.2	146	1	1.50	200	2.7	790
10537	1050	8.9	124	1	1.50	160	2.9	850
10538	160	4.1	48	1	2.40	110	3.2	960
10539	440	7.0	114	1	2.60	140	2.5	880
10540	110	3.1	42	1	2.50	230	2.1	1100
10541	100	3.6	38	1	2.50	220	2.2	960
10542	51	2.8	35	1	3.30	89	4.3	730
10543	1030	5.9	611	1	4.60	89	6.0	530
10544	64	4.9	37	1	3.10	78	4.3	970
10545	926	2.6	32	1	3.00	180	2.6	1000
10546	260	2.2	38	1	4.40	150	3.8	970
10551	956	9.2	246	1	1.50	230	3.0	690
10552	390	8.0	87	1	2.10	280	1.4	700
10553	2090	12.0	234	1	2.40	230	2.4	580
10554	931	12.0	158	1	2.00	230	2.1	610
10555	971	7.8	108	1	2.20	270	1.6	650
10556	5120	8.9	494	7	1.70	190	3.2	530
10557	8050	6.0	140	9	2.10	300	1.4	820
10558	8010	10.0	352	1	2.20	230	2.9	640
10559	4220	7.1	229	1	1.70	150	3.5	700
10560	9780	6.8	198	8	2.80	220	2.2	590
10561	717	5.4	148	1	2.60	150	4.6	640
10562	563	5.6	167	1	2.20	170	4.8	610
10563	1130	5.2	142	1	1.90	160	3.6	520
10564	1060	7.3	359	1	2.10	150	6.0	570
10565	1490	5.4	133	1	2.40	350	1.8	810
10566	1750	3.8	82	1	2.30	150	3.4	870
10567	290	3.3	66	1	2.30	210	3.0	660
10568	940	4.6	115	1	2.00	190	2.9	690
10569	1980	4.9	78	1	1.80	150	2.8	790
10570	742	4.0	57	1	1.90	150	2.6	670
10571	2060	5.8	124	1	2.90	310	2.5	910
10572	1680	10.0	283	1	2.80	120	4.9	730
10573	100	4.7	53	1	2.70	170	3.4	600
10574	150	3.3	70	1	2.40	240	2.8	740
10575	854	4.1	108	1	2.20	140	3.6	860
10576	380	3.7	40	1	2.10	200	1.8	910
10577	1070	5.1	78	1	2.30	250	2.3	860
10578	1070	3.4	34	1	2.10	170	2.6	960
10579	1220	6.3	81	1	1.90	190	3.0	800
10587	62	2.2	66	1	3.10	190	3.3	840
10588	170	2.3	56	1	2.60	110	4.1	910
10589	230	1.4	35	1	3.10	250	3.2	880

Appendix A (Continued)

SAMPLE NUMBER	Au ppb	Sb ppm	As ppm	Ag ppm	Na %	Cr ppm	Fe %	Ba ppm
10590	64	2.2	44	1	3.00	130	4.1	830
10591	49	1.1	22	1	2.90	260	3.2	730
10592	100	2.7	43	1	3.00	140	3.3	890
10593	320	2.5	21	1	3.20	170	3.5	760
10637	975	1.0	27	1	3.50	270	1.9	700
10638	400	2.2	48	1	3.80	160	3.4	990
10639	88	1.8	21	1	3.40	200	3.1	750
10640	598	2.6	88	1	3.20	170	3.4	980
10641	190	2.3	93	1	2.90	270	2.1	720
10642	190	2.7	70	1	2.70	170	4.2	740
10644	1250	28.9	259	1	.80	200	1.7	900
151601	27	.6	4	1	3.04	82	.8	820
151602	2	.5	5	1	3.04	96	1.5	1200
151603	1	.4	3	1	3.21	82	1.4	1100
151604	8	1.0	24	1	2.41	64	2.9	2200
151605	73	1.0	15	1	1.70	110	3.0	910
151606	11	.8	17	1	2.03	89	2.3	1800
151607	8	.9	12	1	1.90	69	3.3	580
151608	24	5.0	49	1	2.01	83	2.1	490
151609	3	10.5	5	1	1.90	69	1.6	370
151610	7	4.9	28	1	2.00	53	1.6	1300
151611	12	4.5	44	1	1.90	79	2.9	590
151612	1	.9	62	1	2.93	96	.7	1400
151614	1	.6	5	1	3.06	63	.7	2000
151615	1	.8	5	1	2.42	170	1.1	1200
151616	1	.7	4	1	2.85	140	.9	1300
151617	1	.5	3	1	2.96	92	.9	1100
151618	1	.7	3	1	2.97	73	1.5	1200
151619	1	1.3	4	1	2.39	170	.9	1200
151620	1	.8	10	1	2.36	120	.5	1200
151621	1	.9	20	1	2.91	70	.9	1800
151622	1	.3	3	1	3.09	68	1.2	1200
151623	1	.4	2	1	2.90	77	1.1	1100

Appendix A (continued)

Instrumental Neutron Activation Analysis For Hf, La, Mo, Cd, Co, Th, W, and U in Wall Rock Samples from the "B" North Ore Body

SAMPLE NUMBER	Hf ppm	La ppm	Mo ppm	Cd ppm	Co ppm	Th ppm	W ppm	U ppm
10534	3	16	14	1	5	3.4	4	1.1
10535	4	26	3	1	12	5.3	2	2.0
10536	3	17	10	1	5	3.6	2	1.4
10537	3	18	7	1	5	3.7	4	1.5
10538	4	24	4	1	12	5.3	2	1.8
10539	2	21	7	1	11	3.9	2	1.4
10540	3	14	15	1	5	2.8	2	1.0
10541	3	17	11	1	5	3.4	2	1.3
10542	4	29	1	1	13	5.5	2	2.0
10543	6	25	1	1	29	4.6	2	1.5
10544	9	55	1	1	11	12.0	2	4.6
10545	3	20	9	1	5	4.2	2	1.4
10546	4	29	5	1	14	5.9	2	2.2
10551	1	22	12	1	5	4.0	2	1.3
10552	2	13	20	1	5	2.4	2	.7
10553	2	15	15	1	5	3.1	2	.7
10554	3	16	15	1	5	3.0	2	1.1
10555	2	12	19	1	5	2.6	2	.8
10556	1	13	15	1	5	3.1		1.0
10557	3	12	23	1	5	2.4	2	.8
10558	3	15	14	1	5	3.6	2	.8
10559	3	18	3	1	13	3.5	6	1.2
10560	3	15	15	1	5	2.5	2	1.3
10561	4	22	5	1	11	4.1	5	1.3
10562	4	22	6	1	17	4.6	4	1.6
10563	3	20	10	1	13	3.8	5	1.4
10564	3	26	1	1	14	5.4	3	1.9
10565	3	14	23	1	5	2.4	2	.8
10566	4	26	4	1	5	4.9	2	1.8
10567	4	21	12	1	5	3.8	3	1.4
10568	4	20	9	1	11	3.7	4	1.4
10569	5	21	6	1	14	4.5	6	1.6
10570	4	20	7	1	5	3.3	4	1.3
10571	4	18	18	1	5	3.4	2	1.1
10572	5	26	1	1	13	4.8	4	1.6
10573	5	23	10	1	5	4.4	3	1.4
10574	3	16	15	1	5	3.2	2	1.0
10575	3	22	6	1	11	4.8	3	1.8
10576	4	16	15	1	5	3.0	2	1.0
10577	5	18	16	1	5	3.1	3	1.1
10578	3	20	11	1	5	3.8	2	1.6

Appendix A (Continued)

SAMPLE NUMBER	Hf ppm	La ppm	Mo ppm	Cd ppm	Co ppm	Th ppm	W ppm	U ppm
10579	3	18	11	1	5	3.4	4	1.3
10587	4	26	9	1	5	4.9	4	1.7
10588	5	27	1	1	11	5.2	3	1.9
10589	4	22	13	1	11	4.4	2	1.4
10590	6	33	5	1	12	6.1	2	2.5
10591	4	21	15	1	5	3.5	2	1.2
10592	4	31	4	1	13	6.1	5	2.1
10593	6	29	6	1	11	5.6	5	2.1
10637	3	16	19	1	5	3.0	2	.9
10638	5	26	7	1	12	5.1	2	1.8
10639	5	24	11	1	5	4.0	2	1.6
10640	4	20	8	1	5	4.3	2	1.6
10641	4	17	16	1	5	3.8	2	1.0
10642	4	28	6	1	13	4.9	3	1.9
10644	1	12	13	1	5	3.0	4	.9
151601	4	22	1	1	5	6.8	1	3.6
151602	4	23	1	1	5	7.3	1	3.9
151603	4	25	1	1	5	6.8	1	3.8
151604	4	18	1	1	7	3.8	1	2.3
151605	2	15	1	1	10	3.5	1	2.0
151606	3	15	1	1	8	3.3	1	1.8
151607	4	16	1	1	8	3.9	2	2.0
151608	5	20	4	1	10	4.6	1	2.5
151609	5	32	2	1	5	10.0	1	5.1
151610	5	18	3	3	8	4.1	1	2.1
151611	4	19	7	3	7	3.5	3	1.9
151612	4	32	20	1	5	7.2	1	4.1
151614	4	15	5	1	5	7.2	1	2.8
151615	4	21	3	1	5	6.4	2	14.0
151616	5	26	1	1	5	7.4	1	3.8
151617	4	23	1	1	5	7.2	1	4.1
151618	4	23	1	1	5	7.3	1	3.8
151619	4	21	1	1	5	6.5	2	3.5
151620	4	22	6	1	5	7.3	1	8.1
151621	4	23	95	1	5	7.6	1	4.1
151622	5	22	1	1	5	7.0	1	3.9
151623	4	23	1	1	5	7.0	1	3.8

APPENDIX B

INSTRUMENTAL NEUTRON ACTIVATION ANALYSIS

DATA BY BONDAR-CLEGG AND COMPANY

FOR VEIN SAMPLES FROM THE

"B" NORTH ORE BODY.

Instrumental Neutron Activation Analysis for Au, Sb, As, Ag, Na, Cr, Fe, and Ba, in Vein Samples from the "B" North Ore Body.

SAMPLE NUMBER	Au ppb	Sb ppm	As ppm	Ag ppm	Na %	Cr ppm	Fe %	Ba ppm
10645	935	21.7	250	1	.75	160	1.5	1000
10646	2810	53.4	176	12	.22	300	.6	450
10647	30000	464.0	108	982	.54	610	.8	600
10648	30000	111.0	198	73	.17	380	.8	400
10649	30000	79.4	101	53	.11	410	.6	200
10650	19500	35.7	59	10	.09	460	.6	100
10651	6890	60.1	354	14	.28	420	1.1	520
10652	5570	40.8	341	9	.67	330	1.0	760
10653	6640	54.6	515	13	.48	340	1.7	760
10654	3340	33.8	264	9	.70	290	1.0	900
10655	30000	135.0	69	98	.14	620	.6	330
10656	22300	53.9	121	18	.19	370	.5	260
10657	30000	35.0	200	29	.48	420	.7	460
10658	30000	204.0	56	360	.31	320	1.1	300
10659	30000	39.7	64	210	.17	370	.8	530
10660	7570	64.3	60	23	.15	490	.5	160
10661	2270	95.5	154	58	.19	480	.7	210
10662	30000	56.6	95	52	.16	410	.6	240
10663	10600	55.0	59	16	.05	540	.5	150
10664	30000	136.0	104	230	.15	410	.1	180
10670	13900	28.1	123	18	.25	400	.6	480
10671	29200	59.1	151	51	.25	310	.6	280
10672	2190	46.5	115	19	.08	200	1.0	280
10673	2820	32.3	95	10	.09	200	1.2	250
10674	3960	52.2	89	35	.09	260	1.0	140
10675	20000	63.6	82	79	.12	310	.8	230
10677	30000	1490.0	238	2210	1.10	1300	1.3	1500
10678	30000	88.5	57	64	.06	470	.1	120
10679	8920	48.3	97	19	.17	430	.5	200
10680	30000	50.3	110	22	.15	480	.8	160
10681	30000	49.0	37	37	.08	350	.1	100
10682	7990	47.3	58	19	.11	500	.1	100
10683	19500	60.5	84	29	.11	480	.6	150
10684	30000	165.0	115	150	.11	420	.5	220
10685	30000	112.0	46	93	.10	500	.1	130
10686	30000	74.7	118	70	.19	380	.7	280
10687	21900	41.6	62	28	.10	540	.6	110
10688	15700	51.2	61	25	.05	470	.1	180
10689	24300	72.7	76	41	.06	350	.5	160
10690	30000	82.6	57	78	.13	370	.1	190
10691	18700	62.6	49	33	.06	450	.1	210
10692	30000	67.4	51	46	.06	510	.6	100
10693	28200	49.9	63	34	.15	510	.1	120
10694	30000	57.3	185	61	.13	460	.9	290

Appendix B (Continued)

SAMPLE NUMBER	Au ppb	Sb ppm	As ppm	Ag ppm	Na %	Cr ppm	Fe %	Ba ppm
10695	30000	107.0	93	120	.16	350	.1	120
10696	27900	45.5	41	41	.16	540	.6	150
10697	25700	71.3	38	48	.08	600	.1	100
10698	12300	19.0	75	11	.13	520	.6	240
10699	18600	21.6	66	8	.21	480	.6	230
10700	19900	49.1	124	39	.17	420	.6	180
151401	3020	18.6	468	5	1.90	200	2.6	810
151402	30000	16.5	74	69	.24	380	.6	290
151403	9100	11.0	243	6	2.16	290	2.0	810
151404	952	16.2	144	3	1.50	400	1.4	590
151405	6230	16.3	43	7	.24	540	.6	200
151406	2110	16.9	139	6	1.20	370	1.0	500
151407	4160	13.5	233	5	1.30	390	1.4	730
151408	4510	21.4	63	5	.28	570	.7	180
151409	3100	24.3	126	5	.52	510	.8	280
151410	6150	22.9	190	14	.52	350	2.3	610
151411	29500	51.5	57	55	.16	530	.8	120
151412	2640	22.2	261	10	.53	310	1.9	600

Appendix B (continued)

Instrumental Neutron Activation Analysis for Hf, La, Mo, Cd, Co, Th, W, and U in Vein Samples from the "B" North Ore Body

SAMPLE NUMBER	Hf ppm	La ppm	Mo ppm	Cd ppm	Co ppm	Th ppm	W ppm	U ppm
10645	1	13	12	1	5	3.5	4	1.2
10646	1	1	22	1	5	1.1	2	.5
10647	13	1	93	68	12	9.0	30	10.0
10648	1	5	9	9	5	.9	3	1.3
10649	1	1	29	8	5	.8	3	.8
10650	1	1	32	1	5	.5	2	.5
10651	1	7	27	1	5	1.1	3	.5
10652	1	9	22	1	5	1.6	2	.5
10653	3	16	20	1	5	3.4	4	1.1
10654	1	10	22	1	5	1.9	2	1.1
10655	3	1	22	14	5	1.3	5	1.5
10656	1	1	26	1	5	.6	2	.5
10657	1	1	24	7	5	.8	2	1.1
10658	7	1	27	34	5	4.6	15	5.3
10659	6	1	34	31	5	5.6	13	8.2
10660	1	1	35	1	5	.5	2	.5
10661	1	1	28	7	5	.6	4	.7
10662	1	1	22	1	5	.5	2	.6
10663	1	1	29	1	5	.5	2	.5
10664	1	1	21	11	5	.9	10	1.4
10670	1	1	36	1	5	.5	2	.5
10671	1	1	26	6	5	.6	2	.7
10672	3	1	15	1	5	1.8	2	.7
10673	2	10	11	1	5	1.9	3	.5
10674	1	7	16	1	5	1.5	2	.5
10675	1	6	19	1	5	1.5	2	.5
10677	28	6	83	140	24	15.0	61	23.0
10678	1	1	32	7	5	.7	3	.7
10679	1	1	30	1	5	.5	2	.5
10680	1	1	30	1	5	.6	2	.6
10681	1	1	24	7	5	.8	2	.9
10682	1	1	38	1	5	.5	2	.5
10683	1	1	31	1	5	.5	2	.5
10684	1	1	18	11	5	1.0	5	1.0
10685	3	1	27	14	5	1.4	5	1.6
10686	3	1	15	13	5	1.3	5	1.5
10687	1	1	39	1	5	.5	2	.5
10688	1	1	34	1	5	.5	2	.5
10689	1	1	30	6	5	.6	2	.6
10690	1	1	29	9	5	1.0	3	1.1
10691	1	1	34	1	5	.5	2	.5
10692	1	1	35	6	5	.6	4	.7

Appendix B (Continued)

SAMPLE NUMBER	Hf ppm	La ppm	Mo ppm	Cd ppm	Co ppm	Th ppm	W ppm	U ppm
10693	1	1	31	1	5	.6	2	.6
10694	1	1	37	8	5	.8	2	1.4
10695	3	1	22	13	5	1.3	4	1.4
10696	1	1	38	1	5	.6	2	.6
10697	1	1	47	6	5	.6	2	.6
10698	1	1	39	1	5	.5	2	.5
10699	1	1	36	1	5	.5	.2	.8
10700	1	1	30	1	5	1.0	2	.5
151401	5	20	1	4	16	4.4	3	1.6
151402	1	3	4	5	5	.6	5	.7
151403	3	14	1	3	8	2.6	2	1.0
151404	3	13	1	1	5	2.4	1	.6
151405	1	1	2	2	5	.1	1	.2
151406	2	9	1	1	5	1.8	2	.6
151407	1	11	1	1	5	1.7	3	1.0
151408	1	3	1	1	5	.3	1	.2
151409	1	4	1	1	5	.6	1	.4
151410	2	12	1	3	5	2.0	3	.3
151411	1	2	2	4	5	.4	4	.5
151412	2	12	1	3	5	2.2	1	.7

APPENDIX C

DIRECTLY-COUPLED PLASMA EMISSION SPECTROGRAPHIC AND COLD VAPOR ATOMIC ABSORPTION ANALYTICAL DATA BY BONDAR-CLEGG AND COMPANY FOR VEIN SAMPLES FROM THE "B" NORTH ORE BODY.

Directly-Coupled Plasma Emission Spectrographic Analyses for Ag, As, Sb, Cu, and Pb, and Cold Vapor Atomic Absorption Analyses for Hg in Vein Samples from the "B" North Ore Body

SAMPLE NUMBER	LEVEL	Ag ppm	As ppm	Sb ppm	Hg ppb	Cu ppm	Pb ppm
2752	700	22	138	15	900	51	5
2755	700	2	172	6	80	59	5
2760	700	11	103	21	220	74	5
2761	700	30	37	9	150	135	8
2764	700	13	20	55	550	198	5
2770	700	24	58	5	110	97	5
2806	650	4	8	10	25	28	5
2807	650	50	1460	2000	1400	18000	102
2808	650	34	39	66	30	84	5
2809	650	25	18	42	210	65	5
2811	650	8	20	12	50	45	5
2812	650	2	153	46	260	38	5
2813	600	26	104	148	80	336	5
2815	700	8	109	112	550	746	5
2819	700	1	25	50	300	151	5
2820	700	6	146	112	550	367	5
2822	700	8	82	84	300	247	5
2823	700	32	40	58	280	315	6
2825	700	31	41	32	100	228	27
2830	755	21	461	60	2600	144	5
2832	755	6	53	5	80	85	5
2833	780	26	36	60	90	315	5
2834	650	50	253	680	1350	509	8
2850	550	50	163	1720	3000	1272	16
2901	500	5	380	106	2000	63	5
2903	500	16	309	137	1200	84	5
2904	500	18	268	41	1200	19	5
2905	500	9	296	66	2000	25	5
2914	755	9	19	12	80	33	5
2915	755	4	17	5	40	10	5
2916	755	24	41	10	250	85	5
2917	600	5	716	115	5000	88	5
2918	700	50	46	496	500	676	5
2919	650	2	46	5	130	170	5
2920	450	3	56	5	350	96	5
2921	650	11	104	230	550	356	5
5001	650	15	125	19	250	133	5
5002	650	49	31	9	190	137	5
5003	650	24	47	19	180	198	5
5004	650	20	20	49	50	159	5
5005	650	17	37	80	340	142	5
5006	650	41	57	5	300	65	5
5007	650	47	123	33	750	66	5
5008	755	29	266	13	150	123	5
5009	755	9	119	5	230	37	5
4510	755	31	130	35	1100	57	5
4511	755	18	36	350	150	655	5

Appendix C (Continued)
DCP Analytical Data for Zn, Se, Fe, Mn, Cr, and Ni

SAMPLE NUMBER	LEVEL	Zn ppm	Se ppm	Fe %	Mn ppm	Cr ppm	Ni ppm
4512	755	23	92	12	300	100	5
2752	700	10	5	.54	802	111	1
2755	700	21	5	.60	317	137	6
2760	700	11	5	.52	60	101	3
2761	700	20	7	.26	63	104	2
2764	700	22	5	.24	61	152	3
2770	700	28	8	.82	192	94	5
2806	650	1	5	.21	25	157	3
2807	650	41	461	.87	420	65	2
2808	650	4	5	.25	866	115	1
2809	650	1	5	.24	214	171	3
2811	650	3	5	.21	37	132	3
2812	650	5	5	.46	34	164	4
2813	600	9	5	.52	275	107	3
2815	700	12	6	.57	28	139	5
2819	700	5	5	.25	88	115	2
2820	700	11	5	.46	26	121	3
2822	700	11	12	.41	20	100	3
2823	700	40	5	.53	1146	119	3
2825	700	78	5	.31	179	86	2
2830	755	9	5	1.62	70	102	3
2832	755	14	5	.81	202	124	5
2833	780	17	5	.30	726	149	2
2834	650	16	66	1.61	88	110	3
2850	550	13	186	.44	141	123	4
2901	500	10	5	1.84	29	131	4
2903	500	8	5	1.42	18	111	3
2904	500	7	5	1.48	249	144	3
2905	500	6	5	2.30	34	125	4
2914	755	4	9	.26	139	147	2
2915	755	6	5	.34	5528	50	1
2916	755	6	5	.29	195	139	3
2917	600	24	8	3.46	100	103	4
2918	700	2	53	.28	14	119	4
2919	650	30	5	.77	194	121	5
2920	450	19	5	1.01	32	114	4
2921	650	4	5	1.34	23	122	3
5001	650	33	5	.67	24	108	5
5002	650	27	5	.23	20	66	2
5003	650	24	5	.29	41	77	3
5004	650	13	5	.23	77	101	3
5005	650	8	5	.25	90	91	3
5006	650	22	5	.26	42	73	3
5007	650	12	5	.54	66	79	3
5008	755	27	5	.80	79	70	4
5009	755	11	5	.54	31	63	3
4510	755	6	5	.73	63	72	3
4511	755	19	39	.32	99	62	2
4512	755	9	5	.53	36	81	3

APPENDIX D

ATOMIC ABSORPTION, FIRE ASSAY, AND INDUCTIVELY COUPLED ARGON PLASMA ANALYSIS BY SILVER VALLEY LABORATORIES FOR COMPOSITE GEOCHEMICAL SAMPLES FROM THE "B" REEF COMPLEX

Atomic absorption analysis for Au, Se, Te, and Hg, and inductively coupled argon plasma analysis for Cu, Pb, and Ag in composite geochemical samples from the "B" reef complex. Au values greater than 10,000 ppb and Ag values greater than 100 ppm obtained by fire assay.

North	Elev.	Au ppb	Ag ppm	Pb ppm	Cu ppm	Hg ppb	As ppm	Sb ppm	Se ppm	Te ppm
5600	1300	21	0.1	12	11	275	33	24.0	0.3	0.05
5600	1350	5	0.1	7	6	49	41	4.0	0.2	0.05
5650	1250	27	0.1	8	6	113	42	123.0	0.2	0.05
6100	1100	16	0.1	7	4	75	9	0.1	0.1	0.05
6100	1150	47	0.1	9	9	400	28	2.0	0.2	0.05
6100	1200	30	0.1	7	13	377	23	5.0	0.3	0.10
6150	900	5	0.1	6	4	26	34	29.0	0.1	0.05
6150	950	15	0.1	6	4	91	12	6.0	0.1	0.05
6150	1000	28	0.1	8	7	197	17	6.0	0.1	0.05
6150	1050	5	0.1	7	4	60	11	10.0	0.1	0.05
6250	800	88	0.1	7	9	109	15	2.0	0.6	0.05
6250	850	5	0.1	6	4	46	12	0.1	0.1	0.05
6250	900	5	0.1	7	4	71	16	0.1	0.1	0.05
6250	1000	86	0.1	11	14	448	29	119.0	0.4	0.05
6250	1050	44	0.1	9	9	163	25	3.0	0.5	0.05
6250	1150	108	0.1	12	19	497	28	7.0	0.5	0.05
6300	1000	5	0.1	8	5	45	10	4.0	0.2	0.05
6300	1050	52	0.1	6	7	86	27	1.0	0.3	0.05
6300	1100	19	0.1	7	8	145	12	2.0	0.3	0.05
6350	800	30	0.1	8	8	234	29	7.0	0.2	0.05
6350	850	25	0.1	8	6	234	18	3.0	0.2	0.05
6350	900	29	0.1	8	7	163	20	8.0	0.1	0.05
6350	1000	38	0.1	8	7	121	20	0.1	0.1	0.05
6350	1050	41	0.1	10	9	217	23	0.1	0.1	0.05
6350	1100	5	0.1	6	7	45	84	0.1	0.1	0.05
6450	1000	28	0.1	10	8	11643	296	24.0	0.2	0.05
6450	1050	22	0.1	8	6	11500	370	9.0	0.1	0.05
6500	950	364	0.1	11	5	2329	246	11.0	0.8	0.10
6550	950	141	0.1	15	13	9000	223	16.0	0.2	0.20
6550	1000	5	0.1	11	4	5486	248	16.0	0.1	0.05
6600	900	5	0.1	8	2	869	161	7.0	0.1	0.10
6600	950	156	0.3	50	12	2029	202	19.0	0.6	0.10
6600	1000	7720	7.1	5	16	240	365	12.0	0.6	0.10
6650	800	388	0.6	13	17	1350	283	17.0	0.5	0.10
6650	850	7540	4.6	7	20	243	400	14.0	0.5	0.10
6650	900	1886	0.2	7	6	282	268	15.0	0.4	0.10
6650	1000	27	0.1	10	3	2128	204	14.0	0.2	0.05
6650	1050	27	0.1	11	67	946	35	14.0	0.4	0.10
6700	700	65	0.1	11	10	140	94	6.0	0.2	0.10
6700	750	465	1.3	9	12	129	64	0.1	0.4	0.10
6700	800	1021	1.8	6	12	148	49	7.0	1.1	0.10
6700	900	210	0.1	12	4	2165	108	8.0	0.5	0.05
6700	950	349	0.1	10	3	1543	138	18.0	0.9	0.10

Appendix D (Continued)

North	Elev.	Au ppb	Ag ppm	Pb ppm	Cu ppm	Hg ppb	As ppm	Sb ppm	Se ppm	Te ppm
6700	1000	3450	4.6	9	14	455	478	14.0	0.5	0.10
6750	850	278	0.3	12	18	631	405	10.0	0.9	0.05
6750	900	739	1.8	10	12	369	262	4.0	0.9	0.05
6750	950	6400	8.3	7	13	322	228	18.0	0.6	0.10
6750	1000	1777	0.9	9	5	1293	177	13.0	1.0	0.05
6750	1050	435	0.1	8	5	1121	199	11.0	1.3	0.10
6800	750	1420	6.3	5	7	511	200	10.0	2.0	0.05
6800	800	1679	6.0	5	10	772	231	14.0	1.4	0.10
6850	700	609	0.2	13	17	5971	246	18.0	1.2	0.10
6850	850	804	7.1	7	14	1207	457	28.0	0.9	0.10
6900	800	1166	4.2	6	7	740	452	17.0	1.0	0.05
6900	850	1049	3.7	10	11	350	608	25.0	1.2	0.10
7150	550	5	0.1	7	3	63	7	0.1	0.3	0.10
7150	800	5	0.1	5	7	103	19	7.0	0.1	0.10
7150	850	25	0.1	6	6	80	7	0.1	0.1	0.10
7150	900	5	2.6	12	13	728	236	23.0	0.9	0.10
7200	750	1715	2.1	8	9	760	440	14.0	0.7	0.05
7200	950	30	0.1	5	6	123	7	2.0	0.3	0.10
7300	100	107	0.1	11	9	370	44	4.0	0.6	0.05
7300	150	1608	1.8	7	18	102	39	0.1	0.4	0.10
7300	350	4150	6.6	13	43	508	426	17.0	1.2	0.10
7300	400	3630	4.3	6	25	280	391	15.0	1.3	0.10
7300	550	81	0.1	11	5	2442	103	0.1	0.2	0.05
7300	600	4010	0.1	11	8	851	128	12.0	0.2	0.05
7300	650	25	0.1	7	9	320	29	0.1	0.2	0.05
7300	700	5	0.1	6	4	54	8	0.1	0.1	0.05
7300	750	37	0.1	8	4	57	6	6.0	0.1	0.10
7300	800	5	0.1	5	8	43	26	2.0	0.1	0.10
7300	850	27	0.1	6	2	51	5	0.1	0.1	0.05
7400	250	27	0.1	9	8	303	12	3.0	0.1	0.05
7400	300	19	0.1	9	9	323	13	3.0	0.2	0.05
7400	350	5	0.1	8	11	206	8	0.1	0.4	0.10
7400	400	39	0.1	9	10	623	18	10.0	0.3	0.05
7400	450	354	1.9	11	11	1100	490	20.0	0.5	0.10
7400	500	53	0.1	10	7	591	284	0.1	0.2	0.05
7400	550	53	0.1	12	9	478	260	11.0	0.3	0.10
7400	600	5	0.1	22	14	917	79	16.0	0.3	0.10
7400	650	12	0.1	10	10	289	27	2.0	0.2	0.05
7400	700	23	0.1	8	9	317	142	0.1	0.2	0.05
7400	750	140	0.1	5	2	51	21	0.1	0.1	0.05
7400	800	5	0.1	9	5	133	49	2.0	0.1	0.10
7400	850	14	0.1	6	4	66	16	2.0	0.1	0.05
7450	350	54	0.1	10	12	637	23	0.1	0.3	0.05
7450	400	71	0.7	10	10	507	132	0.1	0.6	0.05
7450	450	187	2.8	12	16	468	393	10.0	0.8	0.10
7450	500	410	3.1	12	12	609	318	13.0	1.0	0.05
7450	550	5	24.0	8	20	500	437	47.0	2.0	0.05
7450	600	1457	4.9	10	21	570	481	9.0	0.9	0.05
7450	650	5	0.1	12	11	594	36	5.0	0.1	0.10

Appendix D (Continued)

North	Elev.	Au ppb	Ag ppm	Pb ppm	Cu ppm	Hg ppb	As ppm	Sb ppm	Se ppm	Te ppm
7450	700	5	0.1	9	8	248	25	0.1	0.1	0.05
7450	750	5	0.1	13	16	383	59	3.0	0.4	0.10
7450	800	5	0.1	7	2	33	10	0.1	0.1	0.05
7550	500	782	10.4	5	36	609	150	14.0	0.6	0.10
7550	600	5850	0.1	8	6	305	260	11.0	0.2	0.05
7550	650	380	0.8	9	14	689	220	12.0	0.5	0.10
7550	700	729	0.1	7	7	2431	38	0.1	0.2	0.10
7550	850	769	1.4	10	7	2170	176	28.0	1.0	0.10
7600	400	52	0.2	26	12	208	43	0.1	0.1	0.10
7600	450	4100	9.9	9	28	268	335	26.0	1.0	0.05
7600	500	31000	160.0	12	199	117	265	121.0	1.1	0.10
7600	550	3715	11.8	8	22	348	108	19.0	0.9	0.10
7600	600	16100	35.7	12	58	209	53	27.0	0.9	0.10
7600	650	11490	45.6	11	65	156	179	15.0	1.3	0.10
7600	700	680	1.1	7	11	28	145	1.0	0.5	0.10
7600	750	5	0.1	7	7	627	24	0.1	0.1	0.10
7600	800	20	0.1	19	17	434	36	0.1	0.2	0.10
7650	500	146	0.3	11	19	16	73	0.1	0.3	0.10
7650	550	2213	12.4	5	25	339	184	16.0	0.9	0.10
7650	650	6030	10.7	5	28	138	248	2.0	0.8	0.10
7650	700	1435	1.7	7	10	652	159	0.1	0.5	0.10
7650	750	5	0.1	11	5	430	18	0.1	0.1	0.05
7650	850	79	0.1	10	9	335	34	0.1	0.2	0.05
7700	450	1287	5.4	7	11	344	266	8.0	1.9	0.10
7700	500	1286	3.8	9	16	280	236	10.0	0.9	0.10
7700	550	4680	14.1	8	35	148	348	19.0	1.1	0.10
7700	600	2428	12.2	6	32	499	198	13.0	1.2	0.10
7700	650	9750	19.8	6	46	92	105	12.0	0.4	0.10
7750	100	108	0.1	18	13	217	20	4.0	0.3	0.10
7750	150	39	0.1	10	14	301	14	4.0	0.5	0.10
7750	200	29	0.1	8	11	193	13	0.1	0.2	0.10
7750	250	37	0.1	9	12	258	18	0.1	0.3	0.10
7750	300	64	0.1	10	6	100	17	0.1	0.2	0.05
7750	350	13	0.1	8	8	99	16	0.1	0.1	0.10
7750	400	15	0.1	10	9	147	32	0.1	0.3	0.10
7750	450	51	0.1	12	9	117	54	2.0	0.5	0.10
7750	500	9560	11.7	9	19	166	328	7.0	0.6	0.10
7750	550	4940	12.1	7	36	196	319	10.0	1.1	0.10
7750	600	59700	182.0	6	219	68	48	66.0	0.3	0.10
7750	650	97	0.1	9	8	468	72	6.0	0.2	0.20
7750	700	5	0.1	10	7	636	38	8.0	0.2	0.10
7750	750	5	0.1	9	8	348	17	0.1	0.1	0.10
7750	850	13	0.1	7	8	286	28	0.1	0.3	0.10
7800	500	357	2.3	9	11	139	78	8.0	1.5	0.10
7800	550	34600	25.0	7	15	38	344	5.0	0.4	0.05
7800	600	1755	5.4	10	33	160	102	5.0	0.7	0.05
7800	650	6480	16.2	8	82	235	276	19.0	1.2	0.20
7800	700	72	0.1	12	6	268	119	8.0	0.5	0.05
7800	750	18	0.1	13	7	205	21	8.0	0.2	0.05

Appendix D (Continued)

North	Elev.	Au ppb	Ag ppm	Pb ppm	Cu ppm	Hg ppb	As ppm	Sb ppm	Se ppm	Te ppm
7800	800	5	0.1	9	8	385	85	0.5	0.1	0.10
7850	400	37	0.1	10	11	202	13	0.5	0.3	0.10
7850	450	56	0.7	8	8	173	45	0.5	0.3	0.10
7850	500	441	2.3	7	10	162	266	0.5	1.2	0.10
7850	550	2493	5.0	10	11	108	219	5.0	1.0	0.05
7850	650	7260	7.0	7	25	133	159	8.0	0.1	0.10
7900	450	734	1.3	9	1	98	25	3.0	0.5	0.05
7900	500	475	3.3	11	18	162	250	0.5	1.7	0.30
7900	550	7900	7.1	8	14	130	367	6.0	2.0	0.05
7900	600	1861	3.5	14	15	229	350	4.0	1.3	0.10
7900	650	891	6.2	9	17	183	540	7.0	0.8	0.05
7900	700	790	2.8	34	12	201	69	6.0	0.8	0.10
7900	750	28	0.1	7	6	1133	135	5.0	2.4	0.10
7900	800	14	0.1	22	7	320	31	0.5	0.1	0.10
7900	900	5	0.1	7	5	805	67	0.1	0.1	0.05
7950	550	2527	2.7	10	12	158	235	5.0	0.8	0.05
7950	600	2413	2.0	10	16	50	218	0.1	1.0	0.05
7950	650	1377	1.2	12	13	35	171	0.1	0.9	0.05
7950	700	191	0.7	10	21	170	340	5.0	0.6	0.05
7950	800	26	0.1	8	9	2216	106	22.0	0.3	0.10
7950	900	1444	1.8	8	18	268	210	6.0	1.0	0.05
8000	550	52	0.8	14	12	111	34	0.5	0.5	0.10
8000	600	9280	21.1	11	30	70	318	0.1	0.5	0.05
8000	650	3620	3.1	10	24	75	285	0.5	1.2	0.20
8000	700	7040	4.5	13	50	151	163	11.0	0.9	0.30
8000	750	1954	4.1	12	52	94	151	10.0	0.9	0.10
8000	800	99	1.3	11	10	323	54	0.1	0.9	0.05
8000	850	5	0.1	9	3	1005	89	0.5	0.3	0.10
8000	900	5	0.1	9	7	257	22	0.5	0.3	0.10
8050	650	5380	3.1	10	23	95	202	0.5	1.3	0.10
8100	650	1664	1.1	8	16	72	91	3.0	0.6	0.10
8100	700	3800	4.1	12	33	408	209	2.0	0.6	0.10
8100	750	19450	10.1	11	30	31	217	5.0	0.3	0.10
8100	800	466	1.8	17	34	195	200	5.0	1.3	0.10
8100	900	24	0.1	14	7	1850	152	11.0	0.1	0.10
8150	700	9290	5.9	9	48	24	219	0.5	0.8	0.10
8150	750	3230	2.9	9	36	22	194	0.5	0.5	0.10
8150	800	3260	8.8	20	96	89	215	3.0	2.0	0.10
8150	850	96	0.1	12	3	1100	35	13.0	0.8	0.05
8150	900	5	0.1	17	8	545	83	0.1	0.1	0.10
8200	650	27	0.1	11	8	113	10	0.1	0.2	0.05
8200	750	7023	10.2	7	30	117	262	0.5	1.2	0.10
8200	800	3190	5.3	8	106	45	150	2.0	0.6	0.10
8200	850	287	5.1	11	82	212	95	6.0	0.6	0.05
8250	750	5400	3.5	11	28	73	137	0.1	0.6	0.05
8250	800	2223	2.7	11	50	98	164	3.0	1.0	0.10
8250	850	187	1.7	12	9	681	216	37.0	0.7	0.10
8300	550	56	0.1	14	13	217	28	3.0	0.4	0.10
8300	650	2512	3.0	14	16	84	161	0.5	0.8	0.10

Appendix D (Continued)

North	Elev.	Au ppb	Ag ppm	Pb ppm	Cu ppm	Hg ppb	As ppm	Sb ppm	Se ppm	Te ppm
8300	700	1335	1.3	11	17	56	210	4.0	0.5	0.10
8300	750	3270	7.1	13	17	245	209	11.0	1.8	0.10
8300	800	1177	1.4	10	24	63	206	5.0	0.9	0.05
8300	850	4600	5.0	15	35	798	218	14.0	1.1	0.10
8350	800	2014	2.5	13	14	302	189	0.5	1.8	0.10
8350	850	108	0.1	11	4	834	159	20.0	0.4	0.05
8350	900	34	0.1	14	7	368	45	12.0	0.8	0.10

APPENDIX E

SCATTER DIAGRAMS FOR SELECTED ELEMENT PAIRS FROM GEOCHEMICAL DATA SETS

Instrumental Neutron Activation Data, 78 Wall Rock Samples. Au-Cr, Au-As, Au-Ag, and Au-Sb Plots.

INAA DATA
78 WALL ROCK SAMPLES

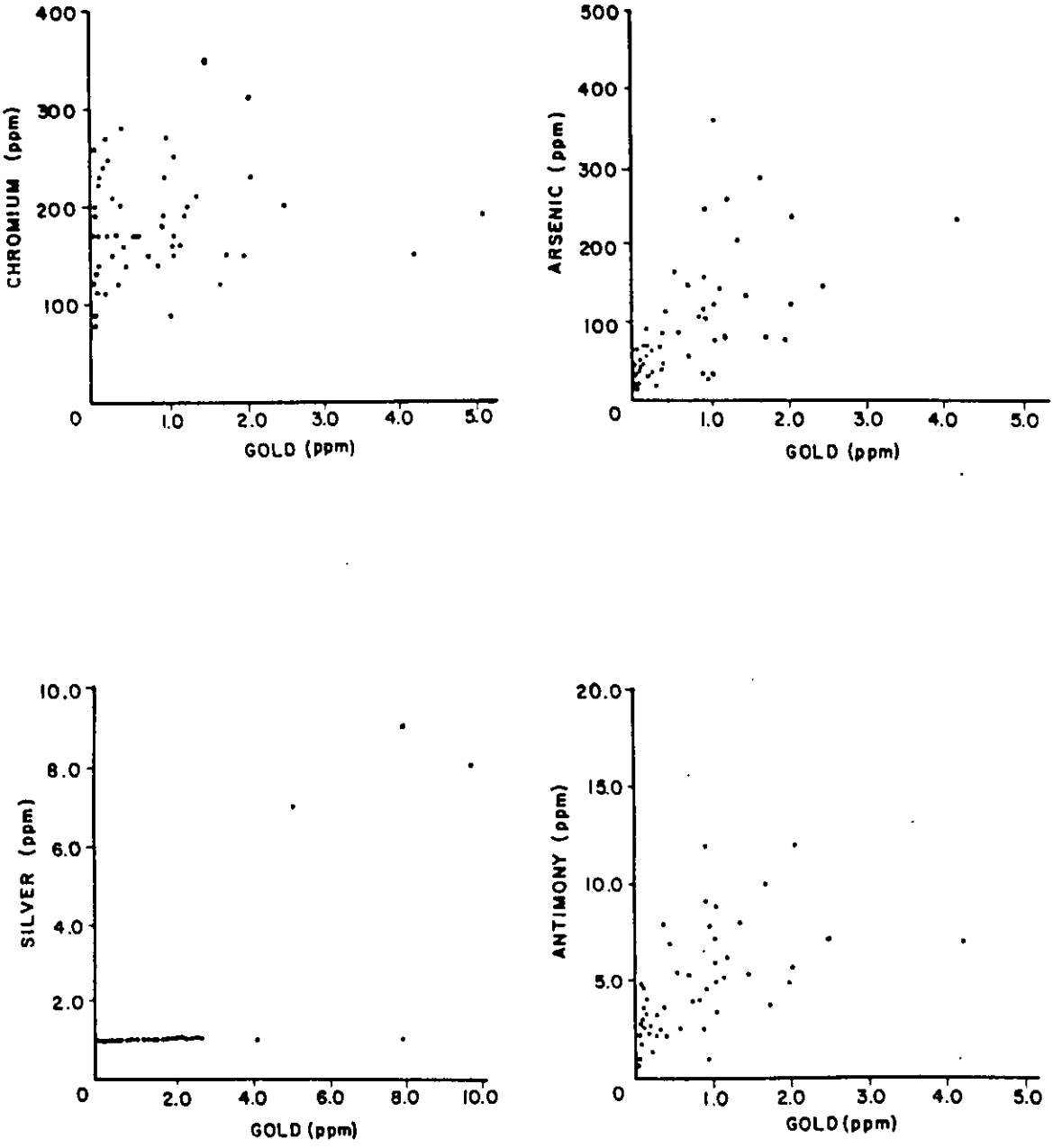

Appendix E (continued)

Instrumental Neutron Activation Data, 78 Wall Rock Samples. Sb-As, and Sb-Na Plots.

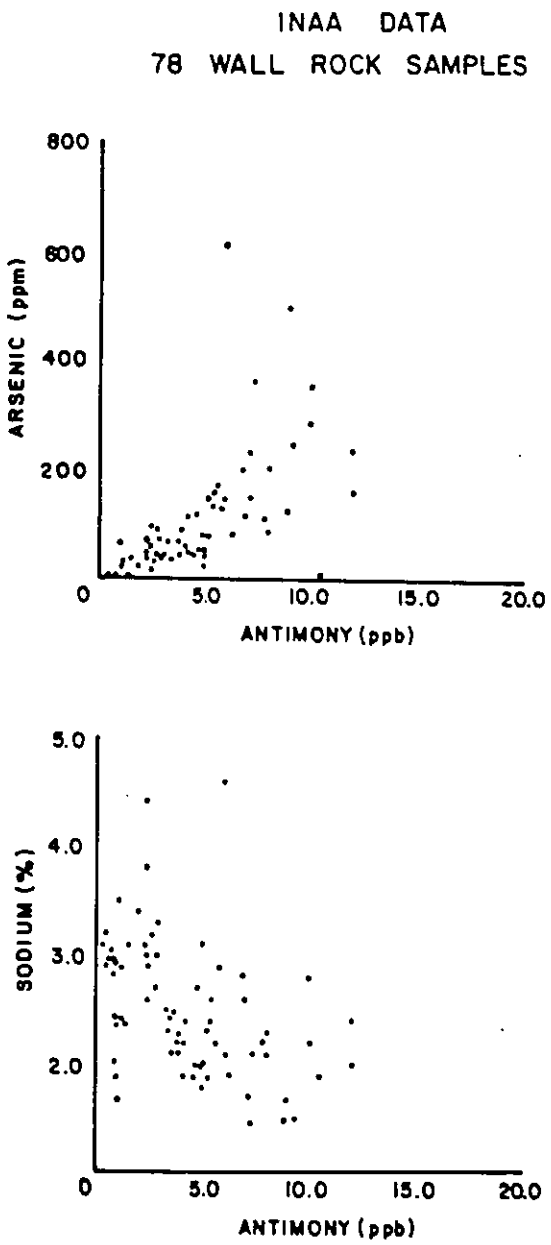

Appendix E (continued)

Instrumental Neutron Activation Data, 62 Vein Samples. Au-Fe, Au-Cr, Au-Ag, and Au-Na Plots.

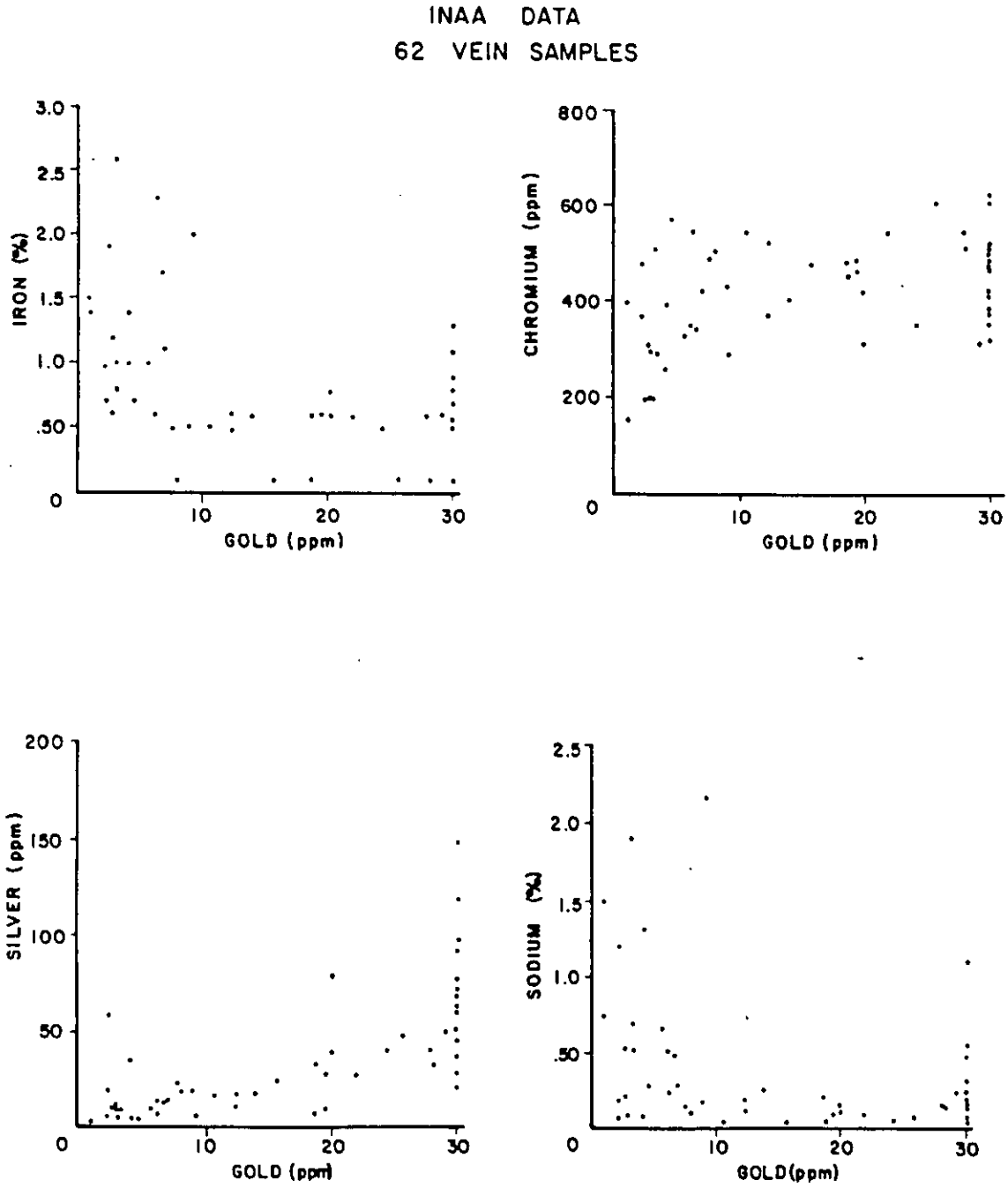

Appendix E (continued)

Instrumental Neutron Activation Data, 62 Vein Samples. As-Na, As-Fe, Sb-Cr, and Sb-Cd Plots.

INAA DATA
62 VEIN SAMPLES

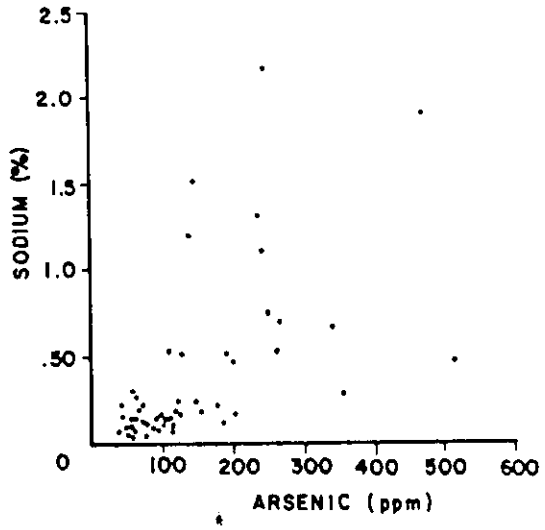

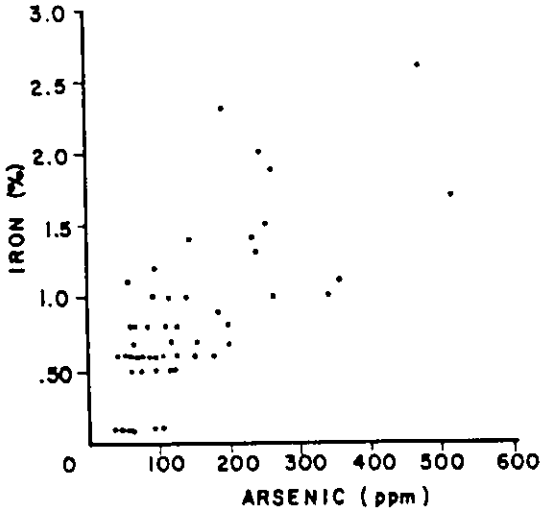

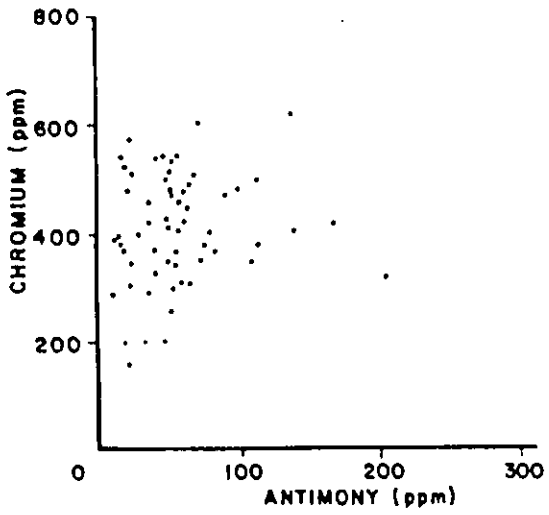

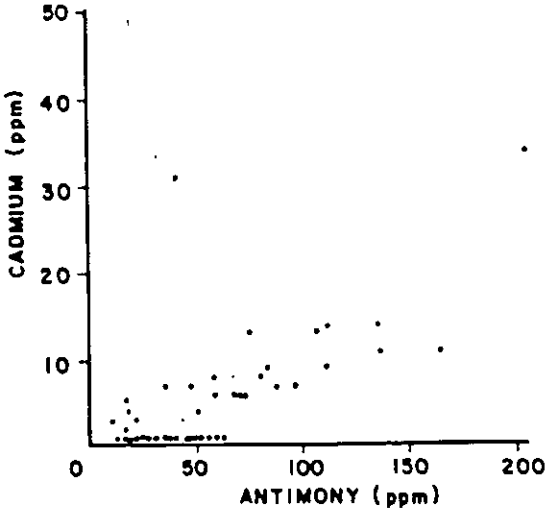

Appendix E (continued)

Instrumental Neutron Activation Data, 62 Vein Samples. Ag-Sb, Ag-Cd, and Na-Fe Plots.

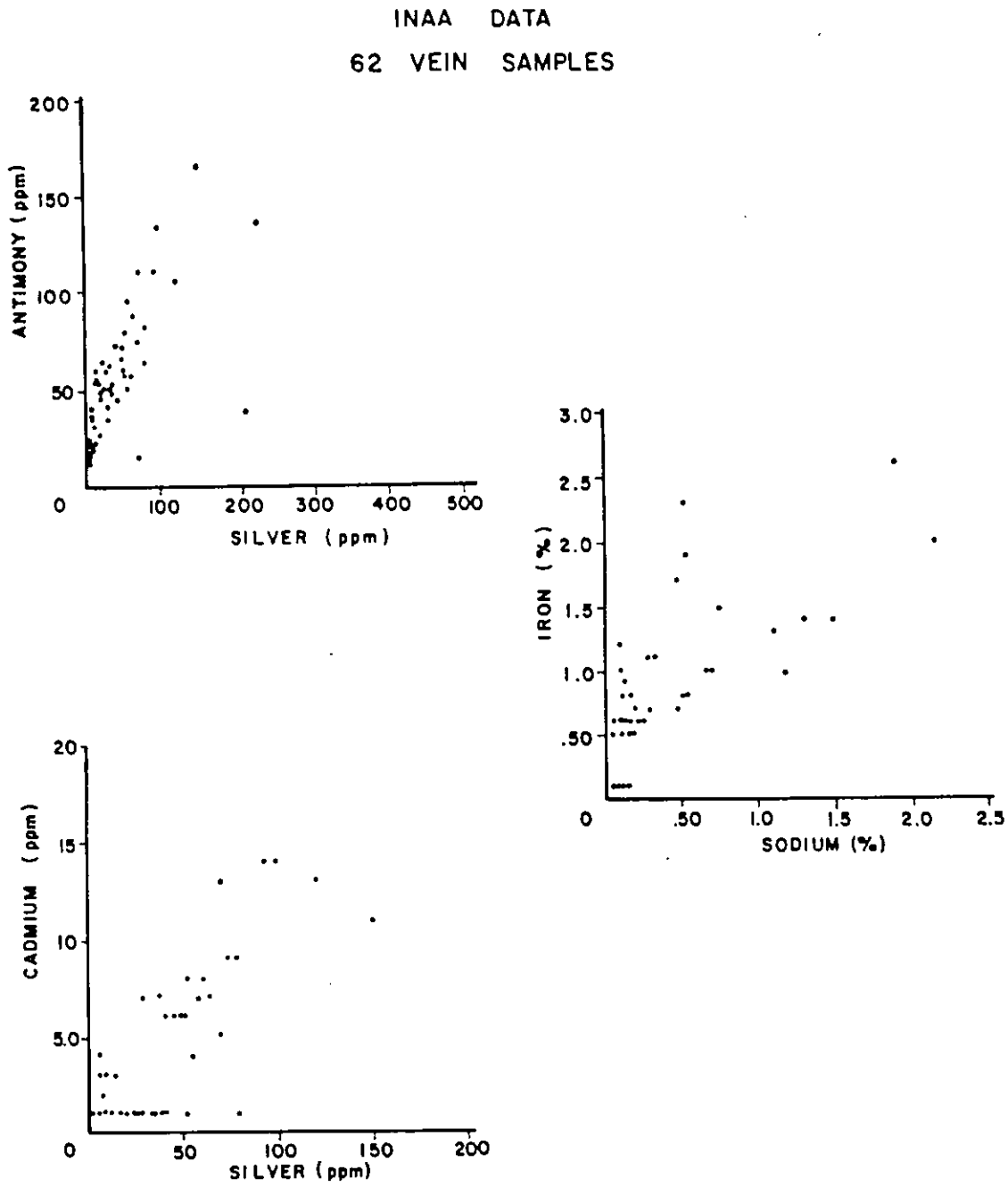

Appendix E (continued)

Directly-Coupled Emission Spectrographic Data,
47 Vein Samples. Ag-Sb, Cu-Pb, Sb-Pb, and Sb-Cu Plots

DCP EMMISSION SPECTROGRAPHIC DATA
47 VEIN SAMPLES

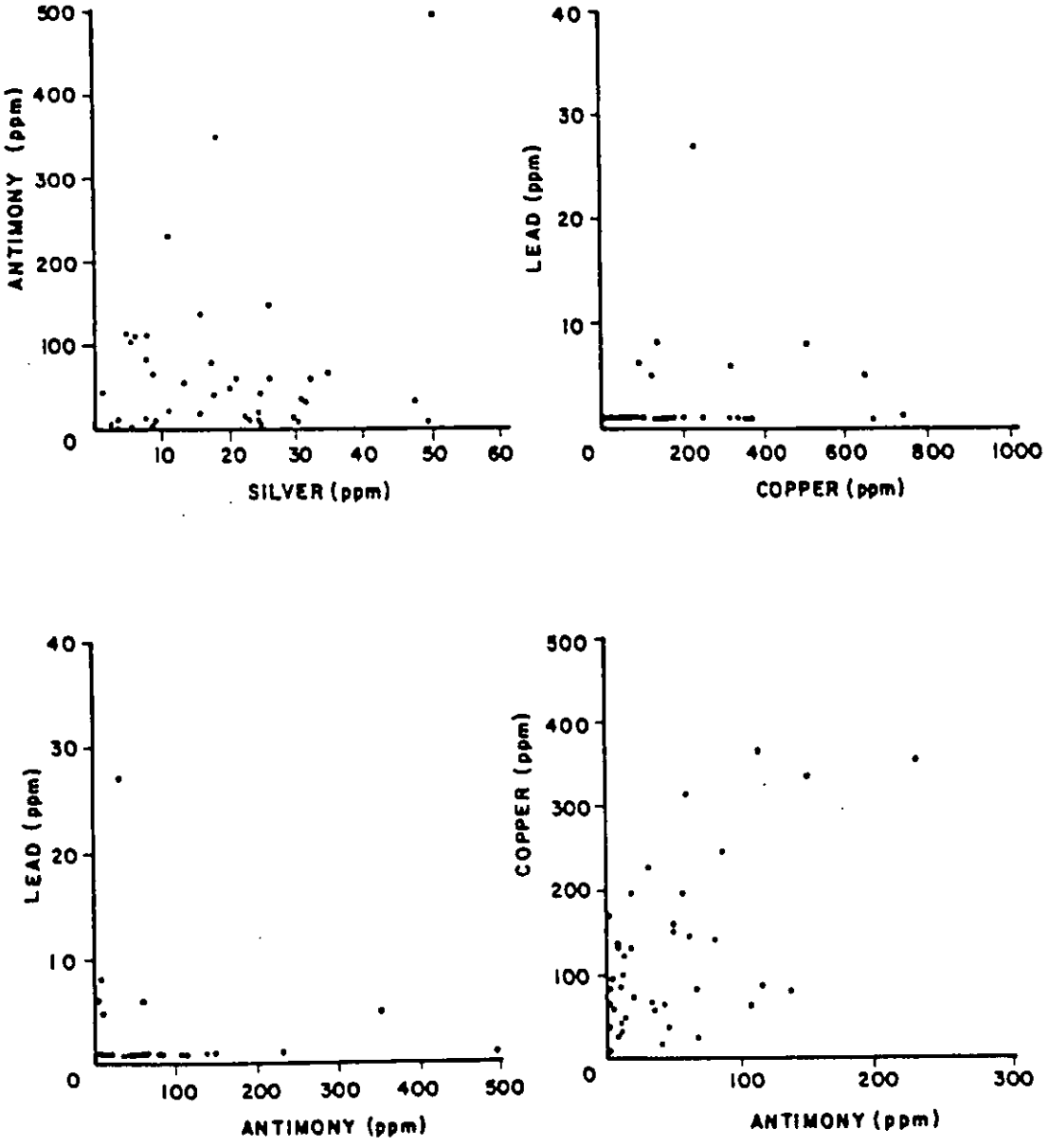

Appendix E (continued)

Directly-Coupled Emission Spectrographic Data, 47 Vein Samples. As-Hg, As-Pb, As-Sb, and As-Cu Plots

DCP EMMISSION SPECTROGRAPHIC DATA

47 VEIN SAMPLES

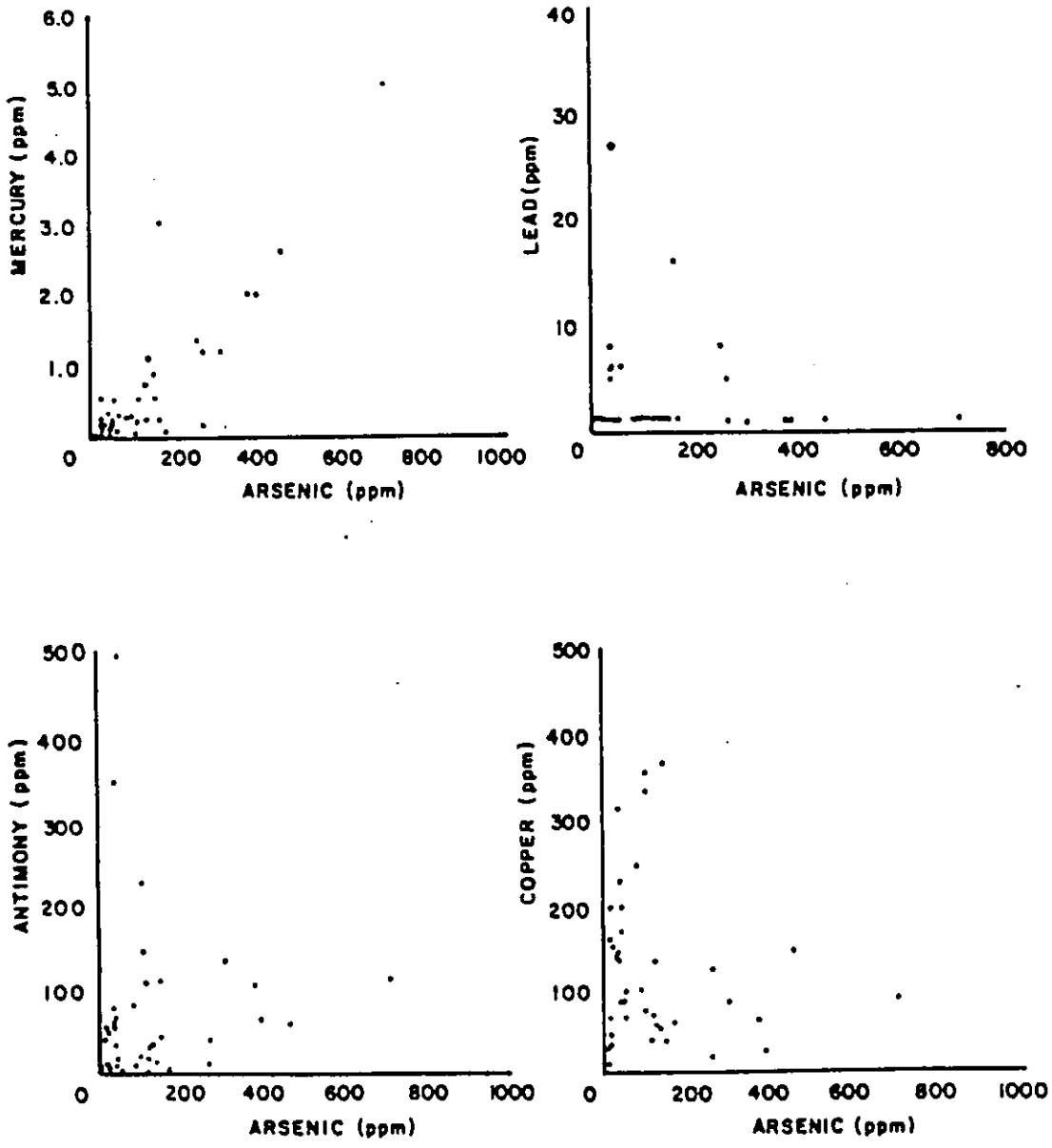

Appendix E (continued)

Atomic Absorption and Fire Assay Analysis 197 Composite Core Samples. Au-Ag, Au-Cu, Au-Sb, and Sb-Cu Plots.

ATOMIC ABSORPTION AND FIRE ASSAY ANALYSIS

197 COMPOSITE CORE SAMPLES

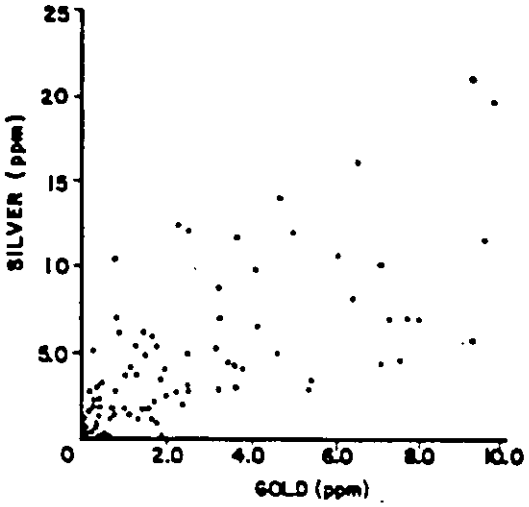

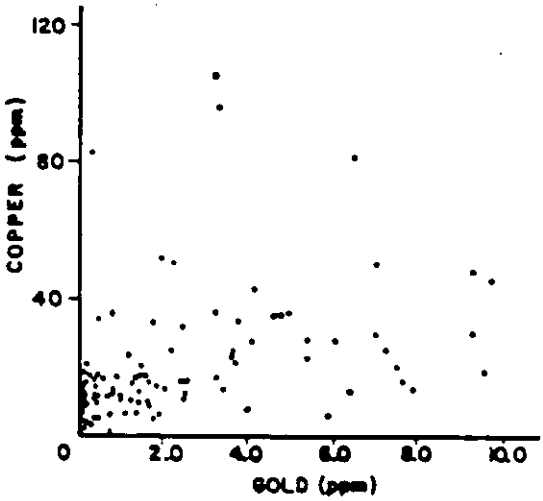

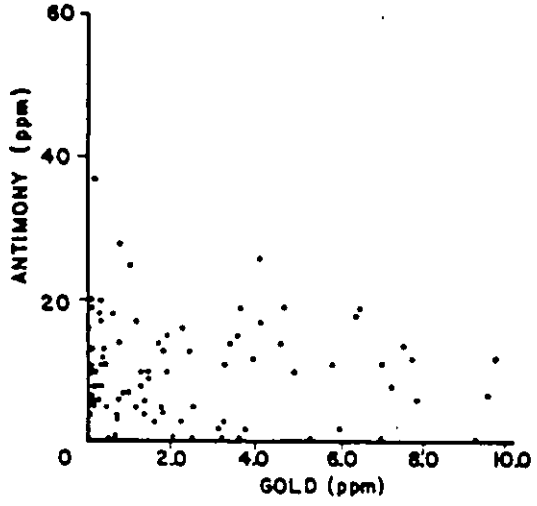

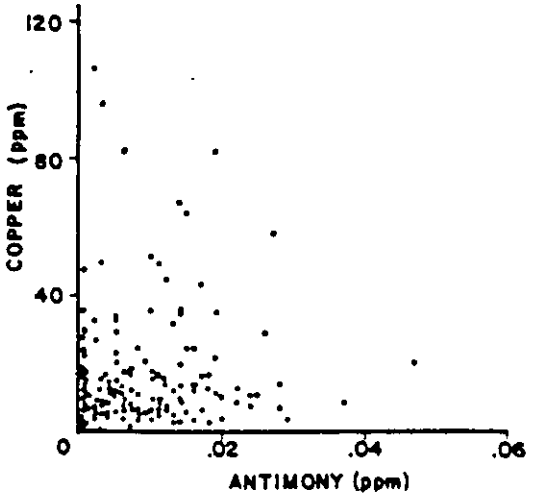

Appendix E (continued)

Atomic Absorption and Fire Assay Analysis 197 Composite Core Samples. Ag-Sb, and Ag-Cu Plots.

ATOMIC ABSORPTION AND FIRE ASSAY ANALYSIS
197 COMPOSITE CORE SAMPLES

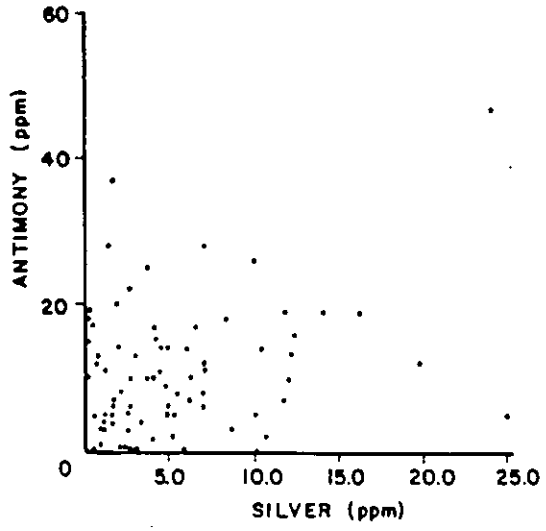

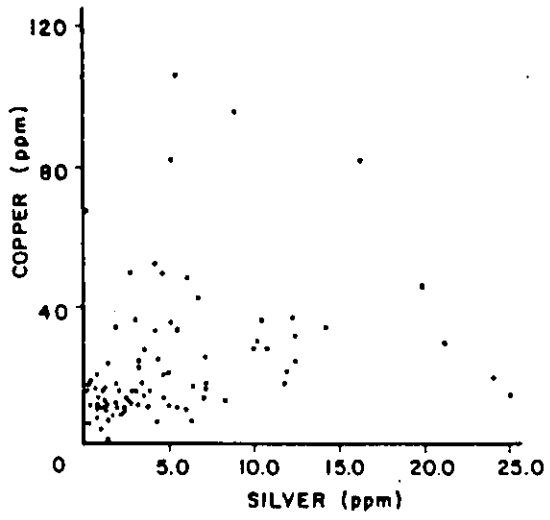

APPENDIX F
TRACE ELEMENT PATTERNS AT THE RHYODACITE - ORE CONTACT ON THE 755, 690, AND 550 LEVELS. SEMI-QUANTITAVE EMISSION SPECTROGRAPHIC ANALYSIS BY CHEMEX LABS, INC.

RHYODACITE CONTACT
755 LEVEL, CANNON MINE
TRACE ELEMENT GEOCHEMISTRY

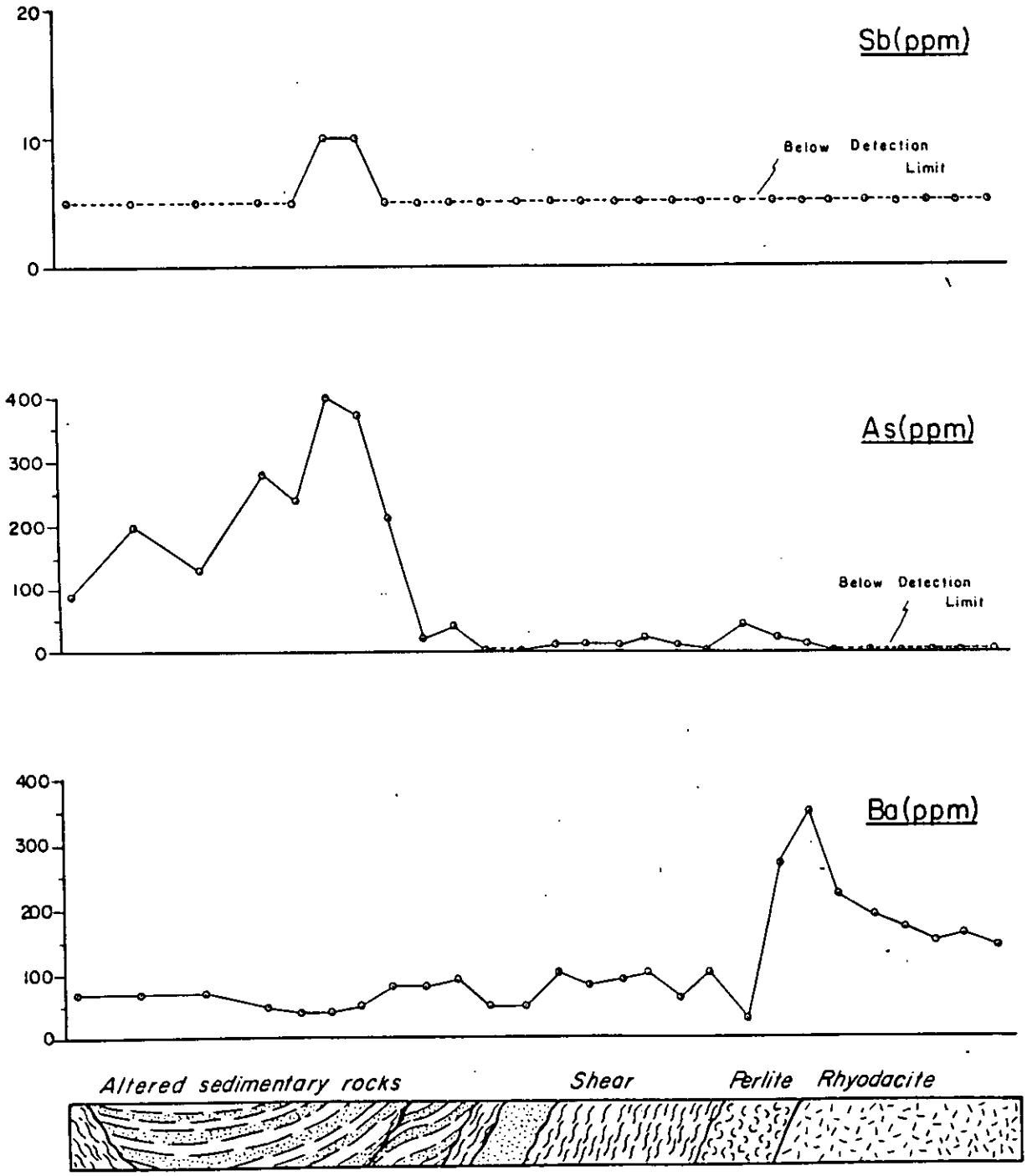

RHYODACITE CONTACT
755 LEVEL, CANNON MINE
TRACE ELEMENT GEOCHEMISTRY

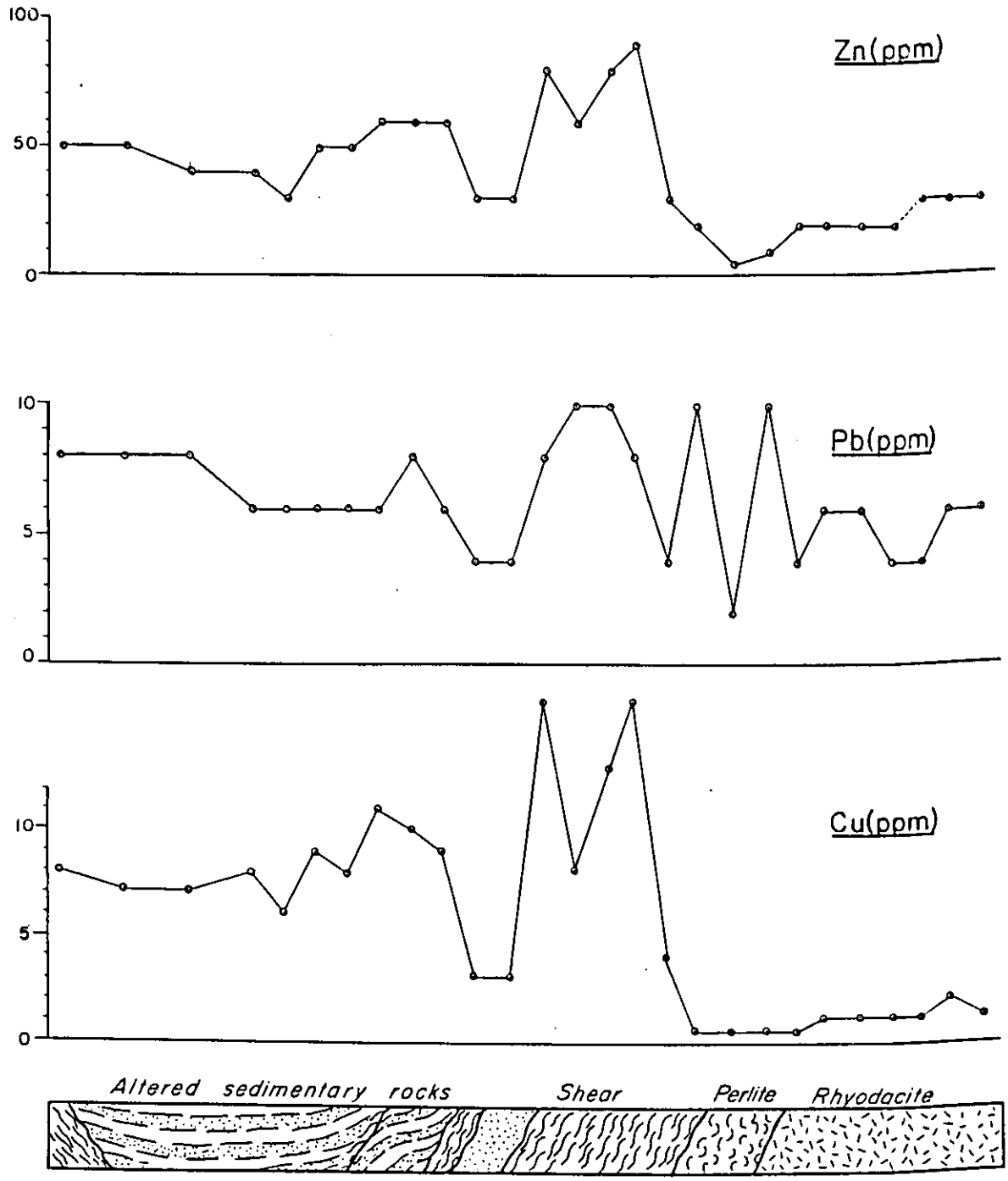

RHYODACITE CONTACT
755 LEVEL, CANNON MINE
TRACE ELEMENT GEOCHEMISTRY

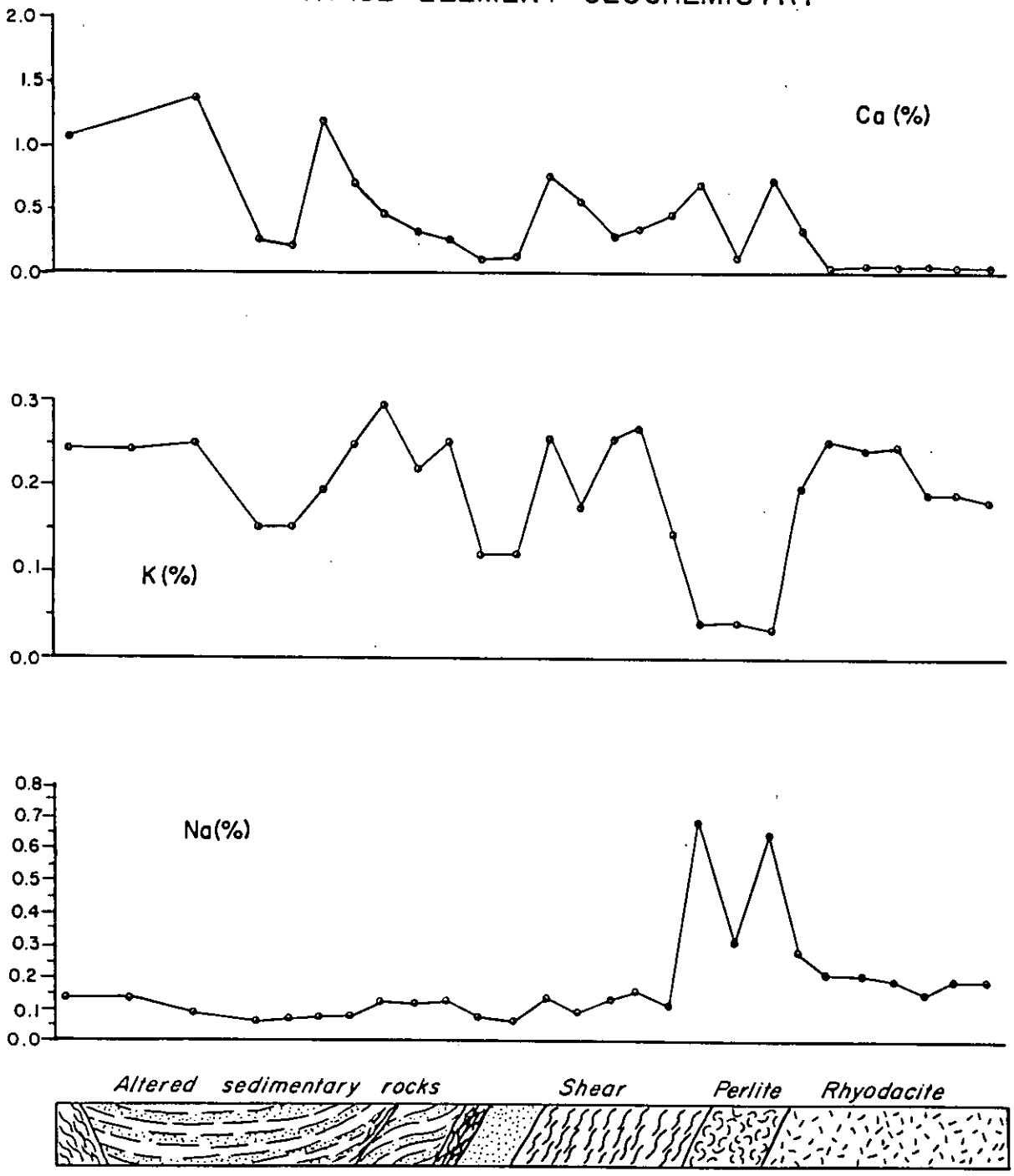

RHYODACITE CONTACT
755 LEVEL, CANNON MINE
TRACE ELEMENT GEOCHEMISTRY

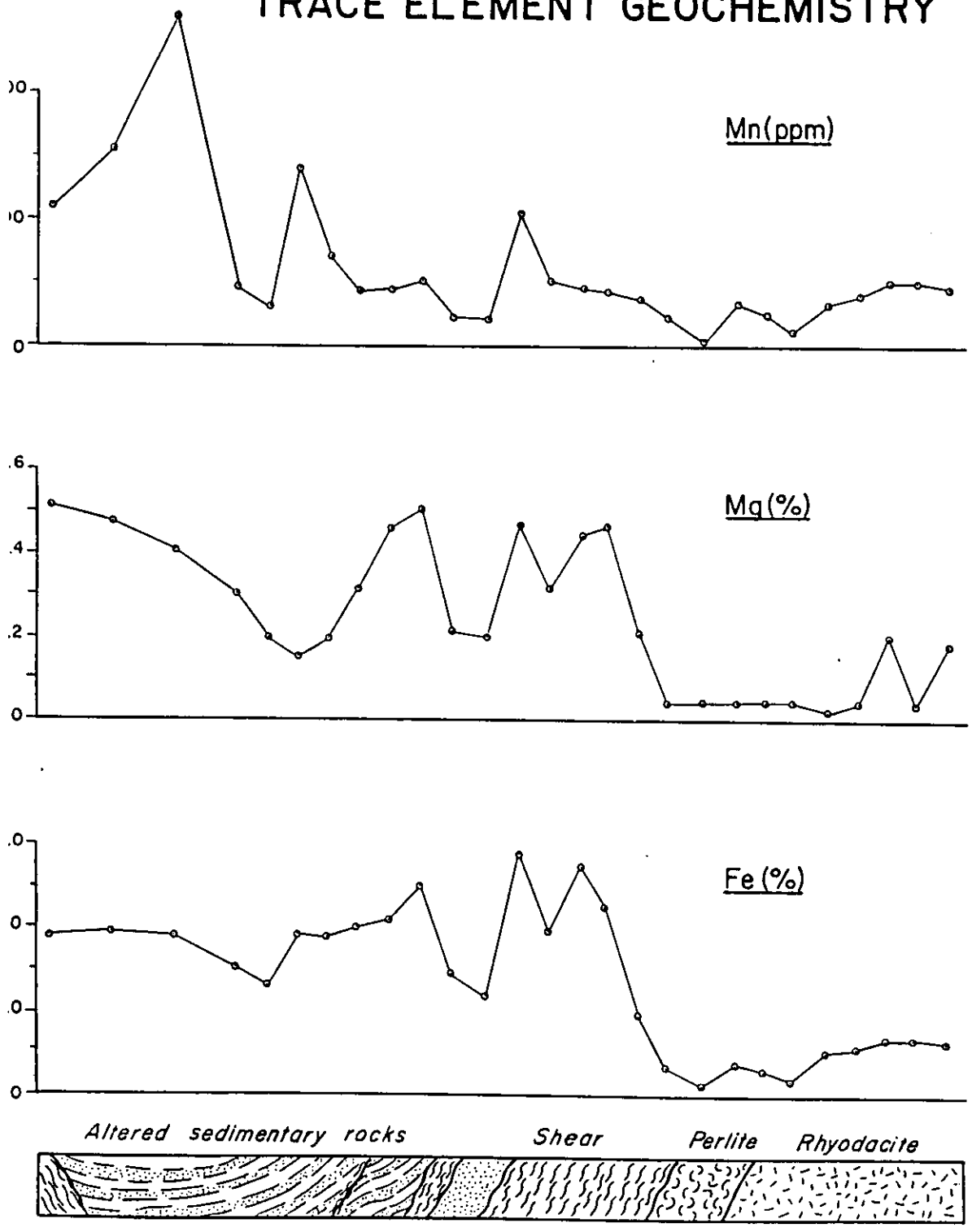

RHYODACITE CONTACT
755 LEVEL, CANNON MINE
TRACE ELEMENT GEOCHEMISTRY

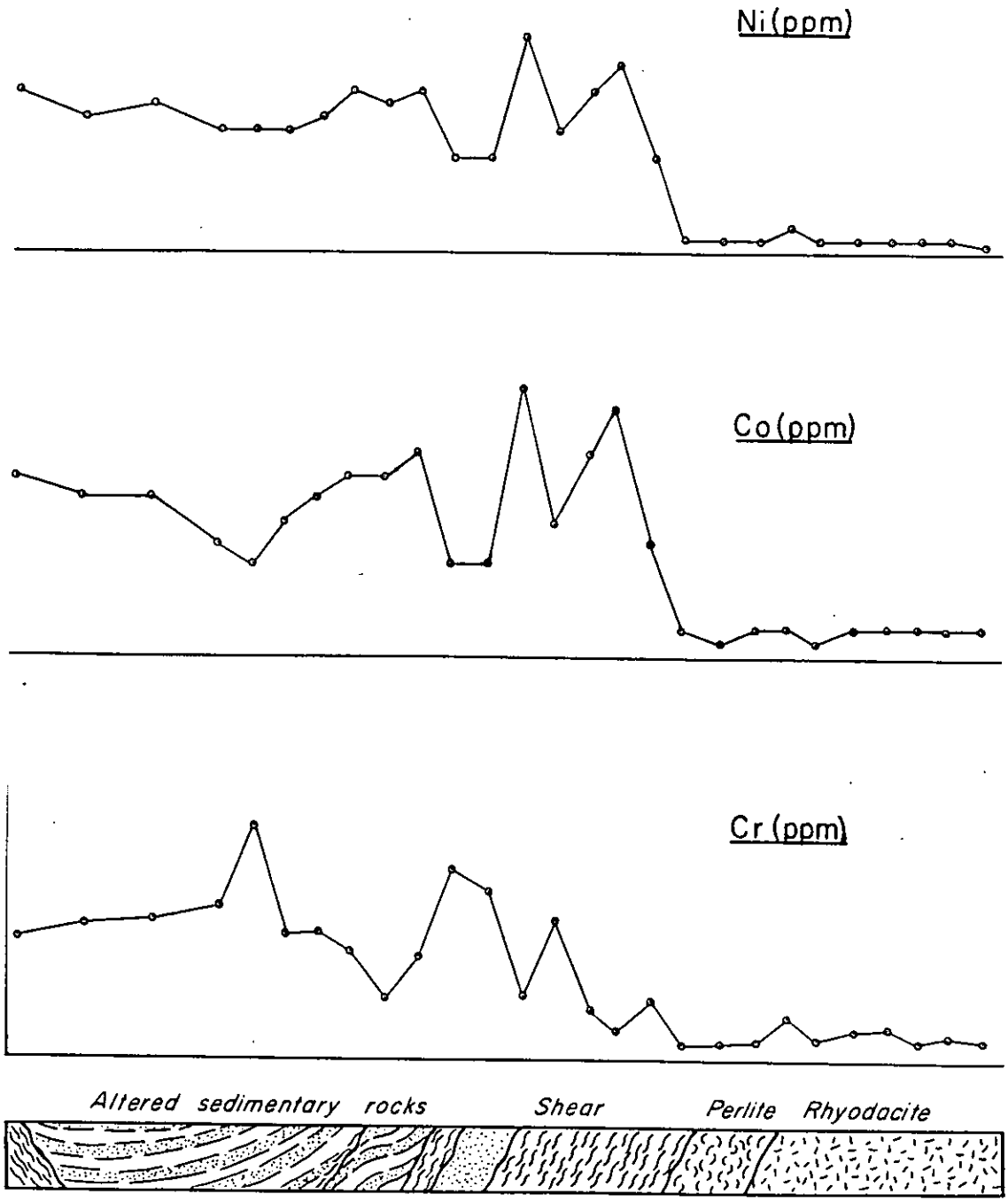

RHYODACITE CONTACT
755 LEVEL, CANNON MINE
TRACE ELEMENT GEOCHEMISTRY

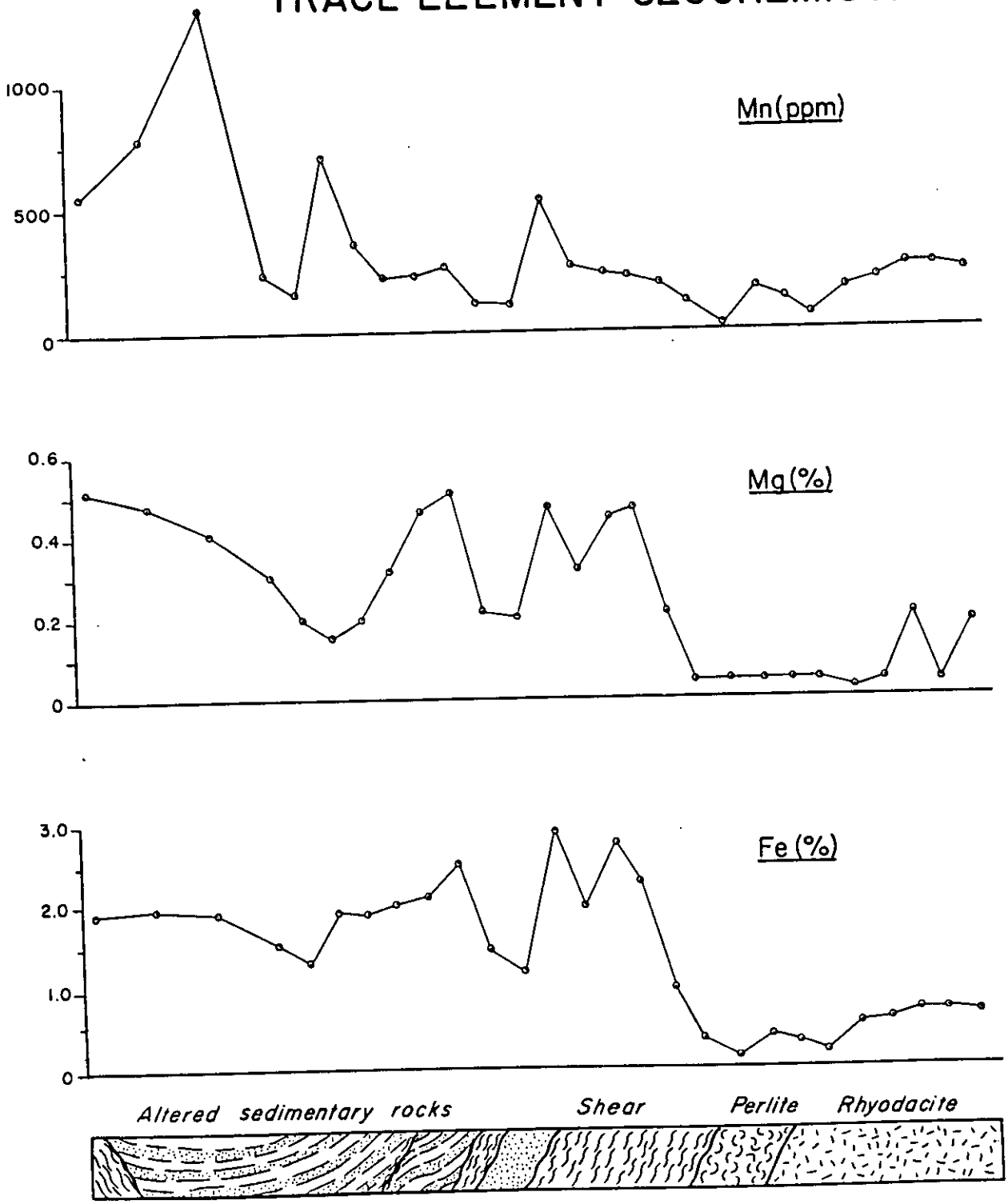

RHYODACITE CONTACT
755 LEVEL, CANNON MINE
TRACE ELEMENT GEOCHEMISTRY

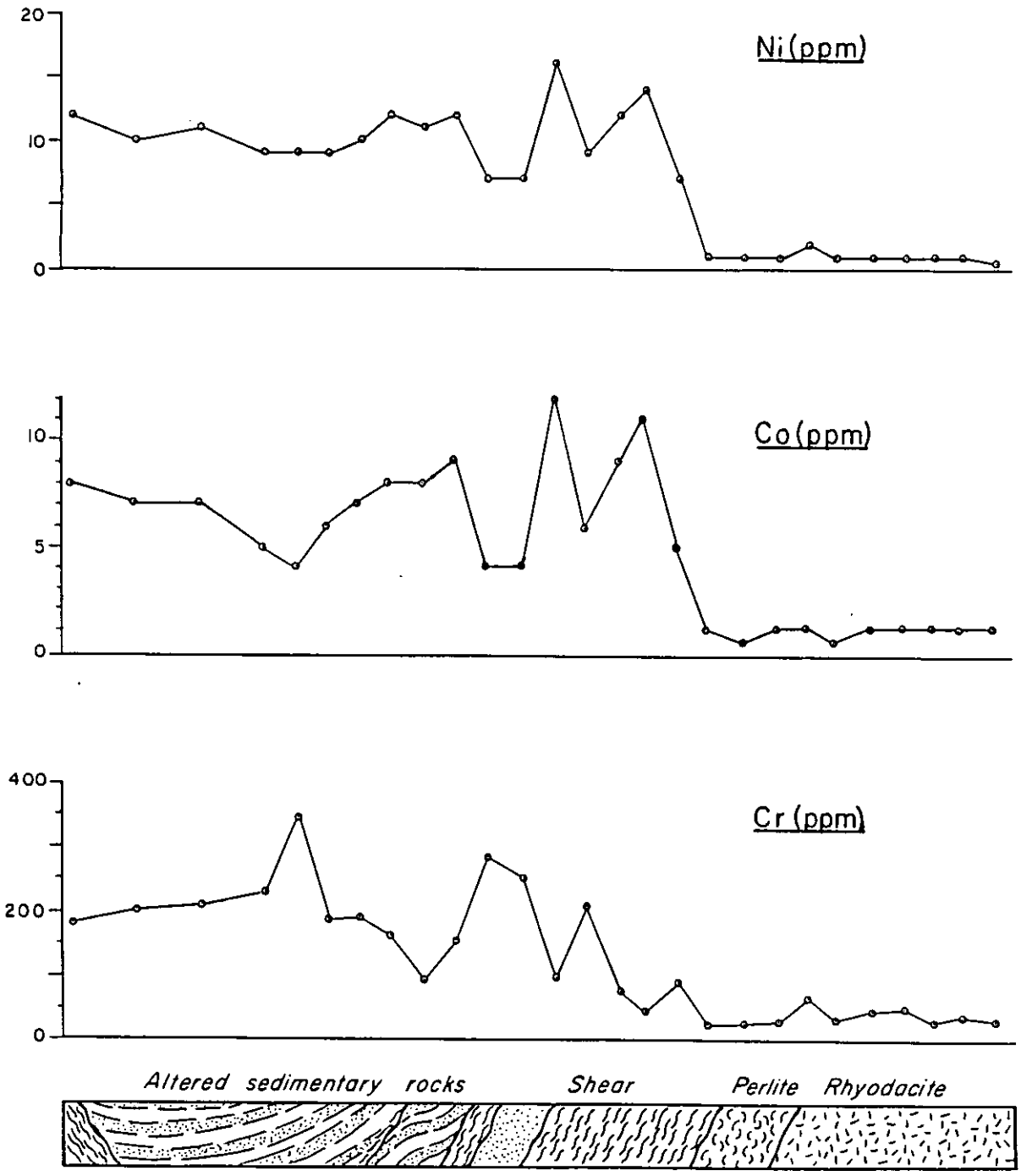

RHYODACITE CONTACT
690 LEVEL, CANNON MINE
TRACE ELEMENT GEOCHEMISTRY

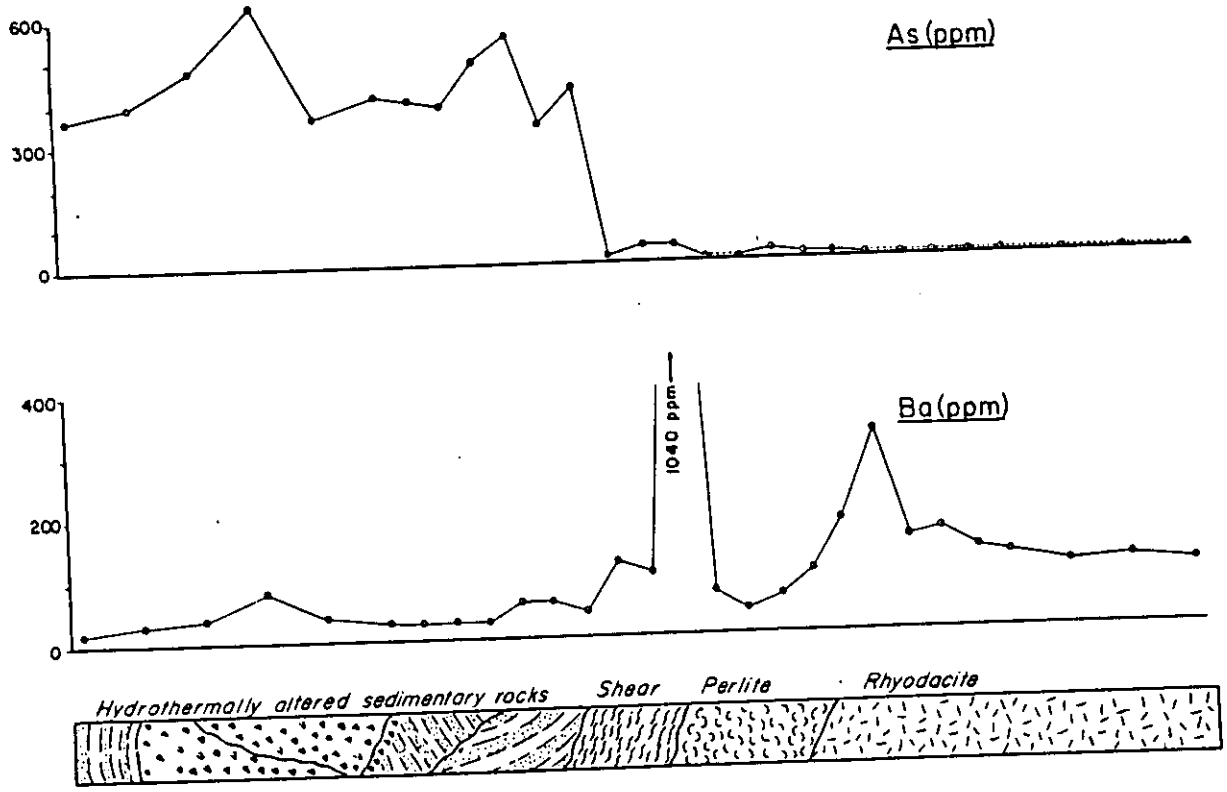

RHYODACITE CONTACT
690 LEVEL, CANNON MINE
TRACE ELEMENT GEOCHEMISTRY

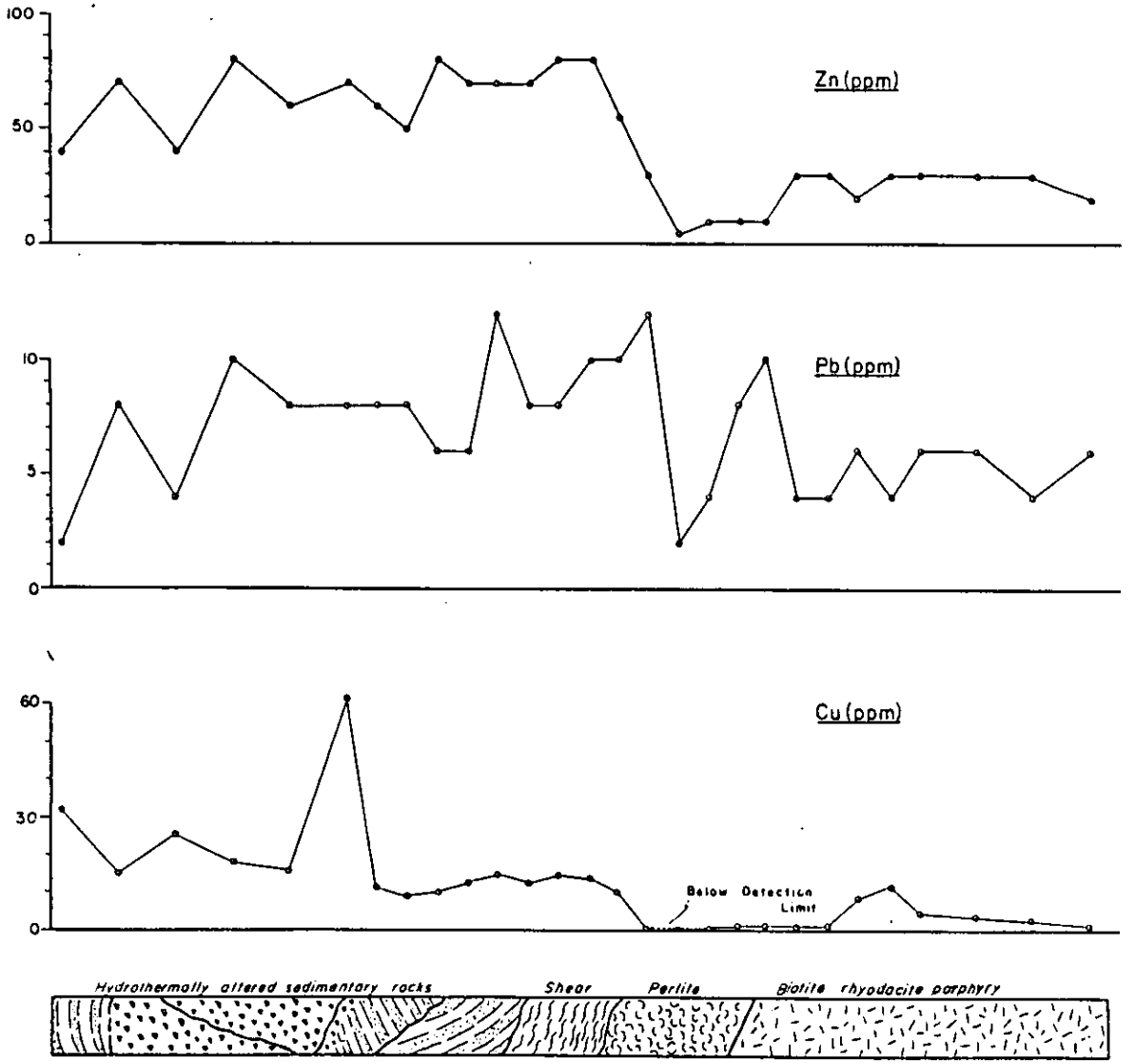

RHYODACITE CONTACT
690 LEVEL, CANNON MINE
TRACE ELEMENT GEOCHEMISTRY

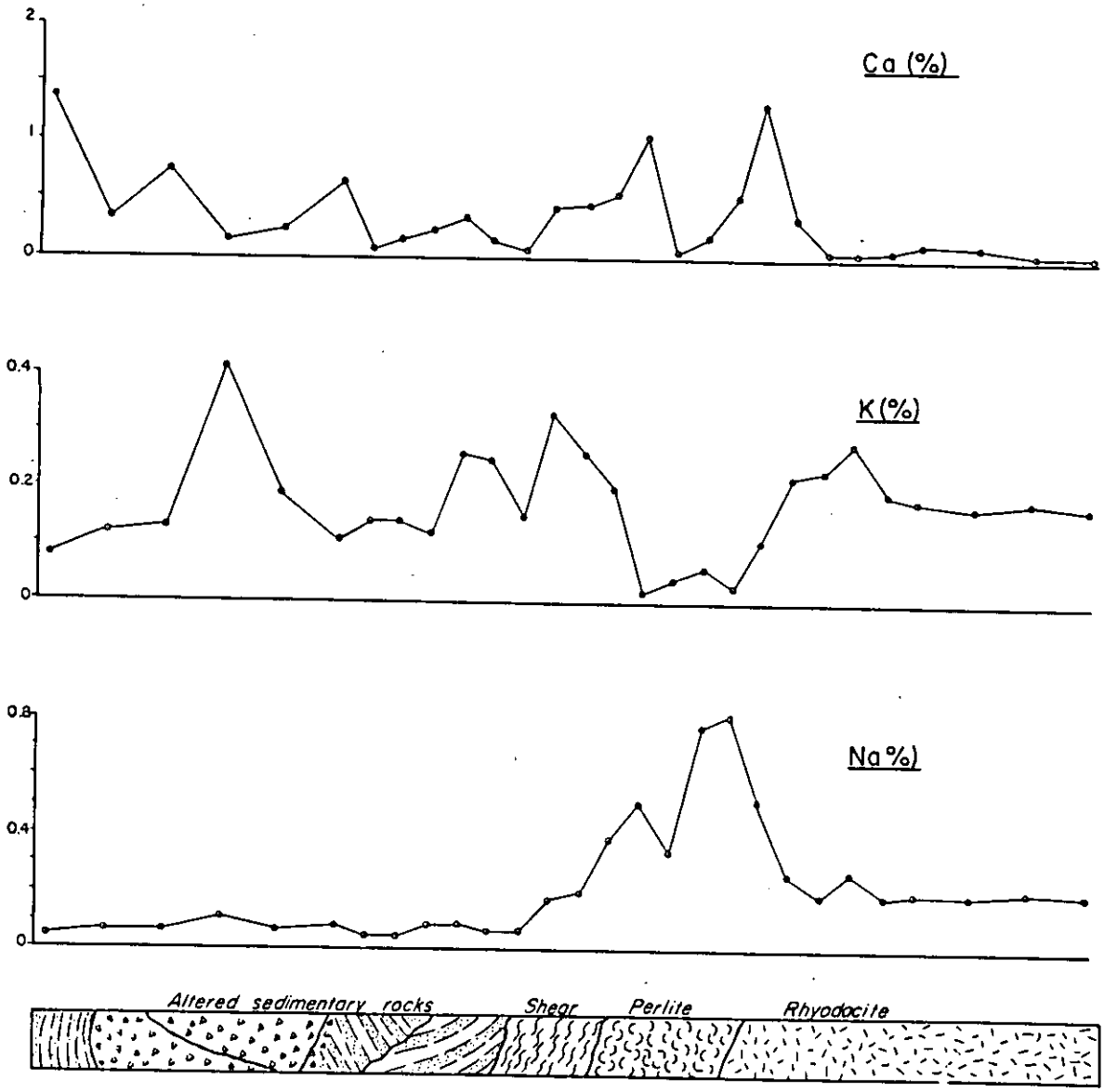

RHYODACITE CONTACT
690 LEVEL, CANNON MINE
TRACE ELEMENT GEOCHEMISTRY

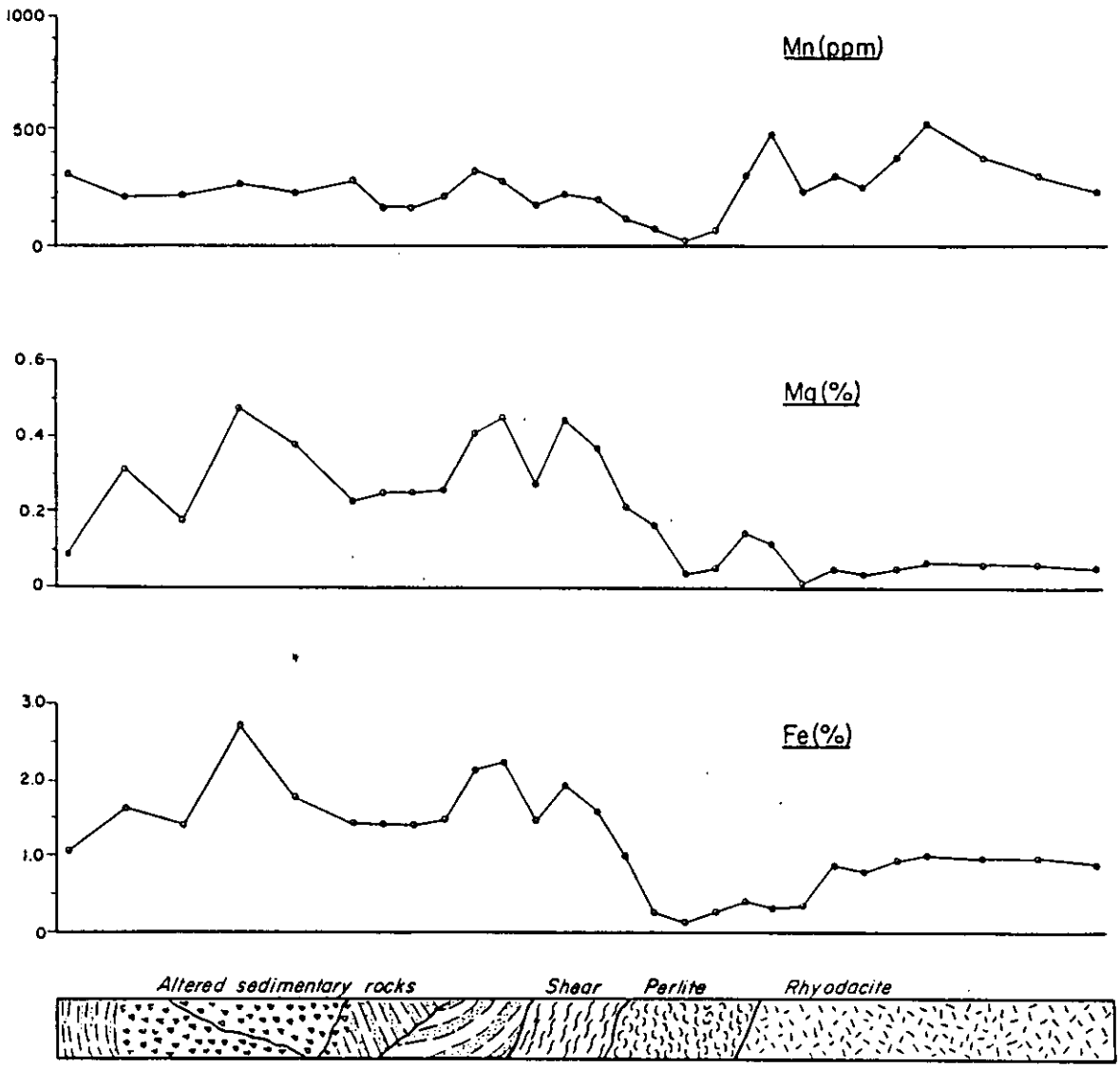

RHYODACITE CONTACT
690 LEVEL, CANNON MINE
TRACE ELEMENT GEOCHEMISTRY

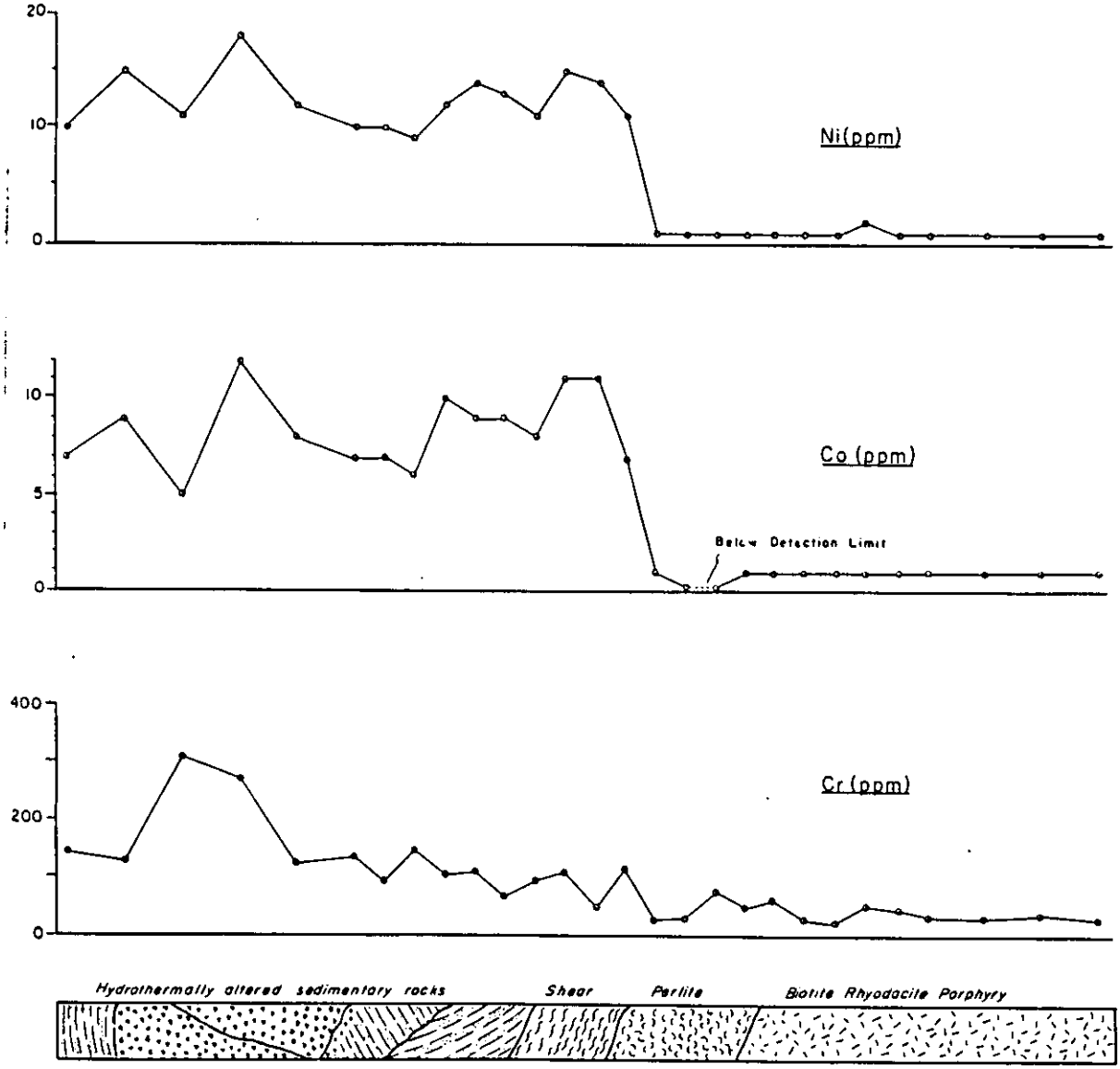

RHYODACITE CONTACT
550 LEVEL, CANNON MINE
TRACE ELEMENT GEOCHEMISTRY

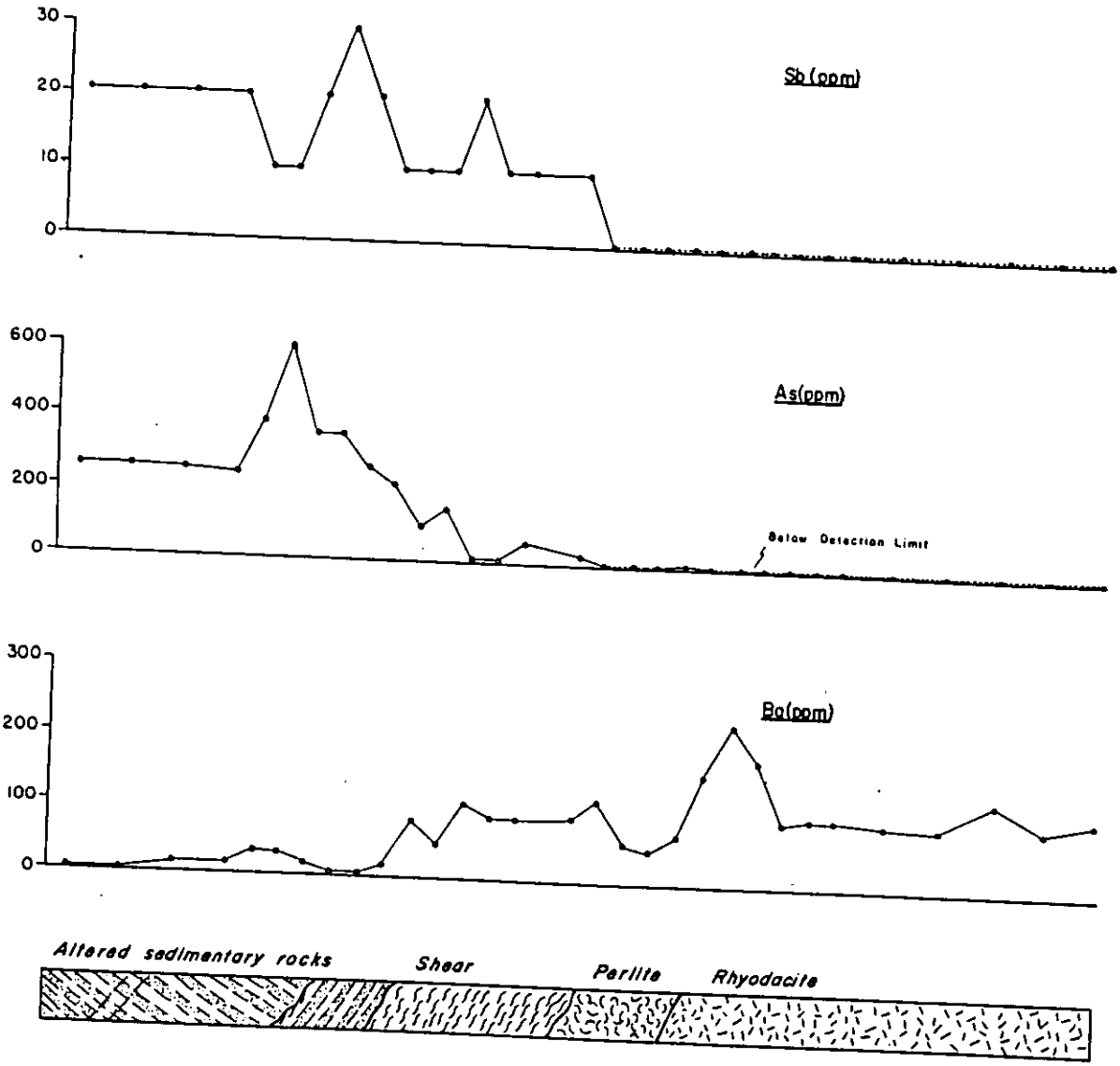

RHYODACITE CONTACT
550 LEVEL, CANNON MINE
TRACE ELEMENT GEOCHEMISTRY

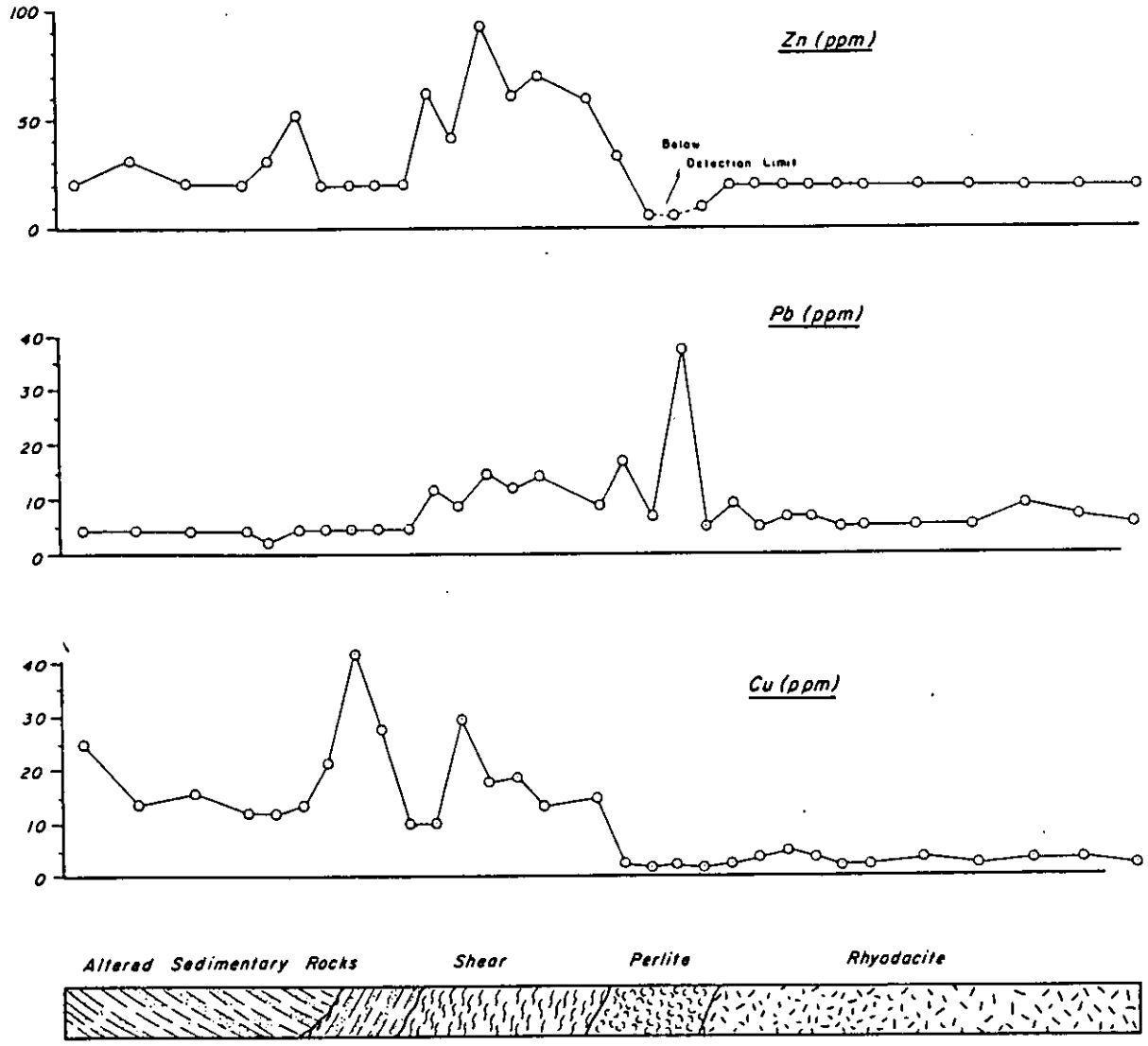

RHYODACITE CONTACT
550 LEVEL, CANNON MINE
TRACE ELEMENT GEOCHEMISTRY

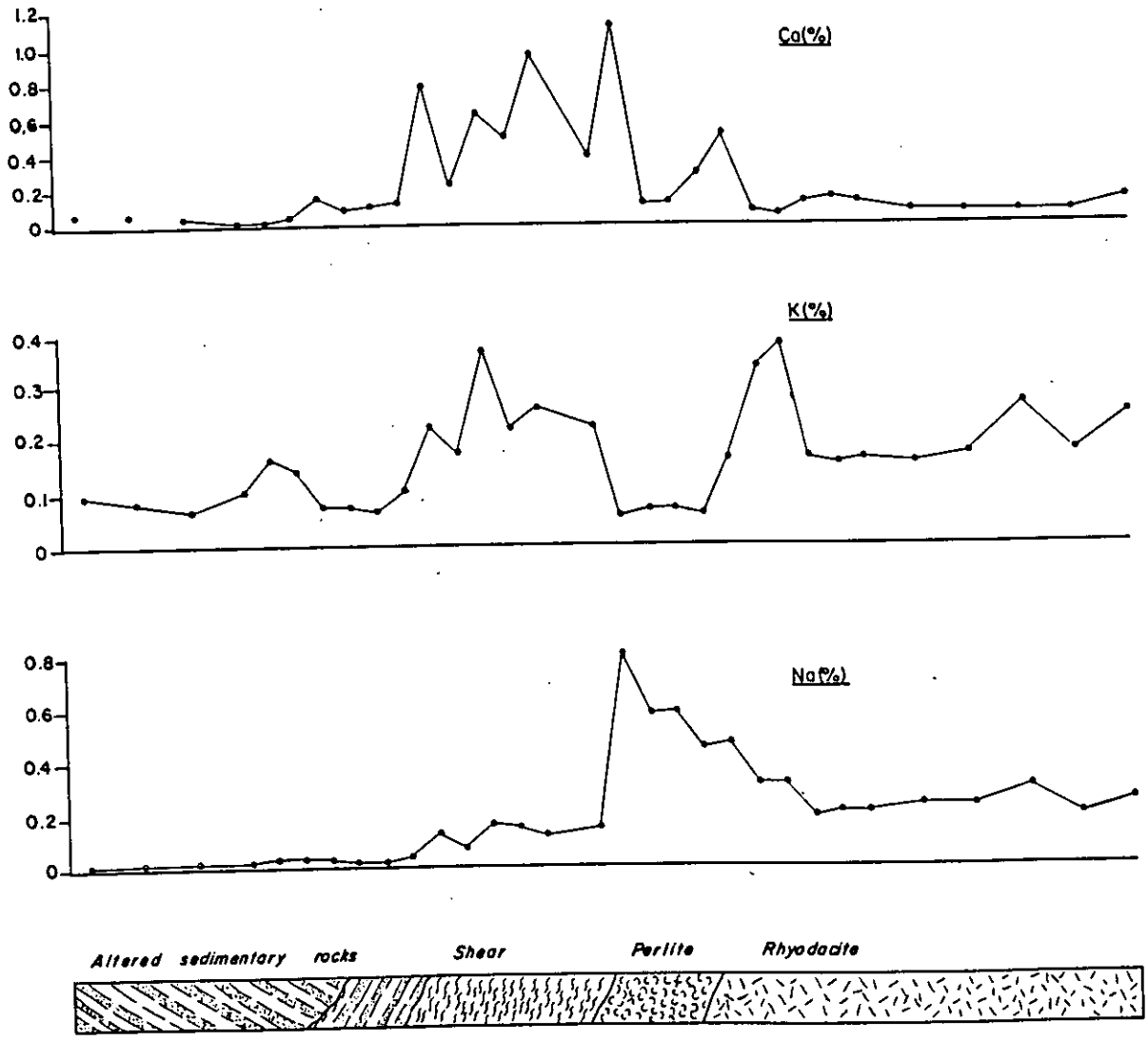

RHYODACITE CONTACT
550 LEVEL, CANNON MINE
TRACE ELEMENT GEOCHEMISTRY

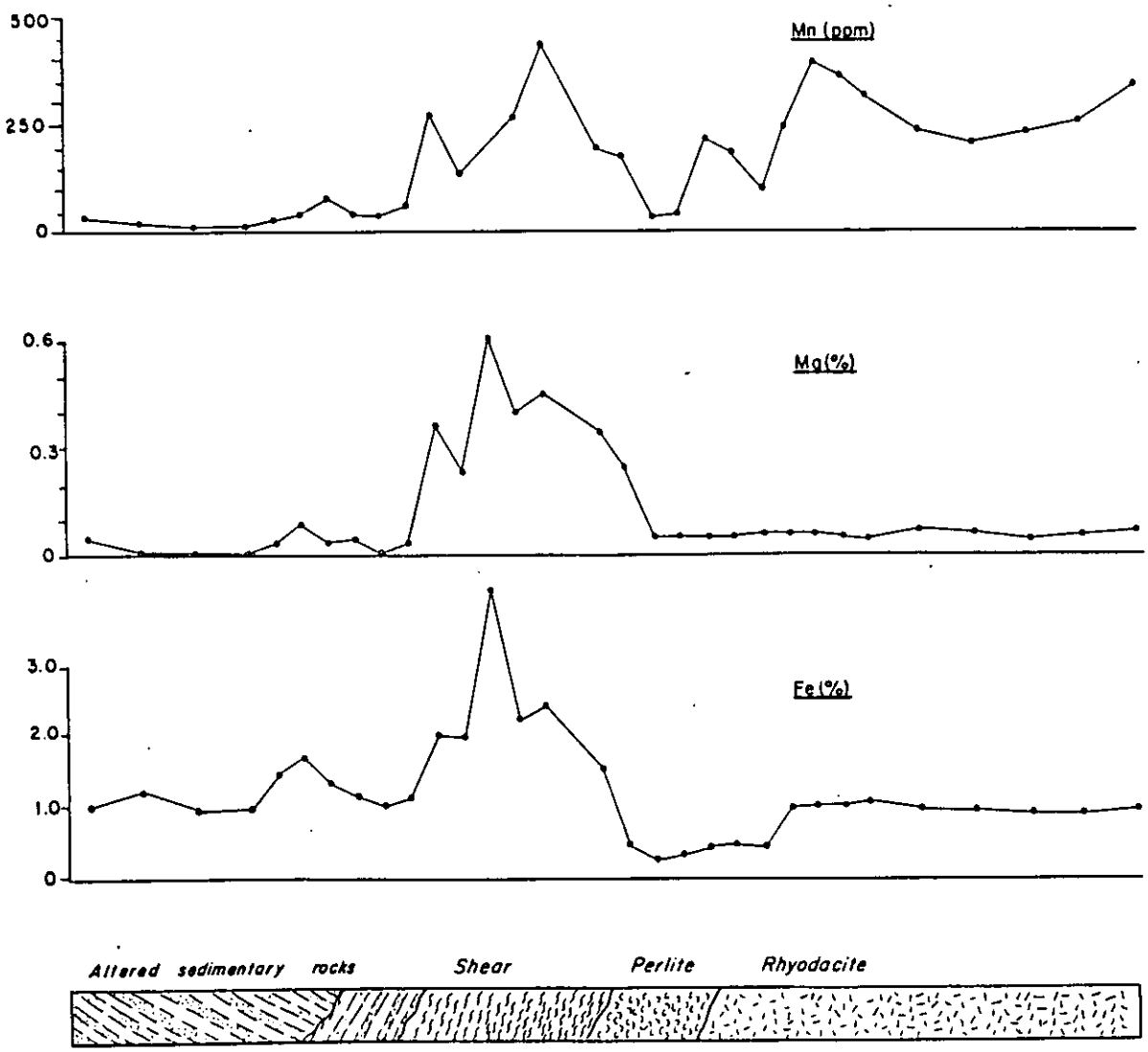
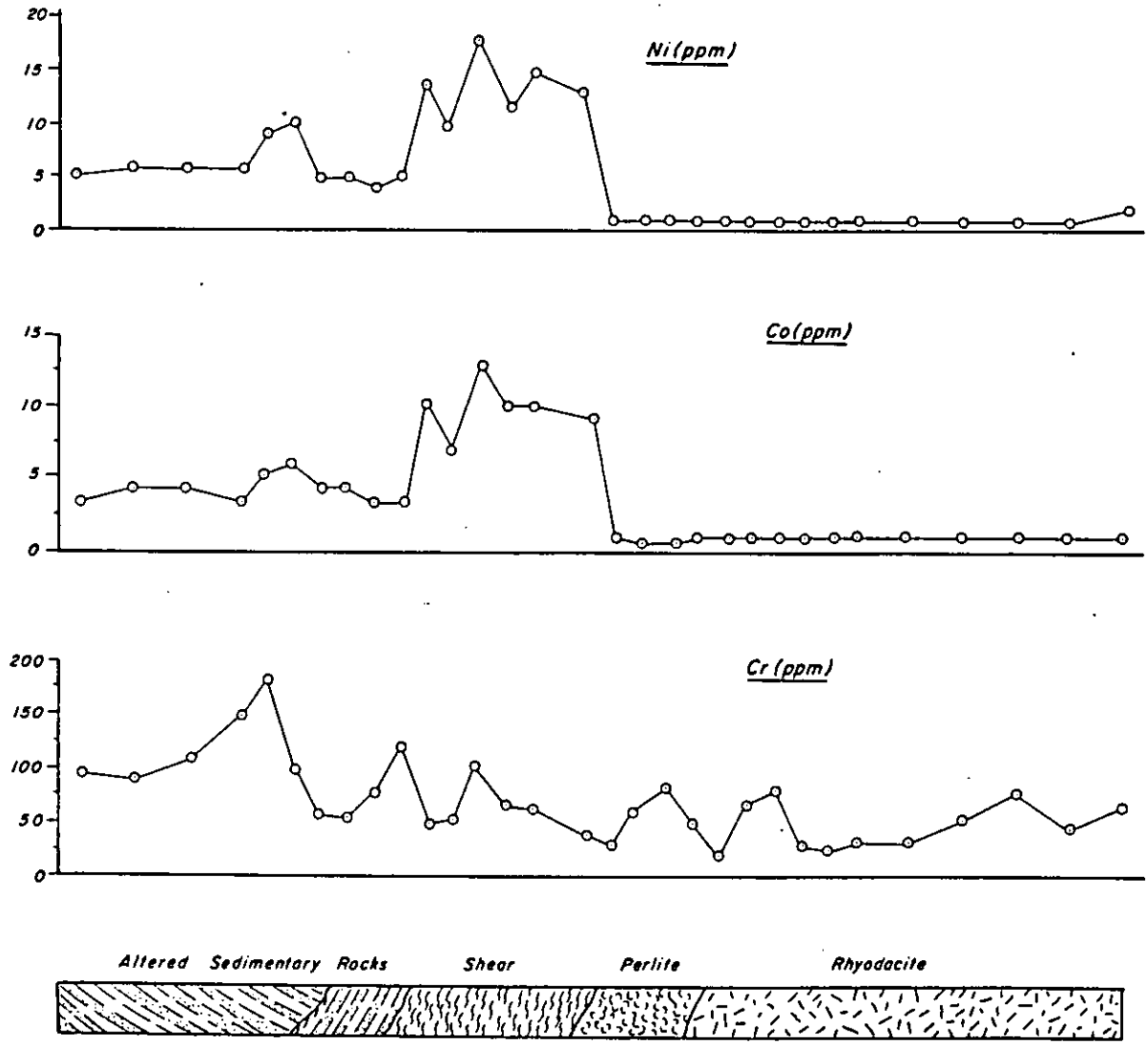
RHYODACITE CONTACT
550 LEVEL, CANNON MINE
TRACE ELEMENT GEOCHEMISTRY